Università degli Studi di Trieste
Dipartimento di Ingegneria ed Architettura

Scienza e tecnologia dei materiali ceramici

Prof. Valter Sergo

Contributi di:
Federico Antonelli
Elisa Favero
Silvia Dalla marta

Taxonomy of Ceramics

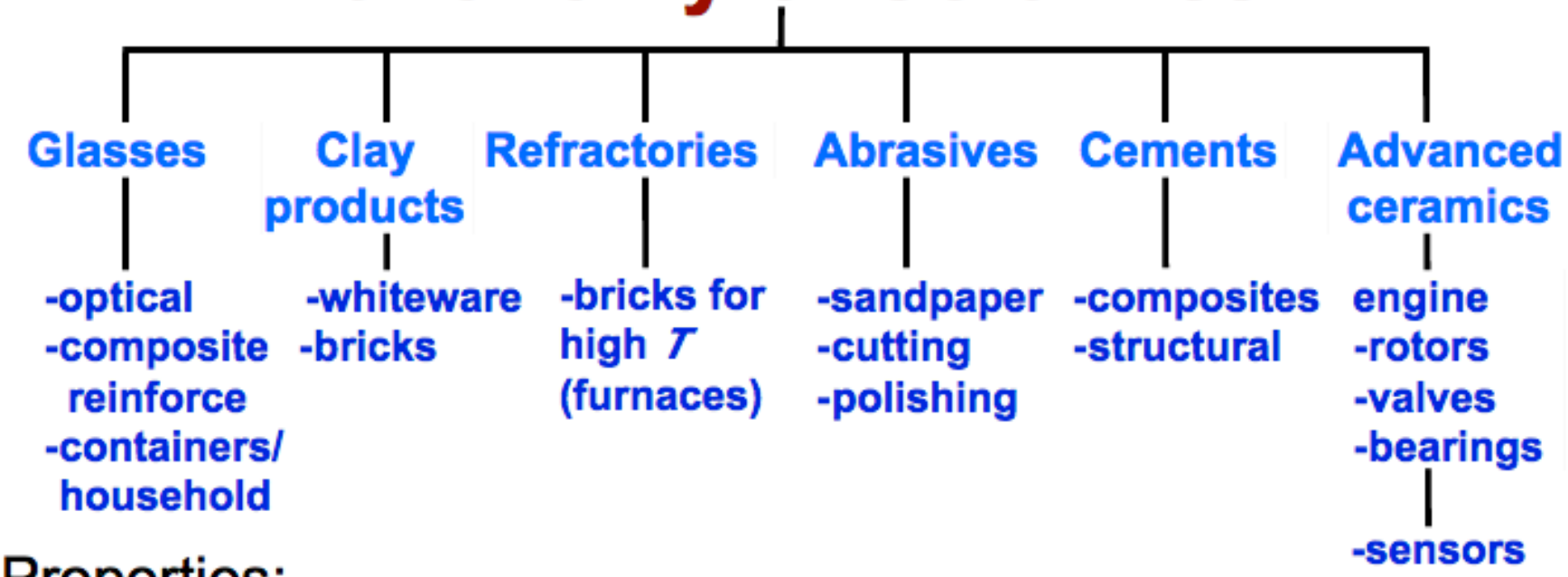

- Properties:
  -- T_m for glass is moderate, but large for other ceramics.
  -- Small toughness, ductility; large moduli & creep resist.
- Applications:
  -- High T, wear resistant, novel uses from charge neutrality.
- Fabrication
  -- some glasses can be easily formed
  -- other ceramics can not be formed or cast.

Packing of atoms determines structures

- Packing efficiency can be characterized by coordination number which depends on cation-anion radius ratio (r_c/r_a)

Cation-anion radius ratio (r_c/r_a)	< 0.155	0.155 – 0.225	0.225 – 0.414	0.414 – 0.732	0.732 – 1.000	> 1.000
Coordination number	2	3	4	6	8	12

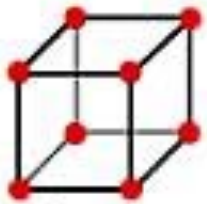

Simple cubic

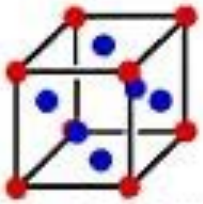

Face-centered cubic

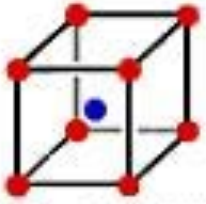

Body-centered cubic

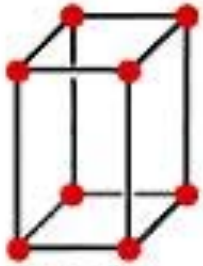

Simple tetragonal

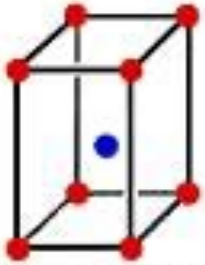

Body-centered tetragonal

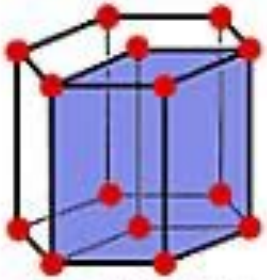

Hexagonal

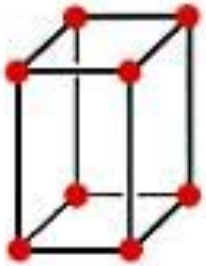

Simple orthorhombic

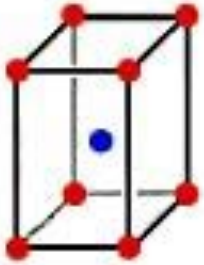

Body-centered orthorhombic

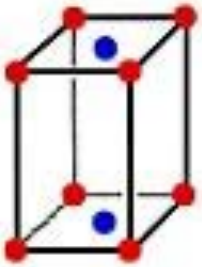

Base-centered orthorhombic

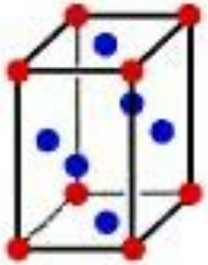

Face-centered orthorhombic

Rhombohedral

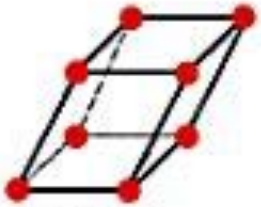

Simple Monoclinic

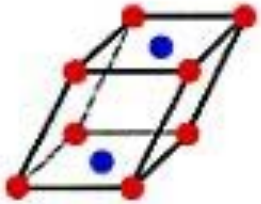

Base-centered monoclinic

Triclinic

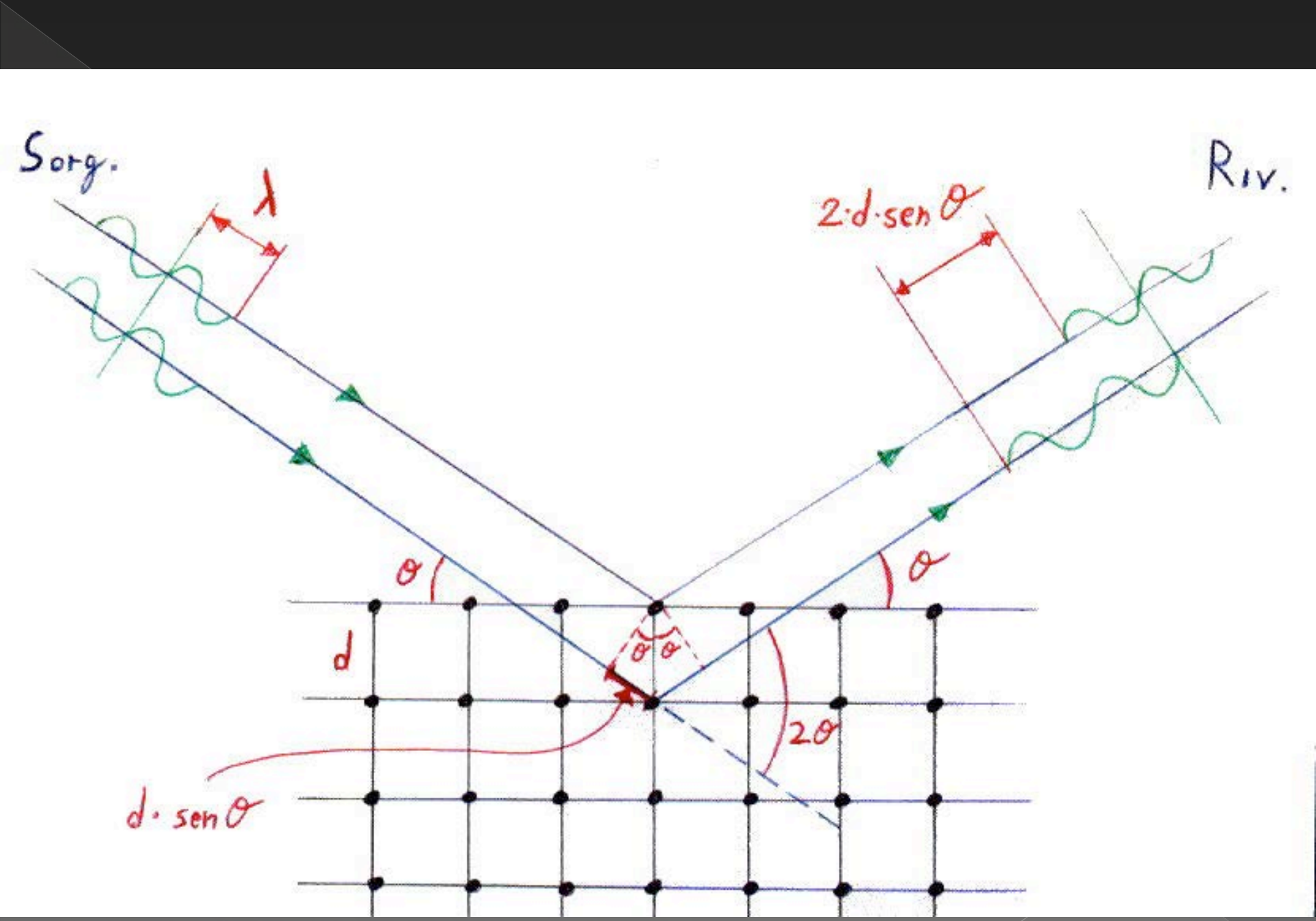
Sorg.
Riv.
λ
2·d·sen θ
θ
θ
d
θ θ
2θ
d · sen θ

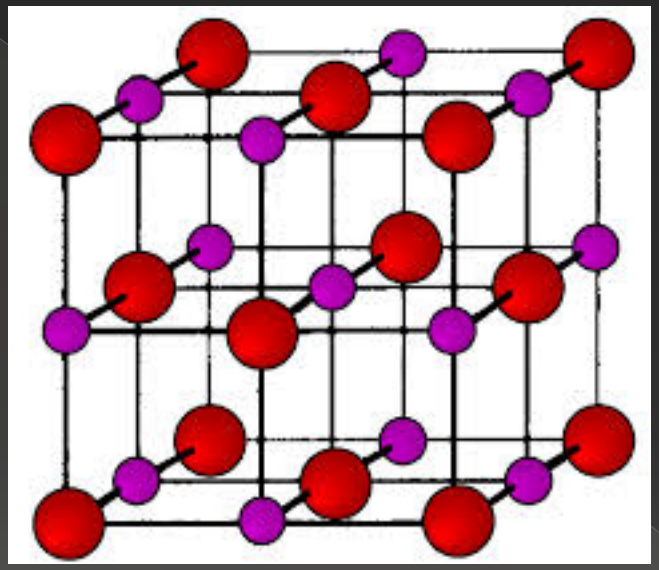

Rock Salt: MgO, CaO, NiO

ROCKSALT (NaCl)

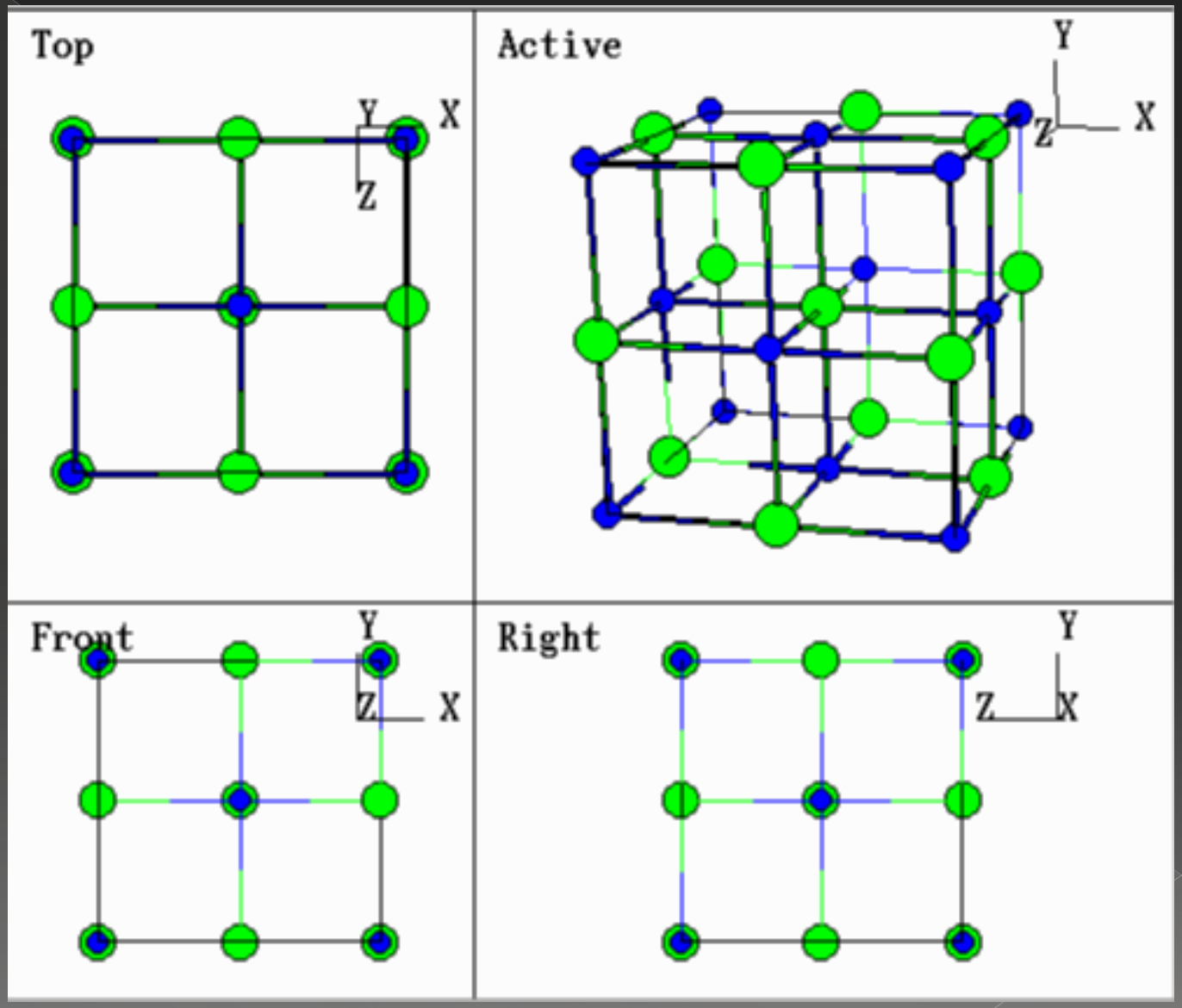

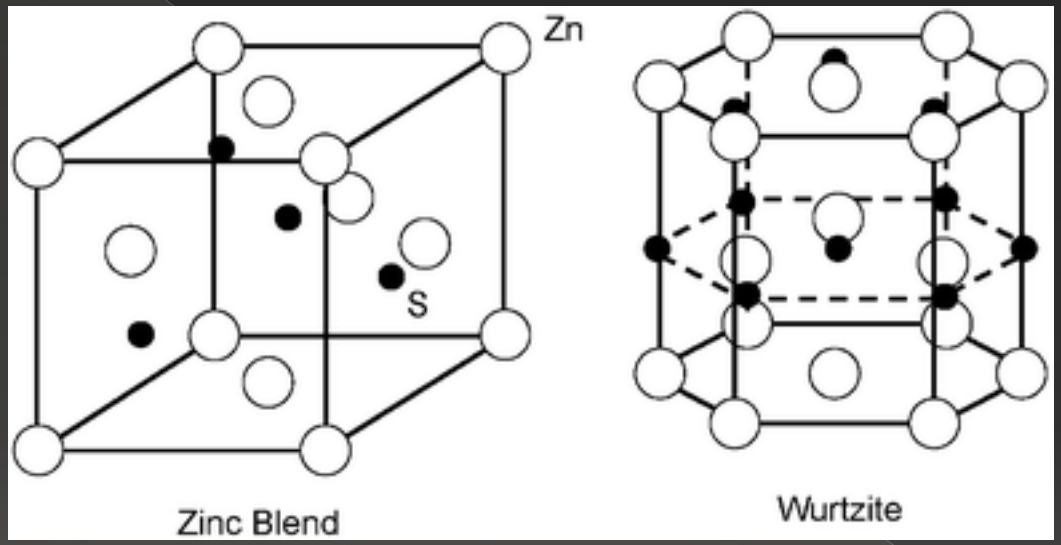

Zinc Blend and wurtzite: ZnO, SiC, BeO

WURTZITE [(Zn,Fe)S]

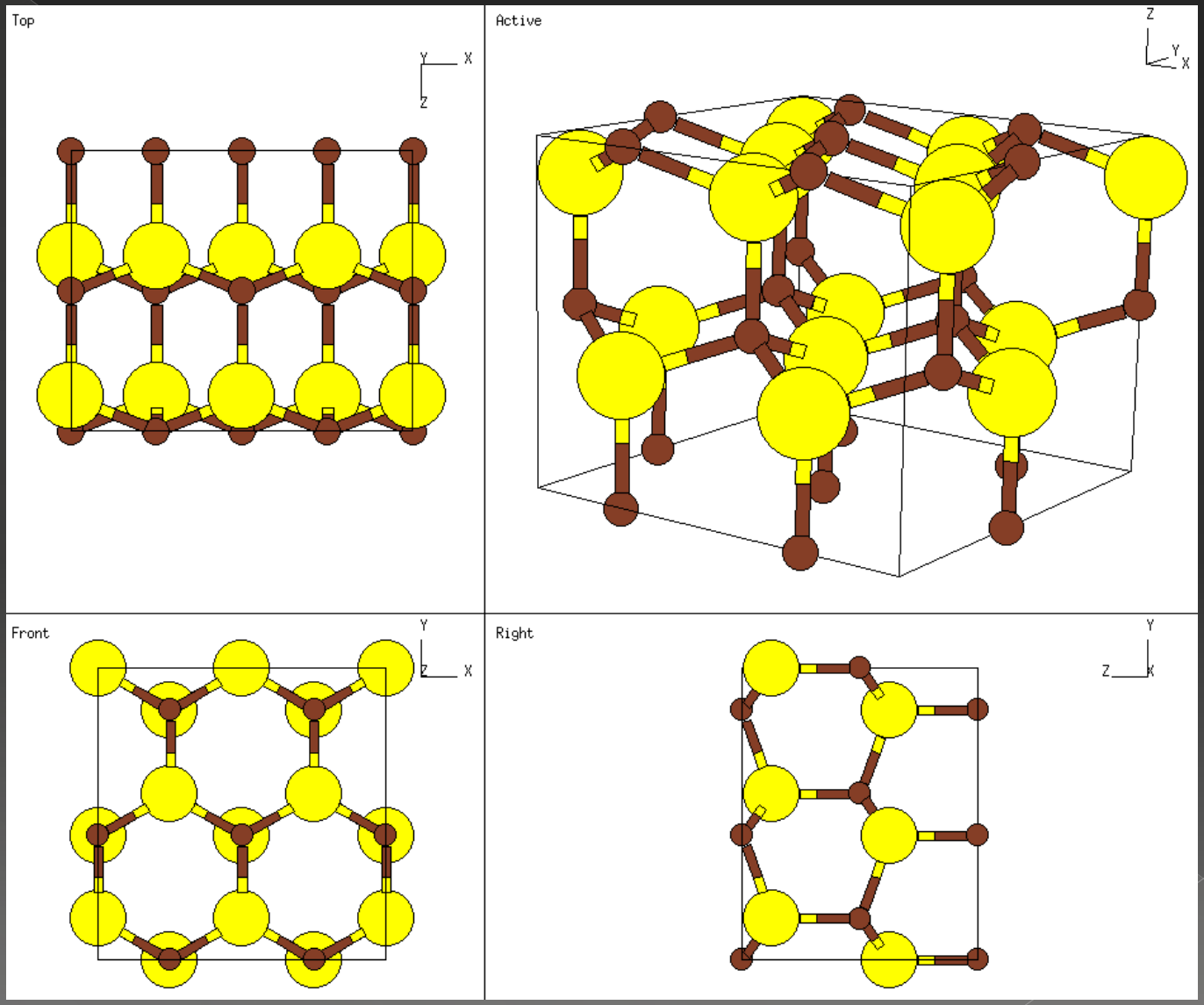

SPHALERITE [(Zn,Fe)s]

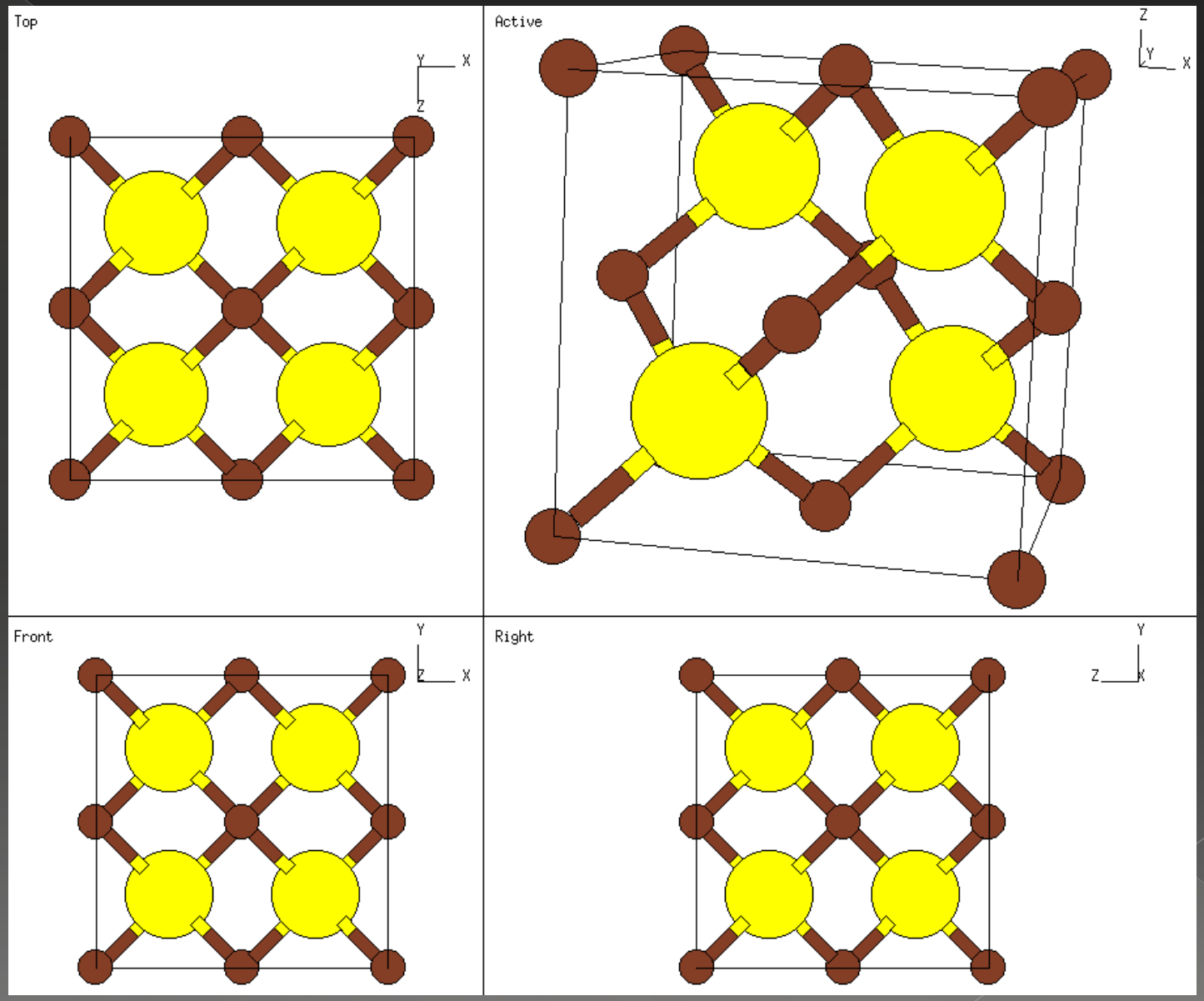

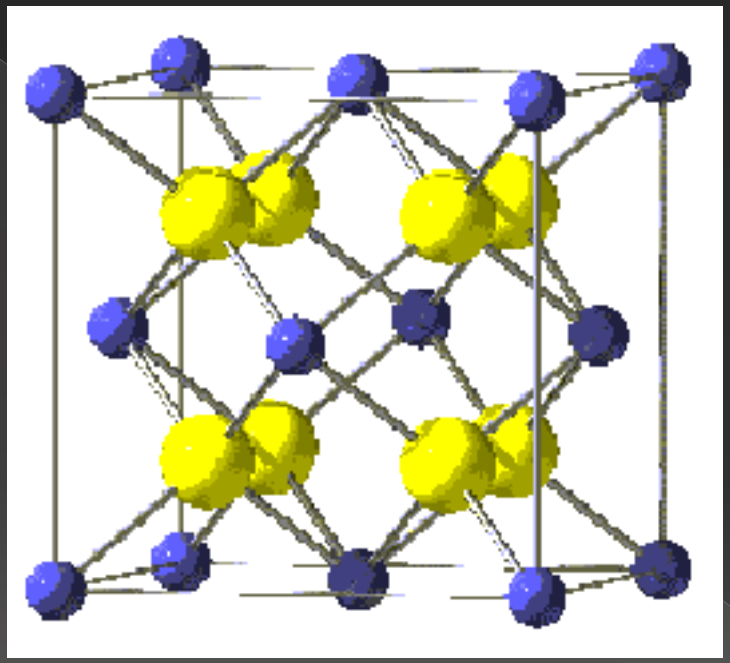

Fluoride struture: ZrO_2, CeO_2, UO_2

FLUORITE (CaF_2)

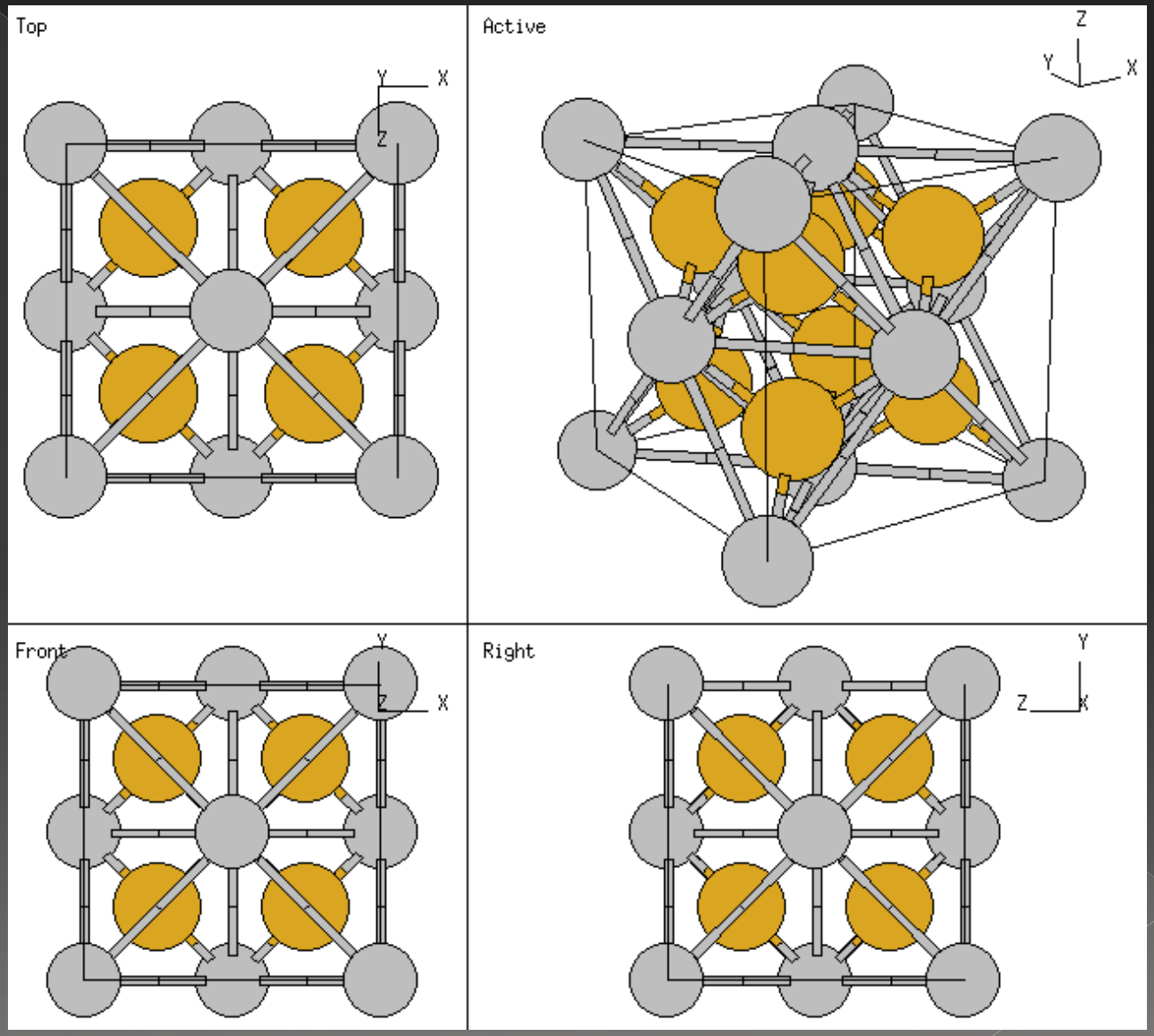

CORUNDUM (Al_2O_3 - α)

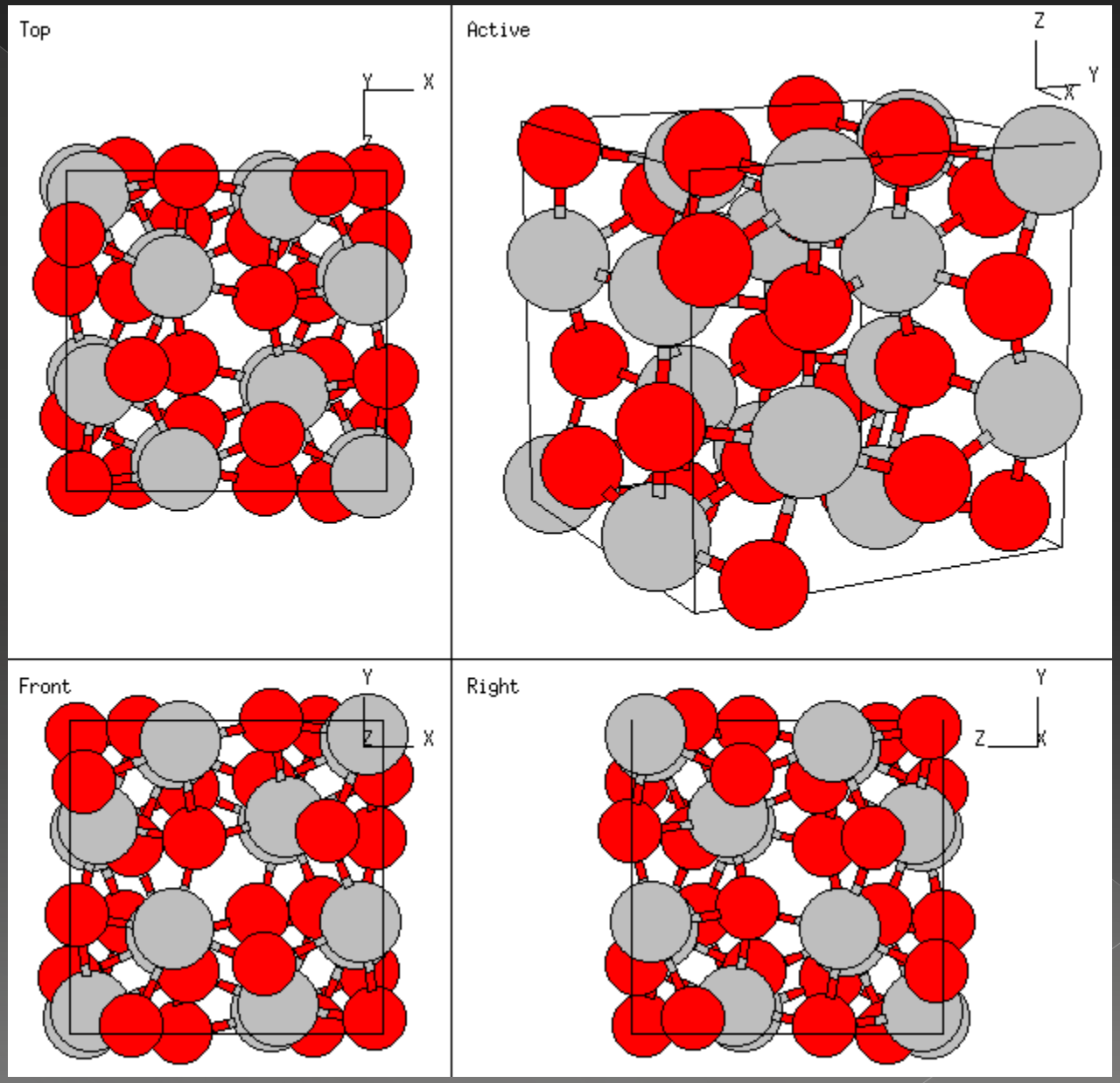

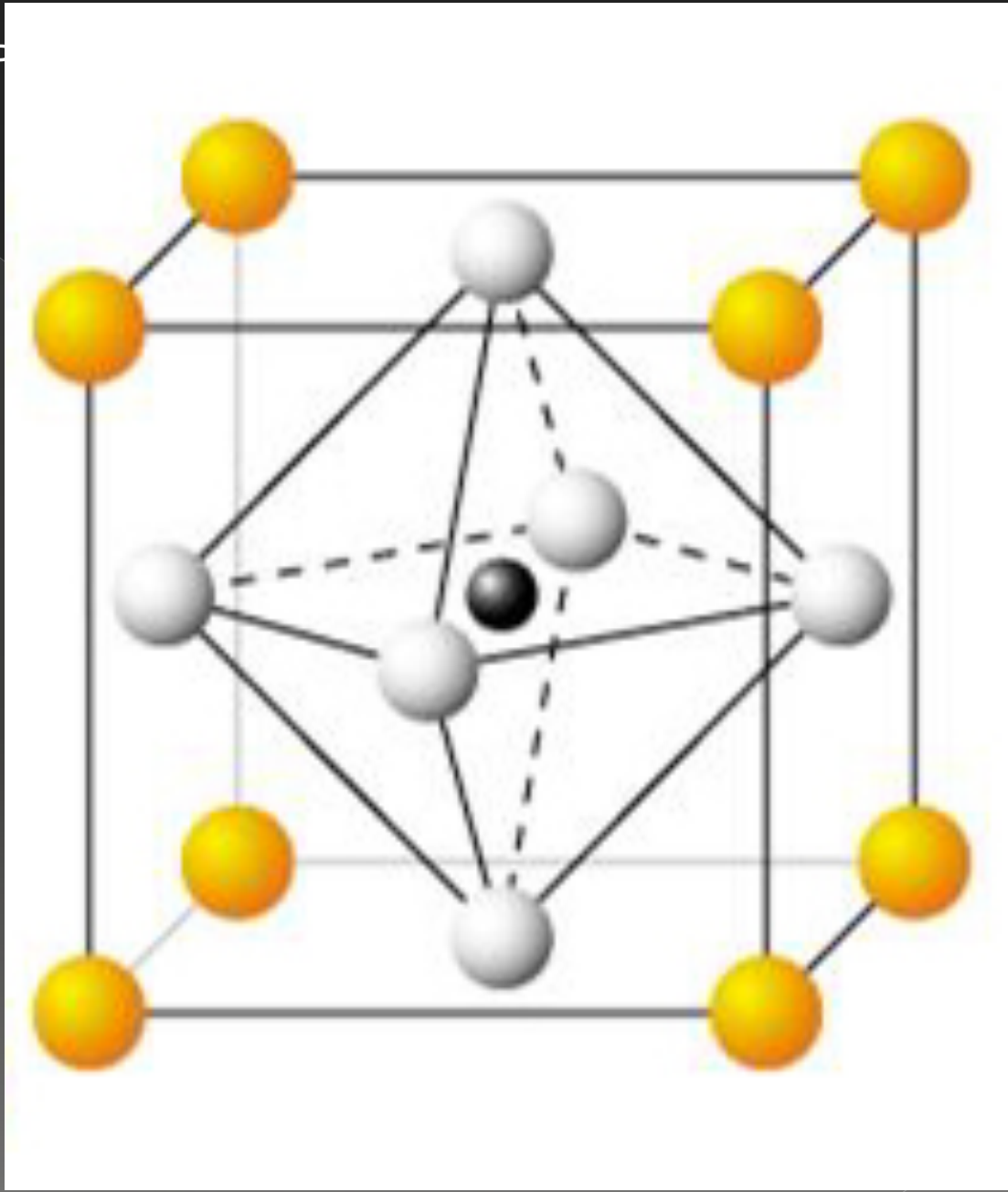

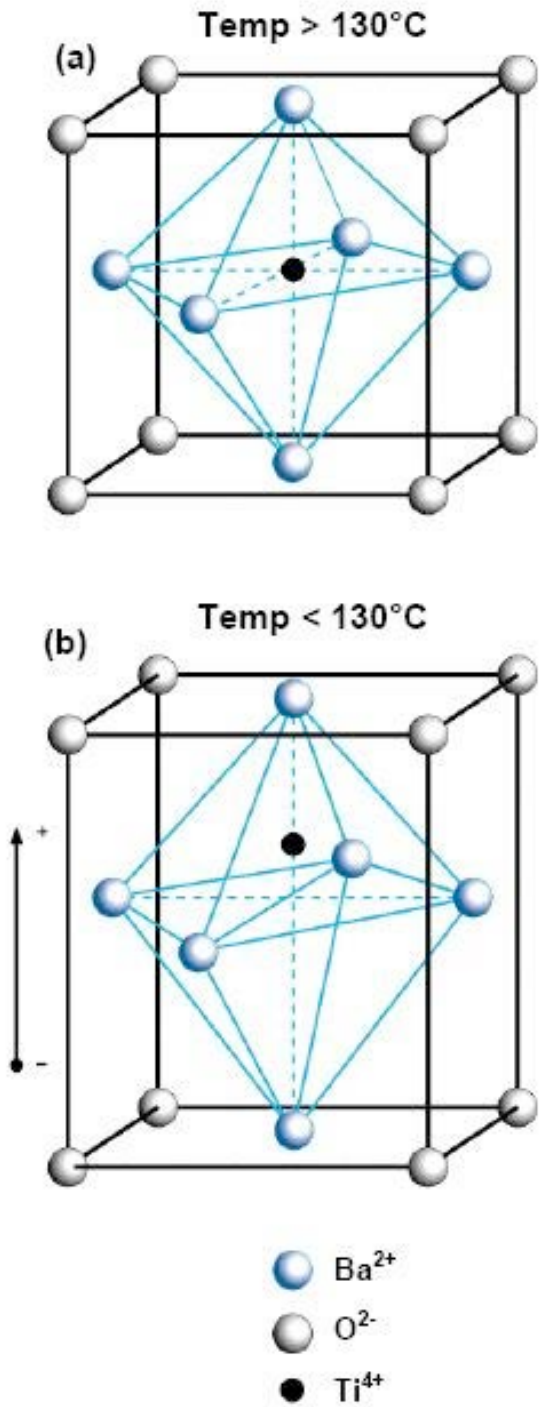
Temp > 130°C
(a)
Temp < 130°C
(b)
+
-
Ba^{2+}
O^{2-}
Ti^{4+}

Cubic Body Centered

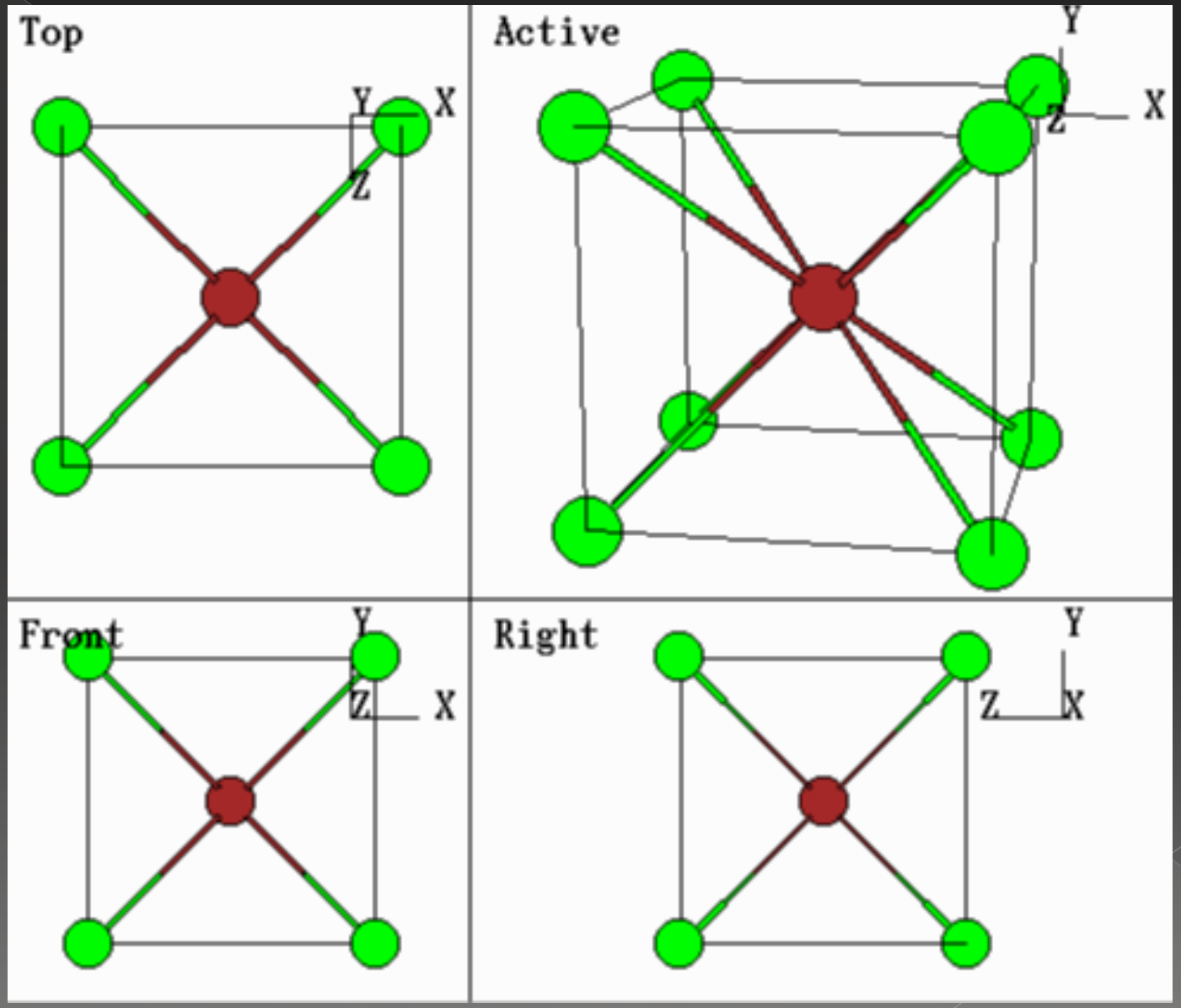

PEROVSKITE ($CaTiO_3$)

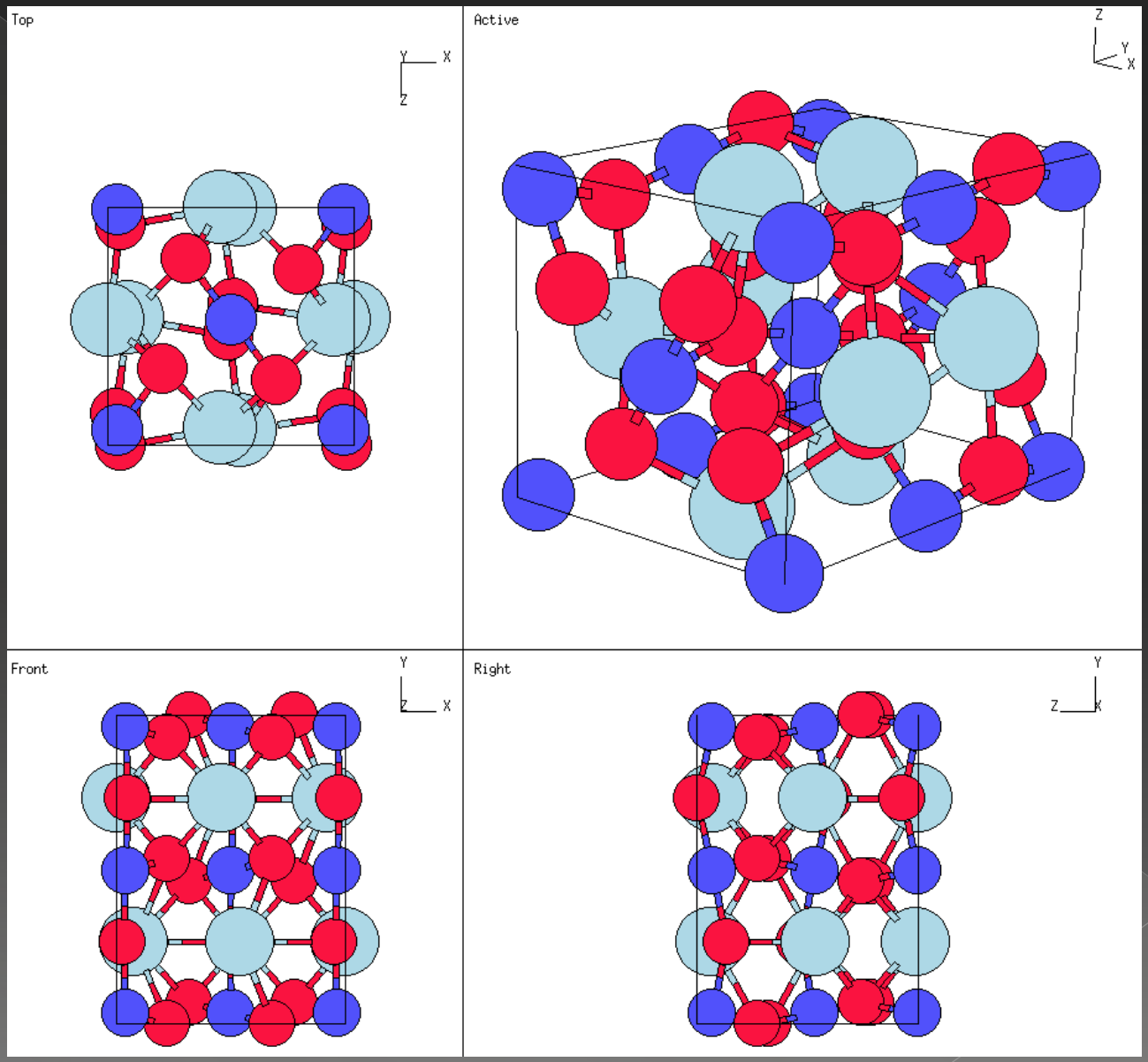

Kröger – Vink Notation

- Proposed in 1956 by F.A. Kröger and H.J. Vink in the journal *Solid State Physics* (*F.A. Kröger, H.J. Vink, Relations between the Concentrations of Imperfections in Crystalline Solids, Solid State Physics, Volume 3, 1956, 307-435*)
- Set of conventions used to describe lattice position and electric charge for point defects in crystalline structures
- The key concept is the crystal lattice to consist of POSITIONS and ATOMS

Vacancy

- There can be <u>unoccupied</u> positions :

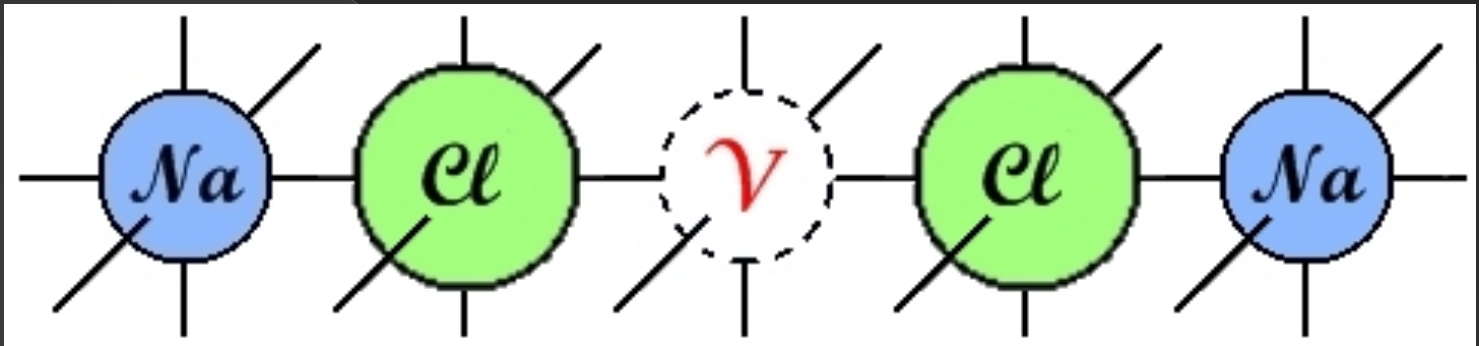

these empty positions are called **VACANCIES**

- In the picture, there is a Na vacancy, which is symbolized by:

$$V_{Na}$$

Vacancy & Charge

- However, like ions, also vacancies have charge:
  e.g. proceeding with the previous example, the absence of a ion Na^+ leads to a lack of positive charge, meaning a *negative charge* concentration!

- **Vacancies have always OPPOSITE CHARGE to the missing ion**

Charge

- $'$ → negative charge e.g. $V_{Na}^{'}$
- $\bullet$ → positive charge e.g. $V_O^{\bullet\bullet}$ [Oxygen vacancy with 2 (+) charges]
- $\times$ → neutrality e.g. $Cl_{Cl}^{\times}$

(neutrality may be unexpressed)

Substitutional defect

- An atom or a ion can be replaced by another:

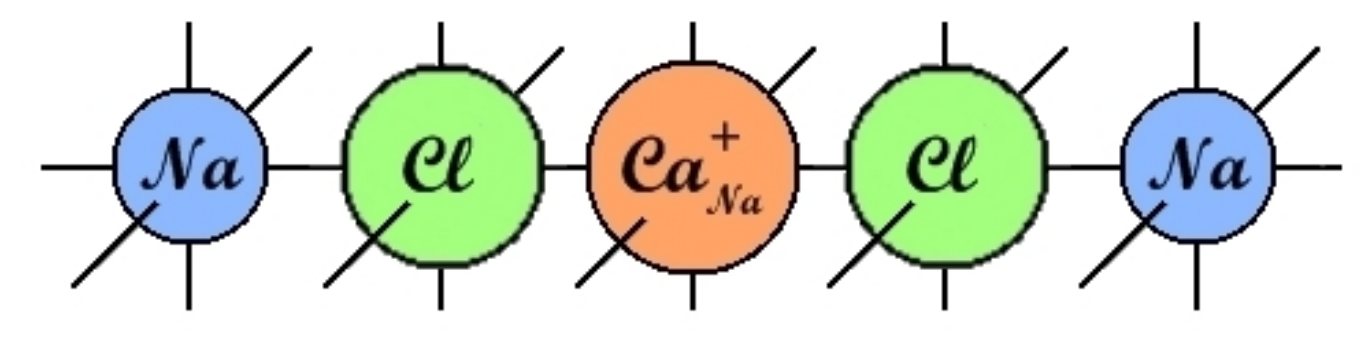

- The Ca ion took the place of the Na ion, which is symbolized by:

$$Ca_{Na}$$

- As Ca ion has 2 (+) charges, while Na ion has only 1 (+) charge, there is a total 1 (+) charge, so:

$$Ca_{Na}^{\bullet}$$

Interstitial defect

- An atom or a ion can be present on any site that would be unoccupied in a perfect crystal, as is typical for H^+ ions in metallic lattice:

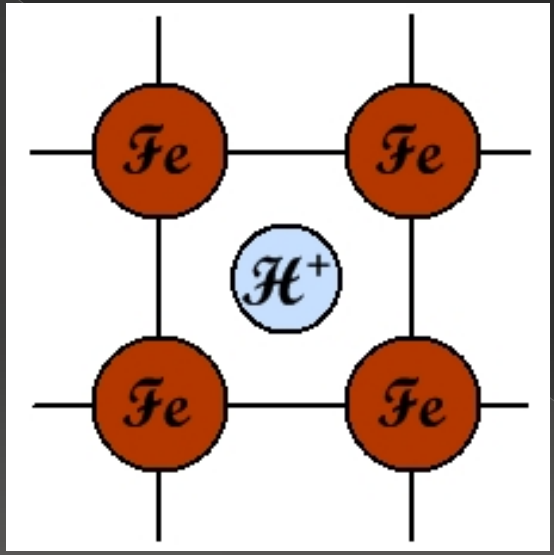

- Interstitial H^+ ion in Fe lattice is symbolized by:

$$H_i^{\bullet}$$

Pure electric charge

pure electric charges

- electrons
- "holes"

- electron: $e^{|}$
- hole: $h^{\bullet}$

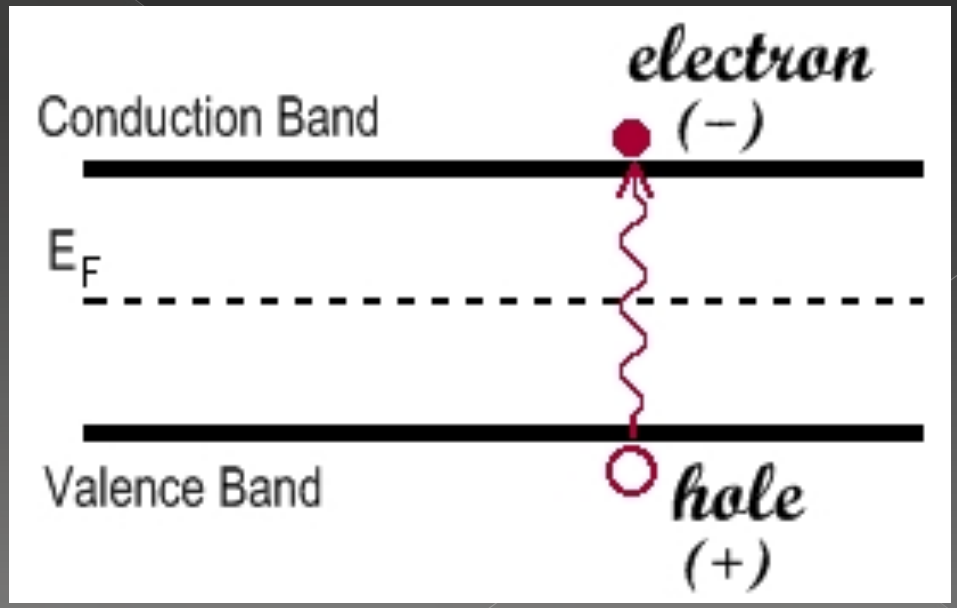

Quasi – Chemical Approach

to defect formation

- Apply Chemical Equilibrium concepts to solid dissolutions of a substance into another
- In order to be able to describe (hence with predictive purposes also) defects formation "reactions"

RULES for defect formation "reactions"

1) **SITE BALANCE,**

2) **MASS BALANCE,**

3) **CHARGE BALANCE.**

Given a generic compound $M_A X_B$:

- **SITE BALANCE**: at equilibrium the ratio of #M SITES (NOT actual atoms) to #X SITES must always be preserved
  - So, creating anionic sites must lead to the creation of cationic sites as well (and vice versa) **IN THE RIGHT RATIO**
- **MASS BALANCE**: defect formation reactions can't create nor destroy mass
- **CHARGE BALANCE** (Electro Neutrality Condition): preservation of crystal global neutrality
  - So, there can't be reactions which leave the crystal charged
  - So, the total sum of negative electric charges must be equal to total sum of positive charges

Defects

Perfect Crystal

- Crystal which has a completely ordered structure with atoms at rest and electrons distributed in the lowest possible energy states.
- But *REAL* crystals contain a variety of imperfections, or *defects*.
- In crystalline ceramics the structure and chemistry of the material will be determined by the kinetics of defect movement.

Defects

- What is special about ceramic defects is that they can be *charged*, while metals cannot.
- *DEFECT HIERARCHY*: defects are often classified in terms of a dimensionality: 0D, 1D, 2D, or 3D.

"Dimension"	Defect
0	Point defects
1	Line defects
2	Surfaces Grain boundaries Phase boundaries
3	Volume defects

- NB: In spite of the classification, ALL these defects are three-dimensional!

Point defects

- Point defects are particularly important in ceramics because of the role they can play in determining the properties of a material.

  e.g. the entire semiconductor industry is possible because of minute concentrations of point defects that are added to Si (dopants determine the whole material electrical properties: if it's n-type, p-type, or semi-insulating).

Point defects

- Types of point defects:
  - ***Misplaced atoms*** & ***Solute atoms*** (*substitutional defects*: atoms or ions are replaced by others),
  - ***Vacancies*** (empty positions),
  - ***Interstitials*** (atoms or ions present on any site that would be unoccupied in a perfect crystal),
  - ***Electronic defects*** (electrons and holes),
  - ***Associated centers*** (two point defects which interact so that they can be considered as a single defect; if more atoms are involved, they would be called a *defect cluster* or a *defect complex*).

Solid Solutions

- If a material crystallizes in the presence of foreign atoms, their inclusion in the main crystalline structure could:
  - *Increase* significantly system's energy ⇒ foreign atoms would be almost completely *excluded* from forming crystalline structure
  - *Decrease* considerably system's energy ⇒ there would be the development of a *new crystalline form*
  - In intermediate cases, foreign atoms would fit in a random way in the forming crystalline structure ⇒ *SS*
- SS are stable, of course, when the mixed crystal has a lower $\Delta G_{formation}$ than the other 2 alternatives.

Let's try to apply Quasi – Chemical Approach rules to 2 real instances:

SS of calcium chloride ($CaCl_2$) in sodium chloride ($NaCl$), which we would assume as a perfect crystal:

- First of all, SS of $CaCl_2$ in $NaCl$ is indicated as follows:

$$CaCl_2 \xrightarrow{NaCl}$$

- MASS BALANCE:

$$CaCl_2 \xrightarrow{NaCl} Ca_{Na} + 2Cl_{Cl}$$

- CHARGE BALANCE: being Ca^{++} the cation, it would probably substitute host Na^{+} cations, leading to an exceeding (+) charge $\Rightarrow$ adding charges to previous equation:

$$CaCl_2 \xrightarrow{NaCl} Ca_{Na}^{\bullet} + 2Cl_{Cl}^{\times}$$

but this equation doesn't balance charges!! So…

- SITE BALANCE: in this example the right ratio anionic/cationic sites is 1:1: our equation doesn't balance lattice sites neither! So…

$$CaCl_2 \xrightarrow{NaCl} Ca_{Na}^{\bullet} + 2Cl_{Cl}^{\times} + V_{Na}^{|}$$

REMARKS:

- All balances are related to a *perfect*, *neutral* crystal.
- Having charge separation, we expect the new crystal to be a better conductor…
- The equation we wrote gives us a better knowledge of the system in an atomic scale:

  e.g. we could represent it as:

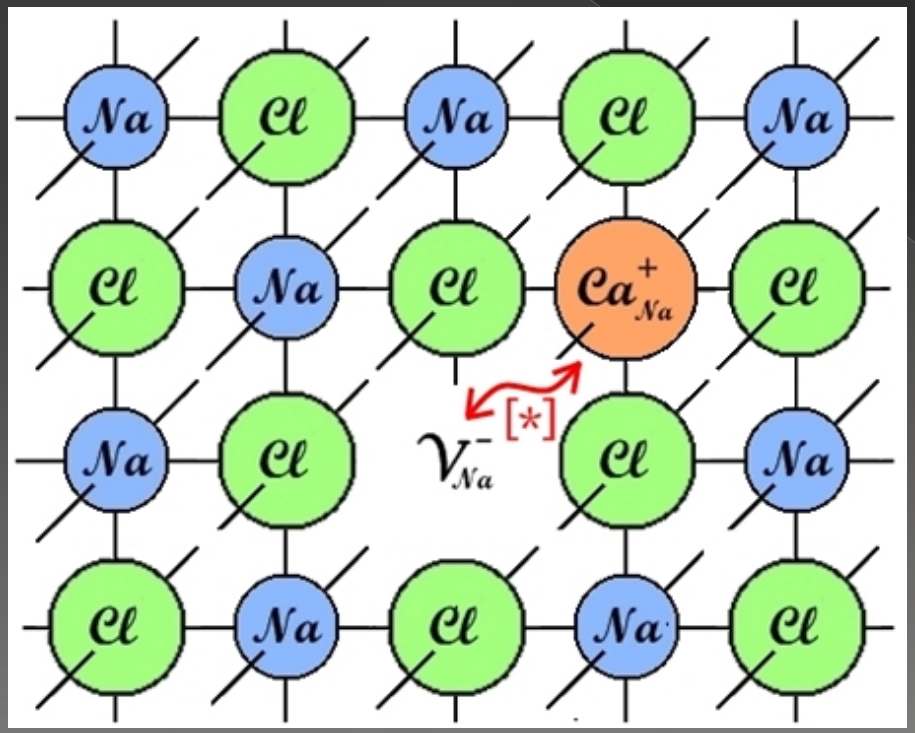

[*] close enough to balance charges!

SS of titania (TiO_2) in magnesia (MgO), which we would still assume a perfect crystal

- Mg has a double valence, while Ti has 4 (+) charges…

$$TiO_2 \xrightarrow{MgO} Ti_{Mg}^{\bullet\bullet} + 2O_O^{\times} + V_{Mg}^{''}$$

Schottky Disorder

- Simultaneous anionic and cationic vacancies.
- Total stoichiometry of the solid isn't compromised by Schottky disorders, because the number of empty M and X sites is balanced as to preserve local electro neutrality.
- Opposite charged vacancies tend to associate (they carry an *effective* charge), so they'd never be too far-away from one another.
- Schottky disorder formation "reaction":

$$\varnothing \xrightarrow{MgO} V_{Mg}^{''} + V_{O}^{\bullet\bullet}$$

Schottky Disorder

- This is a common defect in *alkali halides* at high T.
- In oxides vacancies $\Delta G_{formation}$ is 2x-3x $\Delta G_{formation}$(alkali halides), so at equilibrium the number of S. disorders in not relevant until very high T.

Frenkel Disorder

- Auto-interstitial defect: there is the same number of reticular vacancies and interstitial atoms, cause reticular atoms migrate in interstitial positions.

$$Ti_{Ti} \xrightarrow{TiO_2} V_{Ti}^{''''} + Ti_i^{\bullet\bullet\bullet\bullet}$$

- e.g. halide: $AgBr$ $\quad Ag_{Ag} \xrightarrow{AgBr} V_{Ag}^{'} + Ag_i^{\bullet}$

- e.g. oxide: Y_2O_3 $\quad O_O \xrightarrow{Y_2O_3} V_O^{''} + O_i^{\bullet\bullet}$

Frenkel Disorder

- This is a common defect in:
  - Crystals with *fluorite structure*, which has large interstitial sites.
  - Crystals with high polarizable ions, which can in an easier way set up in interstitial sites.
- The energy change for F. disorder formation depends strongly on reticular structure and ion characteristics.

Some more examples

SS of TiO_2 in MgO

- We wrote

$$TiO_2 \xrightarrow{MgO} Ti_{Mg}^{\bullet\bullet} + 2O_O^{\times} + V_{Mg}^{''}$$

for substitutional SS, but it could be also an interstitial SS:

$$TiO_2 \xrightarrow{MgO} Ti_{Mg}^{\bullet\bullet} + O_i^{''} + O_O^{\times}$$

- Which one is better?

- Evaluate ΔG° and choose the favorite!
- Usually it is $\Delta G_i >> \Delta G_V \Rightarrow$ easier formation of vacancies than interstitials.

SS of TiO_2 in MgO

- This specific instance follows that general rule, too, as the passage of atoms to interstitial positions requires quite high energies:

$$\Delta H_i >> \Delta H_V$$

- $\Rightarrow$ almost the entire part of defects will be substitutional:

$$TiO_2 \xrightarrow{MgO} Ti_{Mg}^{\bullet\bullet} + 2O_O^{\times} + V_{Mg}^{\prime\prime}$$ ✓

$$TiO_2 \xrightarrow{MgO} Ti_{Mg}^{\bullet\bullet} + O_i^{\prime\prime} + O_O^{\times}$$ ✗

Zirconia doped with calcia

- There are, again, 2 possibilities:

① $2CaO \xrightarrow{ZrO_2} Ca_{Zr}^{''} + 2O_O^{\times} + Ca_i^{\bullet\bullet}$

to mantain constant the ratio anionic/cationic sites in zirconia's reticulum
(of course interstitial is *not* considered to this aim)

② $CaO \xrightarrow{ZrO_2} Ca_{Zr}^{''} + O_O^{\times} + V_O^{\bullet\bullet}$

- Zirconia has a Fluorite structure ⇒ lots of empty space inside ⇒ interstitials are *not* automatically privileged…
- So??

Zirconia doped with calcia

- Let's consider the profiles of density in function of mole % of CaO in ZrO_2 (at T_{amb}):

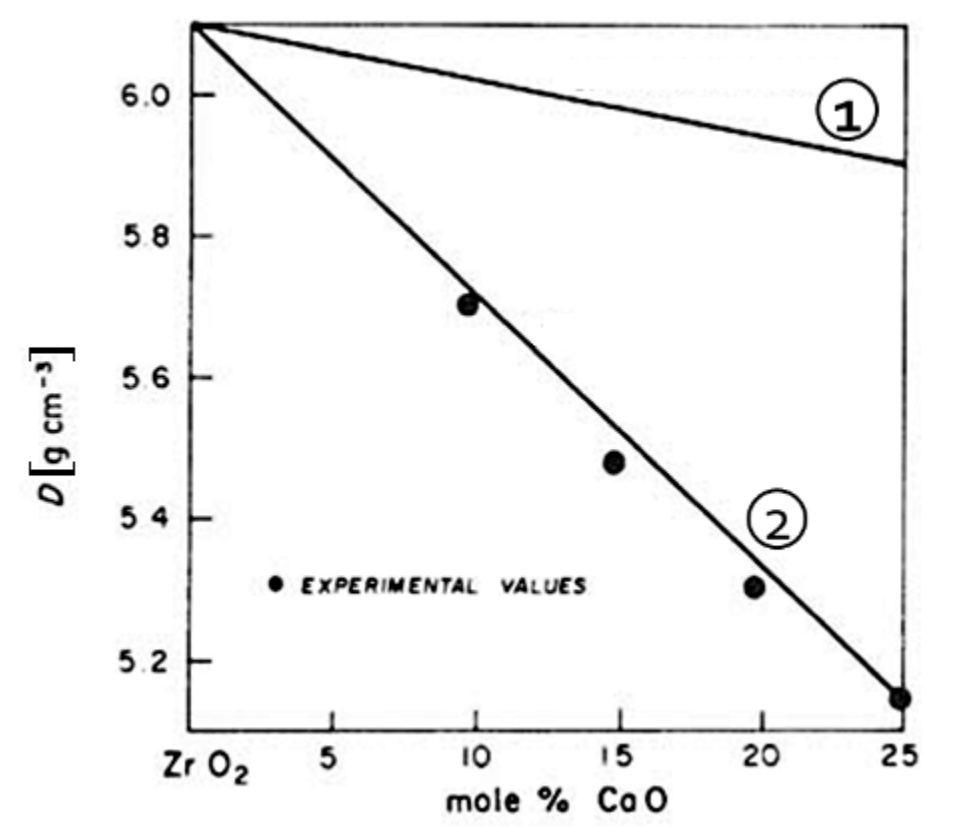

- Experimentally, reaction ② is the favourite.

Lambda sensor (or oxygen sensor)

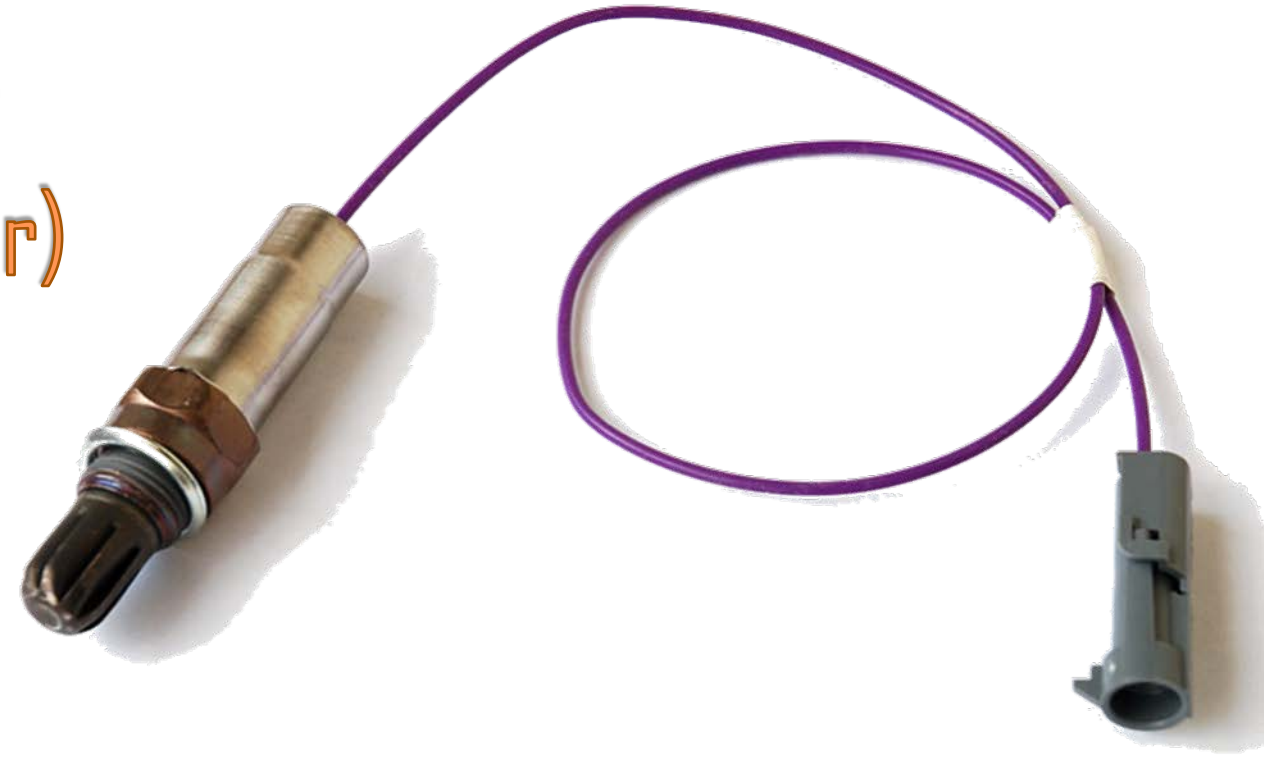

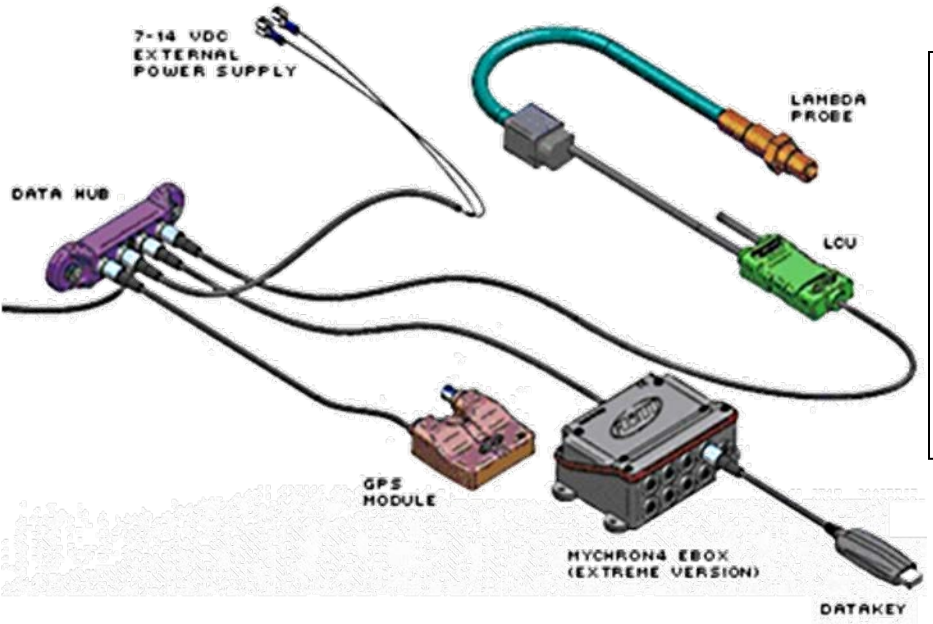

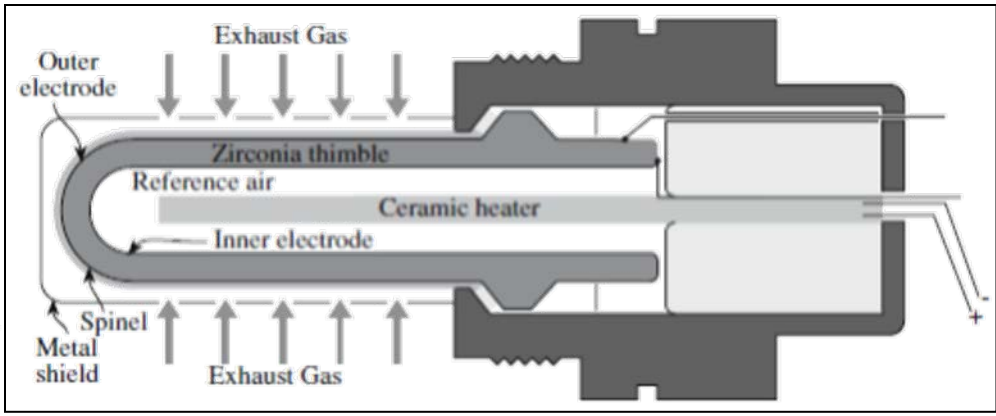

Zirconia doped with yttria

- Applications of *pure* zirconia are restricted because it shows *polymorphism*:
  - It is ***monoclinic*** at room temperature
  - Changes to the denser ***tetragonal*** phase from circa 1000 °C.
- The phase change t-ZrO_2 ⇆ m-ZrO_2 shows a large change in volume (ΔV=5%) which causes *extensive cracking*.
- The addition of some oxides (like CaO, Y_2O_3) results in (meta)stabilizing the t-phase (or c-phase) at room temperature.

Yttria-stabilized Zirconia

Cubic zirconia (or CZ) : hard, optically flawless and usually colorless (but may be made in a variety of different colors).
Single crystals of the cubic phase of zirconia are commonly used as diamond simulant in jewellery.

Magnesia doped with lithium fluoride

$$LiF \xrightarrow{MgO} Li_{Mg}^{'} + F_O^{\bullet}$$

Magnesia doped with alumina

$$Al_2O_3 \xrightarrow{MgO} 2Al_{Mg}^{\bullet} + V_{Mg}^{''} + 3O_O^{\times}$$

Quasi – Chemical Approach

Constant of Reaction

- There's a need of a more immediate way to estimate defect concentration in crystals.
- Applying:
  - Kröger – Vink notation
  - Quasi – Chemical approach

  to equations that represent defect formation's processes
- A "*constant of reaction*" for those equation can be defined.

With e.g. : $TiO_2 \xrightarrow{MgO} Ti_{Mg}^{\bullet\bullet} + 2O_O^{\times} + V_{Mg}^{''}$

Defining: $n_Y = \#\ \underline{sites}\ for\ species\ Y$

$[M_X] =$ *fraction of X species' reticular sites which have been occupied by M atoms*

$$\left[Ti_{Mg}^{\bullet\bullet}\right] = \frac{\#Ti^{4+}/cm^3}{\#Mg^{2+}/cm^3} = \frac{n_{Ti_{Mg}^{\bullet\bullet}}}{n_{Mg}}$$

$$\left[O_O^{\times}\right] = \frac{\#O/cm^3}{\#O/cm^3} = 1$$

$\Rightarrow$

$$\left[V_{Mg}^{''}\right] = \frac{\#V_{Mg}^{''}/cm^3}{\#Mg/cm^3} = \frac{n_{V_{Mg}^{''}}}{n_{Mg}}$$

So:

$$K_r = \frac{\left[Ti_{Mg}^{\bullet\bullet}\right]\left[V_{Mg}^{''}\right]\left[O_O^{\times}\right]^2}{a_{TiO_2}}$$

(where activity of solute specie is at the denominator)

And, going on with the "Quasi – Chemical" approach:

$$K_r = e^{-\frac{\Delta G^\circ}{RT}}$$

Where ΔG° is energy change associated with the dissolution process of TiO_2 in MgO

$$\Rightarrow \quad \frac{\left[Ti_{Mg}^{\bullet\bullet}\right]\left[V_{Mg}^{''}\right]\cancel{\left[O_O^{\times}\right]^2}^{\,1}}{a_{TiO_2}} = e^{-\frac{\Delta G^\circ}{RT}} \qquad (1)$$

ENC (Electro Neutrality Condition):

$$2en_{Ti_{Mg}}^{\bullet\bullet} = 2en_{V_{Mg}}^{''}$$

$$\Rightarrow \quad \frac{n_{Ti_{Mg}}^{\bullet\bullet}}{n_{Mg}} = \frac{n_{V_{Mg}}^{''}}{n_{Mg}} \quad \Rightarrow \quad \left[Ti_{Mg}^{\bullet\bullet}\right] = \left[V_{Mg}^{''}\right]$$

Finally, the (1) becomes:

$$\left[Ti_{Mg}^{\bullet\bullet}\right] = \left(a_{TiO_2}\right)^{1/2} e^{-\frac{\Delta G^\circ}{2RT}} \qquad (2)$$

which permit to *ESTIMATE DEFECTS CONCENTRATION*

NOTE: $0 < \left[Ti_{Mg}^{\bullet\bullet}\right] < 1$

Phase Diagram

In the phase diagram:

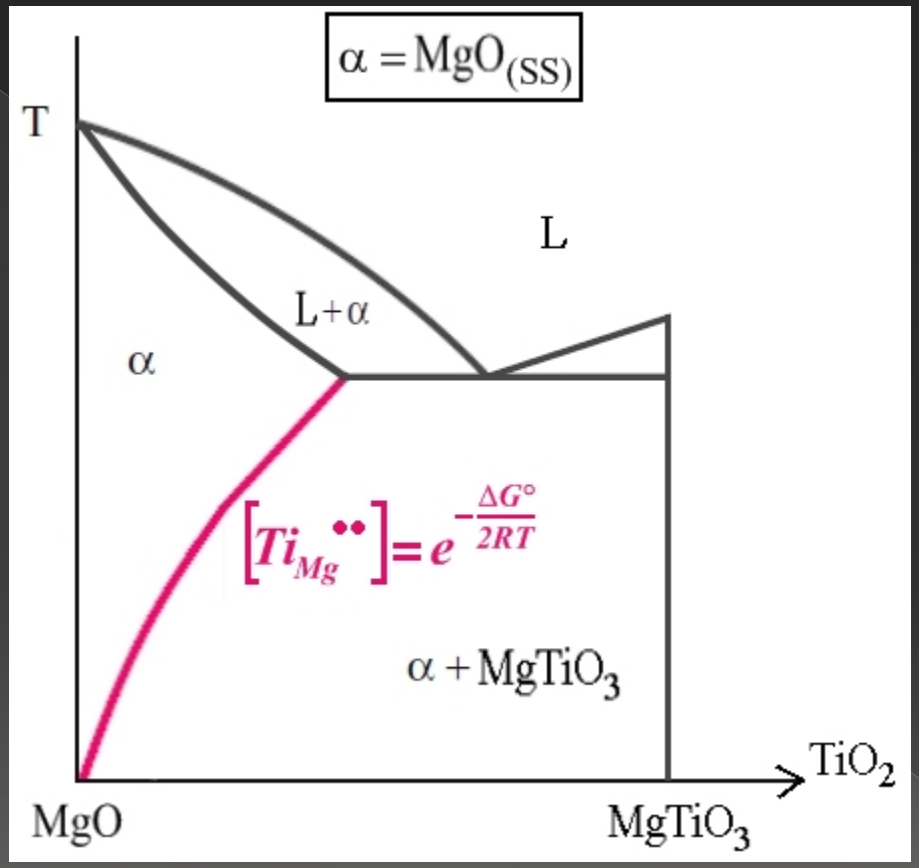

From equation [2] we can also obtain an expression for the SOLVUS LINE (remembering that, for solids, at equilibrium activity is *1*).

Phase Diagram

So, when you come down on a composition line:

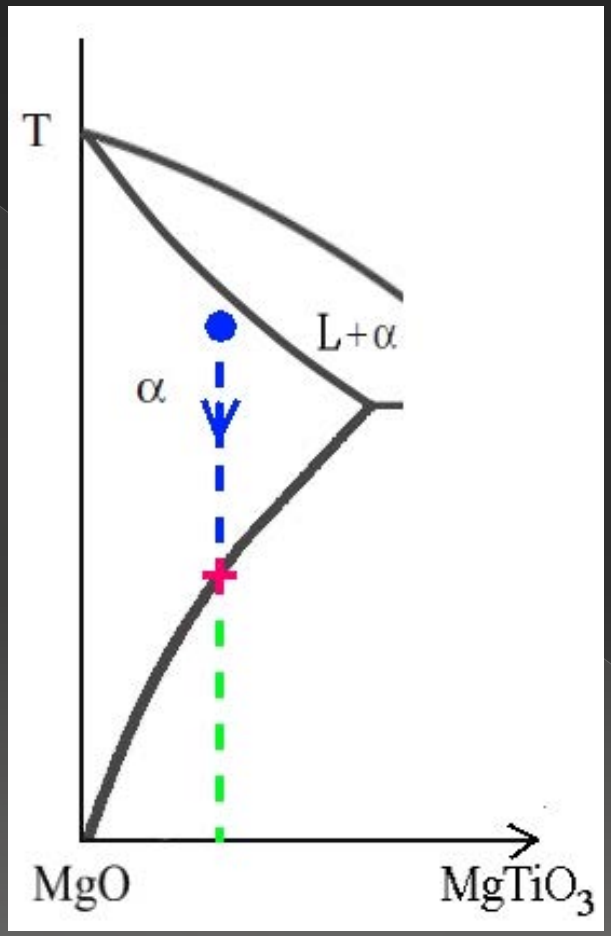

activity changes till when you reach the *solvus line* → then in the microstructure you'll have precipitation of TiO_2.

Some examples

Schottky Disorder in magnesia

$$\emptyset \xrightarrow{MgO} V_{Mg}^{''} + V_O^{\bullet\bullet}$$

$$\Rightarrow \left[V_{Mg}^{''}\right]\left[V_O^{\bullet\bullet}\right] = K_r = e^{-\frac{\Delta H_S}{RT}}$$

With: $\Delta H_S = 7.5\, eV/mol\,\mathcal{V}$

Schottky Disorder in magnesia

$$n_O = n_{Mg} = n_{MgO}$$

$$ENC: \quad 2en_{V_O^{\bullet\bullet}} = 2en_{V_{Mg}^{''}}$$

$$\left[V_{Mg}^{''}\right] = \left[V_O^{\bullet\bullet}\right] = e^{-\frac{\Delta H_S}{2RT}}$$

- So, at T = 2,000 K $\Rightarrow$ [V] $\approx 10^{-9}$
- $\Rightarrow$ in 1 *mol* there'll be $\approx 10^{+14}$ defects. $\left(n_V = [V] \cdot n_{MgO} \right)$
- NB: in a *real* crystal, there'll be, in any case, <u>*AT LEAST*</u> $10^{16} - 10^{17}$ defects/mol
- $\Rightarrow$ [V] $\approx 10^{-6} - 10^{-7}$

Schottky Disorder in alumina

$$\emptyset \xrightarrow{Al_2O_3} 2V_{Al}^{'''} + 3V_O^{\bullet\bullet}$$

$$\left[V_O^{\bullet\bullet}\right]^3\left[V_{Al}^{'''}\right]^2 = e^{-\frac{\Delta H_S}{RT}}$$

With: $\Delta H_S = 25eV$

Schottky Disorder in alumina

$$ENC: \quad 2en_{V_O^{\bullet\bullet}} = 3en_{V_{Al}^{'''}}$$

$$n_{Al} = 2n_{Al_2O_3}$$

$$n_O = 3n_{Al_2O_3}$$

$$2n_O\left[V_O^{\bullet\bullet}\right] = 3n_{Al}\left[V_{Al}^{'''}\right]$$

$$2\left(3n_{Al_2O_3}\right)\left[V_O^{\bullet\bullet}\right] = 3\left(2n_{Al_2O_3}\right)\left[V_{Al}^{'''}\right]$$

$$\Rightarrow \left[V_O^{\bullet\bullet}\right] = \left[V_{Al}^{'''}\right]$$

$$\Rightarrow \left[V_O^{\bullet\bullet}\right] = \left[V_{Al}^{'''}\right] = e^{-\frac{\Delta H_S}{5RT}}$$

Schottky Disorder in alumina

$$\Rightarrow \left[V_O^{\bullet\bullet}\right] = \left[V_{Al}^{'''}\right] = e^{-\frac{\Delta H_S}{5RT}}$$

ΔH_S is sort of "medium E per defect"

- So:
  - 1 Schottky disorder in alumina disarranges **5** points in crystal structure (3 V_O and 2 V_{Al})
  - 1 Schottky disorder in magnesia (previous example) disarranges **2** points in crystal structure (1 V_O and 1 V_{Mg})

Schottky disorder's energy of formation

SPECIE	ΔH_S [eV]	$\Rightarrow$ E/defect [eV]
Al_2O_3	25	~5
MgO	7.5	3.75
CaO	6.1	3.05
NaCl	2.30	1.65
KCl	2.26	1.1
LiF	2.34	1.17
LiCl	2.12	1.1
LiBr	1.80	0.9
LiI	1.30	0.7

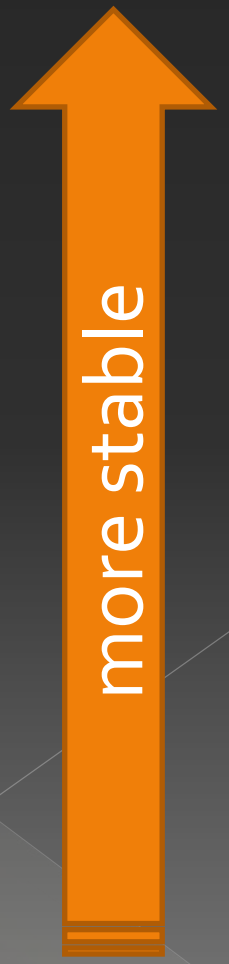

Frenkel Disorder in urania

$$U_U^{\times} \xrightarrow{UO_2} U_i^{\bullet\bullet\bullet\bullet} + V_U^{\text{IIII}}$$

$$\frac{\left[U_i^{\bullet\bullet\bullet\bullet}\right]\left[V_U^{\text{IIII}}\right]}{\left[U_U^{\times}\right]} = e^{-\frac{\Delta H_F}{RT}}$$

- NB: thank to the low defect concentration, $[U_U]$ is SUBSTANTIALLY 1.

Frenkel Disorder in urania

$$ENC: \quad 4en_{U_i^{\bullet\bullet\bullet\bullet}} = 4en_{V_U^{\prime\prime\prime\prime}}$$

As urania has a fluorite structure it is: $n_i = \frac{1}{4} n_U$

$$n_U = n_{UO_2}$$

$$\Rightarrow \quad \frac{n_{U_i^{\bullet\bullet\bullet\bullet}}}{n_i} = 4\frac{n_{U_i^{\bullet\bullet\bullet\bullet}}}{n_U} = 4\frac{n_{V_U^{\prime\prime\prime\prime}}}{n_U} \quad \Rightarrow \quad \left[U_i^{\bullet\bullet\bullet\bullet}\right] = 4\left[V_U^{\prime\prime\prime\prime}\right]$$

$$\Rightarrow \quad \left[U_i^{\bullet\bullet\bullet\bullet}\right]^2 = 4e^{-\frac{\Delta H_F}{RT}}$$

$$\Rightarrow \quad \left[U_i^{\bullet\bullet\bullet\bullet}\right] = 4e^{-\frac{\Delta H_F}{2RT}}$$

Fuel rods for nuclear reactors

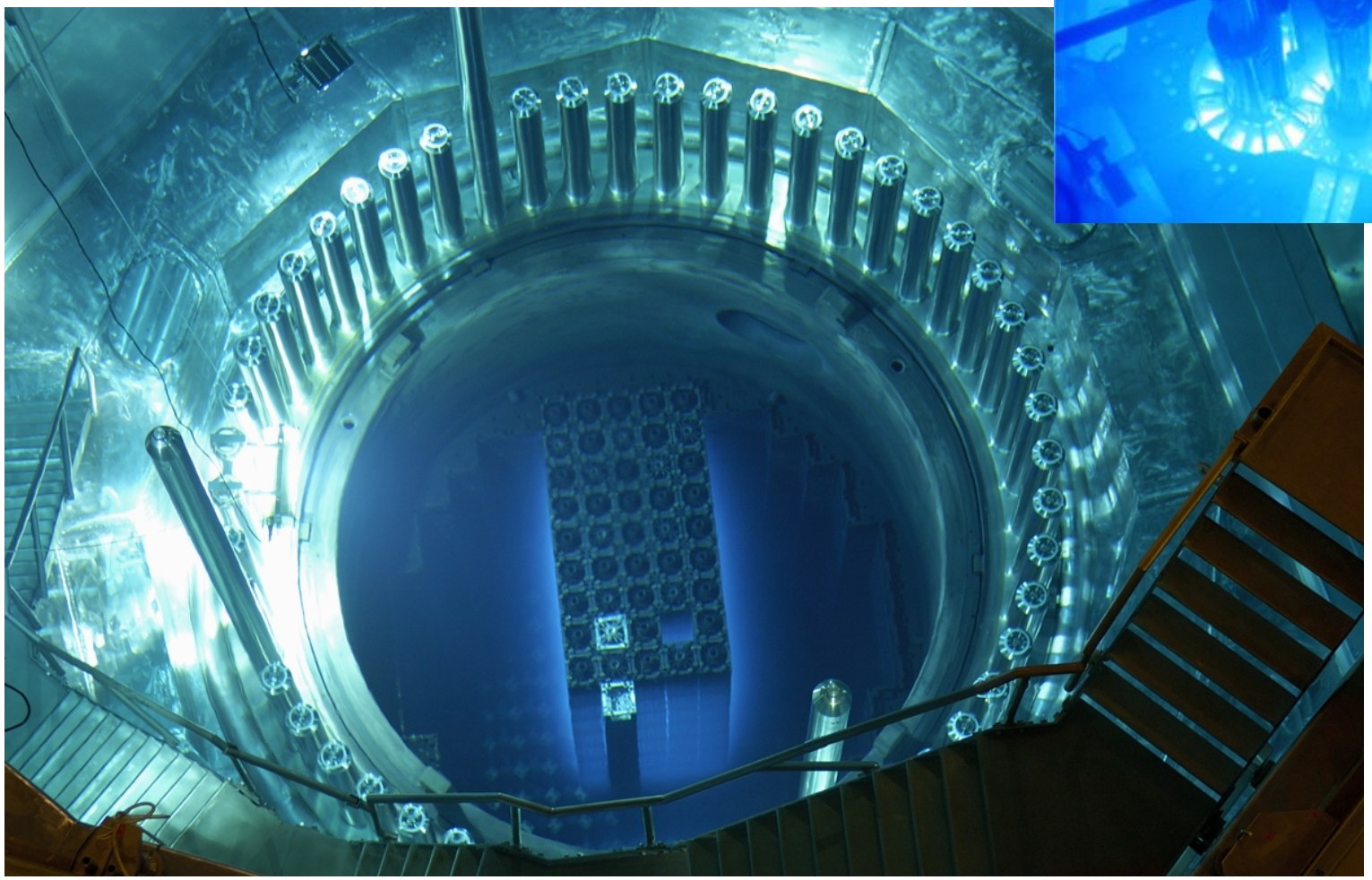

Frenkel disorder's energy of formation

STRUCTURE	MATERIAL – interstitial	ΔG [eV]
Rocksalt str.	$MgO – Mg$	13.5
	$MgO – O$	17.6
Corundum	$Al_2O_3 – Al$	14
	$Al_2O_3 – O$	16.5
Fluorite str.	$UO_2 – U$	3.4
Fluorite	$CaF_2 – Ca$	2.8
till 147 °C: wurtzite (over 147 °C: CBC and there is also a metastable form, with sphalerite str.)	$AgI – Ag$	0.75

Oxygen has also a bigger steric effect

Concentrations of charge carriers (electrons and holes)

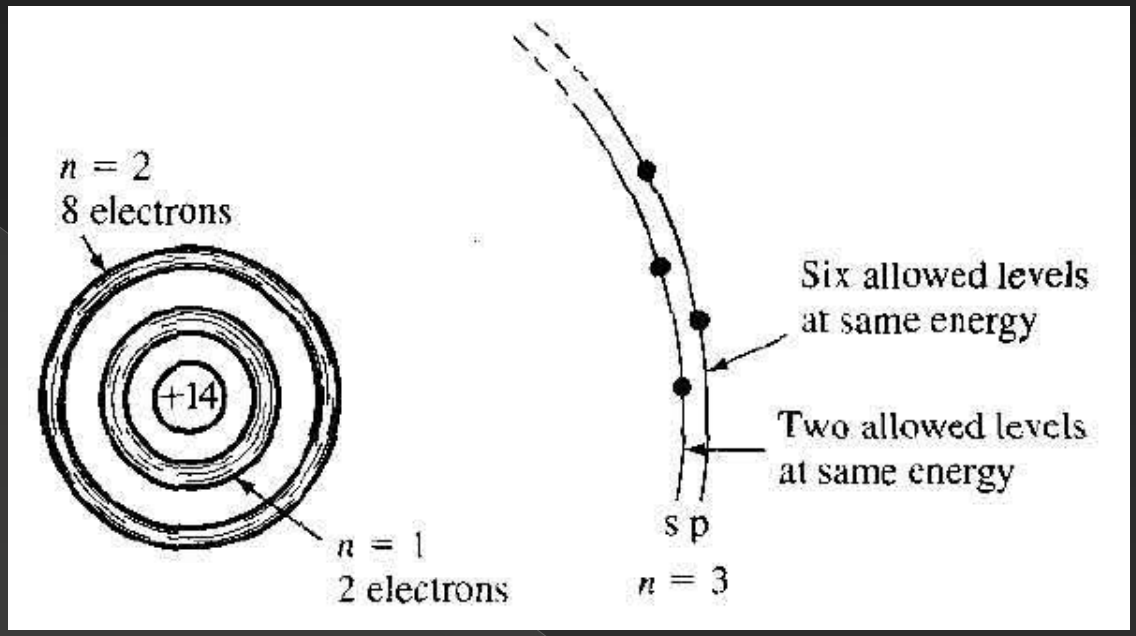

Schematic of an isolated Si atom

- Consider a regular periodic arrangement of atoms in which each atom contains more than one electron (eg Si).
- Suppose the atom in this imaginary crystal contains e^- up through the n=3 energy level.
- If the atoms are initially very far apart , the e^- in adjacent atoms will not interact and will occupy the discrete energy levels.

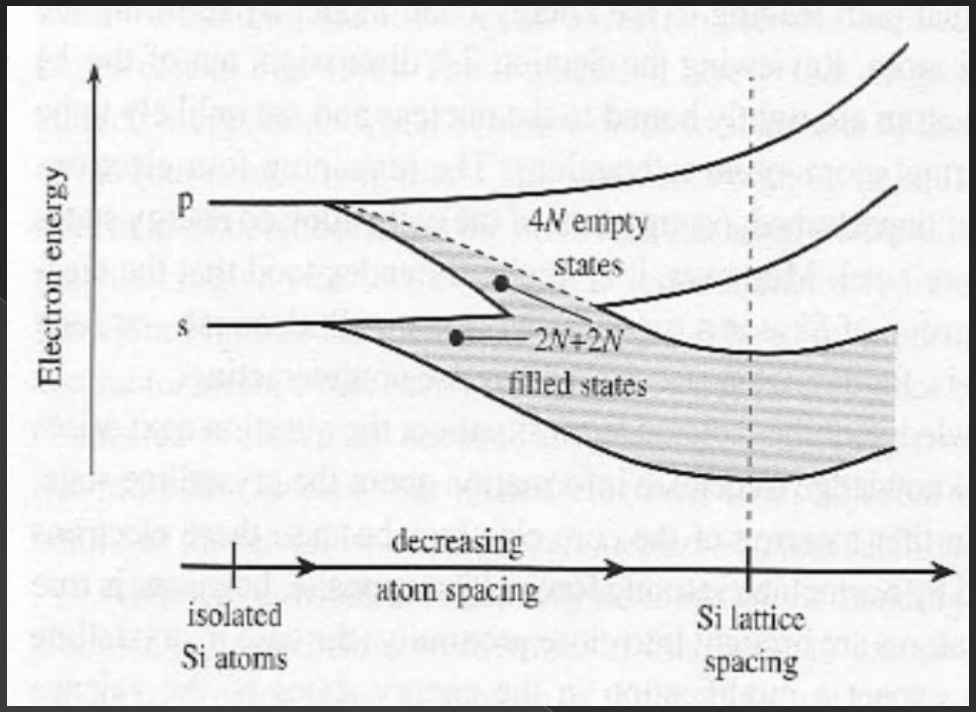

Splitting of the s and p states of Si into the allowed and forbidden energy bands

- If these atoms are brought closer together, somehow (quantum mechanics), their quantized energy levels split and turn into many states grouped in "energy bands" (see diagrams)
- Conduction only happens if electrons have empty "states" available at nearby energy

- Considering an intrinsic semiconductor we have:

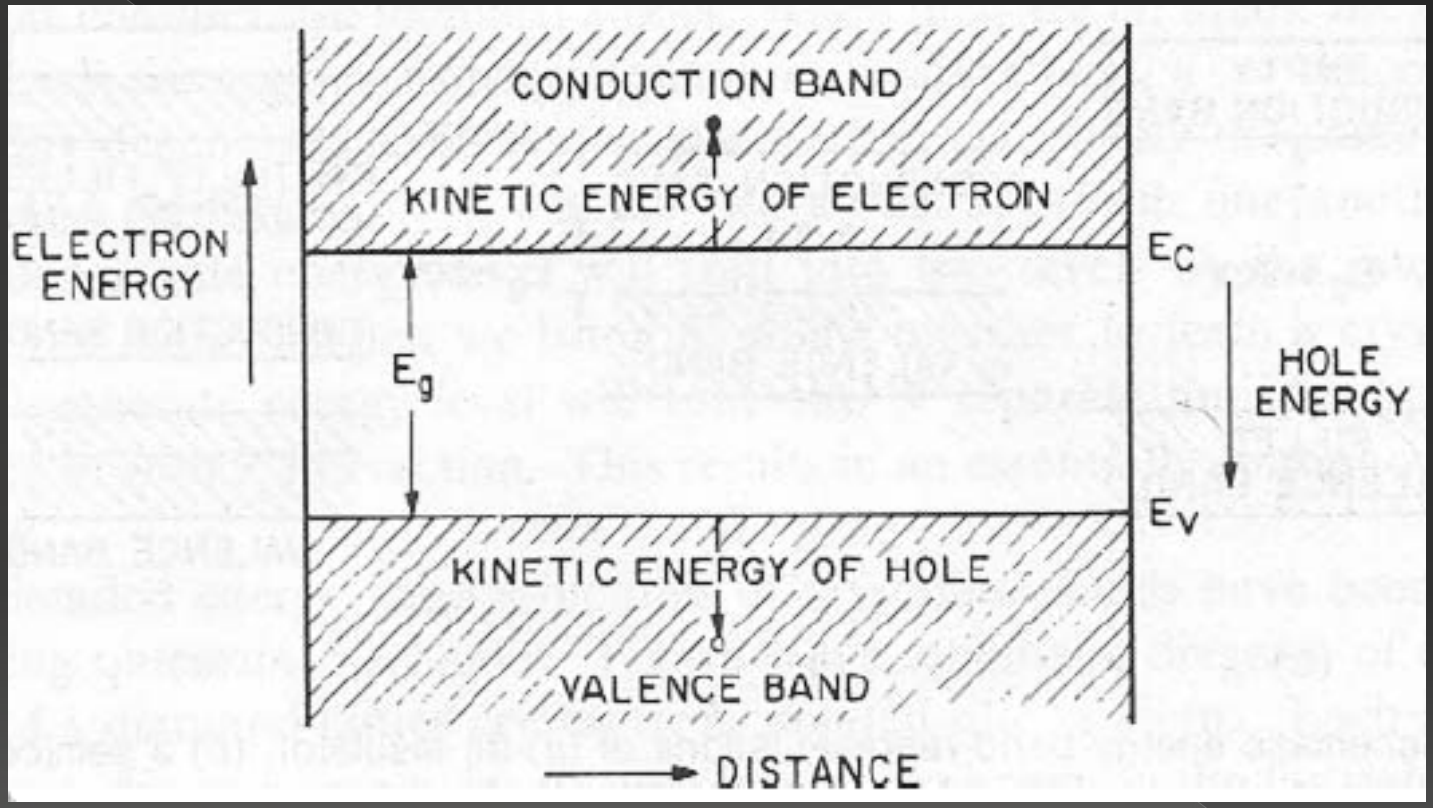

- When an e^- springs from VB to CB, it leaves a hole in VB

- According to Quasi – Chemical approach it's possible to represent this process as:

$$\emptyset \longrightarrow e^{|} + h^{\bullet}$$

$$\Rightarrow \qquad \left[e^{|}\right]\left[h^{\bullet}\right] = e^{-\frac{E_{GAP}}{RT}}$$

$$\left[e^{|}\right] = \frac{n}{N_C} \qquad \left[h^{\bullet}\right] = \frac{p}{N_V}$$

where:

$$n = \frac{\#e^{-}}{CC}$$

$$p = \frac{\#holes}{CC}$$

$$N_C = \#available \;\; states \;\; (= electron \; E \; levels) \; in \; CB$$

$$N_V = \#available \;\; states \;\; (= electron \; E \; levels) \; in \; VB$$

$$\Rightarrow \qquad \frac{n}{N_C}\frac{p}{N_V} = e^{-\frac{E_{GAP}}{RT}}$$

- We have that

$$N_C \cong N_V \cong 2.5 \cdot 10^{19} \frac{\#}{CC}$$

- This is a number little lower than the number of atoms in 1 CC
- So almost every atom contributes with one state

- If, as supposed, the S.C. is intrinsic, we can obtain the concentrations of charge carriers equation:

$$n = p = n_i$$

$$\Rightarrow \quad np = n_i^{\,2} = N_C N_V e^{-\frac{E_{GAP}}{RT}}$$

$$\Rightarrow \quad \boxed{n_i = \sqrt{N_C N_V}\, e^{-\frac{E_{GAP}}{2RT}}}$$

- Some E_{GAP} values for ceramics:

Ceramic	Energy gap [eV]
Al_2O_3	7
Si	1.1
Single crystal ZnO	3.2
Cd doped ZnO	~3.0
Mg doped ZnO	~4.0
Single crystal TiO_2	3.23

(Ceramics Science and Technology: Properties; Volume 2; Ralf Riedel, I-Wei Chen)

- ***Pay attention!!*** There are direct and indirect S.C.s, which means they may have respectively a direct or indirect transition…

Direct transition

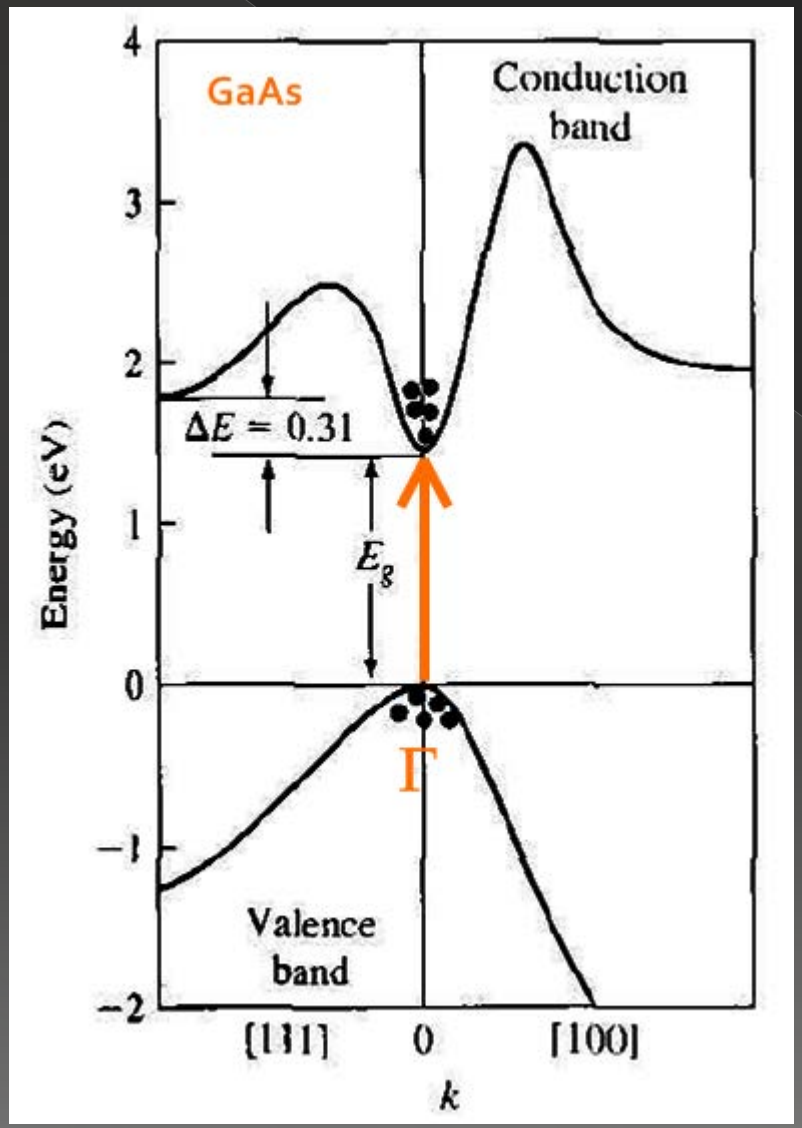

Indirect transition

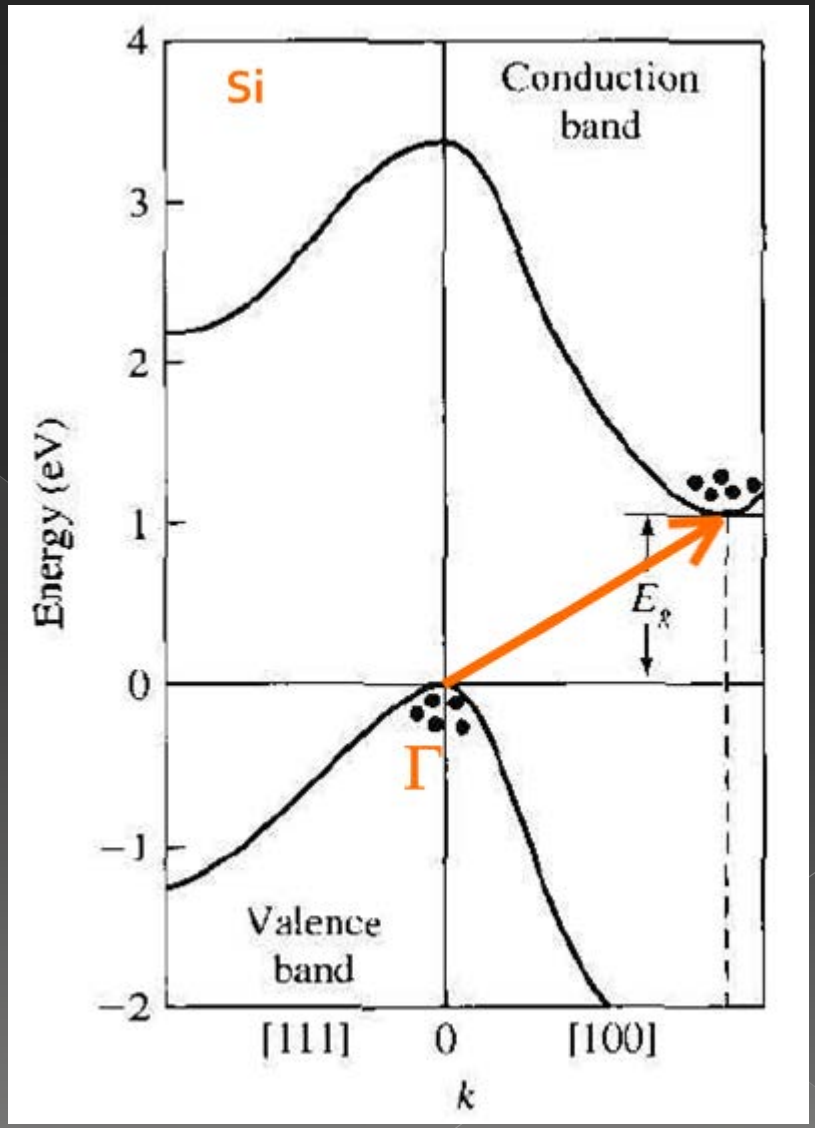

- Why did we evaluate ΔH (instead of ΔG)?
- Usually $\Delta G°$ is due mostly to system's free energy, as:

$$\Delta G = \Delta H - \Delta(TS)$$

Usually ≅ 1-2% of ΔG in solid dissolutions (ppm)

$$\Delta H = \Delta U + \Delta(PV)$$

negligible in SOLIDS

$$\Rightarrow \Delta G \cong \Delta H \cong \Delta U$$

$$0 < \left[Ti_{Mg}^{\bullet\bullet} \right] < 1$$

qualitatively:

$$n_O = n_{Mg} = n_{MgO} = N_A \frac{\rho_{MgO}}{MW_{MgO}} =$$

$$= \frac{6.023 \cdot 10^{23} \frac{molecules}{\cancel{mol}} \cdot 3.58 \frac{\cancel{g}}{cm^3}}{40.03 \frac{\cancel{g}}{\cancel{mol}}} \cong 4 \cdot 10^{22} \, {}^{\#}/_{cm^3}$$

If it is:

$$n_{Ti_{Mg}^{\bullet\bullet}} \cong 4 \cdot 10^{16} \, {}^{\#}/_{cm^3}$$

$$\Rightarrow \left[Ti_{Mg}^{\bullet\bullet} \right] \cong 10^{-6}$$

$$U_U^{\times} \xrightarrow{UO_2} U_i^{\bullet\bullet\bullet\bullet} + V_U^{''''}$$

$[U_U]$ is <u>SUBSTANTIALLY 1</u>:

- Given a generic compound $M_A X_B$,
- With, e.g. 10^9 atoms of M:

$$[V_M] = 10^{-9} = \frac{1\,\#V}{10^9\,\#M}$$

$$[M_M] = \frac{\#M_{left}/CC}{\#M_{in}/CC} = \frac{\#M_{left}}{\#M_{in}} = \frac{\#M_{in} - \#V}{\#M_{in}} = \frac{10^9 - 1}{10^9} \longrightarrow 1$$

Non-stoichiometry in Kroger Vink Notation

- $Cd_{1-x}O$ is non-stoichiometric (and this is due to the fact that more than one oxidation state is available for Cd)

- $\emptyset \rightarrow e^{/} + h^{\cdot}$ $\qquad [e^{/}][h^{\cdot}] = K_e \qquad K_e = e^{-E_g/RT}$

- $\emptyset \longrightarrow V_O^{\cdot\cdot} + V_{Cd}^{//}$ $\qquad [V_O^{\cdot\cdot}]\left[V_{Cd}^{//}\right] = K_S \qquad K_e = e^{-E_S/RT}$

- $O_O^x \longrightarrow \frac{1}{2}O_{2(g)} + V_O^{\cdot\cdot} + 2e^{/}$ $\qquad [V_O^{\cdot\cdot}]\left[e^{/}\right]P_{O_2}^{1/2} = K_P \qquad K_e = e^{-E_P/RT}$

- $\left[e^{/}\right]N_C + 2\left[V_{Cd}^{//}\right]N_A\frac{\rho}{PM} = [h^{\cdot}]\,N_V + 2\,[V_O^{\cdot\cdot}]N_A\frac{\rho}{PM}$

- N_c density of states in the conduction band
- N_v density of states in the valency band
- N_A Avogadro's number
- ρ Density of CdO
- PM molecular weight of CdO

Kroeger-Vink diagram for metal oxide semiconductor MO

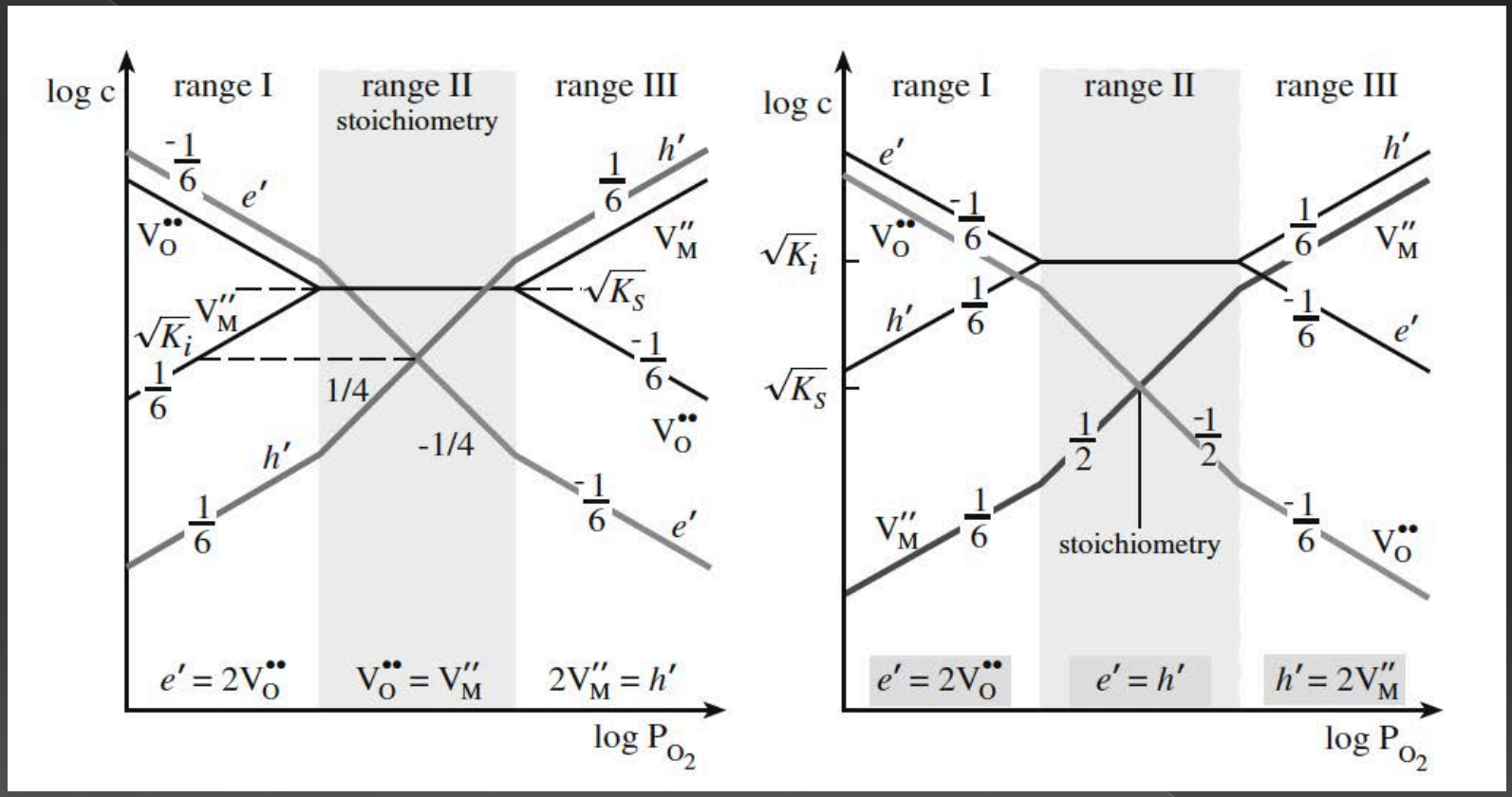

Schottki defects dominate

Electronic defects dominate

Famous case of non-stoichiometric compounds: ceramic superconductors

- $YBa_2Cu_3O_{7-x}$

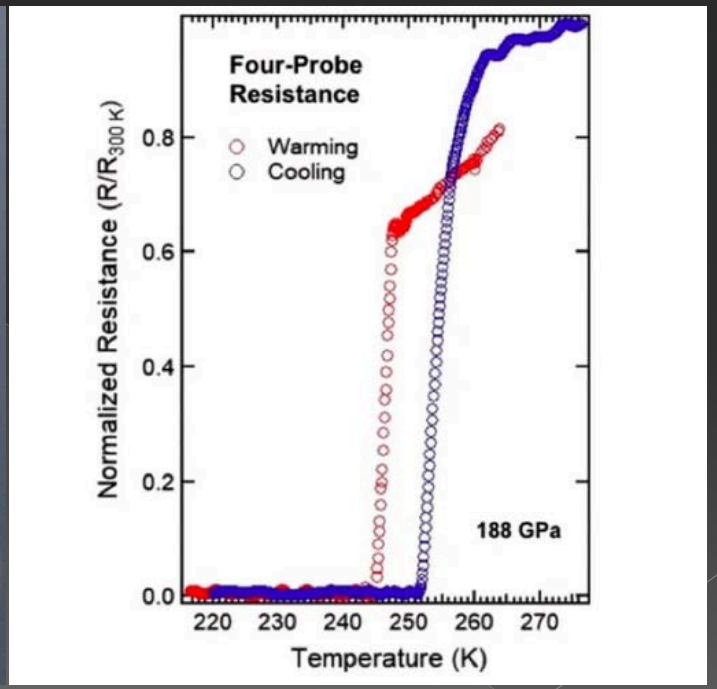

Properties of Ceramics

Melting temperatures

Al_2O_3	2054 ± 6
BaO	2013
BeO	2780 ± 100
Bi_2O_3	825
CaO	2927 ± 50
Cr_2O_3	2330 ± 15
Eu_2O_3	2175 ± 25
Fe_2O_3	Decomposes at 1735 K to Fe_3O_4 and oxygen
Fe_3O_4	1597 ± 2
Li_2O	1570
Li_2ZrO_3	1610
Ln_2O_3	2325 ± 25
MgO	2852
Mullite	1850
Na_2O (α)	1132
Nb_2O_5	1512 ± 30
Sc_2O_3	2375 ± 25
SrO	2665 ± 20
Ta_2O_5	1875 ± 25
ThO_2	3275 ± 25
TiO_2 (rutile)	1857 ± 20
UO_2	2825 ± 25
V_2O_5	2067 ± 20
Y_2O_3	2403
ZnO	1975 ± 25
ZrO_2	2677

B_4C	2470 ± 20
HfB_2	2900
HfC	3900
HfN	3390
HfSi	2100
$MoSi_2$	2030
NbC	3615
NbN	2204
SiC	2837
Si_3N_4	At 2151 K partial pressure of N_2 over Si_3N_4 reaches 1 atm
TaB_2	3150
TaC	3985
$TaSi_2$	2400
ThC	2625

TABLE 34.3 Predominantly Covalent Ceramics with Very High Melting Temperatures

Ceramic	T_m (°C)	*Covalent character of bond (%)*
HfC	3890	70
TiC	3100	78
WC	2775	85
B_4C	2425	94
SiC	2300	88
C (diamond)	3727	100

TABLE 34.4 Melting Temperatures of Alkaline Earth Metal Oxides

Oxide	T_m (°C)	*Covalent character (%)*	ϕ (nm^{-1}) = Z/r
BeO	2780	37	57
MgO	2852	27	28
CaO	2927	21	20
SrO	2665	21	17
BaO	2017	18	15

Heat capacity

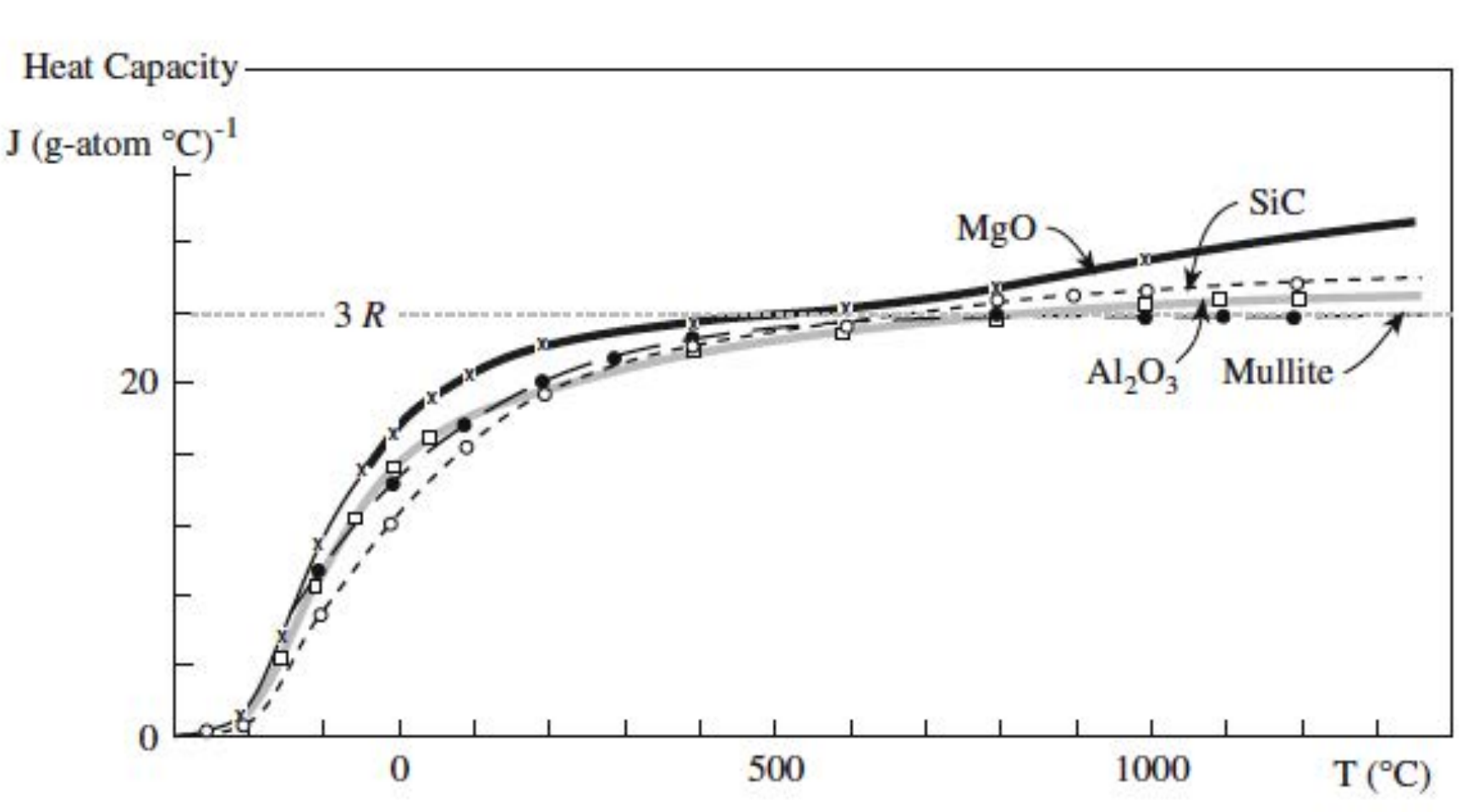

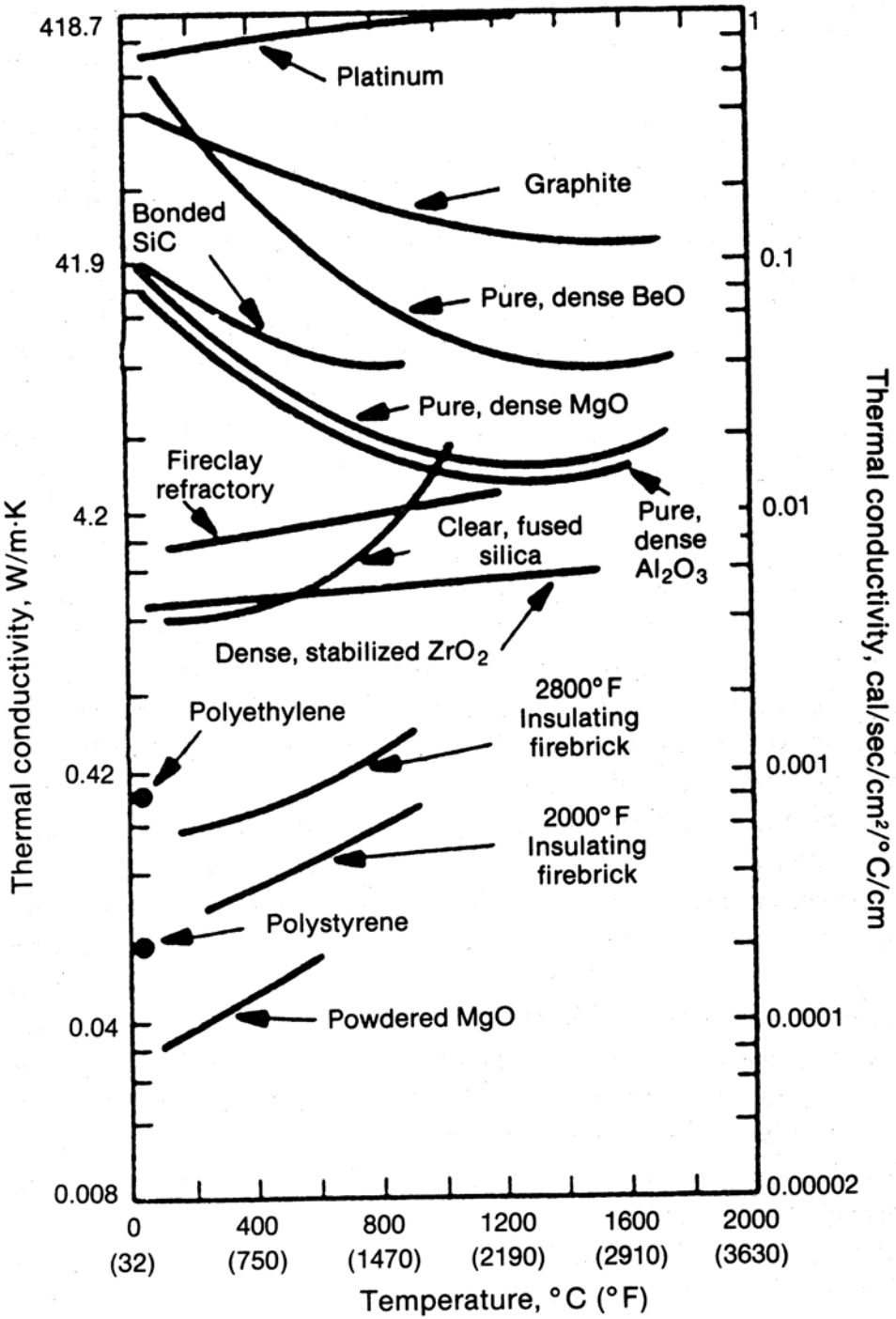
418.7
41.9
4.2
0.42
0.04
0.008
1
0.1
0.01
0.001
0.0001
0.00002
Thermal conductivity, W/m·K
Thermal conductivity, cal/sec/cm²/°C/cm
Platinum
Graphite
Bonded SiC
Pure, dense BeO
Pure, dense MgO
Fireclay refractory
Clear, fused silica
Pure, dense Al_2O_3
Dense, stabilized ZrO_2
Polyethylene
2800° F Insulating firebrick
2000° F Insulating firebrick
Polystyrene
Powdered MgO
0 (32)
400 (750)
800 (1470)
1200 (2190)
1600 (2910)
2000 (3630)
Temperature, °C (°F)

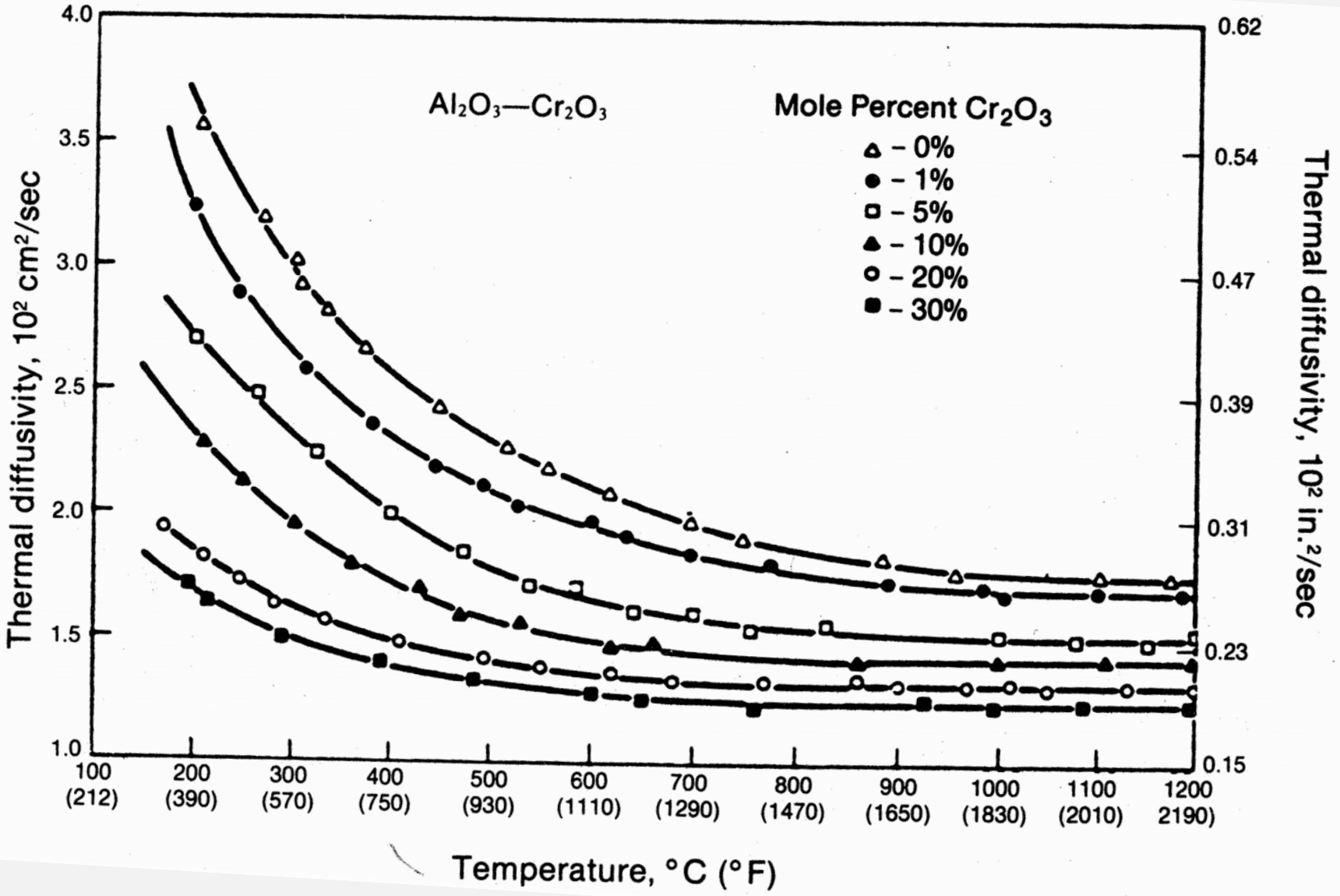
Al_2O_3—Cr_2O_3
Mole Percent Cr_2O_3
△ – 0%
● – 1%
□ – 5%
▲ – 10%
○ – 20%
■ – 30%
Thermal diffusivity, 10^2 cm^2/sec
Thermal diffusivity, 10^2 $in.^2$/sec
4.0
3.5
3.0
2.5
2.0
1.5
1.0
0.62
0.54
0.47
0.39
0.31
0.23
0.15
100 (212)
200 (390)
300 (570)
400 (750)
500 (930)
600 (1110)
700 (1290)
800 (1470)
900 (1650)
1000 (1830)
1100 (2010)
1200 2190)
Temperature, °C (°F)

Thermal expansion

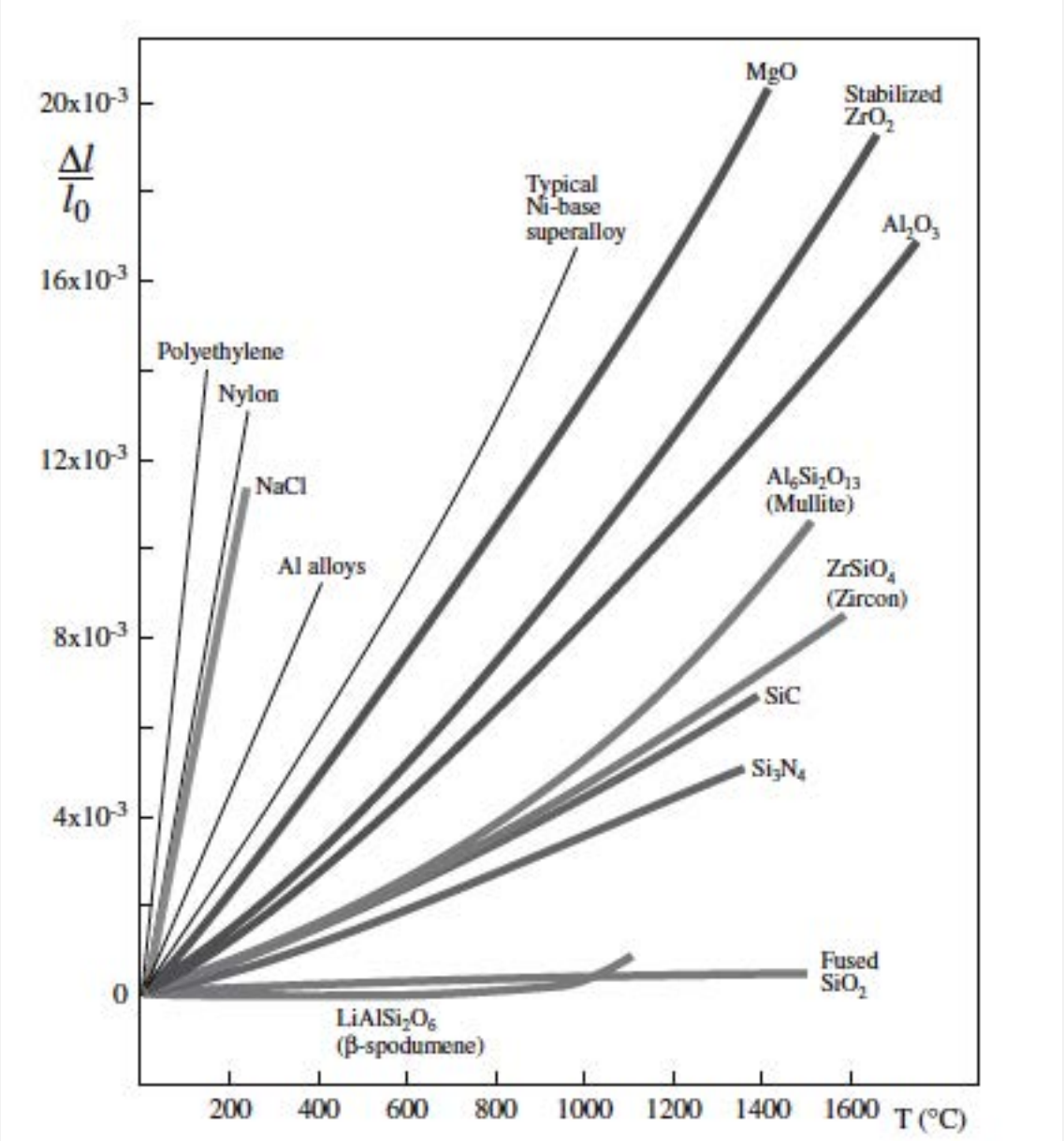

Thermal expansion

TABLE 34.9 Mean Thermal Expansion Coefficients of Various Ceramics

Ceramic	α *(ppm/°C)*	*Ceramic*	α *(ppm/°C)*
	Binary oxides		
α-Al_2O_3	7.2–8.8	ThO_2	9.2
BaO	17.8	TiO_2	8.5
BeO	8.5–9.0 (25–1000)	UO_2	10.0
Bi_2O_3 (α)	14.0 (RT–730°C)	WO_2	9.3 (25–1000)
Bi_2O_3 (δ)	24.0 (650–825°C)	Y_2O_3	8.0 (*c* axis)
Dy_2O_3	8.5	ZnO	4.0 (*a* axis)
Gd_2O_3	10.5	ZrO_2 (monoclinic)	7.0
HfO_2	9.4–12.5	ZrO_2 (tetragonal)	12.0
MgO	13.5		

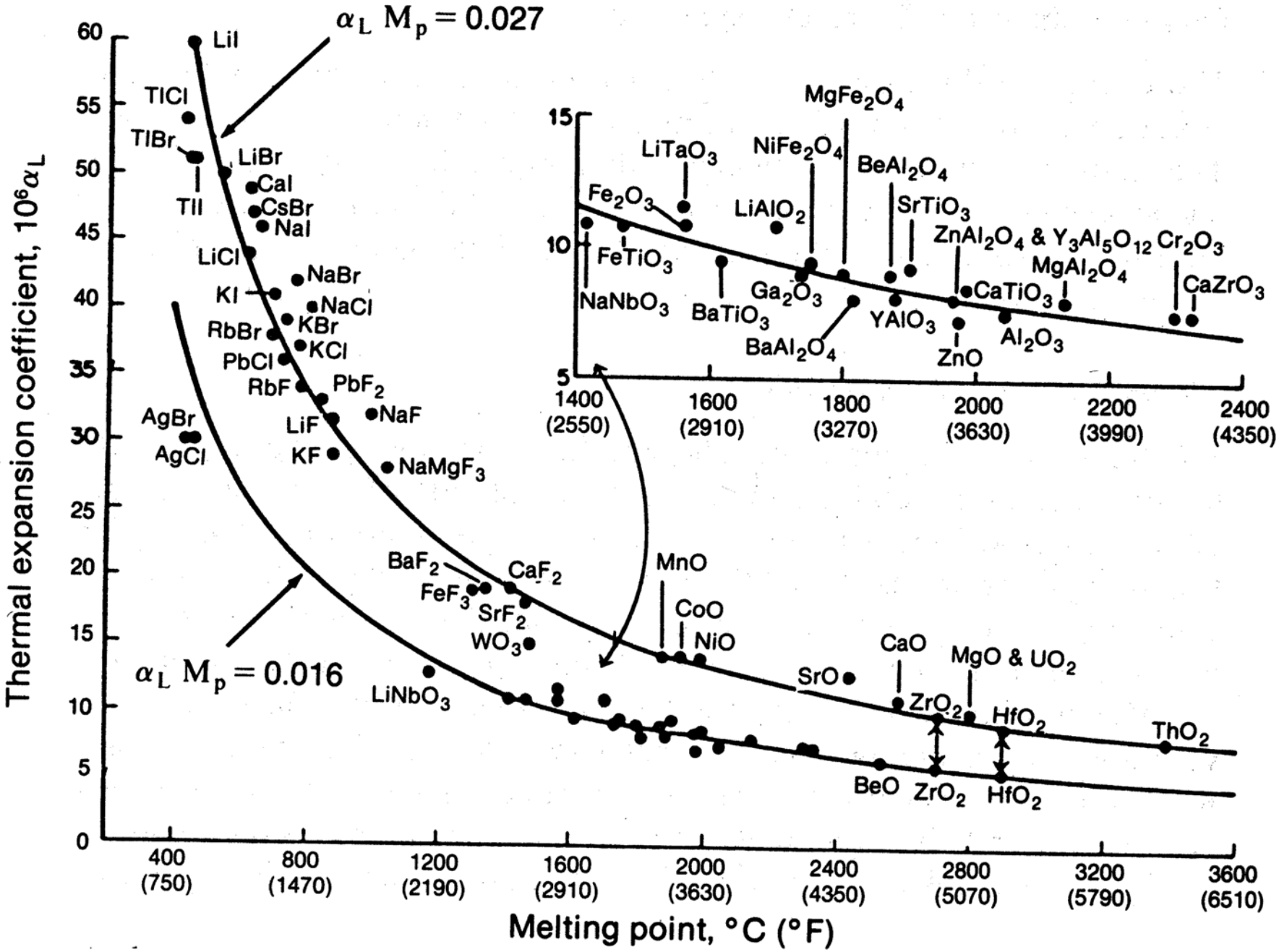
α_L $M_p = 0.027$
α_L $M_p = 0.016$
Thermal expansion coefficient, $10^6\alpha_L$
Melting point, °C (°F)
LiI
TlCl
TlBr
LiBr
CaI
CsBr
NaI
TlI
LiCl
NaBr
KI
NaCl
KBr
RbBr
KCl
PbCl
RbF
PbF_2
NaF
AgBr
AgCl
LiF
KF
$NaMgF_3$
BaF_2
CaF_2
FeF_3
SrF_2
WO_3
$LiNbO_3$
MnO
CoO
NiO
SrO
CaO
MgO & UO_2
ZrO_2
HfO_2
ThO_2
BeO
ZrO_2
HfO_2
$MgFe_2O_4$
$LiTaO_3$
$NiFe_2O_4$
$BeAl_2O_4$
Fe_2O_3
$LiAlO_2$
$SrTiO_3$
$ZnAl_2O_4$ & $Y_3Al_5O_{12}$
Cr_2O_3
$MgAl_2O_4$
$FeTiO_3$
$CaZrO_3$
$NaNbO_3$
$BaTiO_3$
Ga_2O_3
$CaTiO_3$
$YAlO_3$
$BaAl_2O_4$
Al_2O_3
ZnO
60
55
50
45
40
35
30
25
20
15
10
5
0
15
10
5
400 (750)
800 (1470)
1200 (2190)
1600 (2910)
2000 (3630)
2400 (4350)
2800 (5070)
3200 (5790)
3600 (6510)
1400 (2550)
1600 (2910)
1800 (3270)
2000 (3630)
2200 (3990)
2400 (4350)

Asby map Young modulus/density

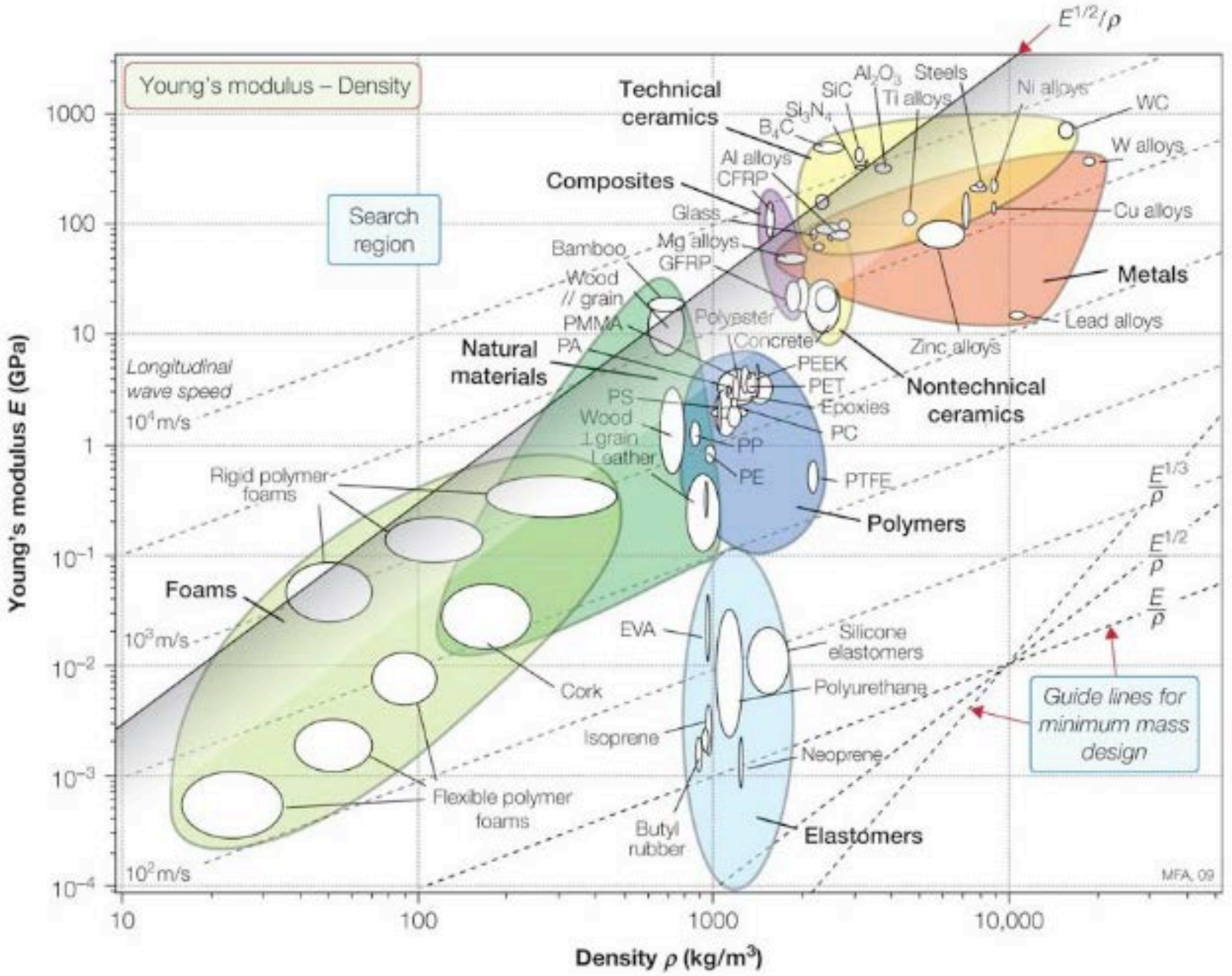

TABLE 16.2 Elastic Constants of Selected Polycrystalline Ceramics (20°C)

Material	*Crystal type*	*μ (GPa)*	B *(GPa)*	*ν*	*E (GPa)*
Carbides					
C	Cubic	468	416	0.092	1022
SiC	Cubic	170	210	0.181	402
TaC	Cubic	118	217	0.270	300
TiC	Cubic	182	242	0.199	437
ZrC	Cubic	170	223	0.196	407
Oxides					
Al_2O_3	Trigonal	163	251	0.233	402
$Al_2O_3 \cdot MgO$	Cubic	107	195	0.268	271
$BaO \cdot TiO_2$	Tetragonal	67	177	0.332	178
BeO	Tetragonal	165	224	0.204	397
CoO	Cubic	70	185	0.332	186
$FeO \cdot Fe_2O_3$	Cubic	91	162	0.263	230
Fe_2O_3	Trigonal	93	98	0.140	212
MgO	Cubic	128	154	0.175	300
$2MgO \cdot SiO_2$	Orthorhombic	81	128	0.239	201
MnO	Cubic	66	154	0.313	173
SrO	Cubic	59	82	0.210	143
$SrO \cdot TiO_2$	Cubic	266	183	0.010	538
TiO_2	Tetragonal	113	206	0.268	287
UO_2	Cubic	87	212	0.319	230
ZnO	Hexagonal	45	143	0.358	122
$ZrO_2–12Y_2O_3$	Cubic	89	204	0.310	233
SiO_2	Trigonal	44	38	0.082	95

Relations among elastic constants

- E , Young modulus
- ν , Poisson modulus
- G, Rigidity (shear) modulus
- B, bulk modulus

- $E = 2G(1 + \nu)$ $\quad$ $E=3K(1-2\nu)$

- $E=9KG/(3K-G)$ $\quad$ $\nu=(3K-2G)/(6K+2G)$

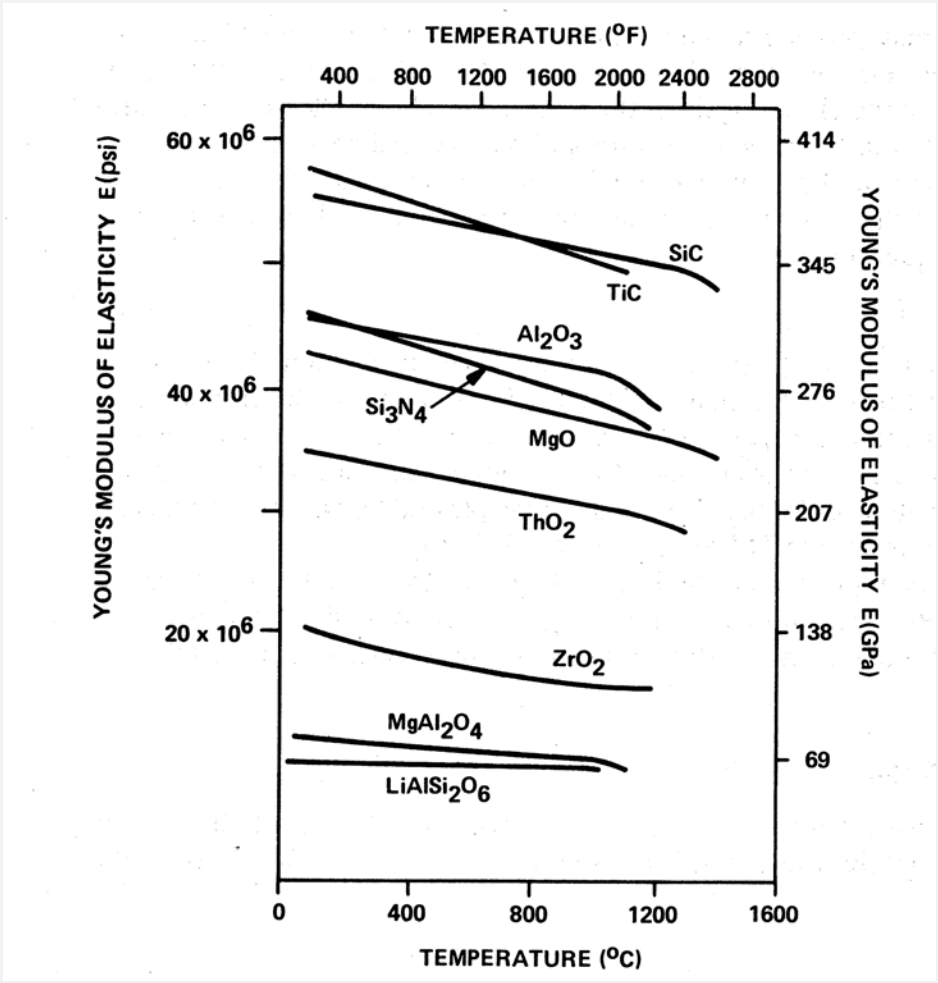
TEMPERATURE (°F)
400
800
1200
1600
2000
2400
2800
YOUNG'S MODULUS OF ELASTICITY E(psi)
60 x 10^6
40 x 10^6
20 x 10^6
YOUNG'S MODULUS OF ELASTICITY E(GPa)
414
345
276
207
138
69
SiC
TiC
Al2O3
Si3N4
MgO
ThO2
ZrO2
MgAl2O4
LiAlSi2O6
0
400
800
1200
1600
TEMPERATURE (°C)

Commonly Used Mechanical Testing Techniques

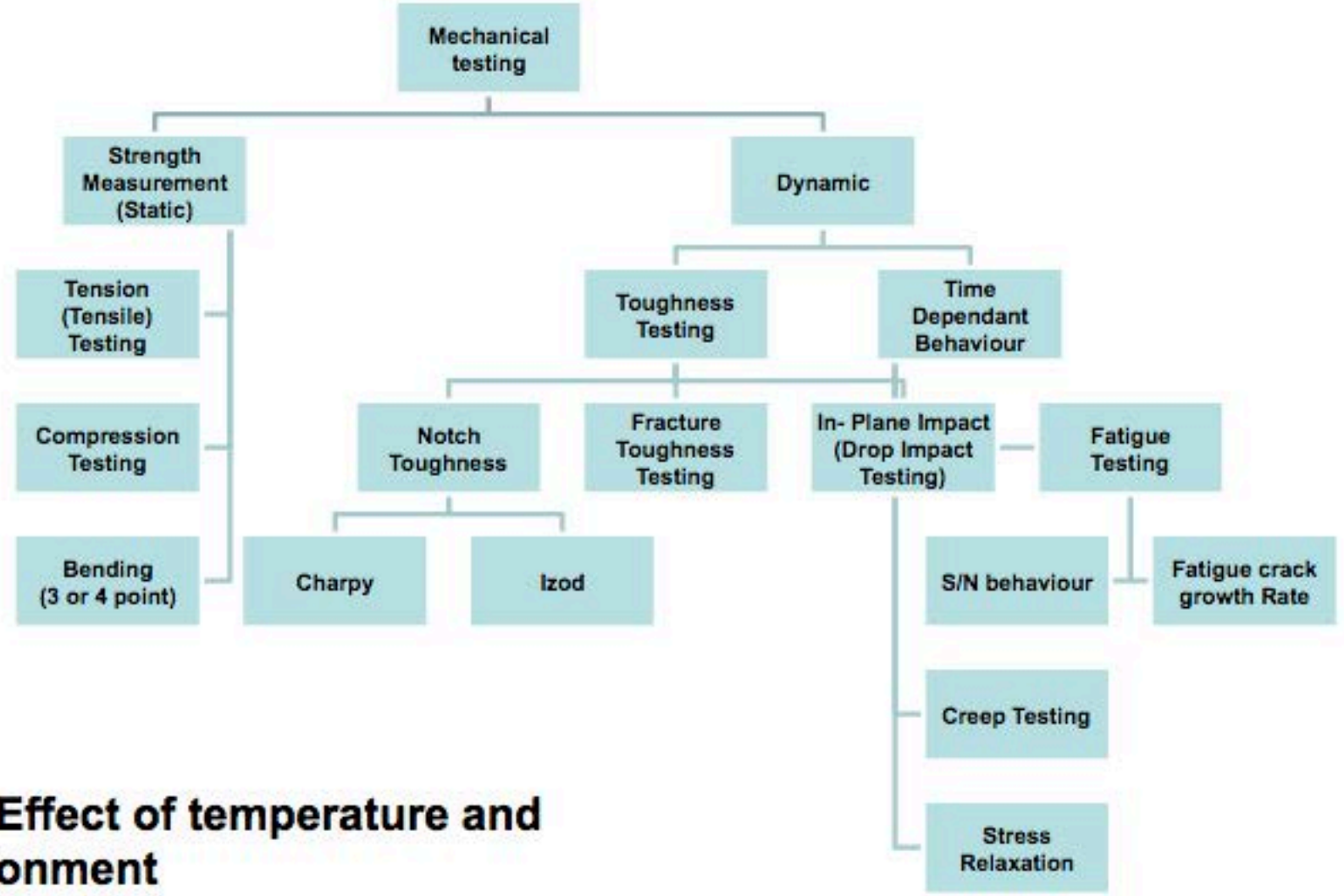

Plus Effect of temperature and environment

Strength

Tensile tests with and without luders behaviour
https://www.youtube.com/watch?v=D8U4G5kcpcM

Ashby map strength/density

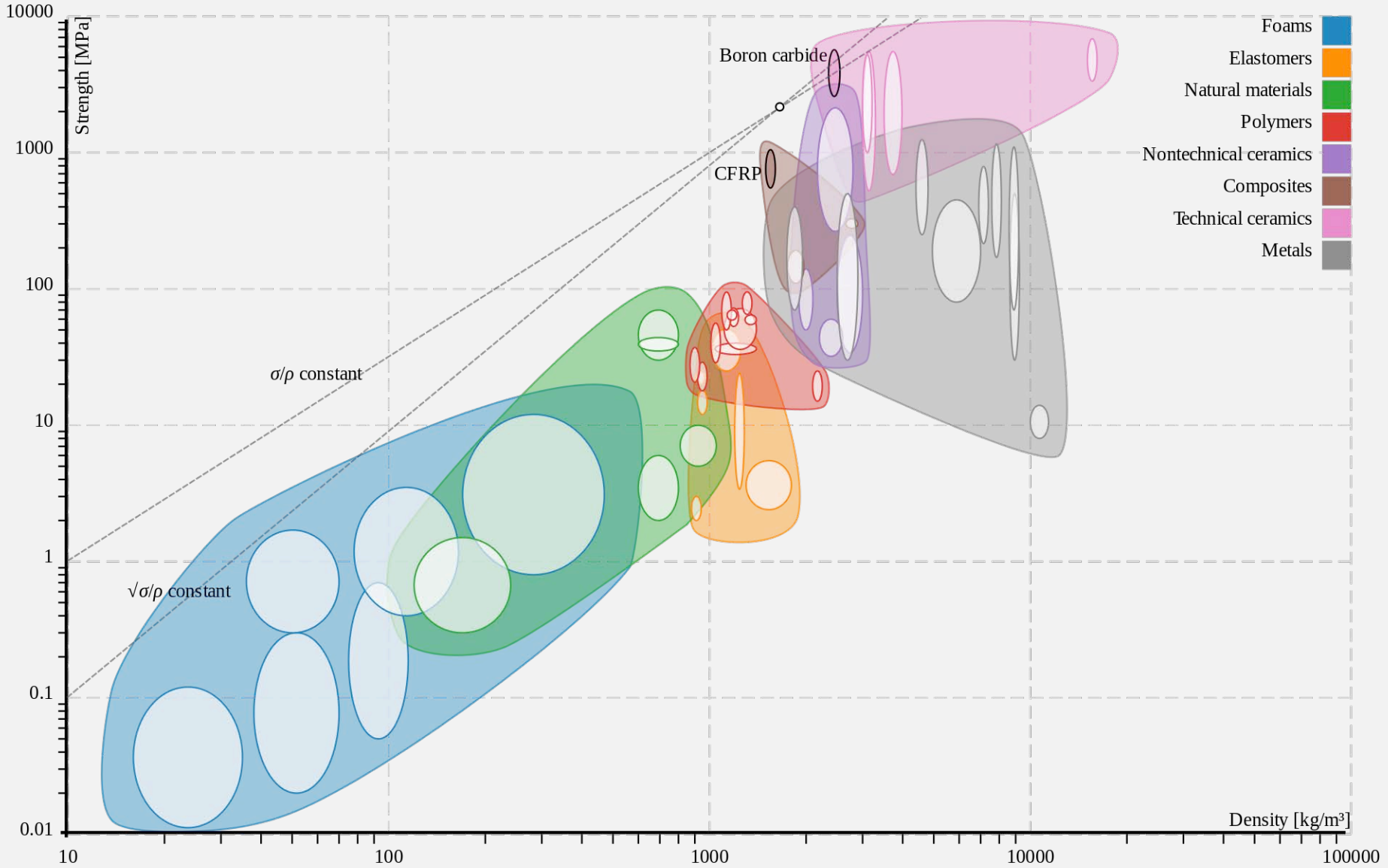

Ashby map strength/density

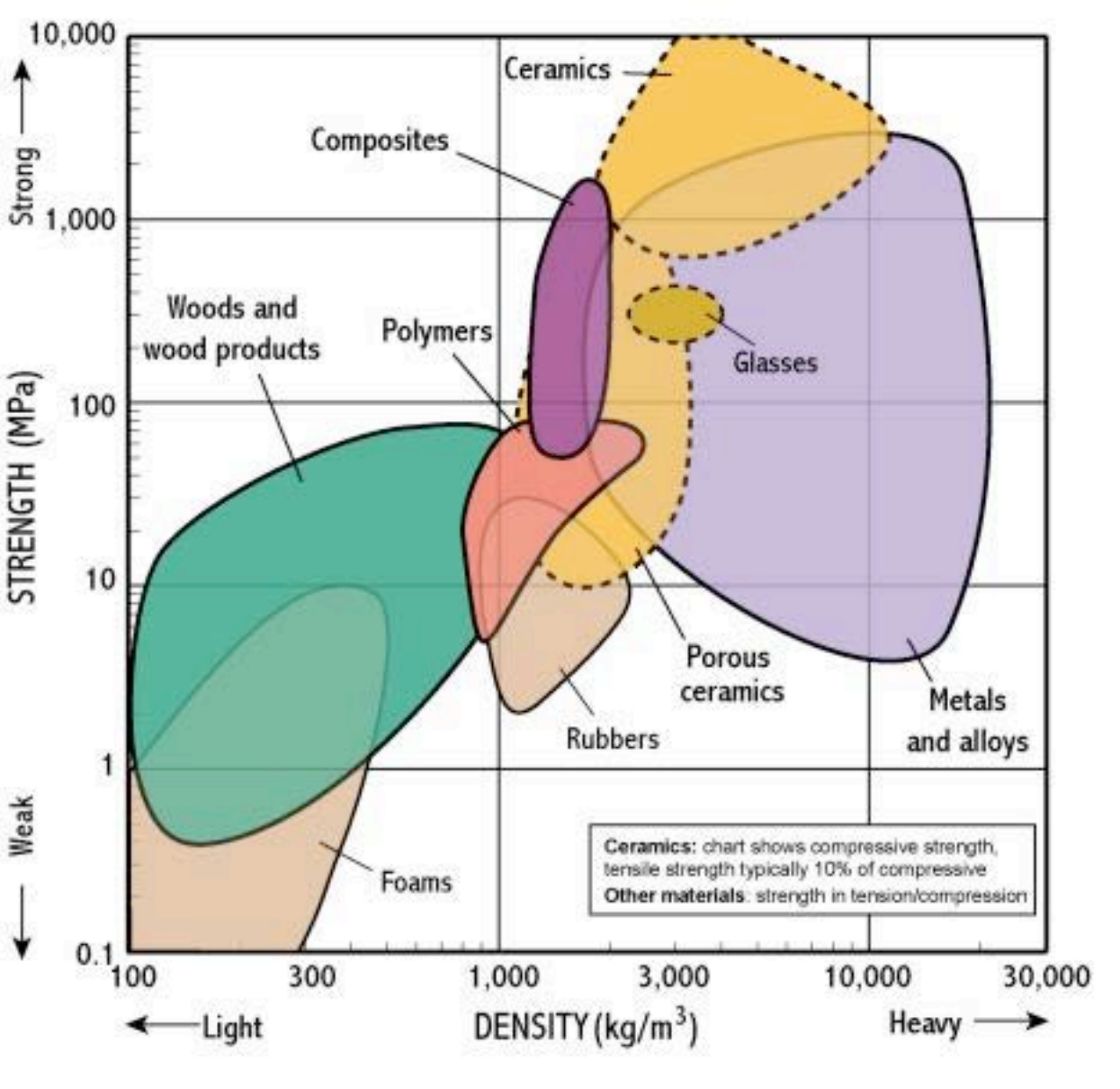

Table 5.3 Comparison of Theoretical Strength and Actual Strength

Material	E [GPa (psi)]	Estimated theoretical strength [GPa (psi)]	Measured strength of fibers [GPa (psi)]	Measured strength of polycrystalline specimen [GPa (psi)]
Al_2O_3[a]	380 (55×10^6)	38 (5.5×10^6)	16 (2.3×10^6)	0.4 (60×10^3)
SiC	440 (64×10^6)	44 (6.4×10^6)	21 (3.0×10^6)	0.7 (100×10^3)

[a]From R. J. Stokes, *The Science of Ceramic Machining and Surface Finishing*, NBS Special Publication 348, U.S. Government Printing Office, Washington, D.C., 1972, p. 347.

Flaws are Stress Concentrators

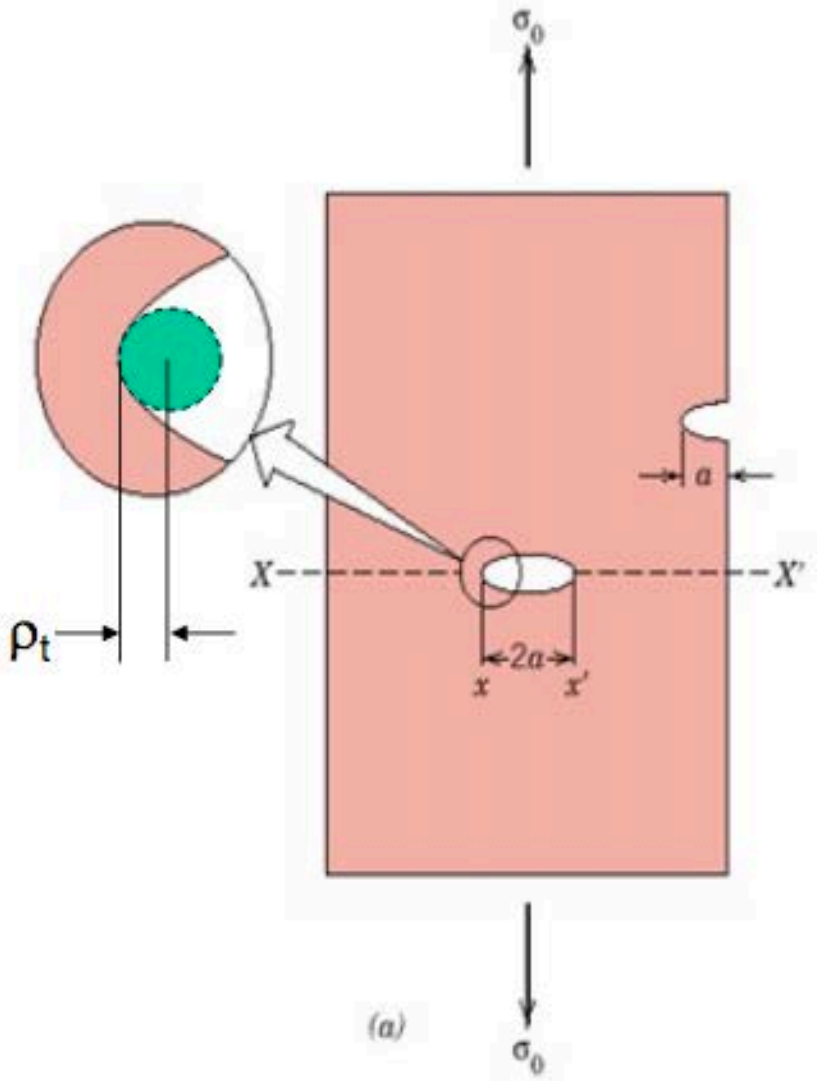

If the crack is similar to an elliptical hole through plate, and is oriented perpendicular to applied stress, the maximum stress σ_m=

$$\sigma_m = 2\sigma_o\left(\frac{a}{\rho_t}\right)^{1/2} = K_t\sigma_o$$

where

ρ_t = radius of curvature

σ_o = applied stress

σ_m = stress at crack tip

a = length of surface crack or ½ length of internal crack

$\sigma_m/\sigma_o = K_t$ the stress concentration factor

Concentration of Stress at Crack Tip

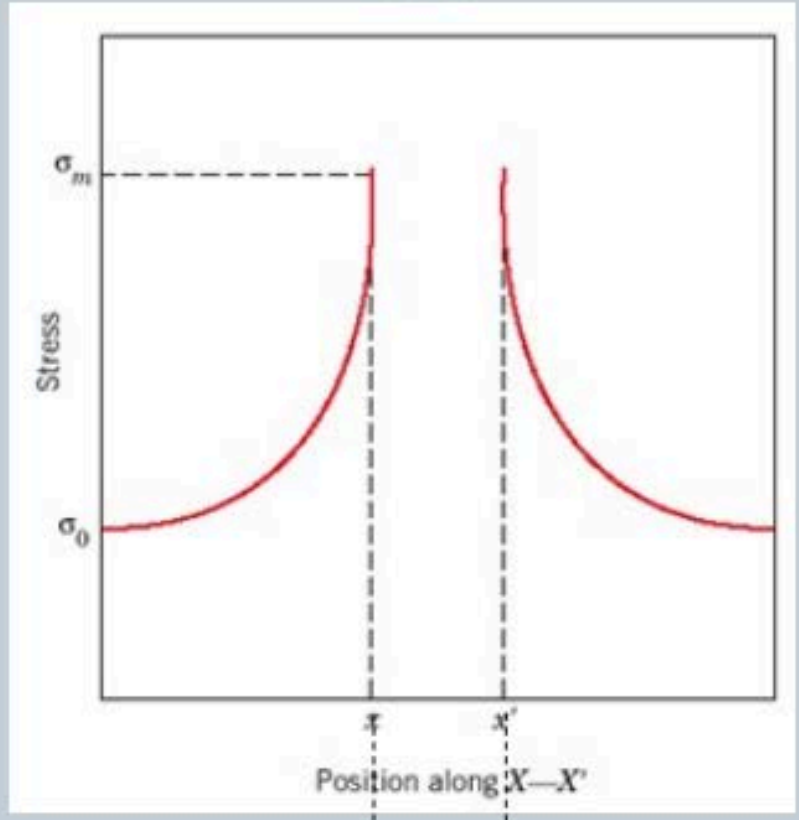

$$K = Y\sigma\sqrt{\pi\, a}$$

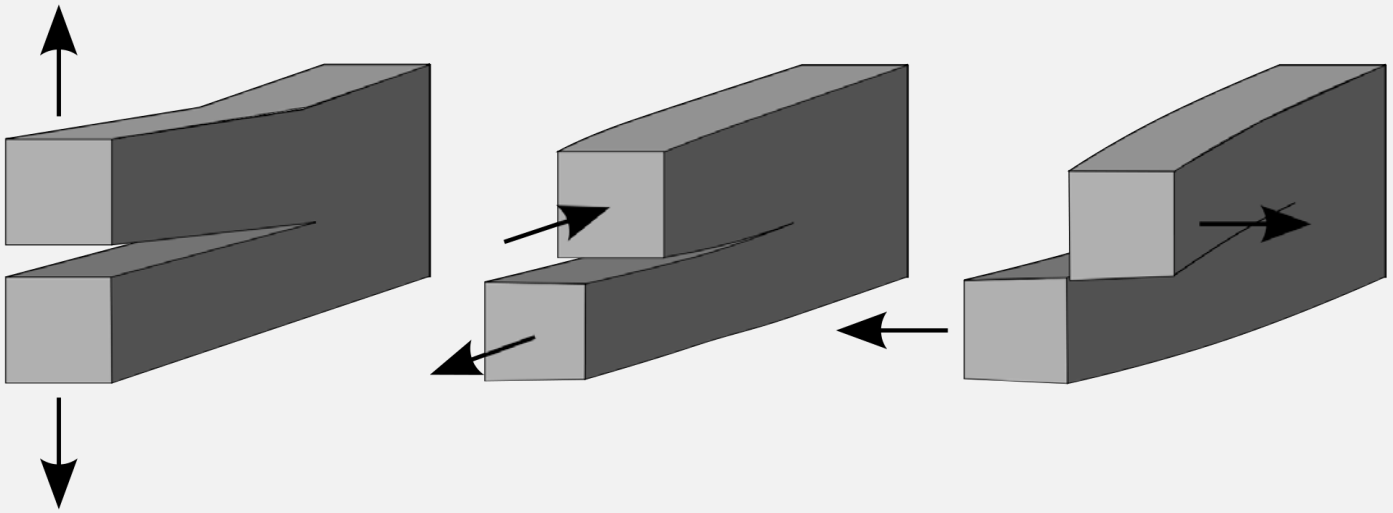

Mode I:
Opening

Mode II:
In-plane shear

Mode III:
Out-of-plane shea

$$K = Y\sigma\sqrt{\pi\, a}$$

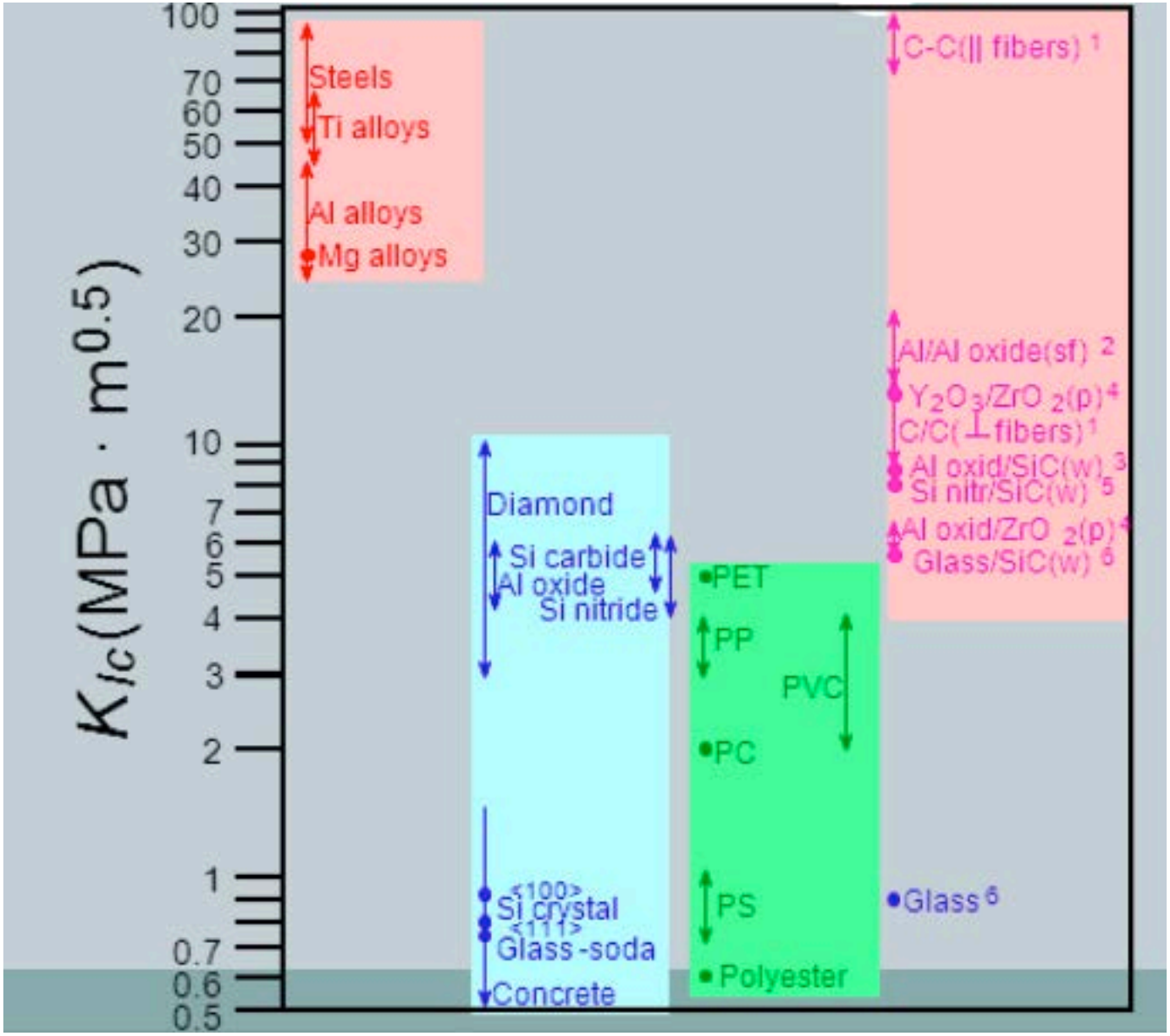

DESIGN AGAINST CRACK GROWTH

- **Crack growth condition:** $K \geq K_c$

$$K = Y\sigma\sqrt{\pi a}$$

- **Largest, most stressed cracks grow first.**

--Result 1: Max flaw size dictates design stress.

$$\sigma_{design} < \frac{K_c}{Y\sqrt{\pi a_{max}}}$$

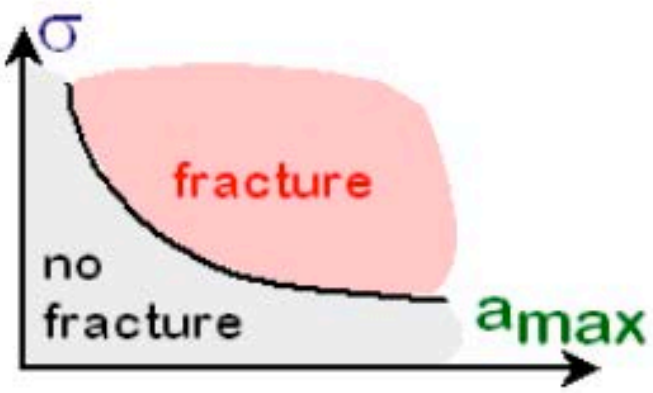

--Result 2: Design stress dictates max. flaw size.

$$a_{max} < \frac{1}{\pi}\left(\frac{K_c}{Y\sigma_{design}}\right)^2$$

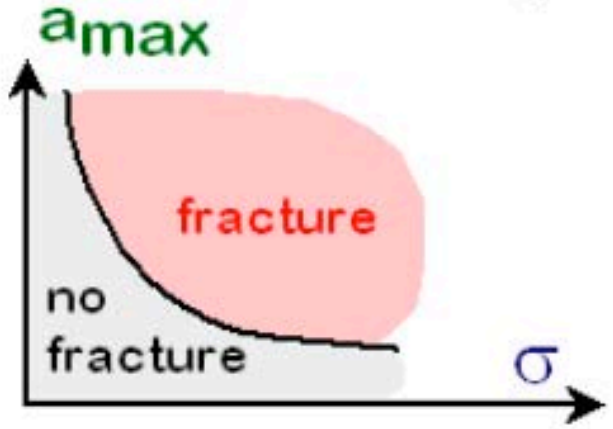

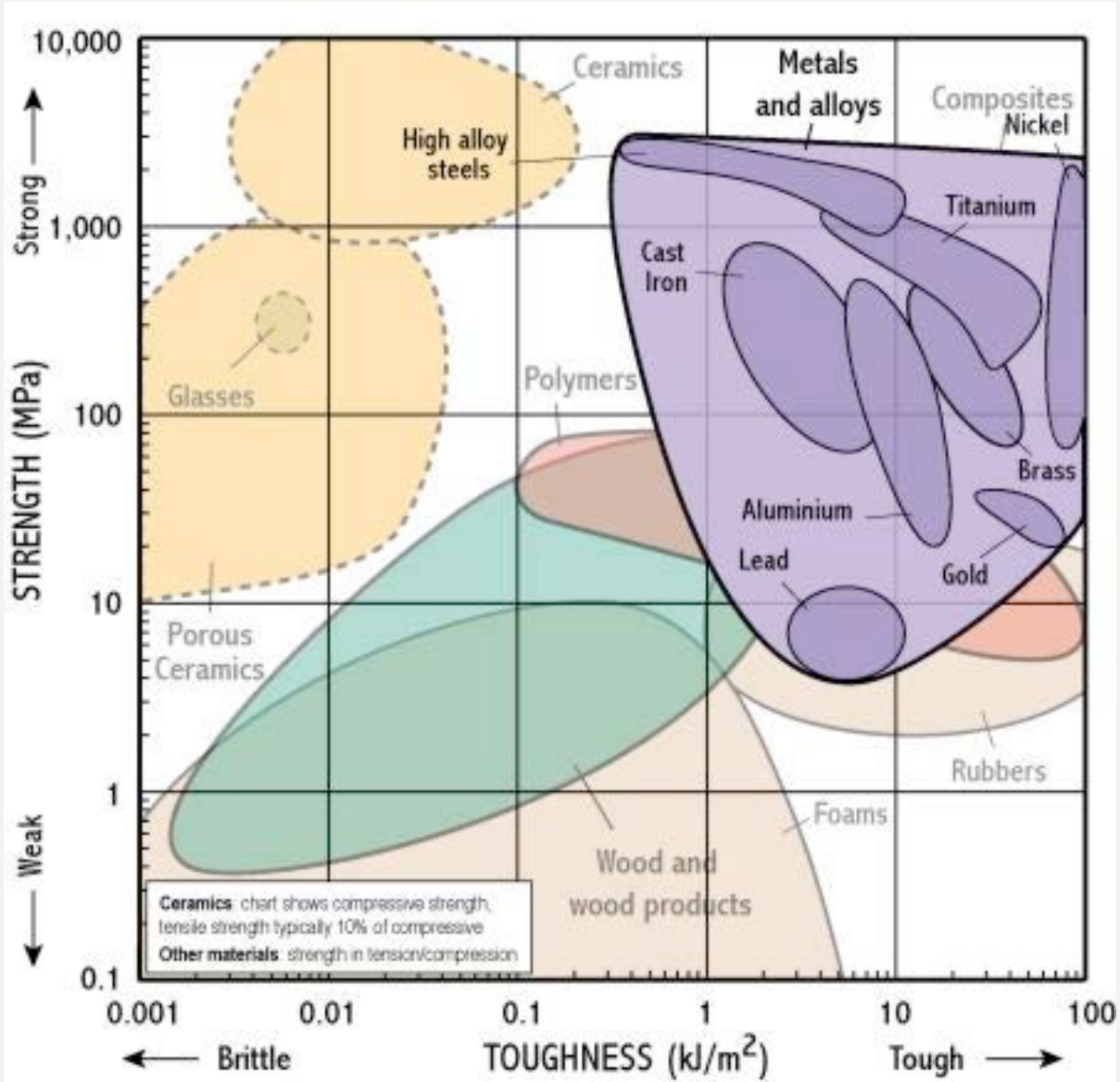
10,000
1,000
100
10
1
0.1
Strong
Weak
STRENGTH (MPa)
0.001
0.01
0.1
1
10
100
Brittle
TOUGHNESS (kJ/m²)
Tough
Ceramics
Metals and alloys
Composites
High alloy steels
Nickel
Titanium
Cast Iron
Glasses
Polymers
Brass
Aluminium
Lead
Gold
Porous Ceramics
Rubbers
Foams
Wood and wood products
Ceramics: chart shows compressive strength, tensile strength typically 10% of compressive
Other materials: strength in tension/compression

III.4 FRACTURE TOUGHNESS – STRENGTH

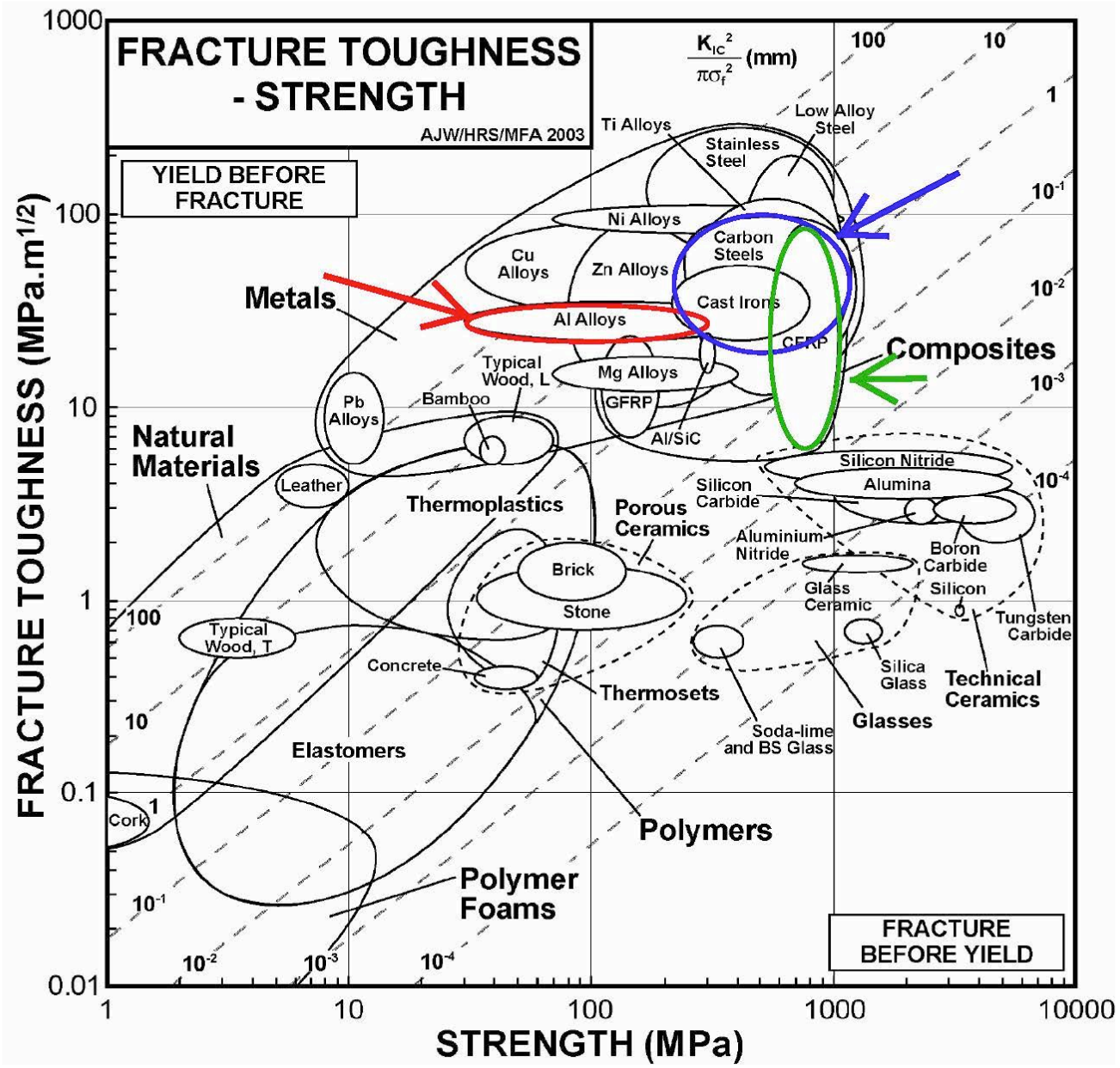

COMPARING CERAMICS AND METALS PART I					
Property	Density (g/cm2)	Elastic modulus (GPa)	Flexural strength (GPa)	Fracture toughness (MPa*m2)	Max. service temperature (°C)
Aluminum oxide (sintered)	3.9	395	300	38	1,700
Zirconium oxide (sintered)	6.1	210	1,050	7	1,500
Silicon carbide (hot press)	3.1	400	380	3	1,600
Silicon nitride (Reaction bonded and sintered)	3.2	310	600	6	1,000
Boron nitride (hot press)	2.3	675	51	2.6	1,000
Silicon carbide (including fiber composite0	2.5	270	360	39	1,600
Advanced high-strength steel (QuesTek C61)	7.9	200	1,650	140	430

Accurate determinations of K_{IC}

(a) SINGLE-EDGE NOTCHED BEAM (SENB) SPECIMEN

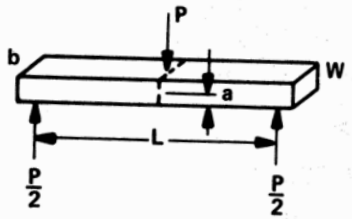

$$K_I = Y \frac{3PL}{2bW^2} \sqrt{a}$$

$$Y = 1{\cdot}96 - 2{\cdot}75\left(\frac{a}{W}\right) + 13{\cdot}66\left(\frac{a}{W}\right)^2$$
$$-23{\cdot}98\left(\frac{a}{W}\right)^3 + 25{\cdot}22\left(\frac{a}{W}\right)^4$$

(b) DOUBLE TORSION (DT) SPECIMEN

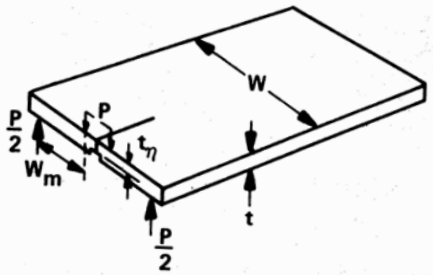

$$K_I = PW_m \left[\frac{3(1+\nu)}{Wt^3 t_\eta}\right]^{1/2}$$

(c) CONSTANT-MOMENT SPECIMEN

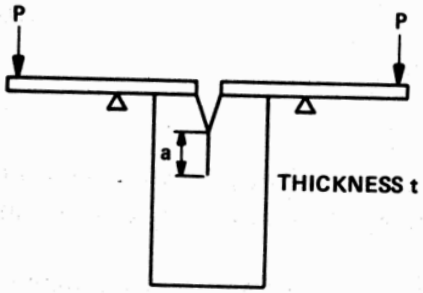

$$K_I = \frac{\text{MOMENT}}{\sqrt{It}}$$

I IS INERTIA OF ONE ARM.

(d) TAPERED DOUBLE CANTILEVER BEAM (TCB) SPECIMEN

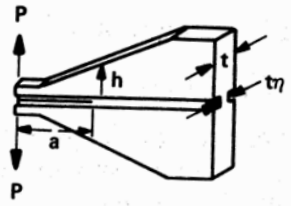

$$K_I = 2P\left(\frac{m}{tt_\eta}\right) \qquad M = \frac{1}{t}$$

SENB Specimen

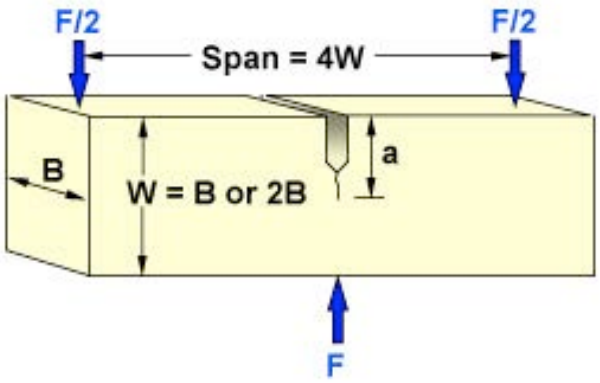

CT Specimen

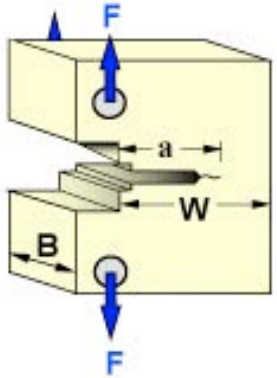

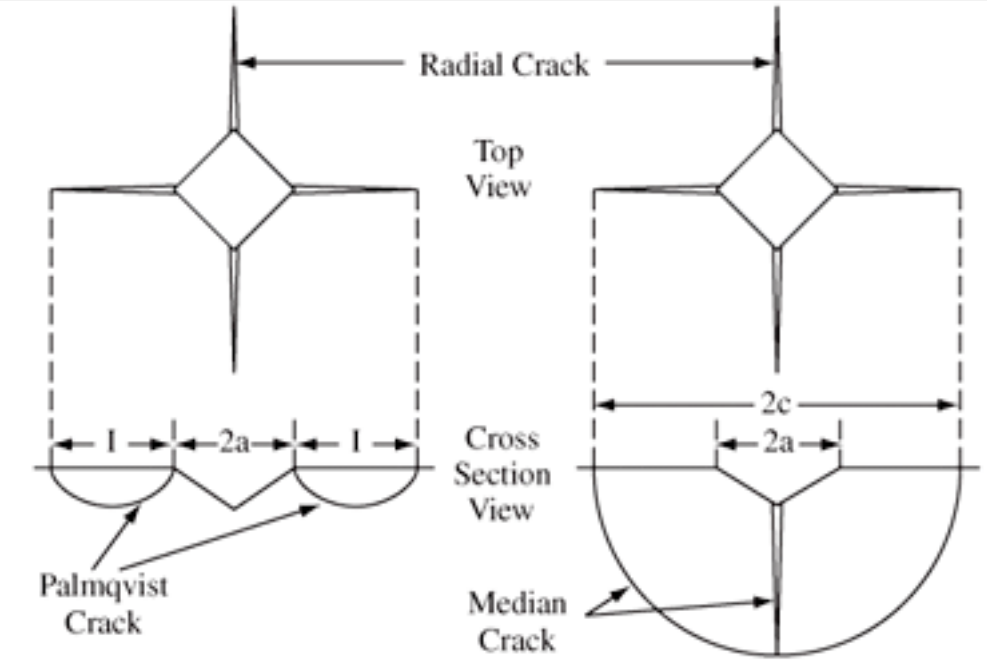

Figure 1. Crack formation by Vickers indentation.

$$K_c = 0{,}016\left(\frac{E}{H_V}\right)^{0,5}\frac{P}{c^{1,5}}$$

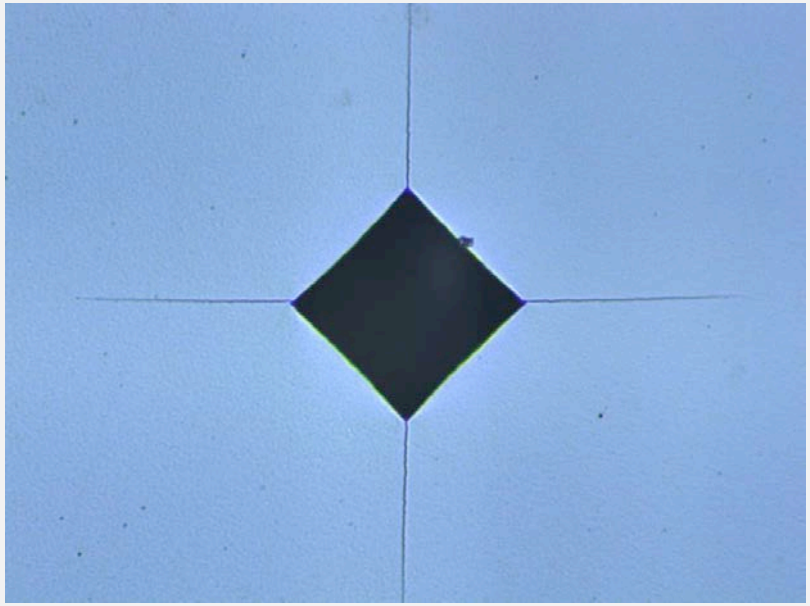

Table I. Materials Used in Indentation Toughness Studies

Material	Characterization	Grain size (μm)	E(GPa)	H(GPa)	K_c(MPa•m$^{1/2}$)	Toughness measurement[e]
Glass-ceramic (C9606)[a]	Glass-ceramic	1	108	8.4	2.5	DCB (standard)
Soda-lime glass I[b]	Amorphous		70	5.5	0.74	DCB (standard)
Soda-lime glass II[c]	Amorphous		73	5.6	0.75	DCB (standard) (Ref. 27)
Aluminosilicate glass[c]	Amorphous		89	6.6	0.91	DCB (standard) (Ref. 27)
Lead alkali glass[c]	Amorphous		65	4.9	0.68	DCB (standard) (Ref. 27)
Al_2O_3 (AD999)[d]	Polycrystal	3	406	20.1	3.9	DCB (standard)
Al_2O_3 (AD90)[d]	Polycrystal	4	390	13.1	2.9	DCB (standard)
Al_2O_3 (Vi)[e]	Polycrystal	20	305	19.1	4.6	DCB (D. B. Marshall)
Al_2O_3 (sapphire)[f]	Monocrystal[j]		425	21.8	2.1	DT (A. G. Evans[*] and E. A. Charles,[†] Ref. 20)
Si_3N_4 (NC132)[g]	Polycrystal	2	300	18.5	4.0	DCB (standard)
Si_3N_4 (NC350)[g]	Polycrystal	10	170	9.6	2.0	DT (S. M. Wiederhorn[‡] and N. J. Tighe[‡])
SiC(NC203)[g]	Polycrystal	4	436	24.0	4.0	DT (S. M. Wiederhorn[‡] and N. J. Tighe[‡])
ZrO (Ca-stabilized)[h]	Polycrystal	50	210	10.0	7.6	DCB (D. B. Marshall)
Si[i]	Monocrystal[k]		168	10.6	0.7	DT (S. M. Wiederhorn[‡] and E. R. Fuller[‡])
WC (Co-bonded)[c]	Polycrystal	3	575	13.2	12	DT (S. W. Freiman[‡])

[a]Pyroceram, Corning Glass Works, Corning, N. Y. [b]Commercial sheet glass. [c]National Bureau of Standards, Washington, D. C. [d]Coors Porcelain Co., Golden, Colo. [e]Vistal, Coors Porcelain Co. [f]Linde, Union Carbide Co., New York, N. Y. [g]Norton Co., Worcester, Mass. [h]CSIRO, Australia. [i]Texas Instruments, Inc., Dallas. [j]Rods, [0001] 30° to axis. [k]Disks, [111] parallel to axis. [l]DT = double torsion, DCB = double cantilever beam. [*]University of California, Berkeley. [†]Rockwell International Science Center, Thousand Oaks, Calif. [‡]National Bureau of Standards.

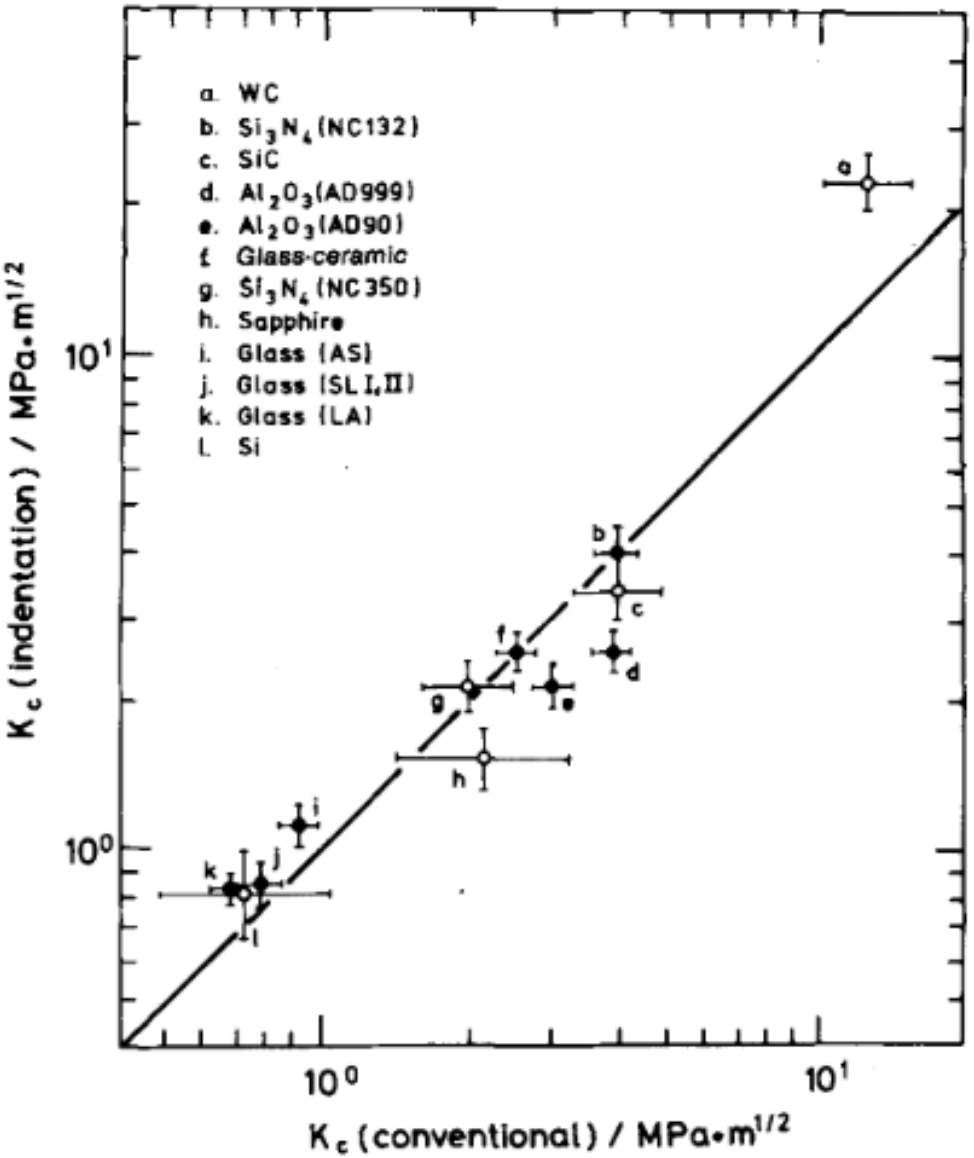

Fig. 5. Plot demonstrating correlation between toughness values determined by indentation and by conventional means. Filled symbols denote reference materials used to evaluate constant $\S_V^R$ in Eq. (4). Vertical error bars represent uncertainty (standard deviation) in parameter $P/c_0^{3/2}$ obtained from Fig. 4, horizontal error bars nominal accuracy of K_c values taken from Table I.

ISB determination of K_{Ic}

$$K_{IC} = 0{,}59 \left(\frac{E}{H_V} \right)^{\frac{1}{8}} \left(\sigma_f \cdot p^{\frac{1}{3}} \right)^{\frac{3}{4}}$$

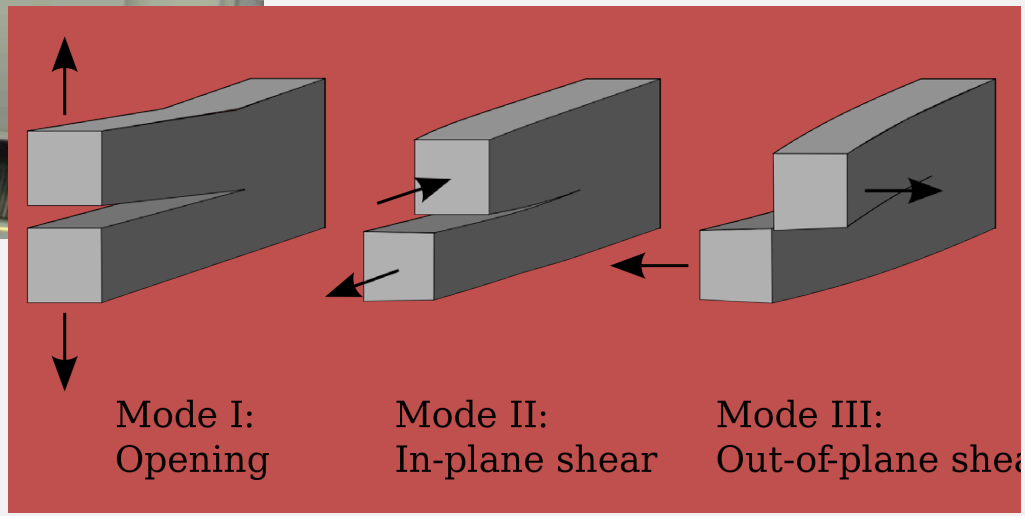

Creep

Sample deformation at a constant stress (σ) vs. time

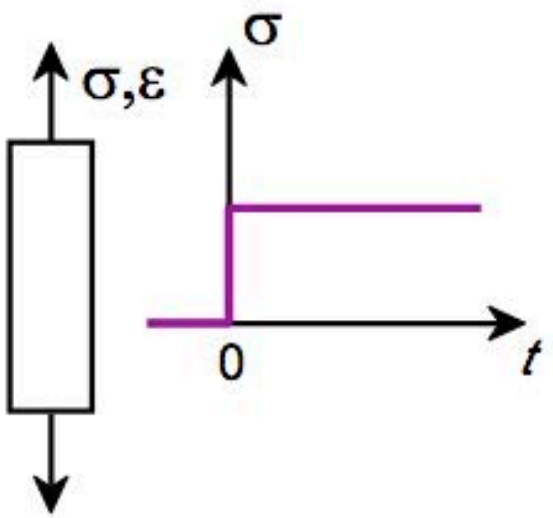

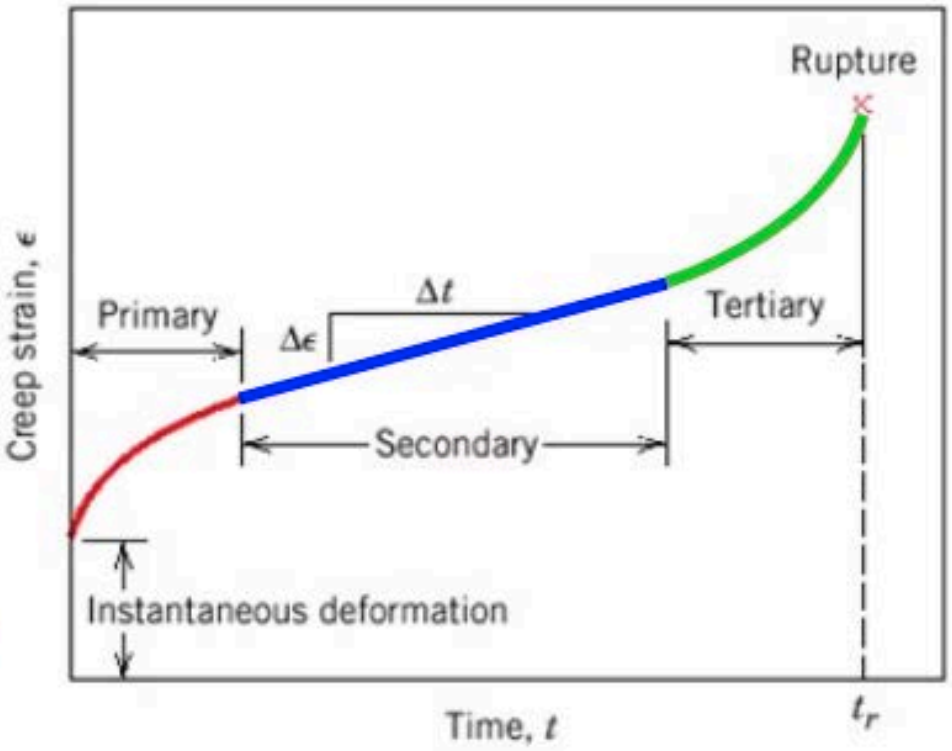

Primary Creep: slope (creep rate) decreases with time.

Secondary Creep: steady-state i.e., constant slope.

Tertiary Creep: slope (creep rate) increases with time, i.e. acceleration of rate.

Creep

- A typical creep test consists of subjecting a specimen to a constant load or stress while maintaining constant temperature.
- Upon loading, there is instant elastic deformation. The resulting creep curve consists of 3 regions: primary or transient creep adjusts to the creep level (creep rate may decrease); secondary creep- steady state-constant creep rate, fairly linear region (strain hardening and recovery stage); tertiary creep, there is accelerated rate of strain until rupture (grain boundary separation, internal crack formation, cavities and voids).

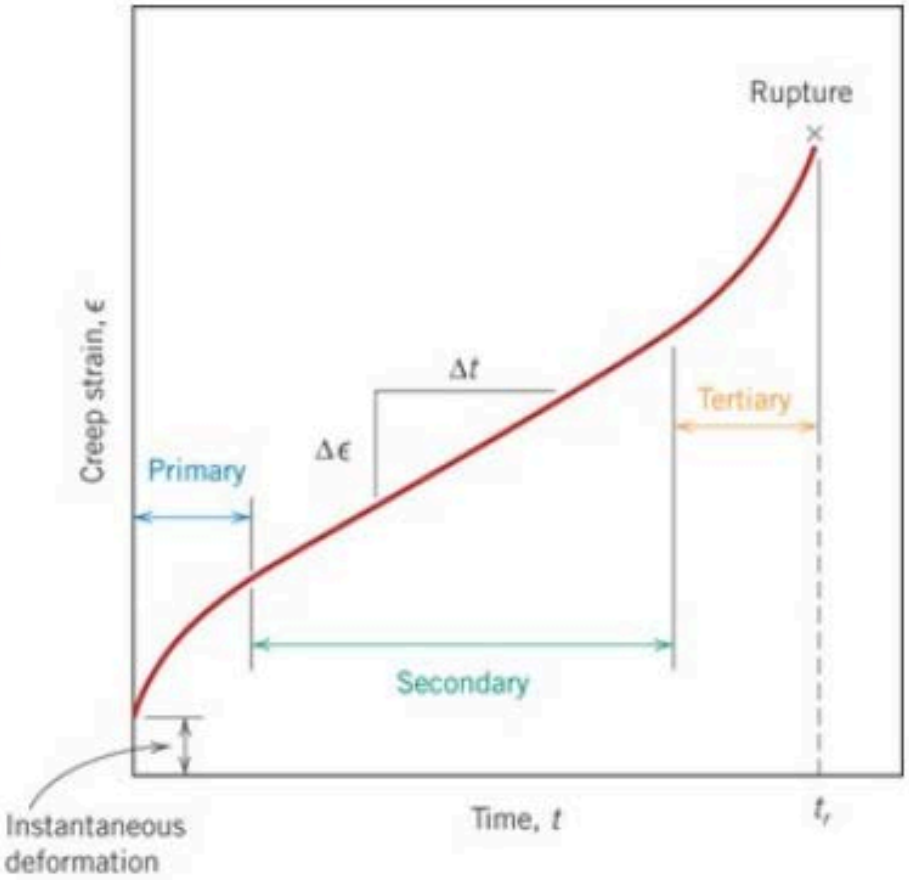

Creep strain vs time at constant load and constant elevated temperature. Minimum creep rate (steady-state creep rate), is the slope of the linear segment in the secondary region. Rupture lifetime t_r is the total time to rupture.

Secondary Creep

- Strain rate is constant at a given T, σ
  -- strain hardening is balanced by recovery

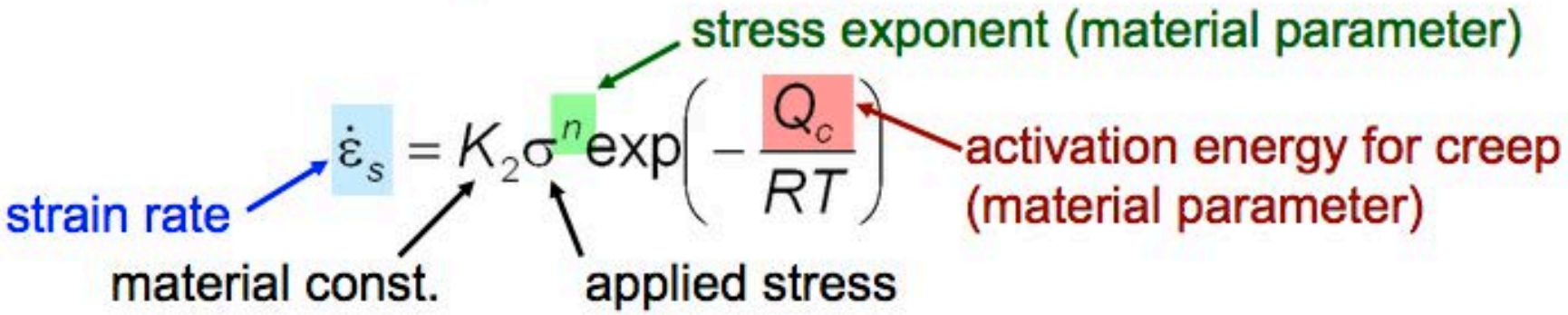

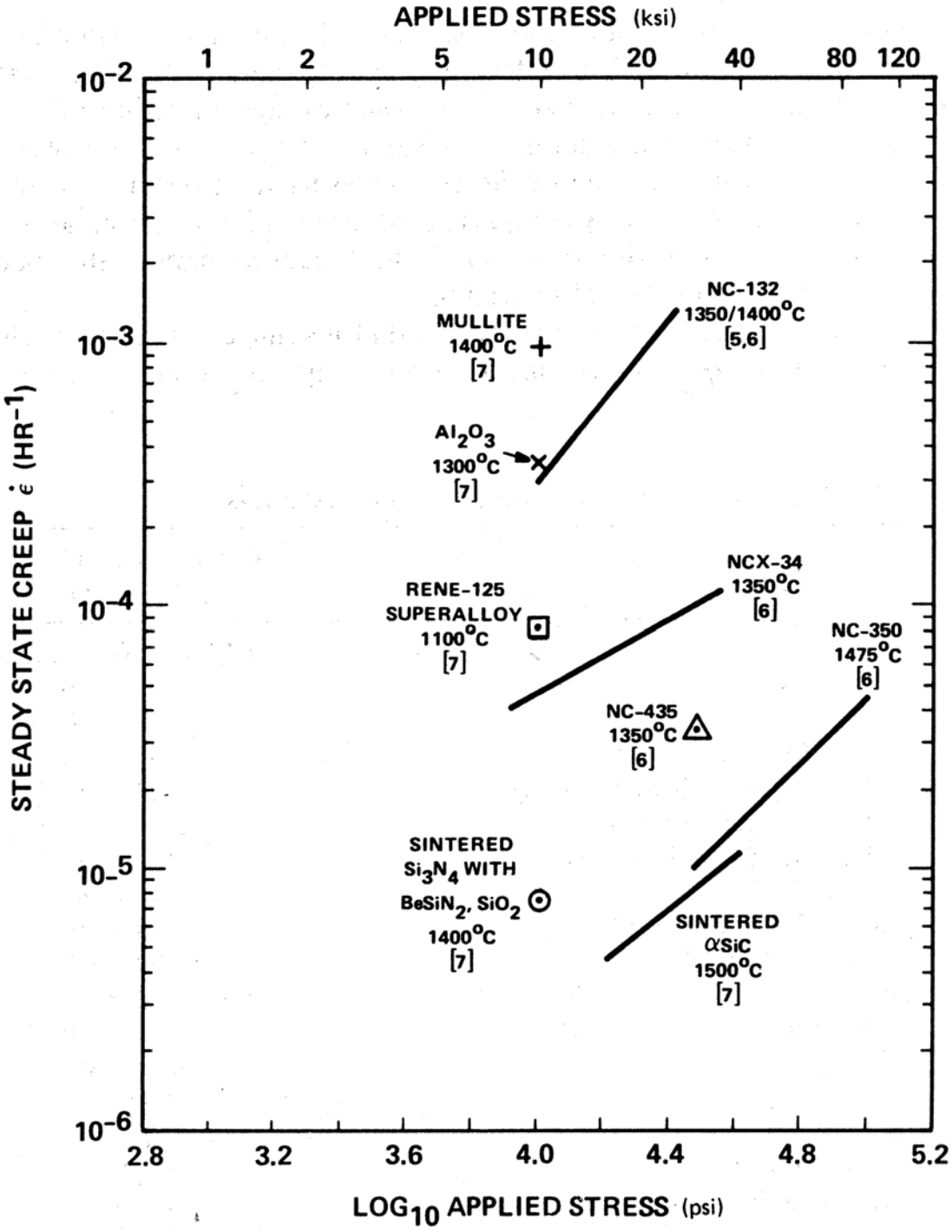
APPLIED STRESS (ksi)
1
2
5
10
20
40
80
120
10^{-2}
10^{-3}
10^{-4}
10^{-5}
10^{-6}
STEADY STATE CREEP $\dot{\epsilon}$ (HR^{-1})
MULLITE
1400°C
[7]
Al_2O_3
1300°C
[7]
NC-132
1350/1400°C
[5,6]
RENE-125
SUPERALLOY
1100°C
[7]
NCX-34
1350°C
[6]
NC-350
1475°C
[6]
NC-435
1350°C
[6]
SINTERED
Si_3N_4 WITH
$BeSiN_2$, SiO_2
1400°C
[7]
SINTERED
αSiC
1500°C
[7]
2.8
3.2
3.6
4.0
4.4
4.8
5.2
LOG_{10} APPLIED STRESS (psi)

Ashby map Therm. Expan./therm Conduc

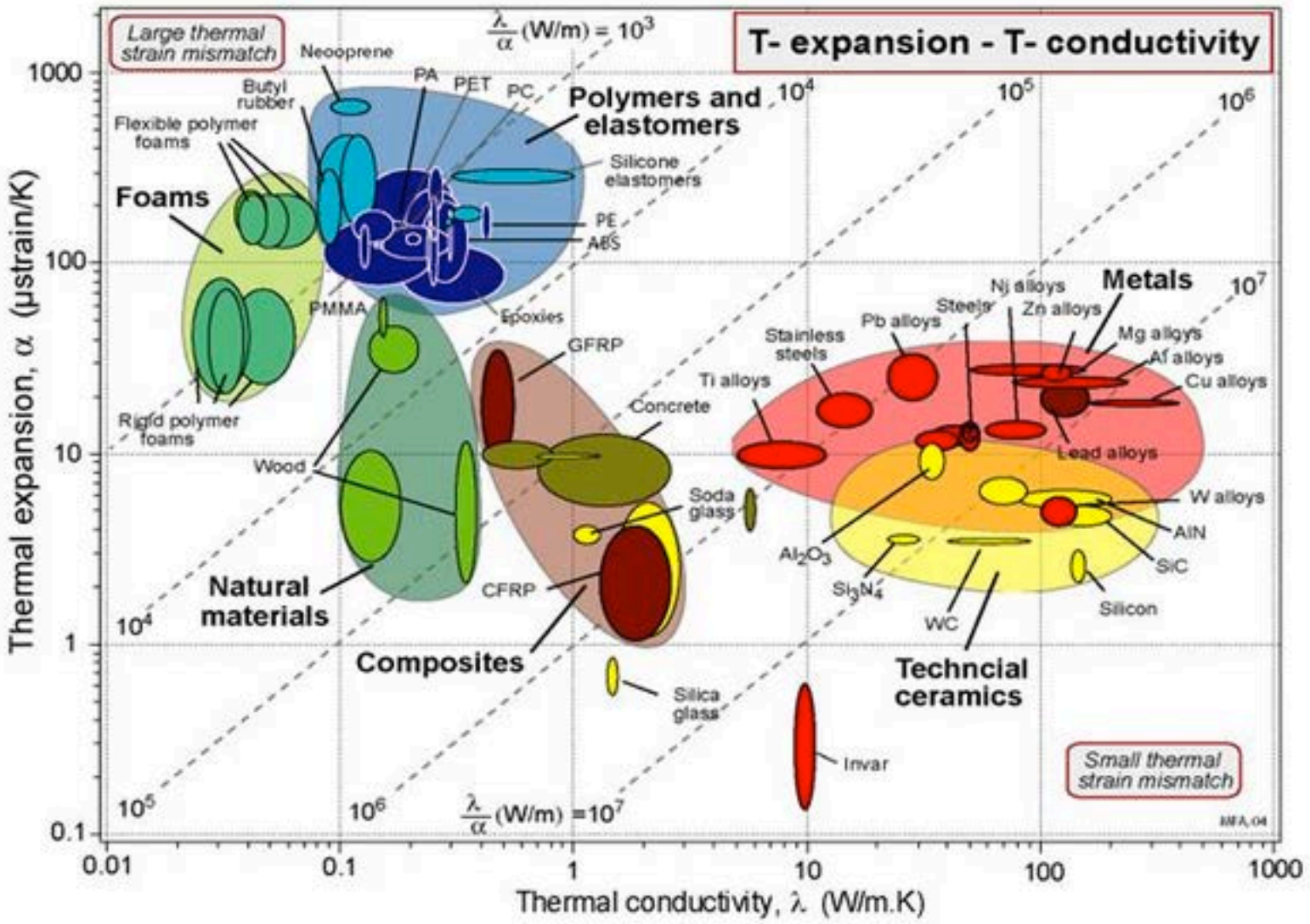

Thermal shock resistance

Table 8.8 Calculated Values of the Thermal Shock Parameter R for Various Ceramic Materials Using Typical Property Data

Material	Strength,[a] σ (psi)	Poisson's Ratio, ν	Thermal Expansion, α (in./in. · °C)	Elastic Modulus, E (psi)	$R = \frac{\sigma(1-\nu)}{\alpha E}$ (°C)
Al_2O_3	50,000	0.22	7.4×10^{-6}	55×10^6	96
SiC	60,000	0.17	3.8×10^{-6}	58×10^6	230
RSSN[b]	45,000	0.24	2.4×10^{-6}	25×10^6	570
HPSN[b]	100,000	0.27	2.5×10^{-6}	45×10^6	650
LAS[b]	20,000	0.27	-0.3×10^{-6}	10×10^6	4860

[a]Flexure strength used rather than tensile strength.
[b]RSSN, reaction-sintered silicon nitride; HPSN, hot-pressed silicon nitride; LAS, lithium aluminum silicate (β-spodumene).

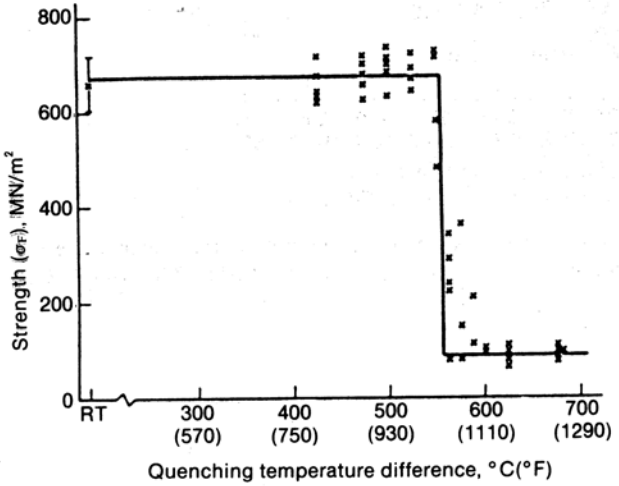

Figure 8.32 Typical results of retained strength versus thermal shock ΔT for quench test. Example is for hot-pressed Si_3N_4 material containing 3% MgO as a densification aid. (From G. Ziegler, in *Progress in Nitrogen Ceramics* [F. L. Riley, ed.] Martinas Nijhoff Publishers, The Hague, 1983.)

Thermal shock testing of Schott glasses

Stress data for Weibull plot

Ergebnisse:

Nr	P N	σ MPa	P_f	d mm	r3 mm
1	998,3	1190	0,00	1,185	6,735
2	993,3	1190	0,00	1,181	6,875
3	1034,9	1200	0,00	1,2	6,895
4	994,4	1190	0,00	1,181	6,88
5	1002,2	1180	0,00	1,192	6,935
6	1026,4	1210	0,00	1,192	6,9
7	1035,1	1210	0,00	1,194	6,915
8	940,4	1120	0,00	1,184	6,9
9	1026,8	1190	0,00	1,199	6,935
10	1000,4	1180	0,00	1,192	6,935
11	971,5	1170	0,00	1,176	6,945
12	993,2	1190	0,00	1,183	6,885

Nr	P N	σ MPa	P_f	d mm	r3 mm
13	1013,2	1200	0,00	1,19	6,885
14	1018,6	1210	0,00	1,185	6,945
15	994,4	1180	0,00	1,189	6,9
16	980,9	1170	-	1,186	6,9
17	1016,7	1210	-	1,186	6,92
18	992,1	1170	-	1,191	6,945
19	1033,9	1240	-	1,184	6,865
20	989,6	1170	-	1,188	6,88
21	998,7	1190	-	1,187	6,94
22	1025,5	1210	-	1,19	6,895
23	985,1	1170	-	1,188	6,915

Seriengrafik:

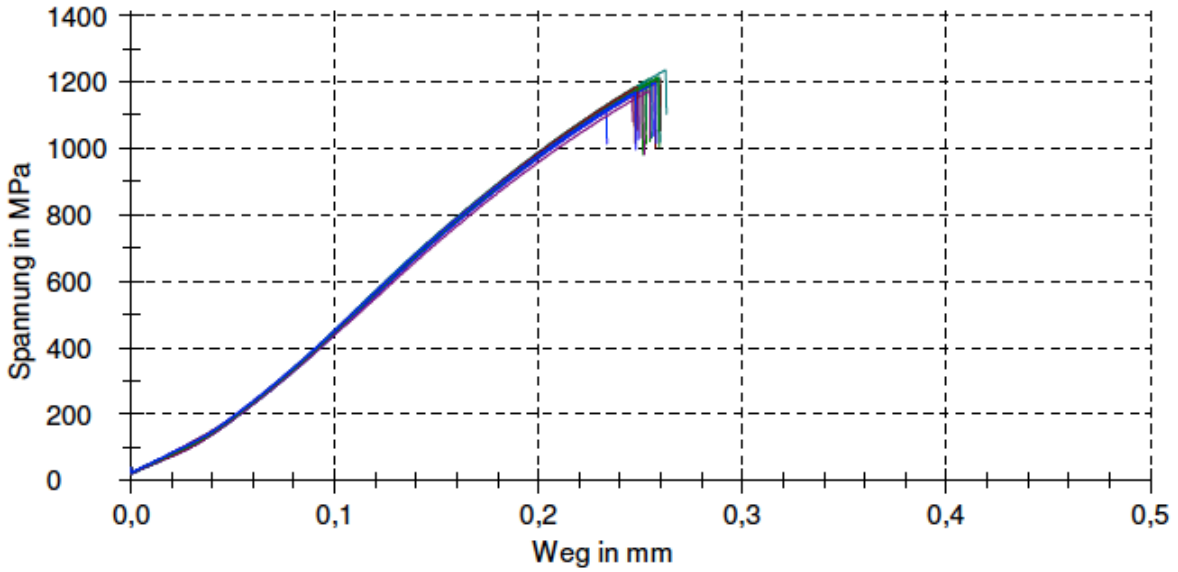

Data from SKF

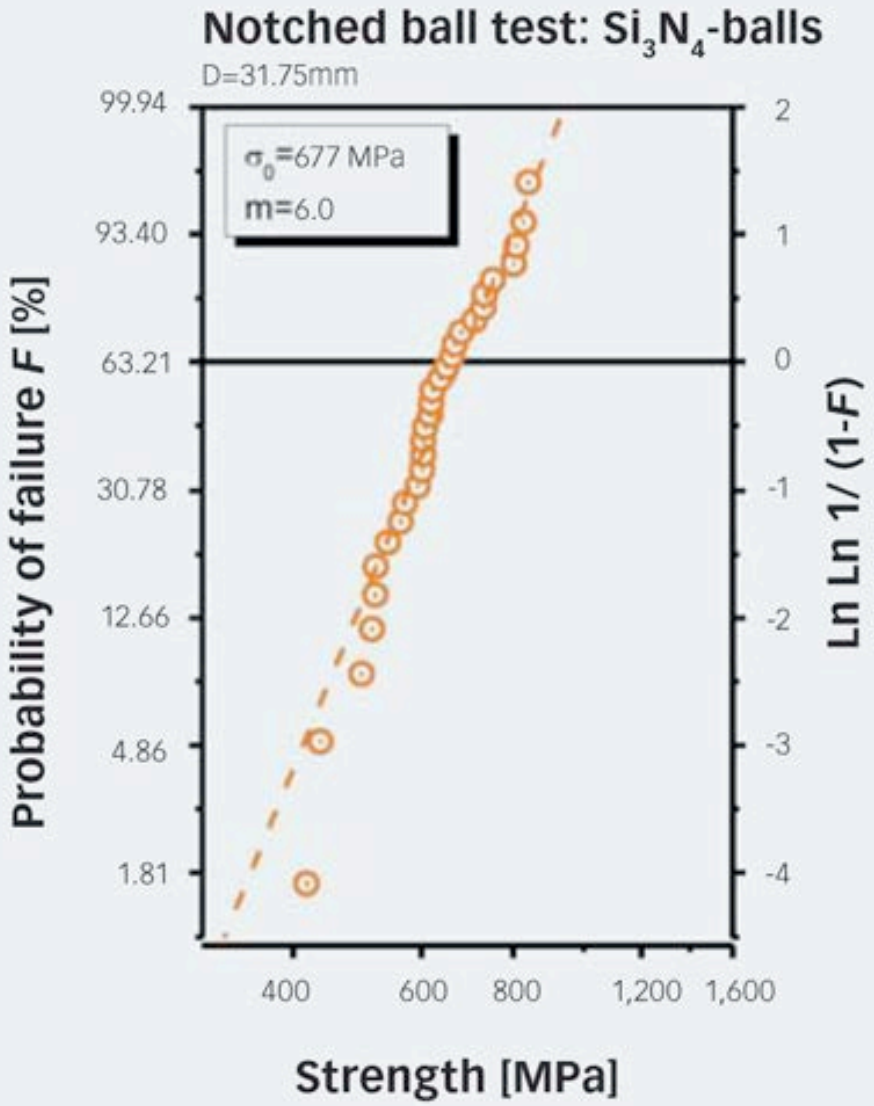

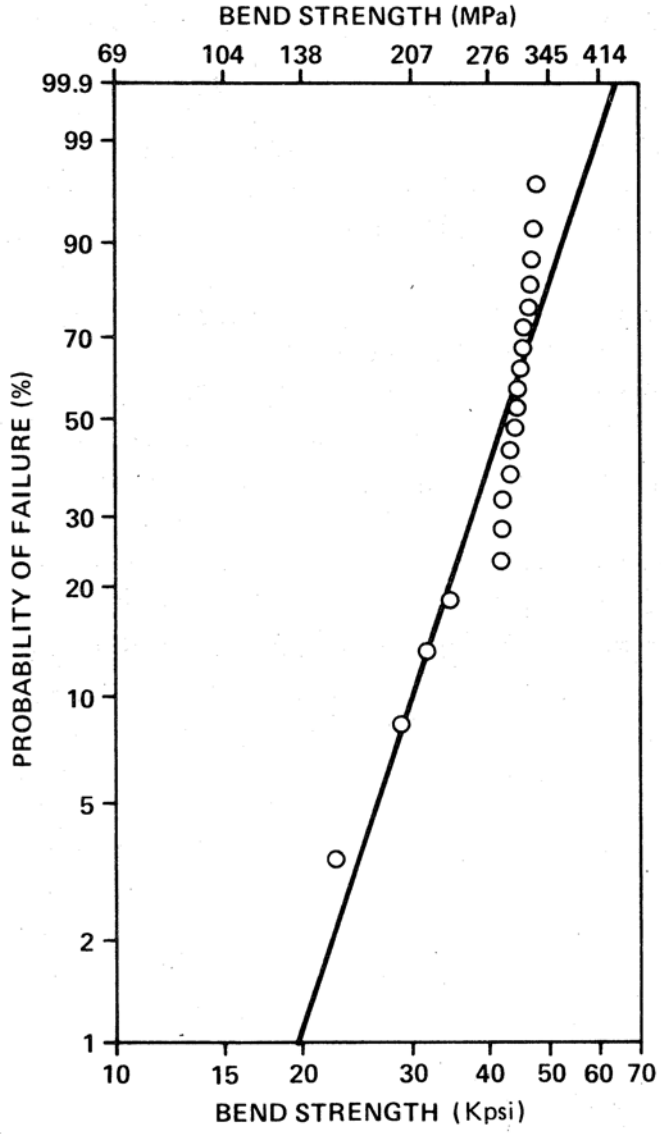

Figure 15.6 Example of Weibull curve generated from strength test data for reaction-bonded Si_3N_4. (Data from Ref. 6.)

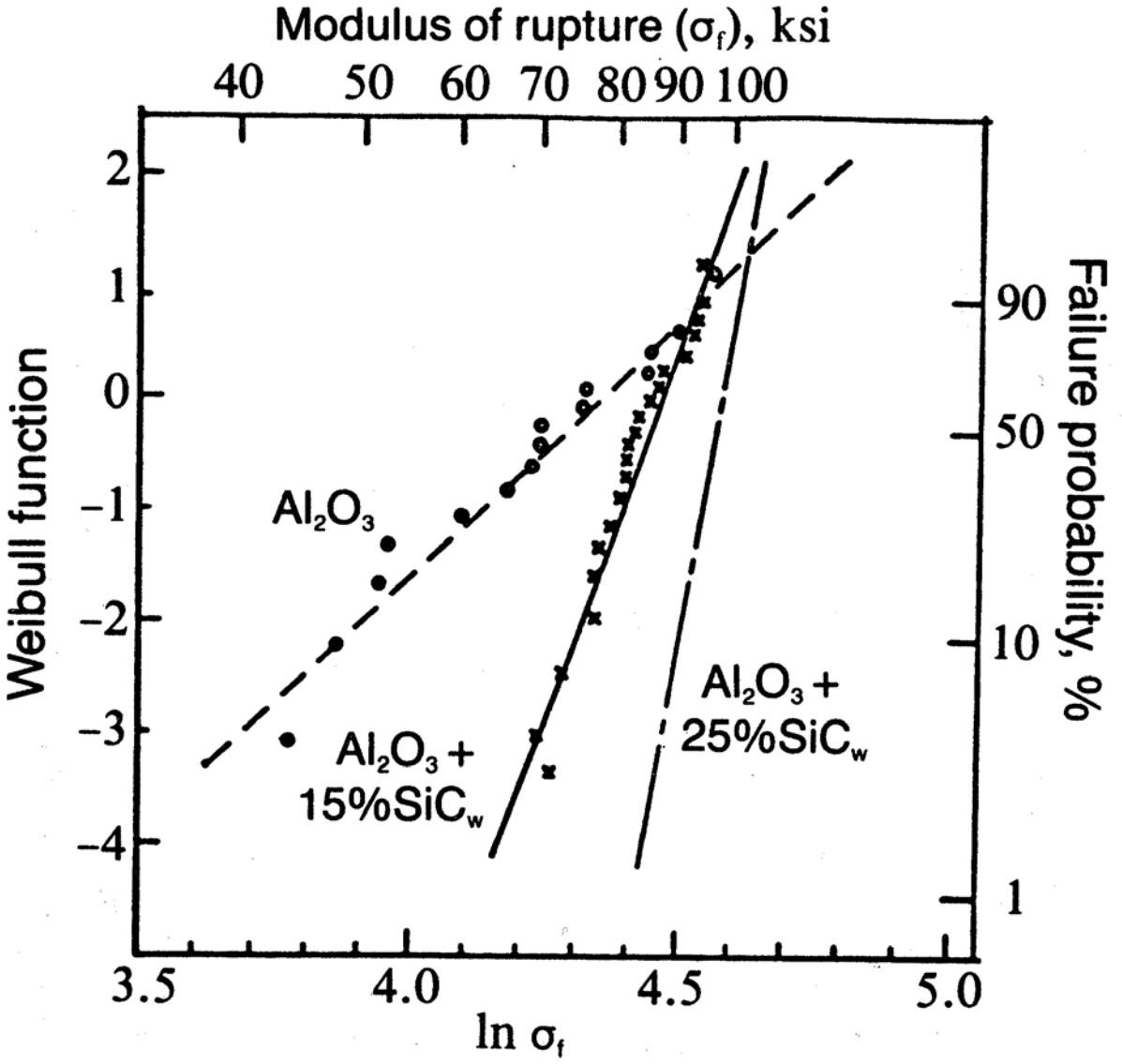

Figure 15.8 Example of the use of Weibull plots to compare material. (Adapted from J.F. Rhodes, H.M. Rootare, C.A. Springs, and J.E. Peters, data presented at the 88th Annual Meeting of the American Ceramic Society, Chicago, Ill. April 28, 1986.)

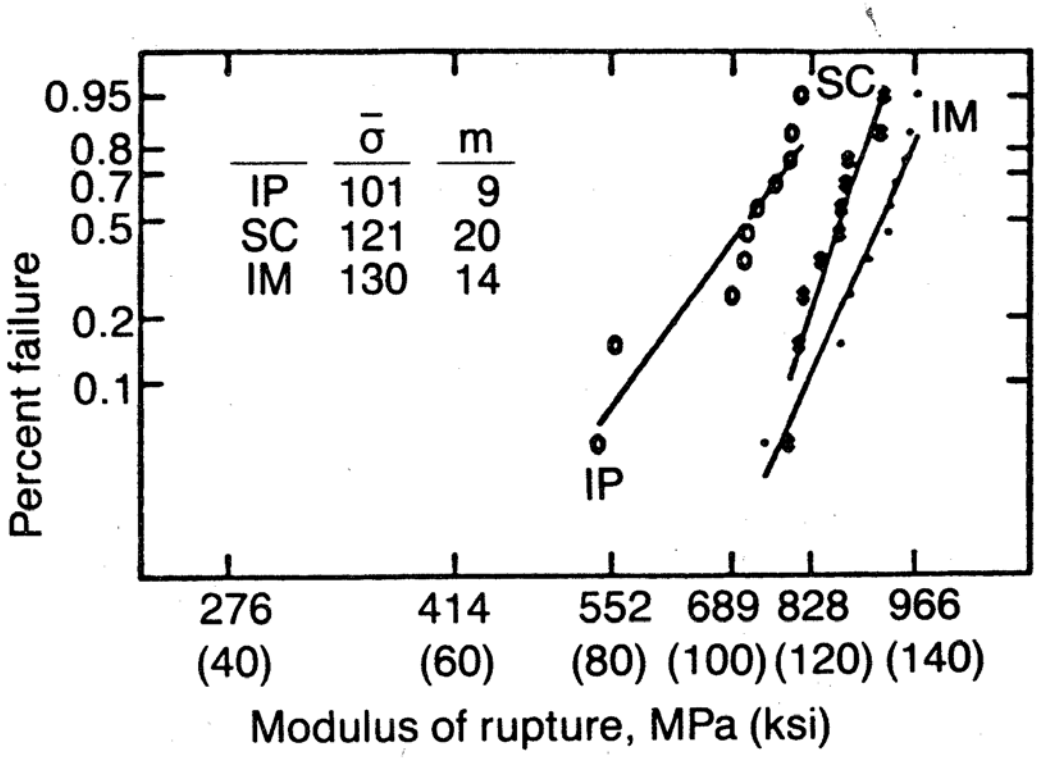

Figure 15.10 Weibull plots comparing the strength of a sintered Si_3N_4 fabricated by various techniques. IP is isostatically pressed, SC is slip-cast, and IM is injection-molded. (From A. Pasto, J. Neil, and C.L. Quackenbush, paper presented at International Conference on Ultrastructure Processing of Ceramics, Glasses and Composites, Gainesville, Florida, Feb. 13–17, 1983.)

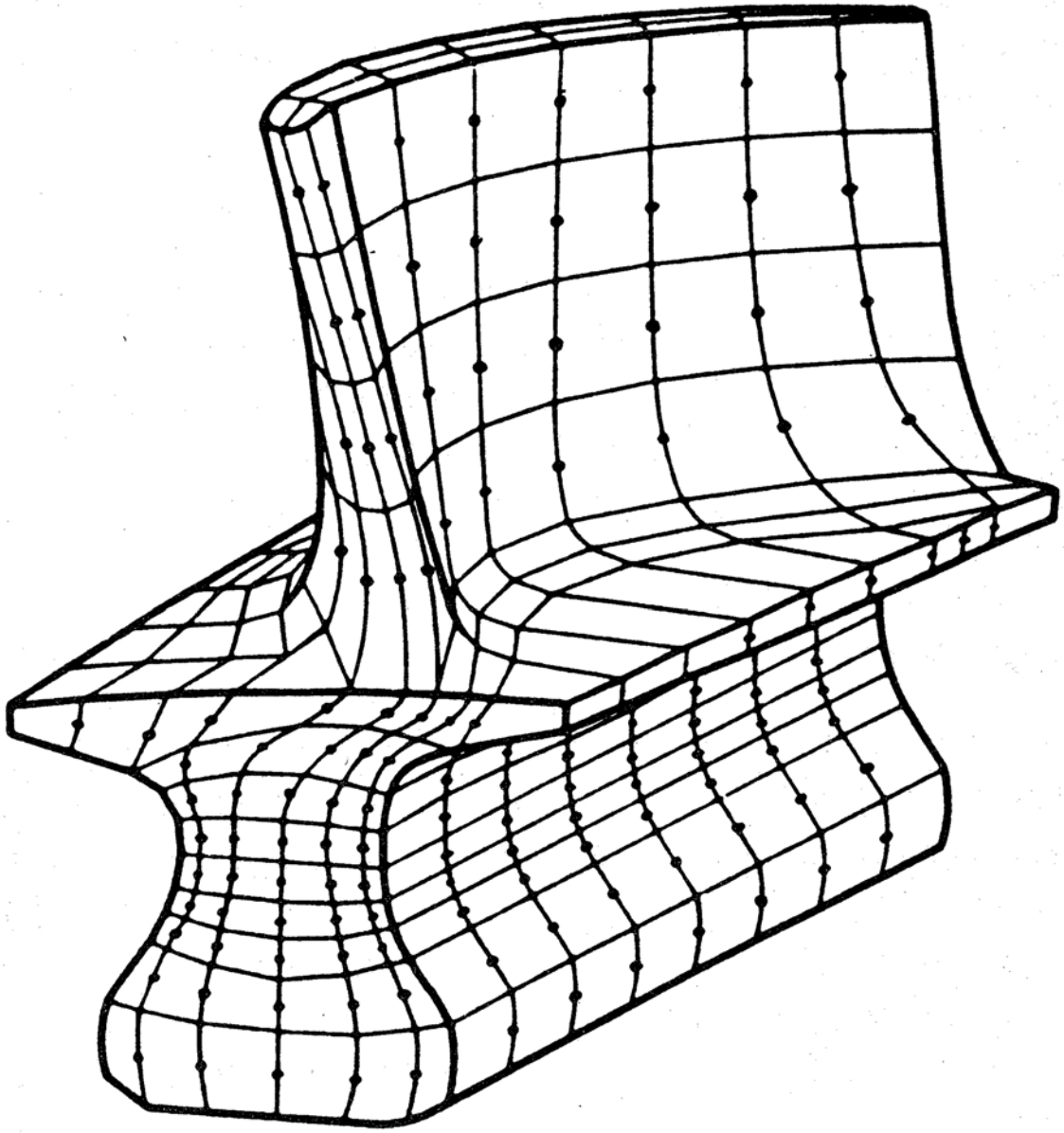

Figure 15.11 Finite-element analysis model for a ceramic rotor blade for a gas-turbine engine. (© ASM International.)

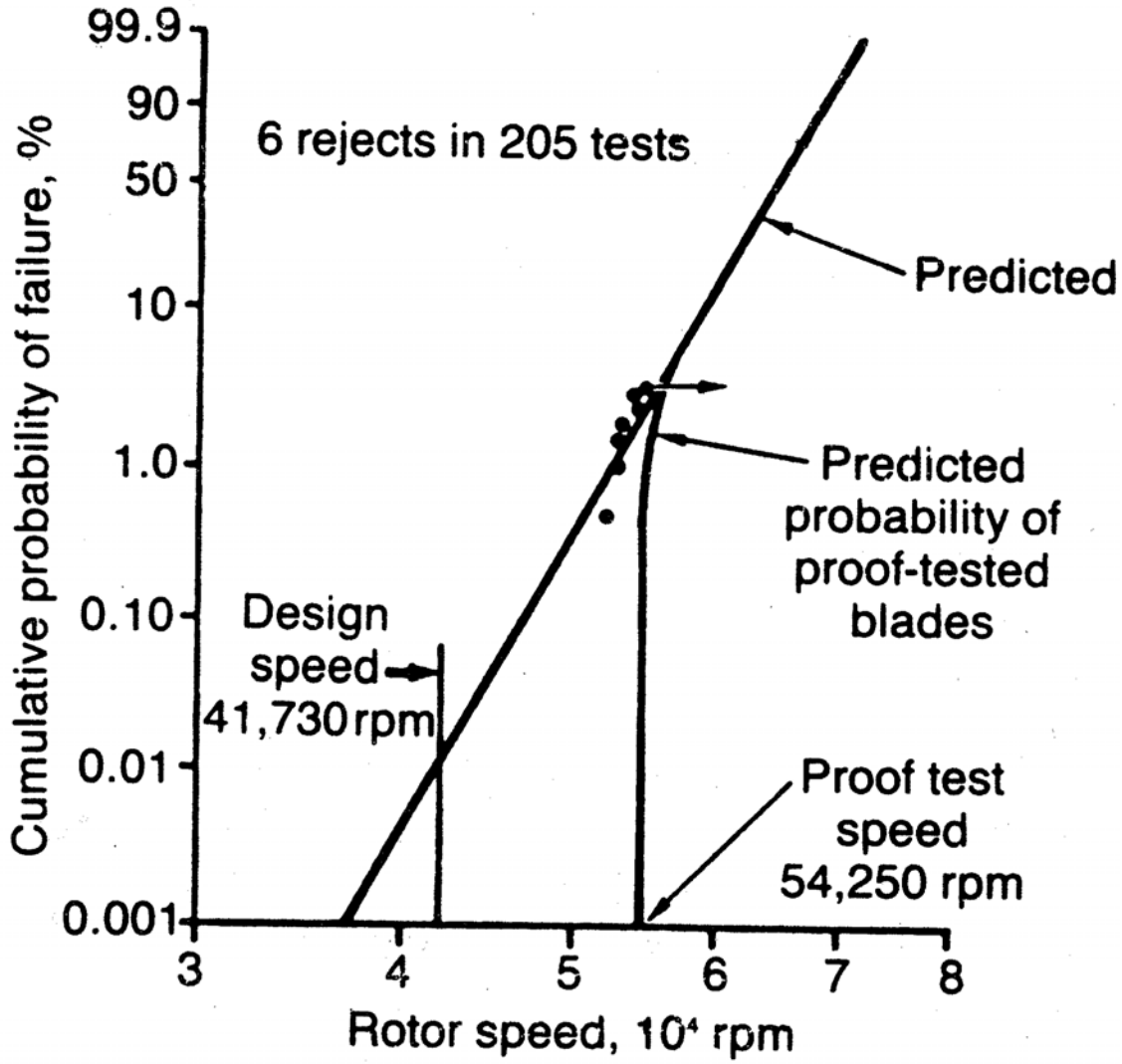

Figure 15.12 Rotor blade spin proof-test results that show good correlation between predicted and actual probability of failure for hot-pressed Si_3N_4 rotor blades. (From D. W. Richerson, Design with ceramics for heat engines, paper presented at U.S./Japan Seminar on Structural Ceramics, Seattle, Wash., Aug. 13–15, 1984.)

Raw materials for traditional ceramics

- Halloysite $Al_2Si_2O_5(OH)_4 \cdot 2H_2O$
- Montmorillonite $(Na,Ca)_{0,3}(Al,Mg)_2Si_4O_{10}(OH)_2 \cdot n(H_2O)$

- In genere prodotto di dilavamento feldspatico:
- Feldspati $(Ba,Ca,Na,K,NH_4)(Al,B,Si)_4O_8$

Clay Mineral Structure

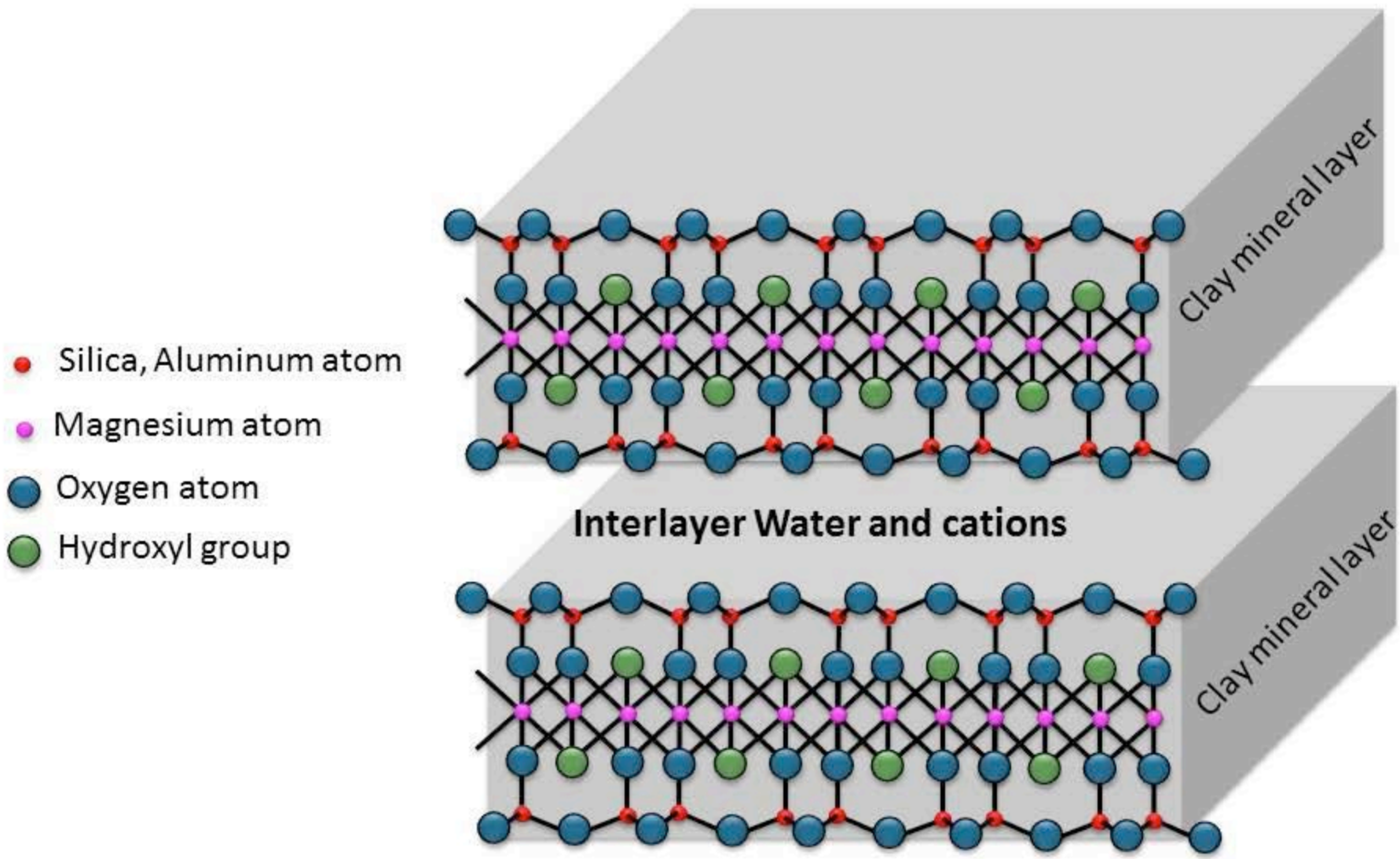

Montmorillonite

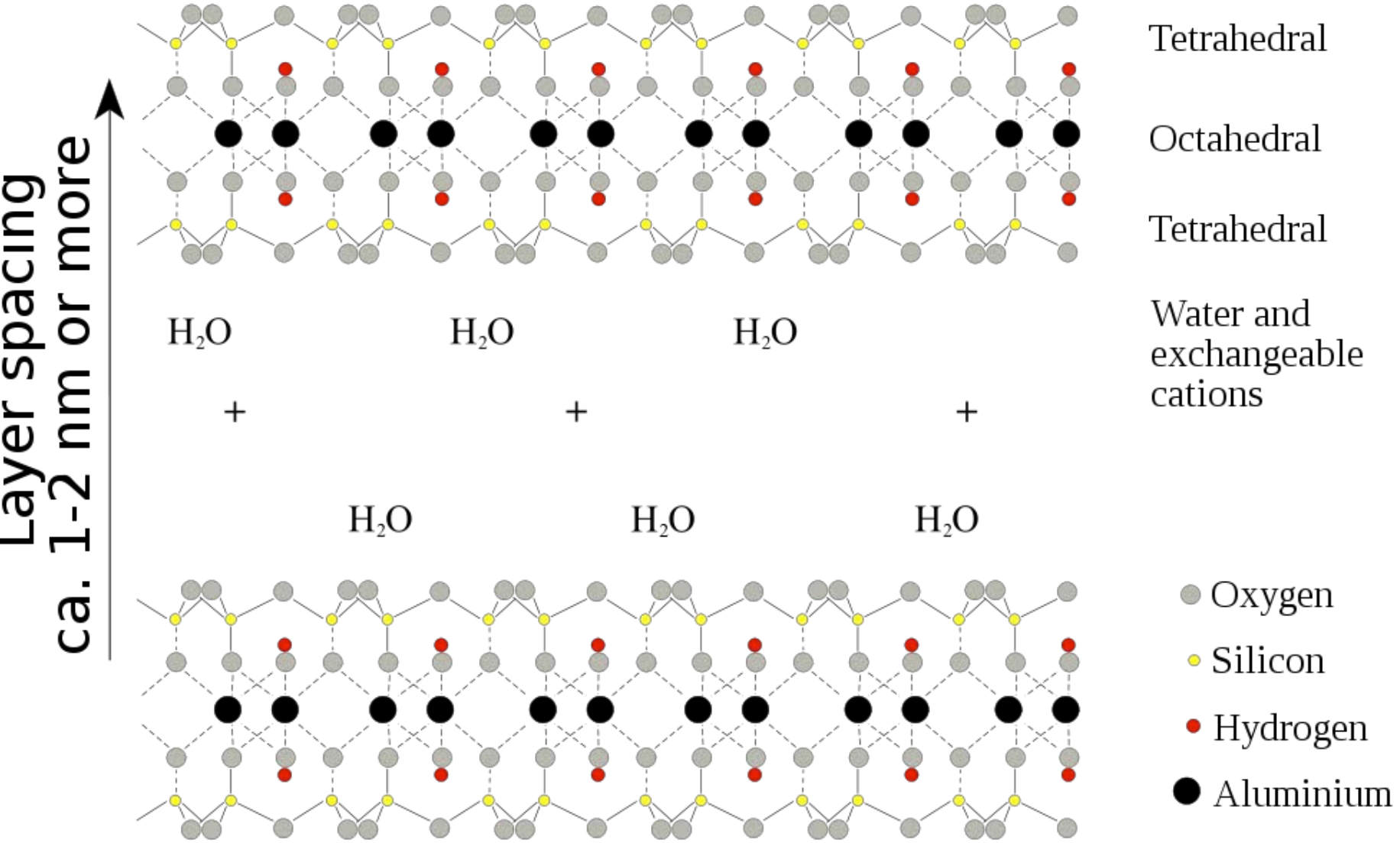

Processo Bayer

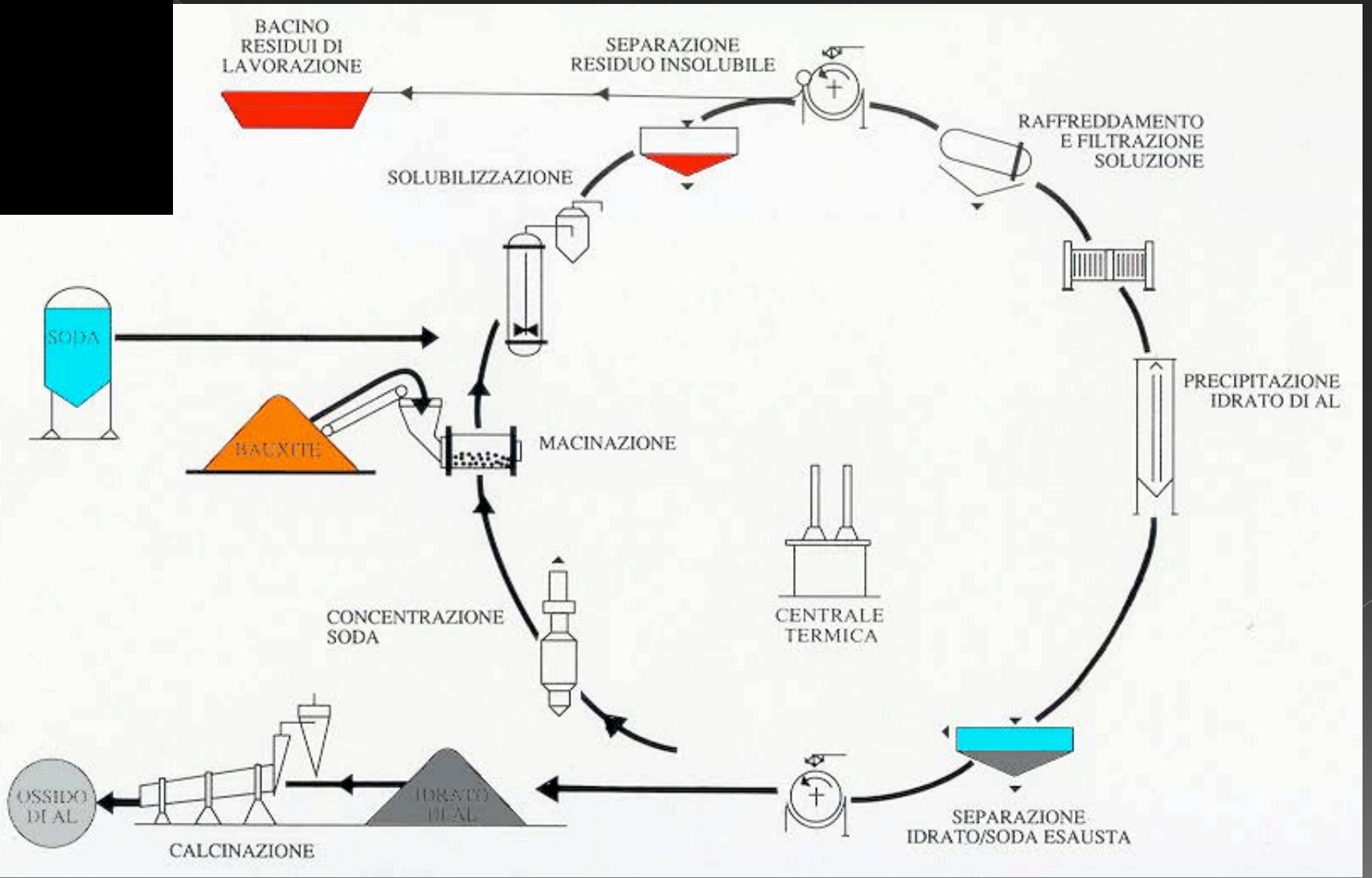

Zirconia powder preparation

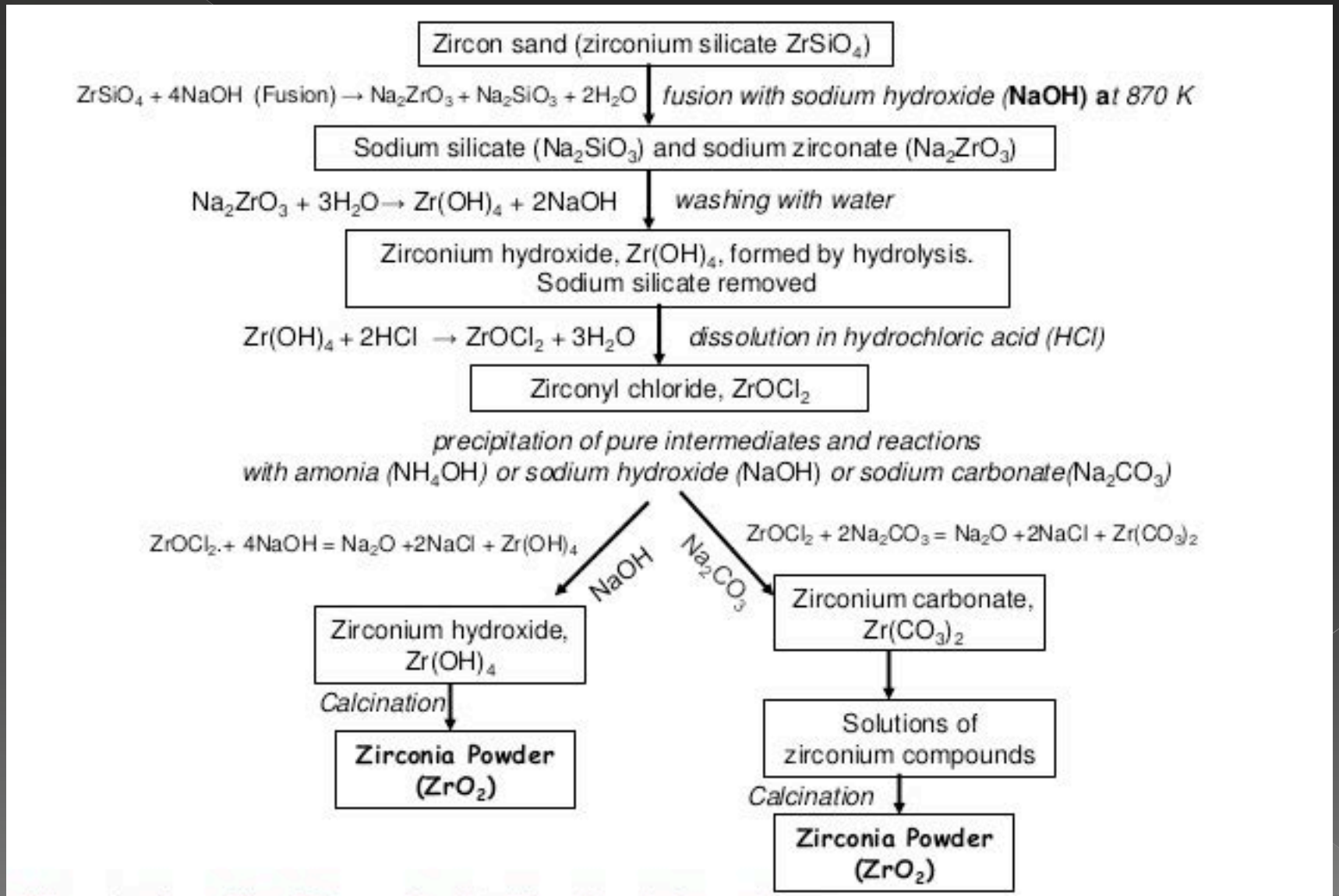

Acheson process: $3C + SiO_2 => SiC + 2CO$

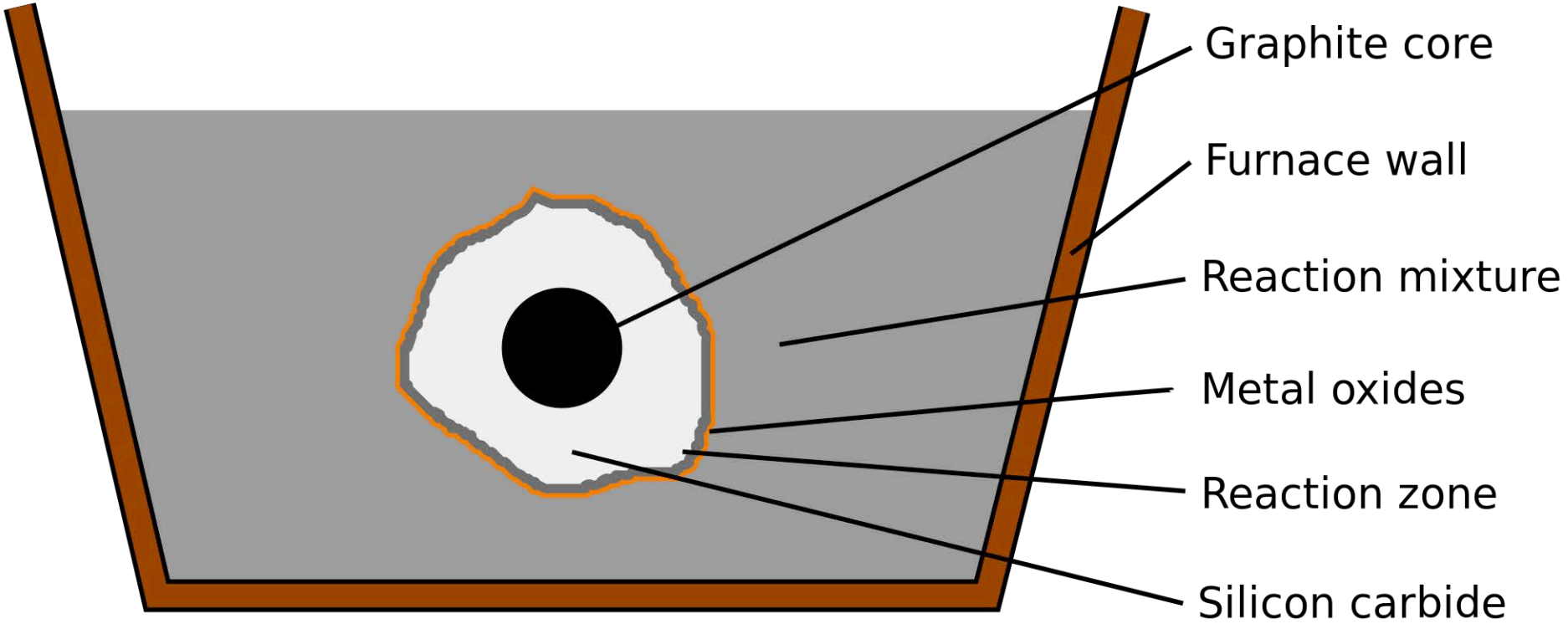

Measuring Particle Size

- Most common method uses screens of different mesh sizes
- *Mesh count* - refers to the number of openings per linear inch of screen
  - A mesh count of 200 means there are 200 openings per linear inch
  - Since the mesh is square, the count is equal in both directions, and the total number of openings per square inch is $200^2 = 40{,}000$
  - Higher mesh count = smaller particle size

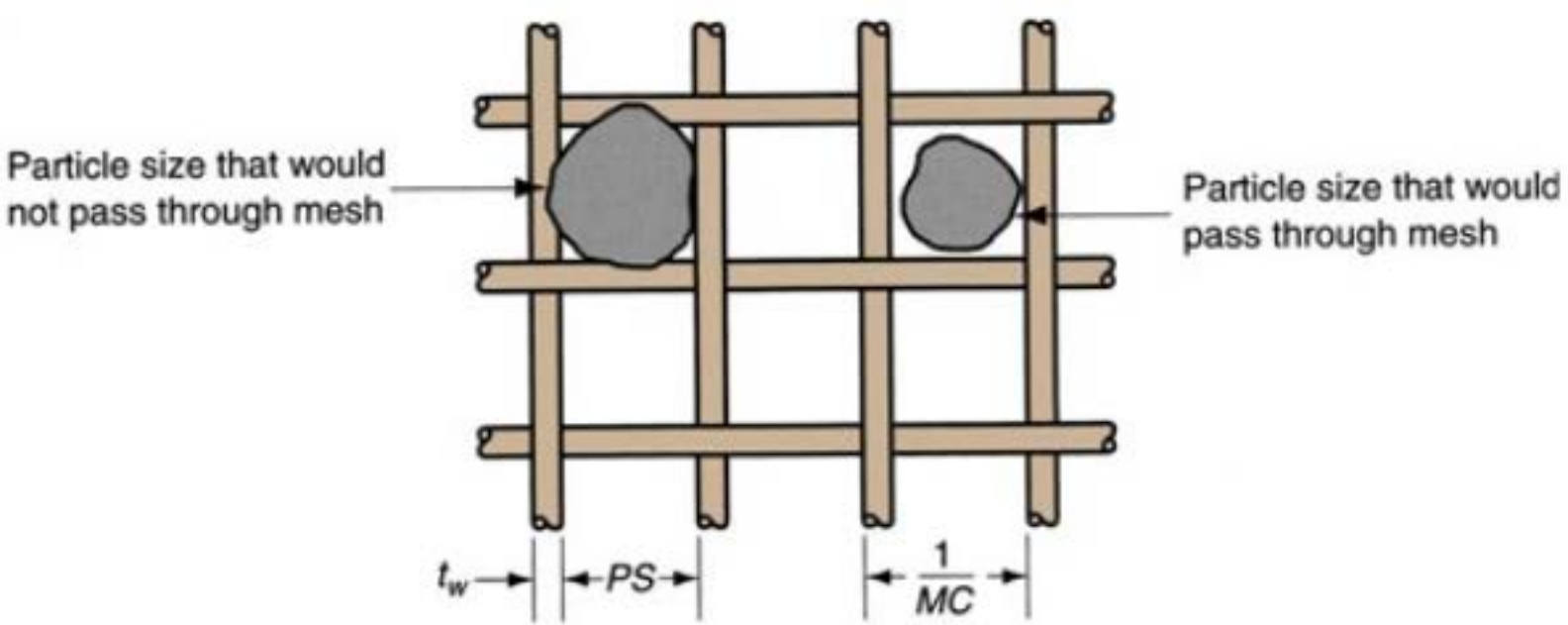
Particle size that would not pass through mesh
Particle size that would pass through mesh
t_w
PS
1
MC

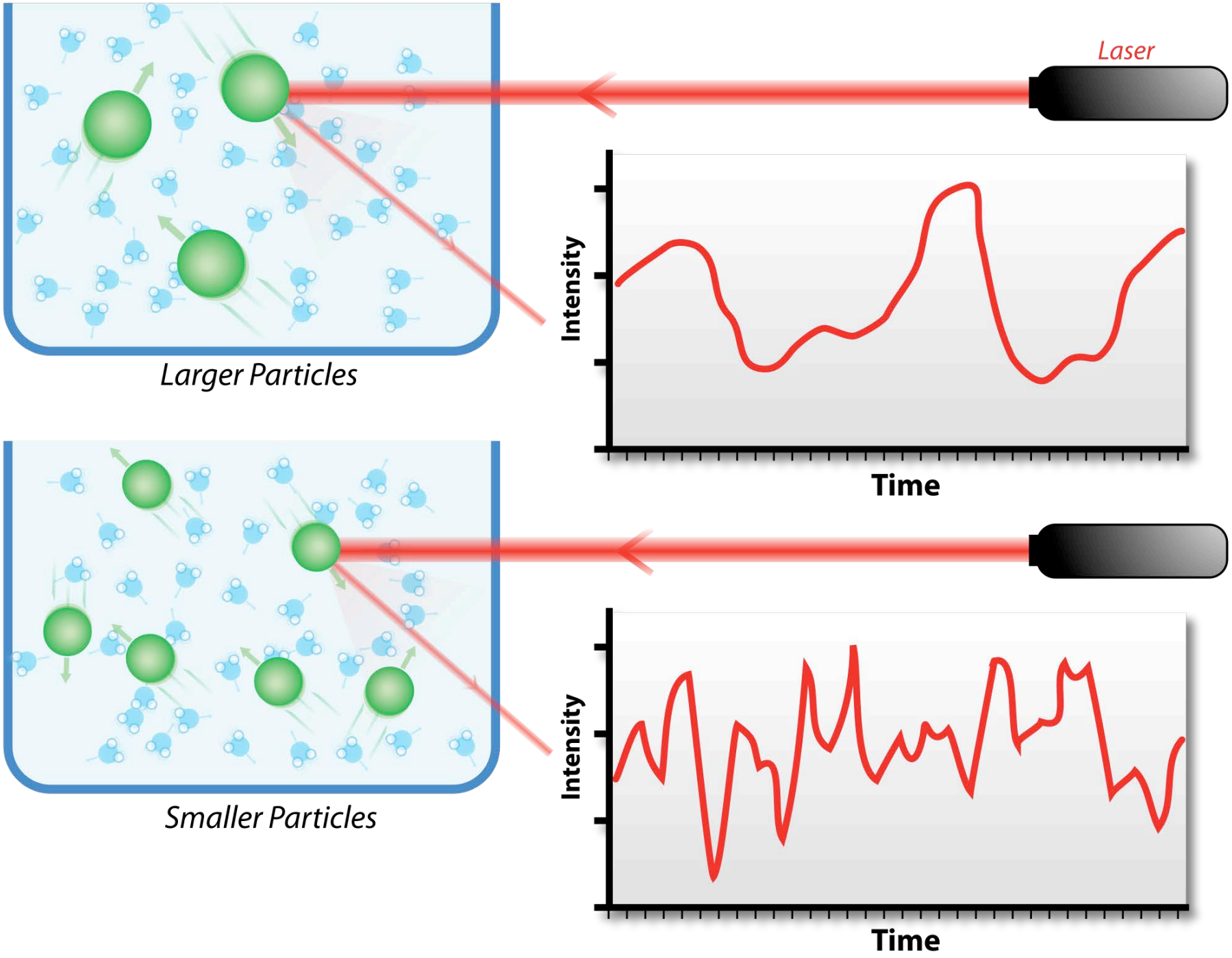
Laser
Larger Particles
Intensity
Time
Smaller Particles
Intensity
Time

Dynamic light scattering

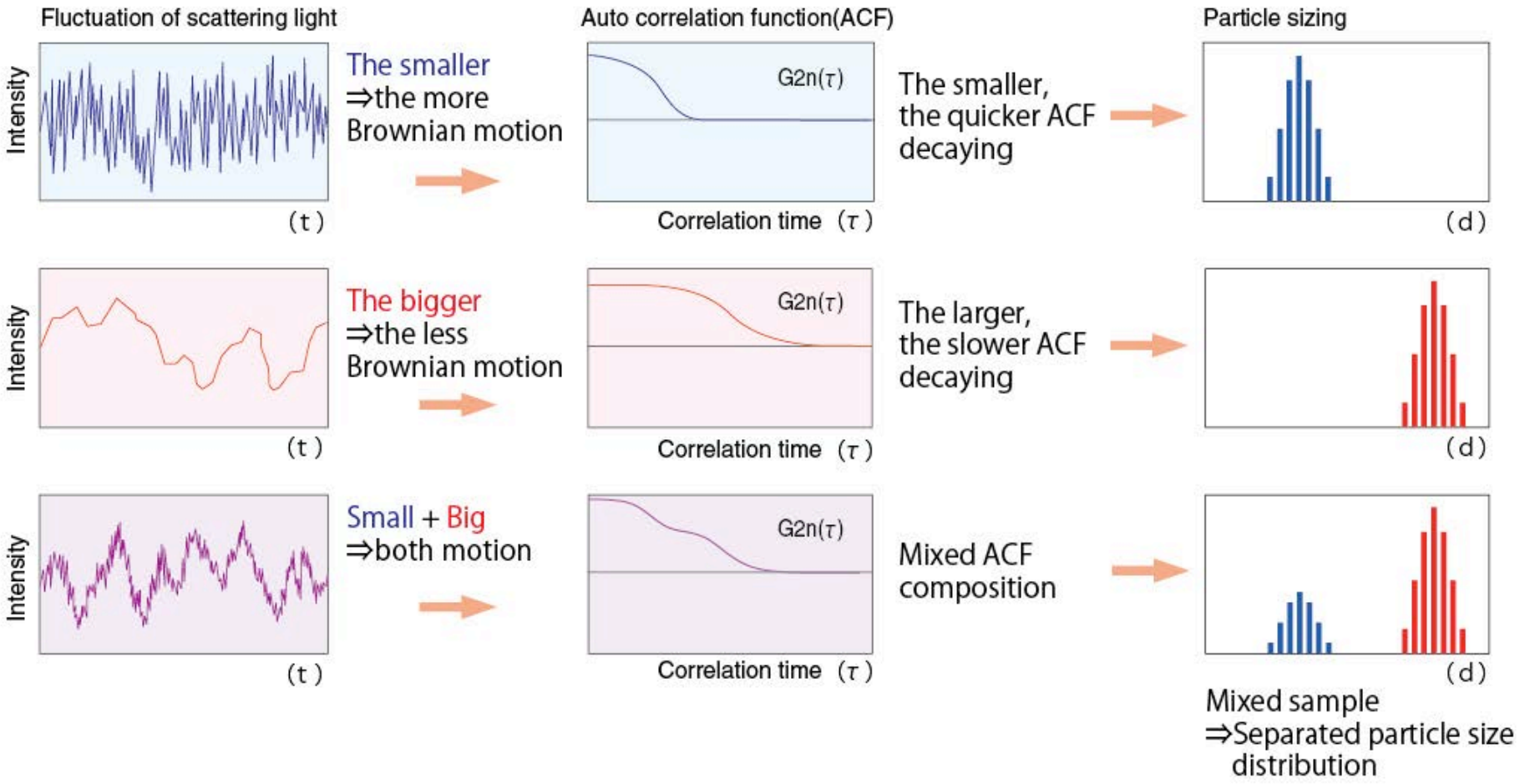

Si3N4

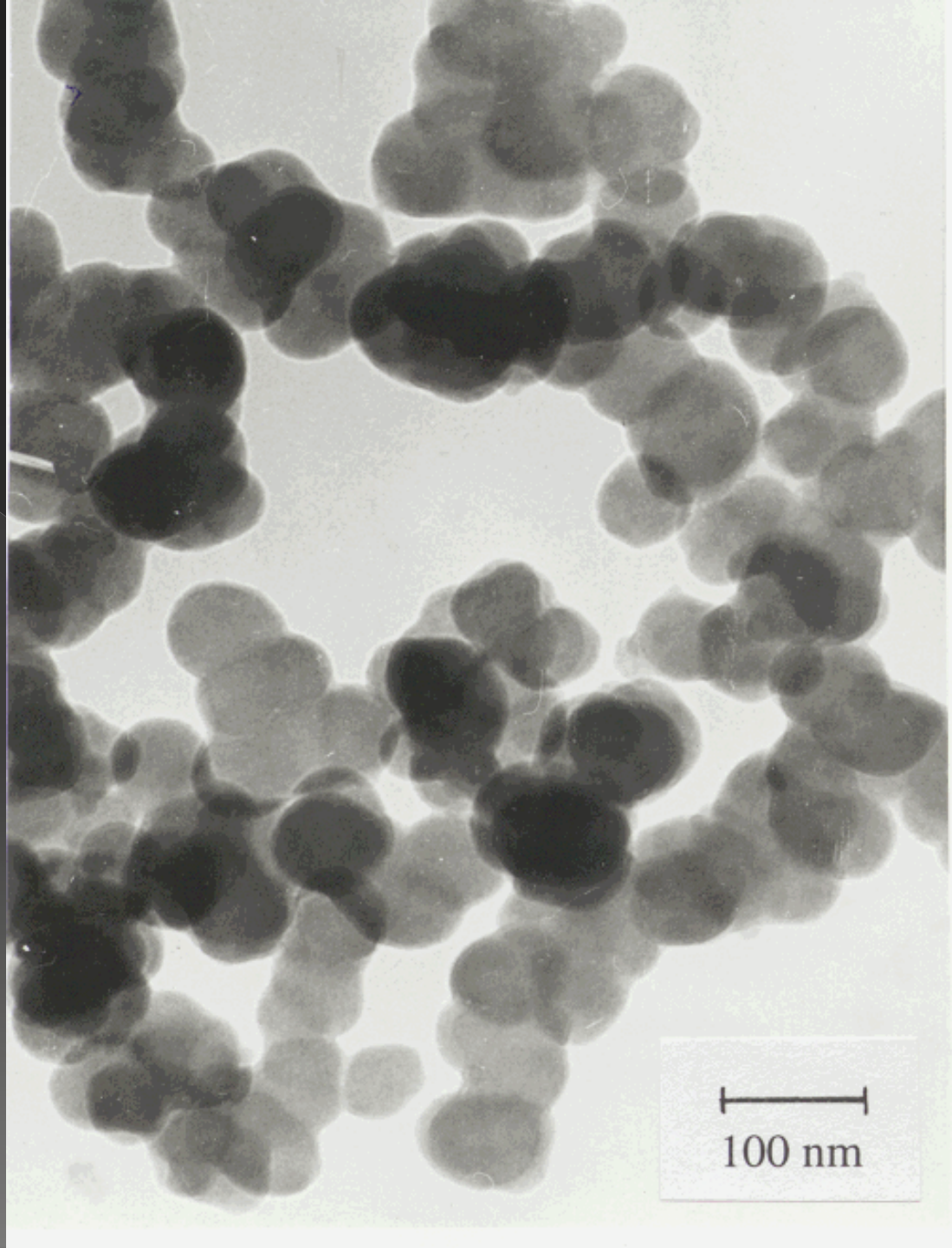

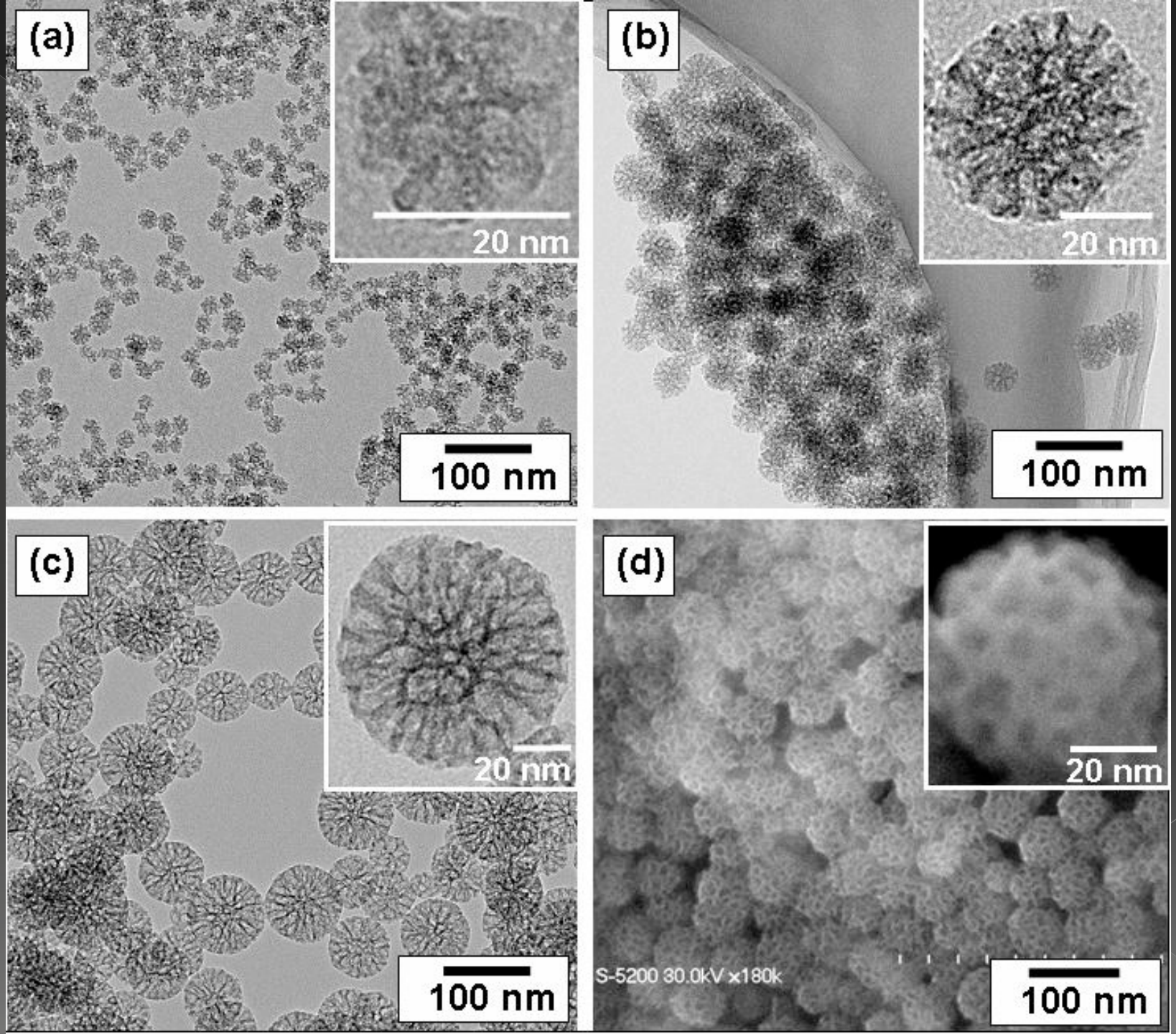
(a)
20 nm
100 nm
(b)
20 nm
100 nm
(c)
20 nm
100 nm
(d)
20 nm
S-5200 30.0kV ×180k
100 nm

Ball milling

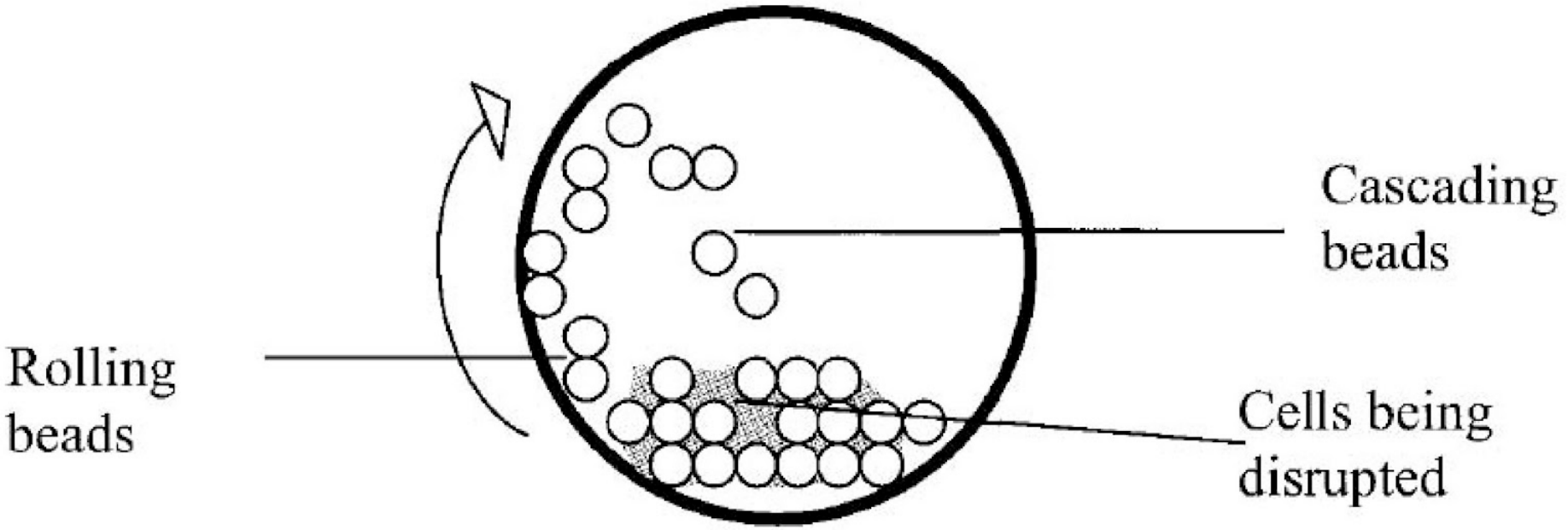

Industrial ball mills

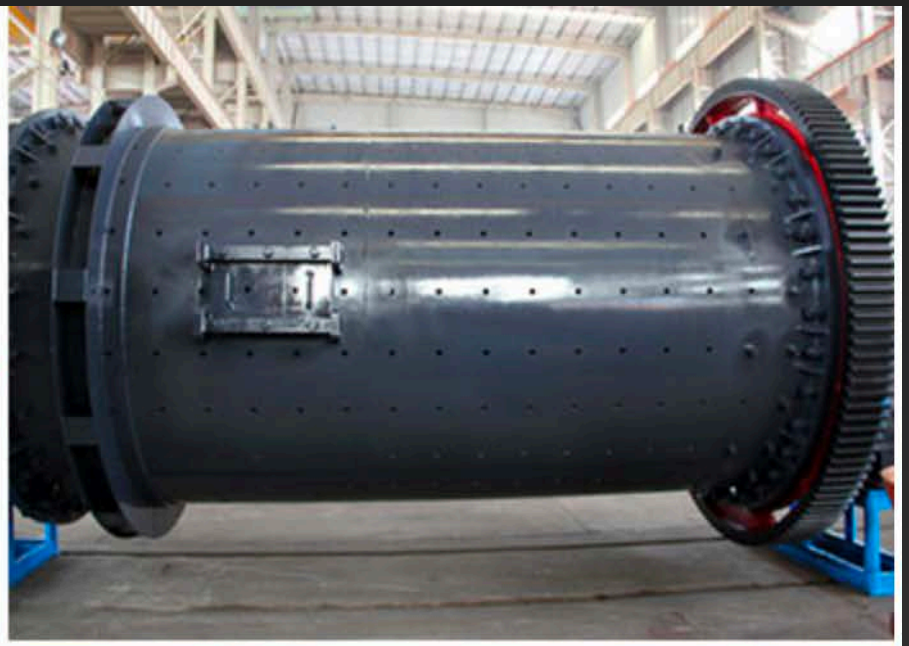

Attrition milling

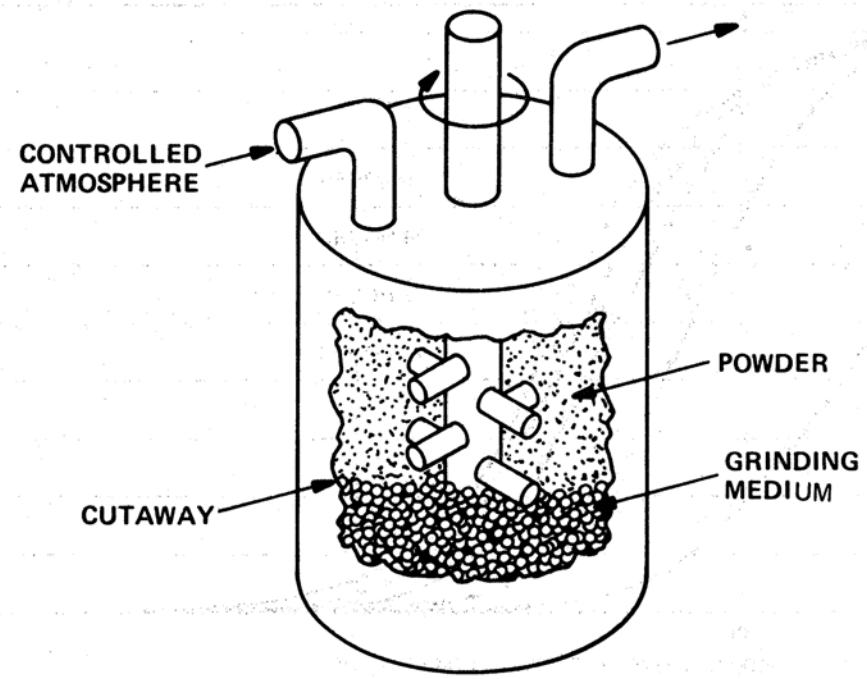

Figure 9.7 Schematic of an attrition mill. (Adapted from T. P. Herbell and T. K. Glasgow, NASA, paper presented at the DOE Highway Vehicle Systems Contractors Coordination Meeting, Dearborn, Mich., Oct. 17–20, 1978.)

Industrial attrition mills

CENTRIFUGAL IMPACT MILLS

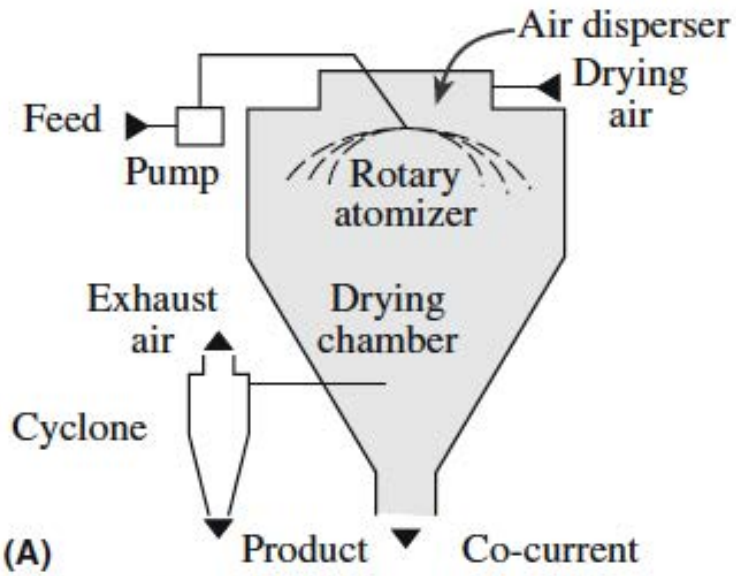

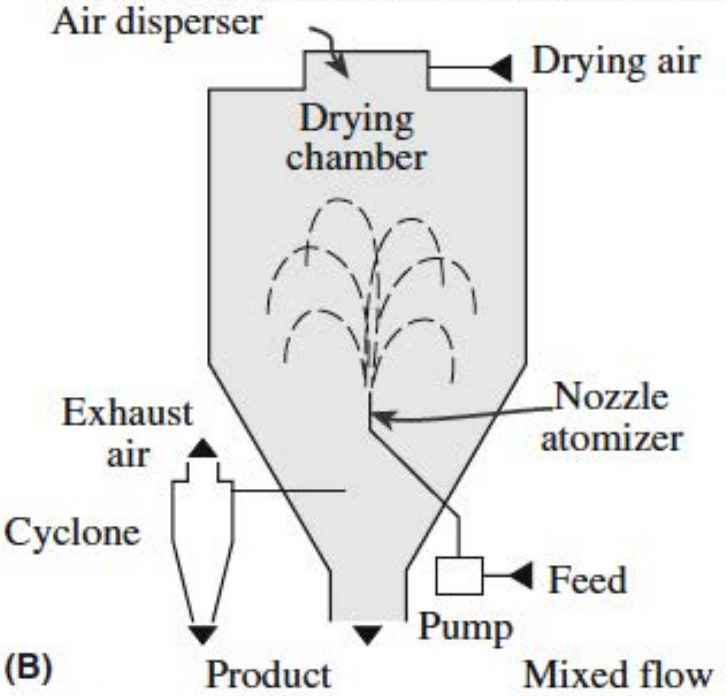

FIGURE 20.3 Spray dryers: (a) Centrifugal atomizer with cocurrent air flow. (b) Nozzle atomizer using mixed-flow conditions.

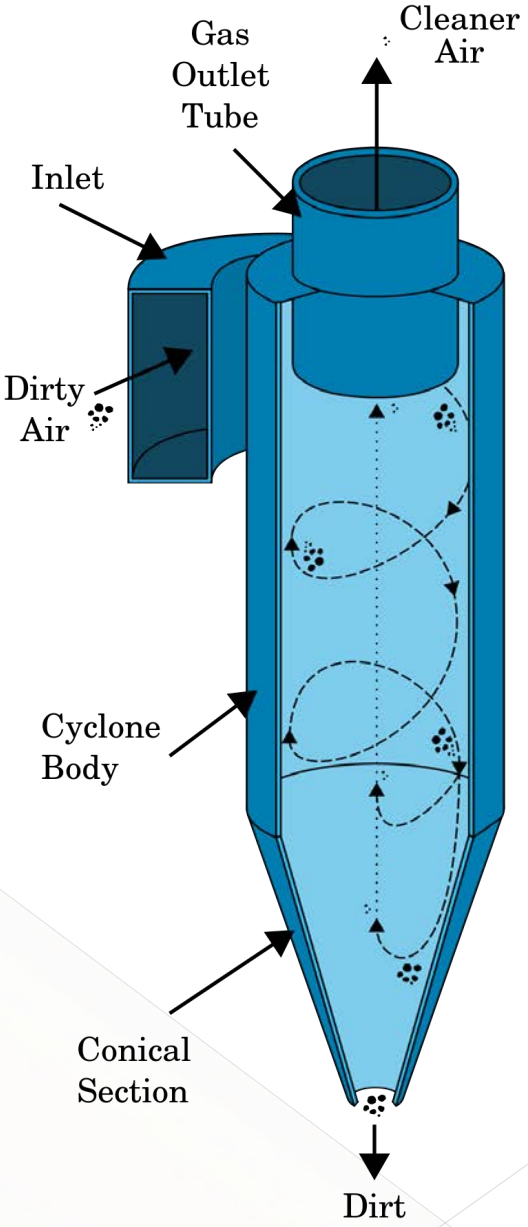

Cyclone

Shaping

- Pressing
  - Uniaxial
    - Cold
    - Hot
  - isostatic
    - Cold
    - Hot
- Casting
  - -Drain
  - -Squeeze
  - -Centrifugal
  - TAPE casting
- Extrusion
- Injection Moulding (very rare)

Overall process from starting powder to slurry:
https://www.youtube.com/watch?v=UHD1SzAJjU8

Slurry preparation (impasto/barbottina)

- Ceramic powder 50%
- Water (or other suspension media) 40%
- Binder (legante) 5%
  - Organic: PVA, PEG, Cellulose, starch
  - Inorganic: Clay, colloidal silica, aluminates
- Plasticizer (plasticizzante) 2-3%
- Lubricant (lubrificante) 1-2%
  - Stearic acid or stearata
  - Graphite, BN, steatite

Typical composition of slurry

Components	Amounts (%)
PZT powder	65–70
Dispersant	1.25
Solvent	25
Plasticizer	1.75
Binder	2

TABLE 23.3 Examples of Compositions of Extruded Bodies (Composition in vol%)

Refractory alumina		*High alumina*		*Electrical porcelain*	
Alumina (<20 μm)	50	Alumina (<20 μm)	46	Quartz (<44 μm)	16
Hydroxyethyl cellulose	6	Ball clay	4	Feldspar (<44 μm)	16
Water	44	Methylcellulose	2	Kaolin	16
$AlCl_3$ (pH > 8.5)	<1	Water	48	Ball clay	16
		$MgCl_2$	<1	Water	36
				$CaCl_2$	<1

TABLE 23.4 Additives for Injection Molding of SiC

Function	*Example*	*Quantity (wt%)*	*Volatilization temperature*
Thermoplastic resin	Ethyl cellulose Polyethylene Polyethylene glycol	9–17	200–400°C
Wax or high-temperature volatilizing oil	Paraffin Mineral oils Vegetable oils	2–3.5	150–190°C
Low-temperature volatilizing hydrocarbon or oil	Animal oils Vegetable oils Mineral oils	4.5–8.5	50–150°C
Lubricant or mold release	Fatty acids Fatty alcohols Fatty esters	1–3	
Thermosetting resin	Epoxy Polyphenylene Phenol formaldehyde		Gives carbon 450–1000°C

Uuniaxial pressing

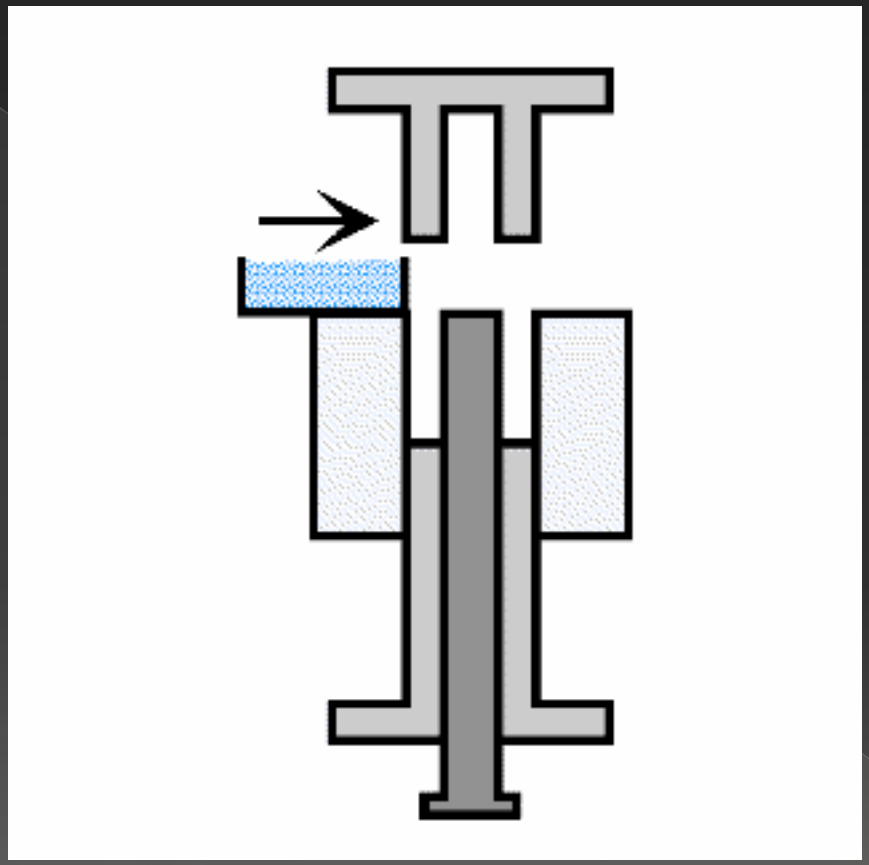

https://www.youtube.com/watch?v=WuxRkt_icso

Cold Isostatic Pressing

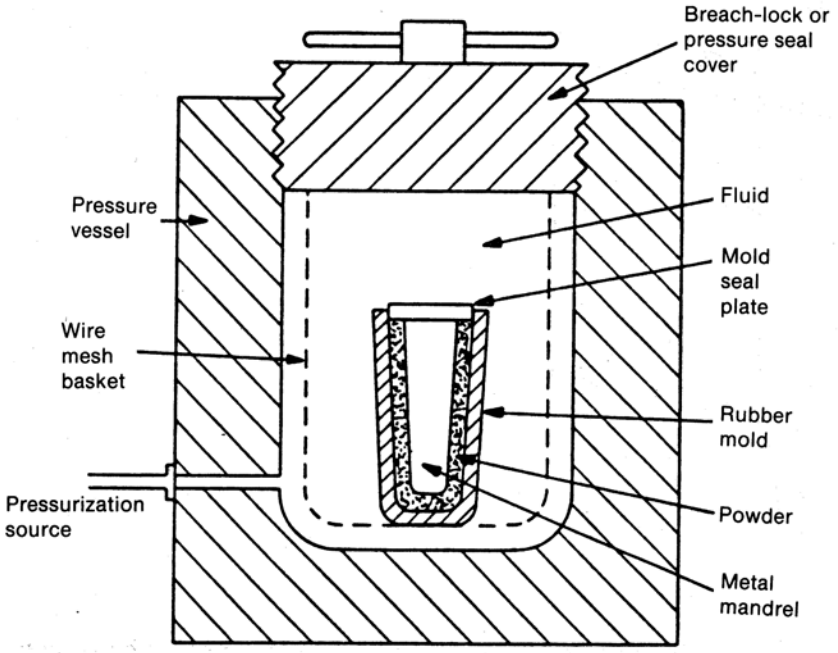

Figure 10.18 Schematic of a wet-bag isostatic pressing system. (© ASM International.)

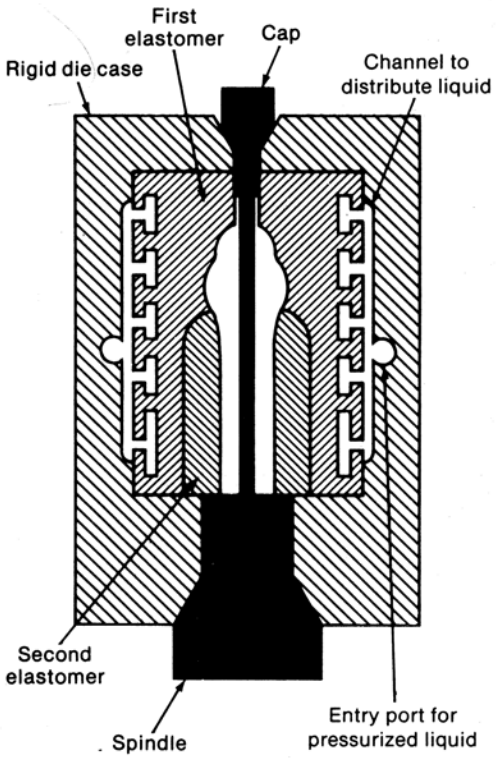

Figure 10.19 Schematic of a die for dry-bag isostatic pressing of a spark plug insulator. (© ASM International.)

Uniaxial hot press

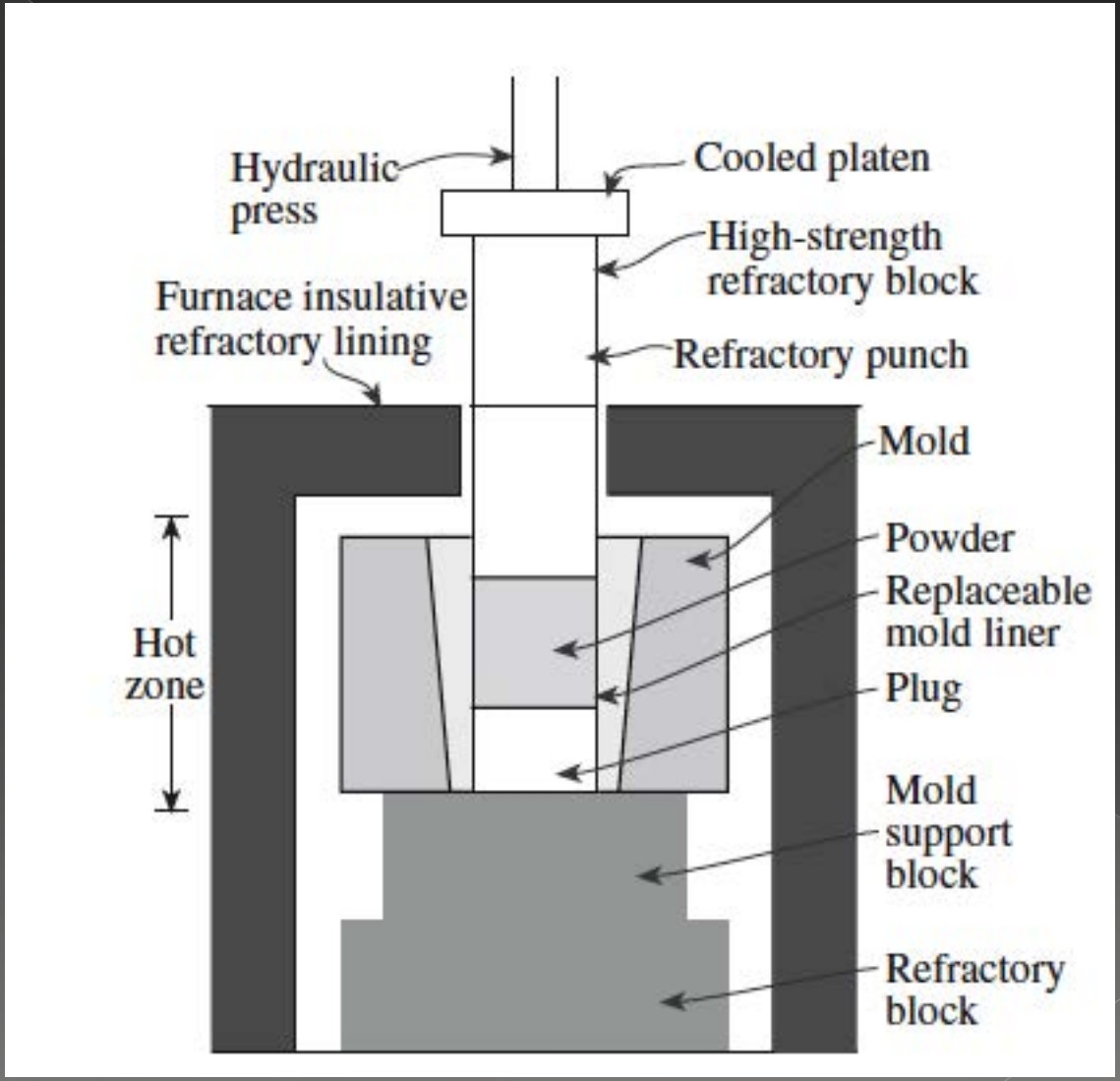

Isostatic Hot press

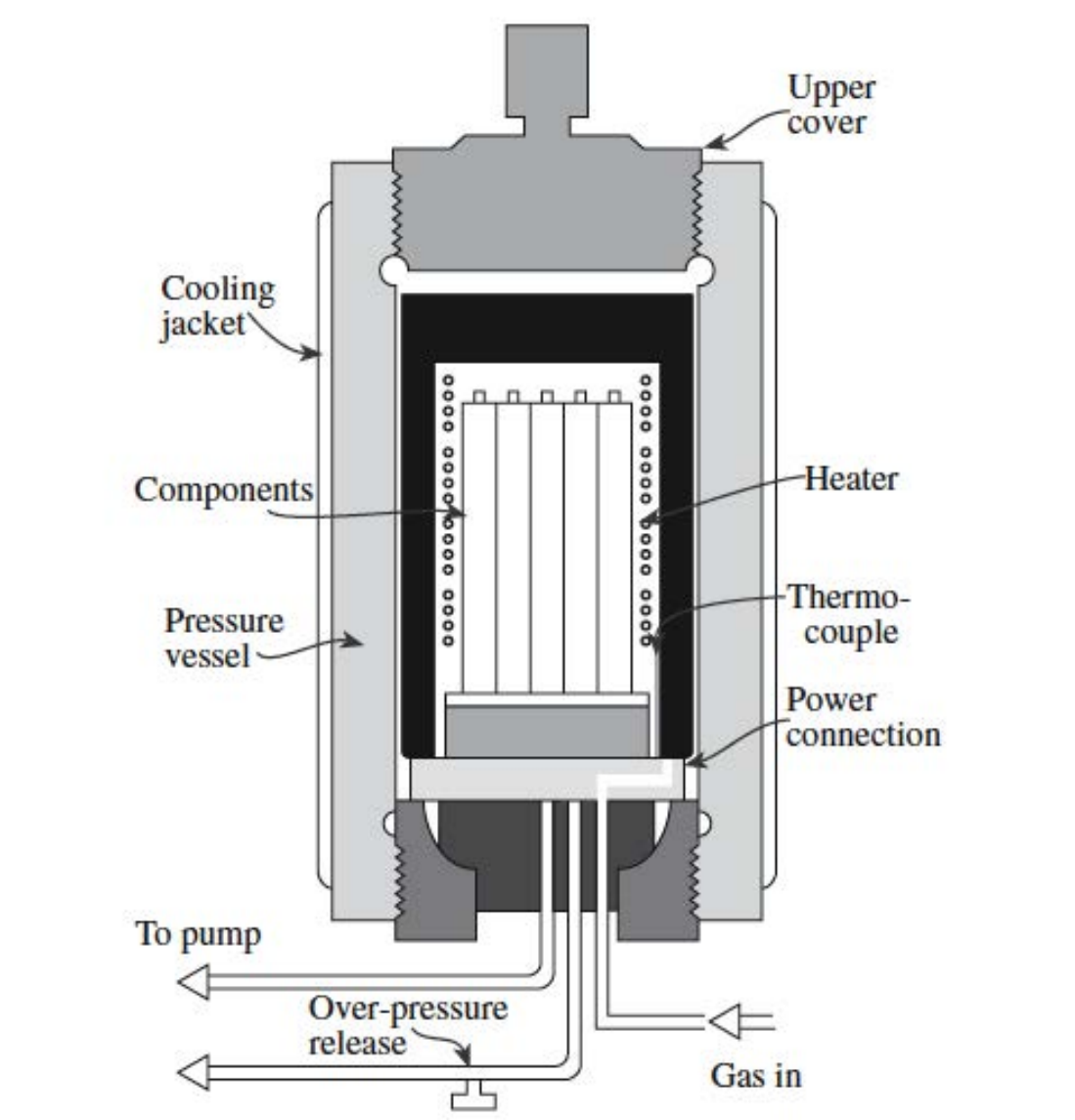

Drain Casting

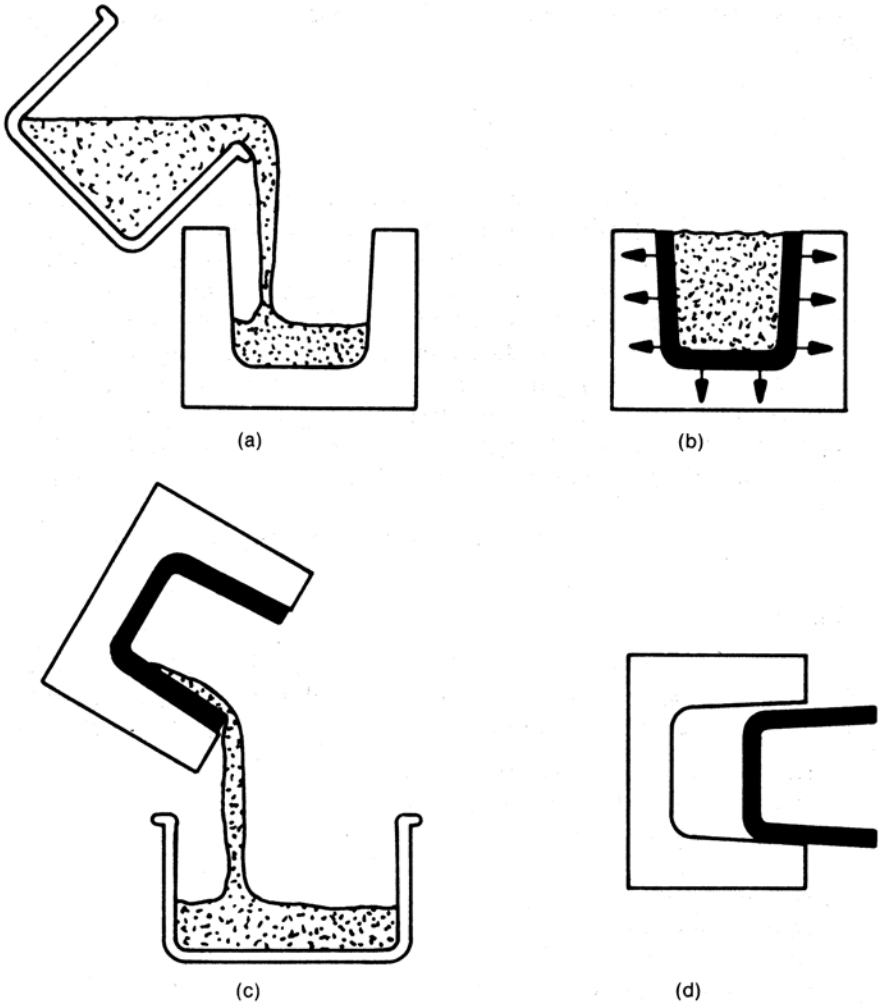

Figure 10.34 Schematic illustrating the drain-casting process. (a) Fill mold with slip, (b) mold extracts liquid, forms compact along mold walls, (c) excess slip drained, and (d) casting removed after partial drying.

Casting

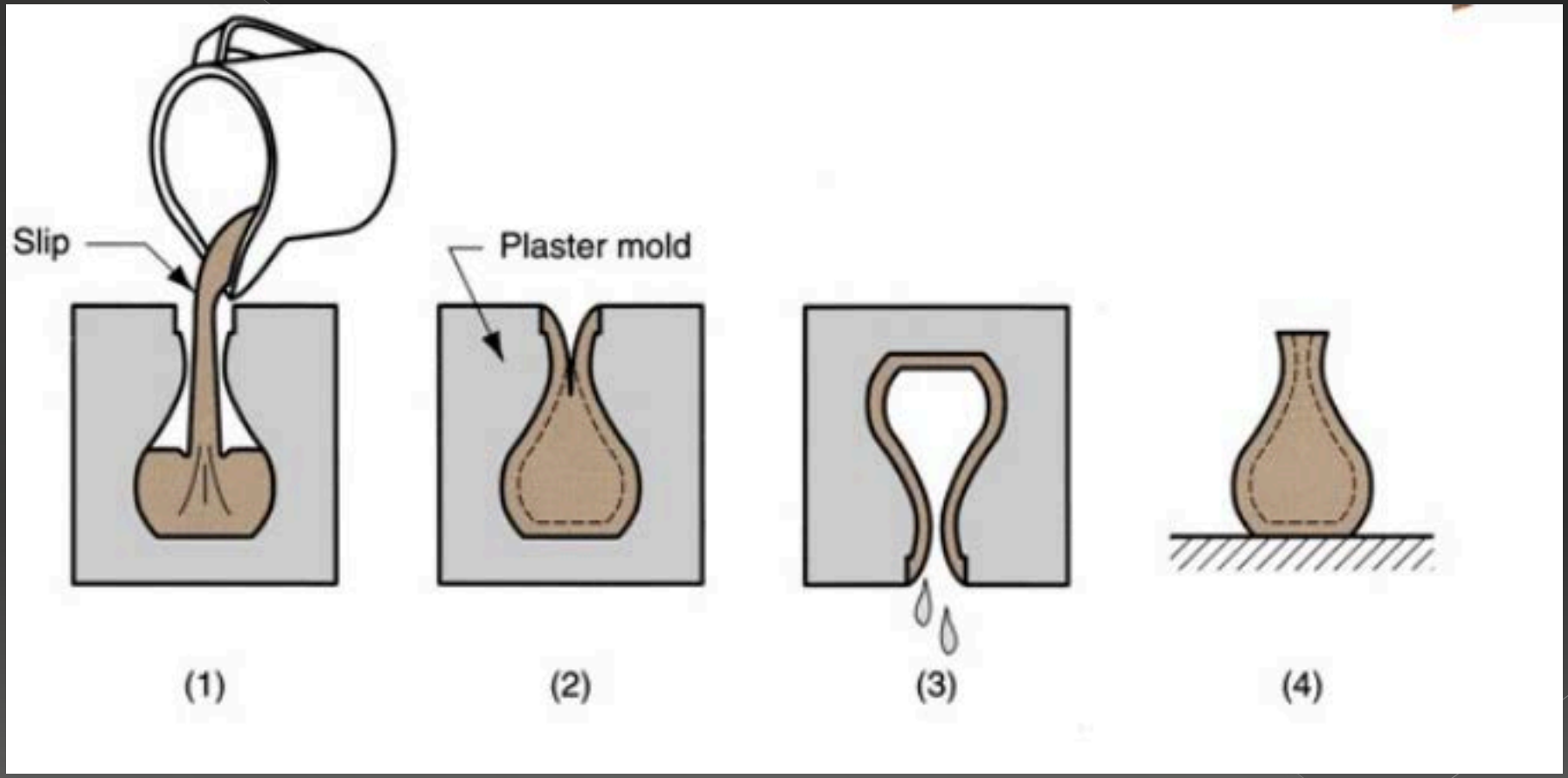

https://www.youtube.com/watch?v=FZzOTXgIhqs

SLIP CASTING

Tape Casting

Fabrication process for thin ceramic sheets

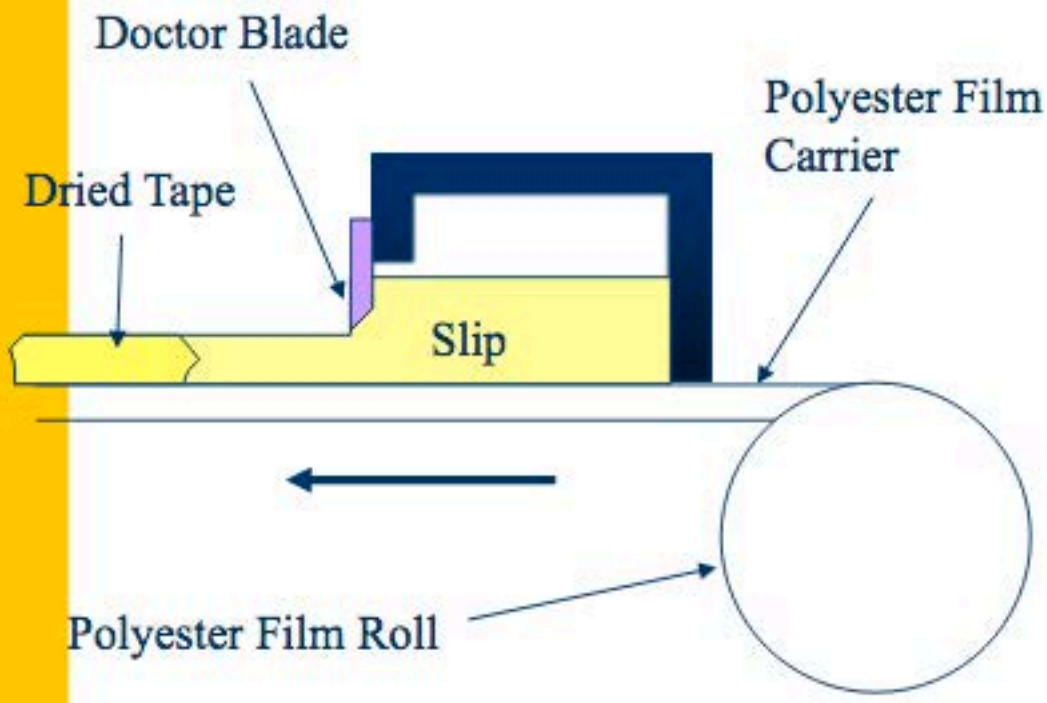

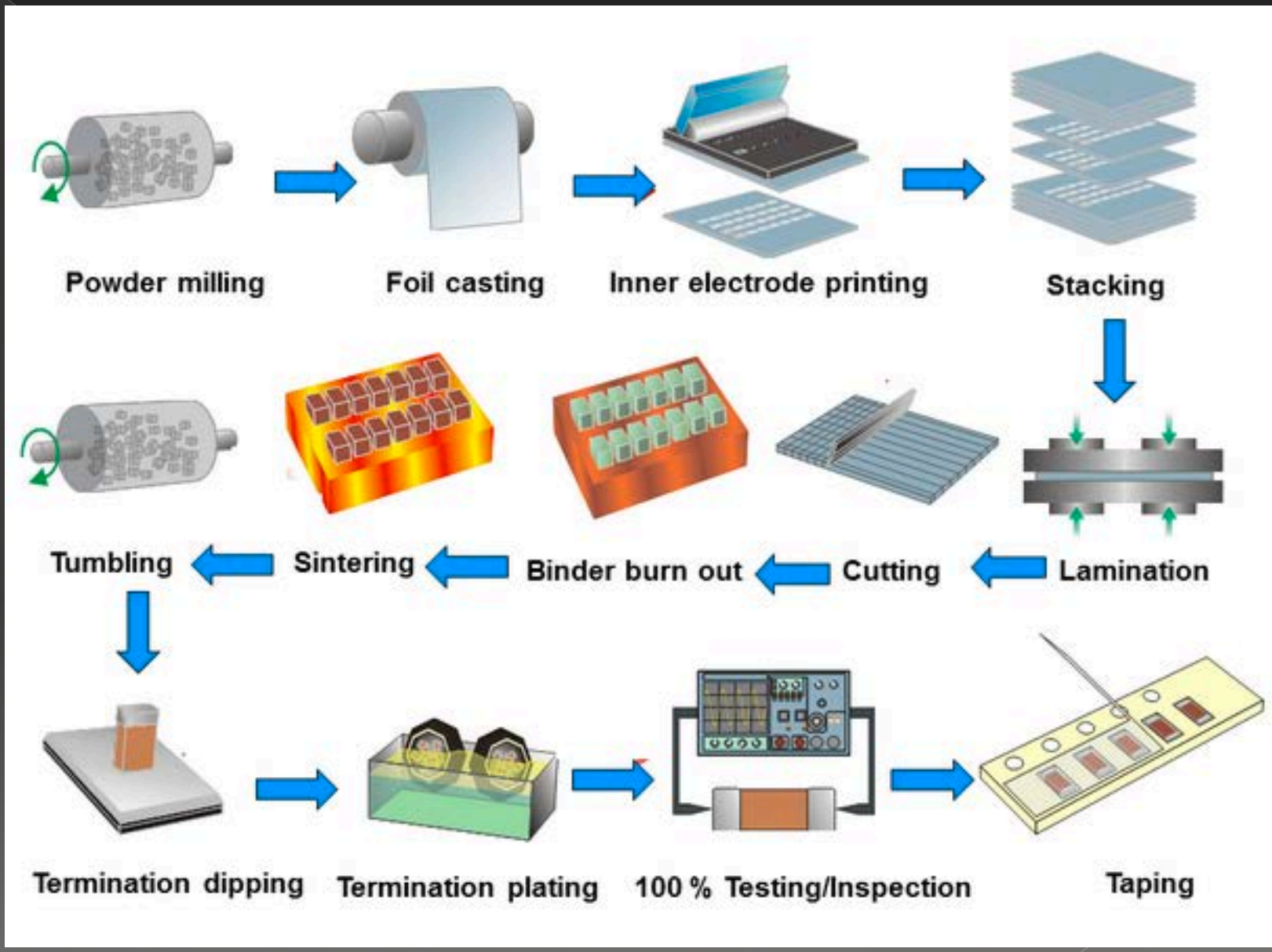
Powder milling
Foil casting
Inner electrode printing
Stacking
Lamination
Cutting
Binder burn out
Sintering
Tumbling
Termination dipping
Termination plating
100 % Testing/Inspection
Taping

Extruder Sectional View

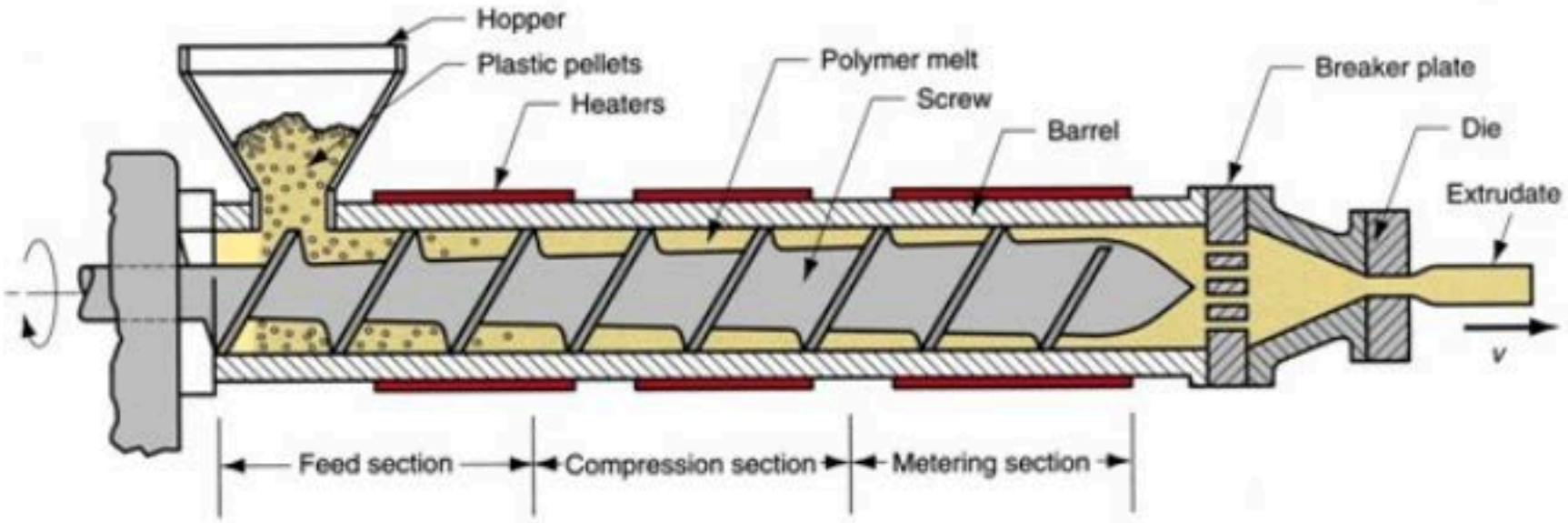

Components and features of a (single-screw) extruder for plastics and elastomers

https://www.youtube.com/watch?v=OqloeOubnmY

TABLE 23.3 Examples of Compositions of Extruded Bodies (Composition in vol%)

Refractory alumina		*High alumina*		*Electrical porcelain*	
Alumina (<20 μm)	50	Alumina (<20 μm)	46	Quartz (<44 μm)	16
Hydroxyethyl cellulose	6	Ball clay	4	Feldspar (<44 μm)	16
Water	44	Methylcellulose	2	Kaolin	16
$AlCl_3$ (pH > 8.5)	<1	Water	48	Ball clay	16
		$MgCl_2$	<1	Water	36
				$CaCl_2$	<1

SINTERING PROCESS

Silvia Dalla Marta
(dal corso di Scienza e tecnologia dei materiali ceramici
prof. V. Sergo)

It is a thermal process of microstructural rearrangement in which the particles of powder are compacted and the porosity decreases to form a dense piece of ceramic.

monodisperse powder fcc or hcp: PF=74.5%

ceramic matherial with porosity:
before sintering

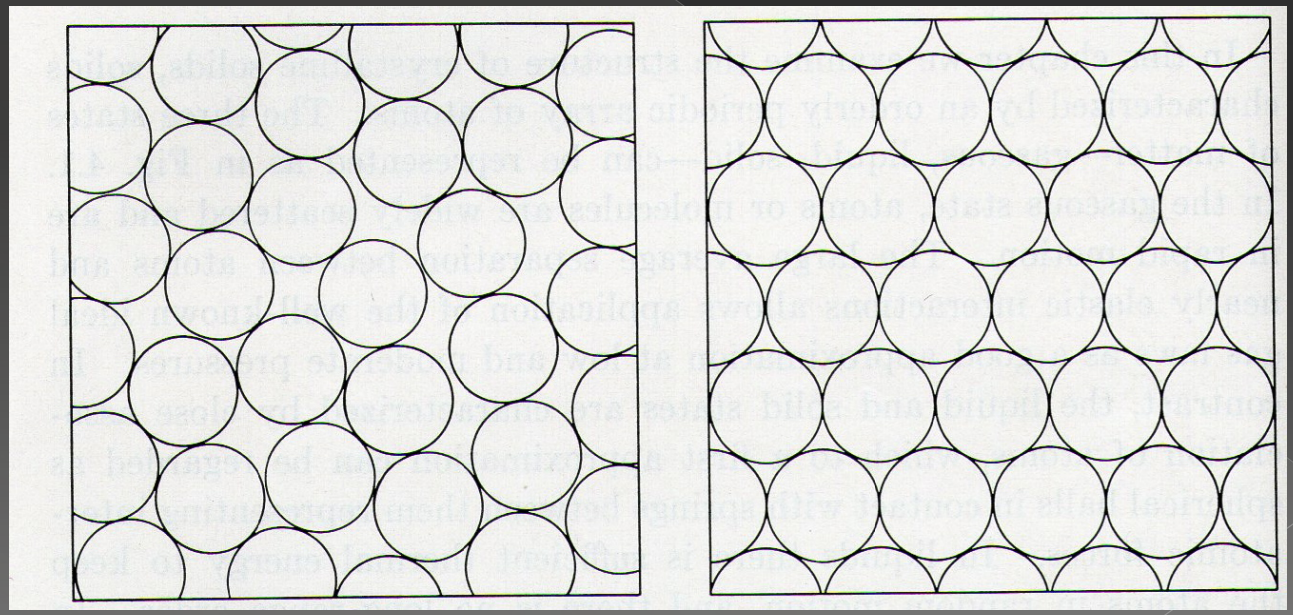

FORMATURE?

The absence of defects and porosity is very important for the *mechanical properties*:

$$K_{IC} = y\sigma\sqrt{c}$$

K: the parameter for the determination of the stress at the tip of the crack.
y: dimensionless constant that depends on defect's geometry and load
c: length of defect (m)

For the polycrystalline alumina: $K_{IC} = 3MPa\sqrt{m}$

In ceramics materials these values are very low compared to metals.
A very small defect or porosity lead to failure during an application of stress.

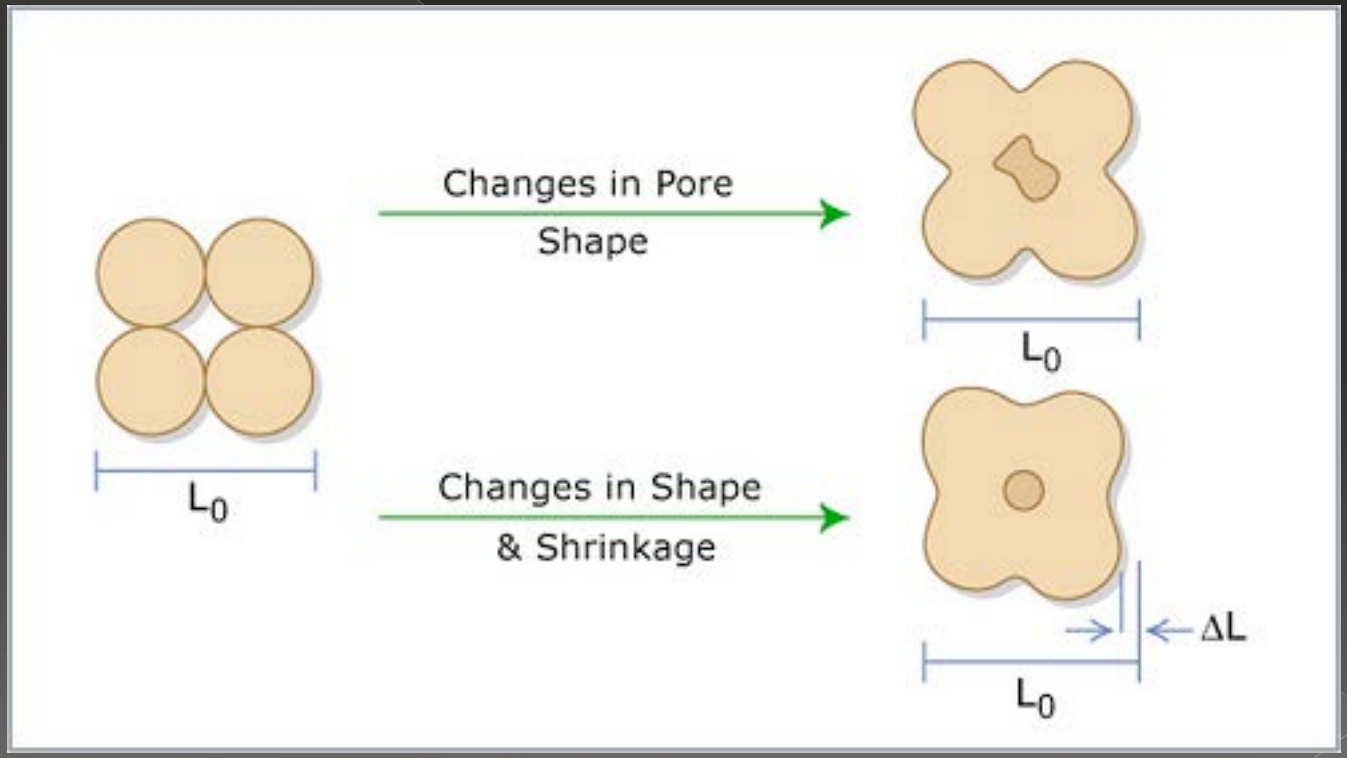
Changes in Pore
Shape
L_0
L_0
Changes in Shape
& Shrinkage
ΔL
L_0

BEFORE SINTERING:

- powder compact united by weaks Van der Waals forces
- individual grains separated by 25-60% of volume porosity

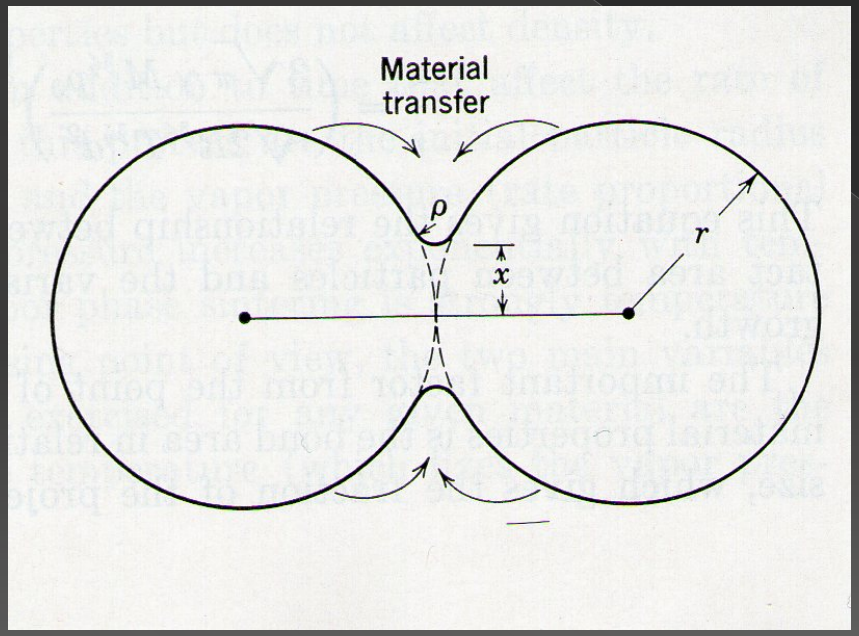

Considering two particles of ceramic material in contact with each other:

- concave zone
- convex zone

The atoms in a convex zone tend to *migrate* in a concave zone in according to a diffusion process actived by temperature.

DIFFUSION PROCESS

- Thermodinamically favored
- kinetically slow

FICK'S LAW (1D):

$$\frac{dC}{dt} = D\frac{d^2C}{dx^2}$$

Diffusion coefficient:

$$D = D_0 e^{-\frac{Ea}{RT}}$$

In order of kinetics to be fast enough for microstructural rearrangment to occur in *short time*, the sintering temperature must be:

$$T = \frac{2}{3}T_m$$

SINTERING MECHANISMS

- *SURFACE DIFFUSION*
- *VAPOR TRANSPORT*

NO ***densification***

thinning of the particles

- *BULK DIFFUSION*
- *GRAIN BOUNDARY DIFFUSION*

densification

decrease of the distance between particle centres

Thinning due to vapor phase matherial transfer:

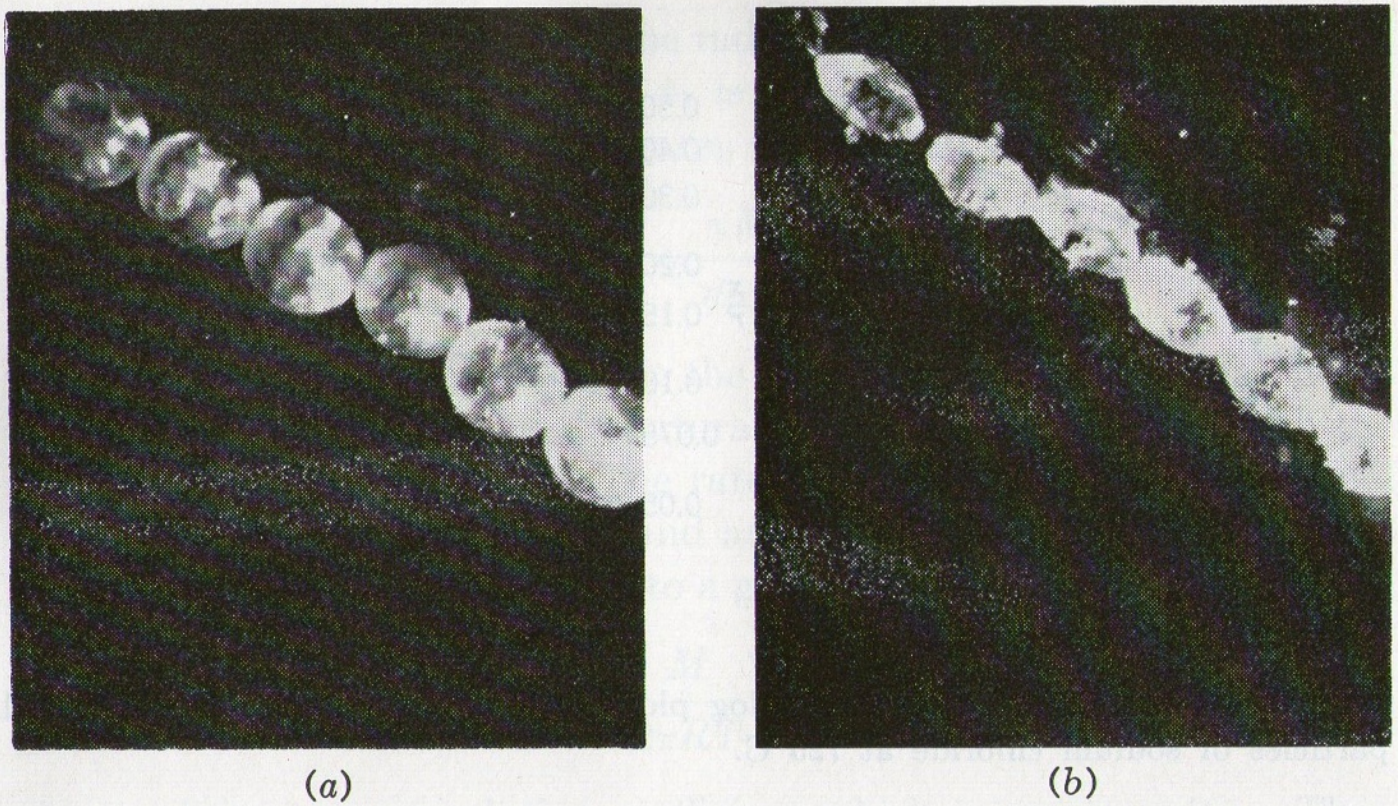

(*a*) (*b*)

Fig. 12.17. Photomicrographs of sintering sodium chloride at 750°C: (*a*) 1 min, (*b*) 90 min.

DENSIFICATION:

- atoms migration in the neck zone
- pores disappearence
- obtaining straight grain boundaries
- same chemical potential
- thermodynamically stable

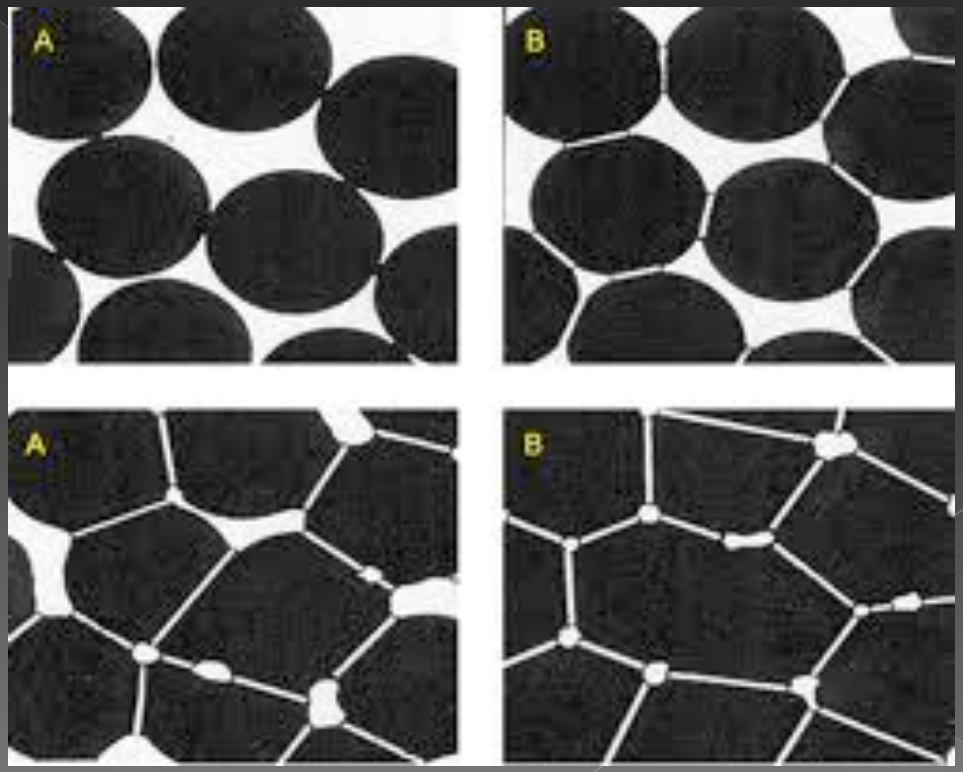

Monodispersed powder:
rare and expensive!

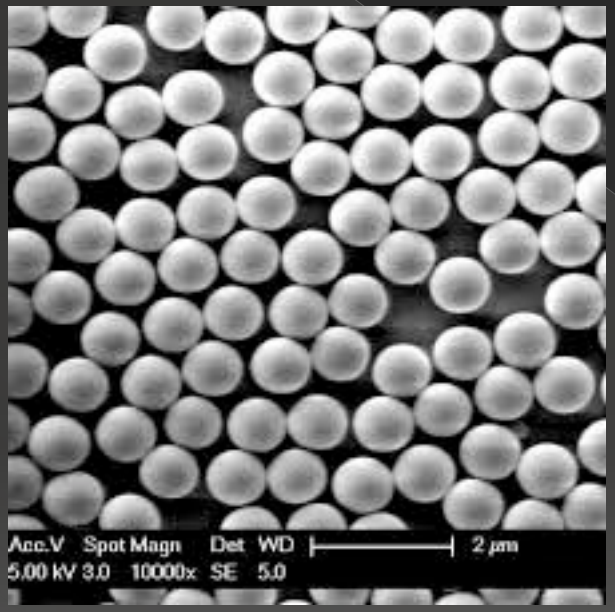

More frequent:
Grain size distribution!

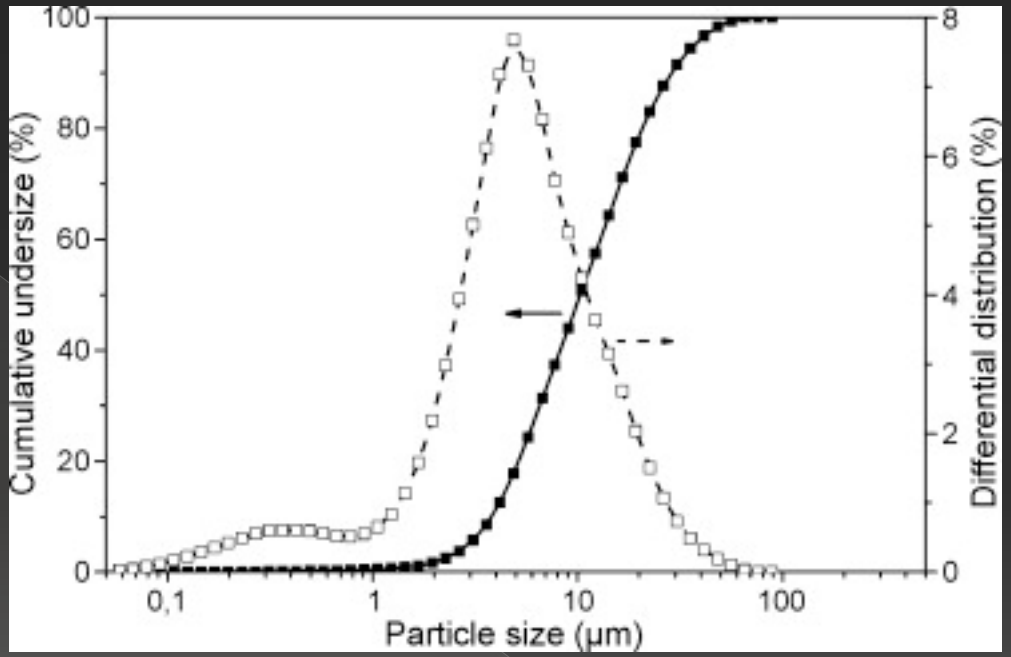

SECONDARY ABNORMAL OF BOUNDARY

Since grain boundaries migrate toward their centre of curvature,
grains with more than 6 sides tend to incorporate grains with less than 6 sides.

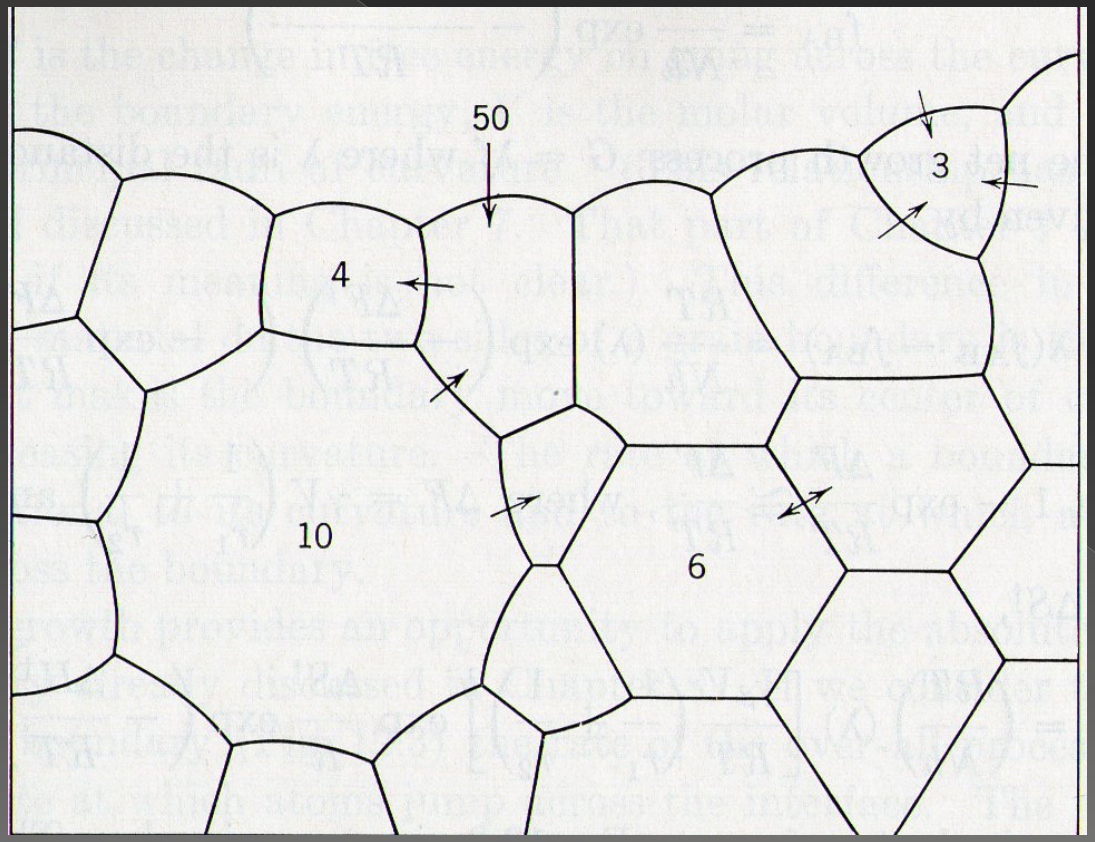

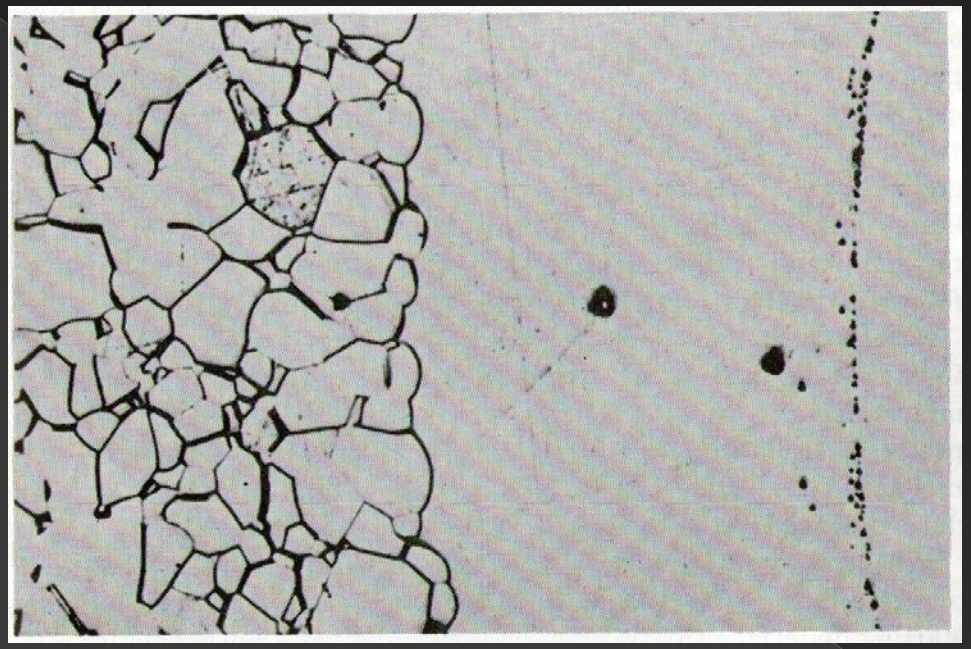

Growth of a large Al_2O_3 crystal into a matrix of uniformly sized grain.

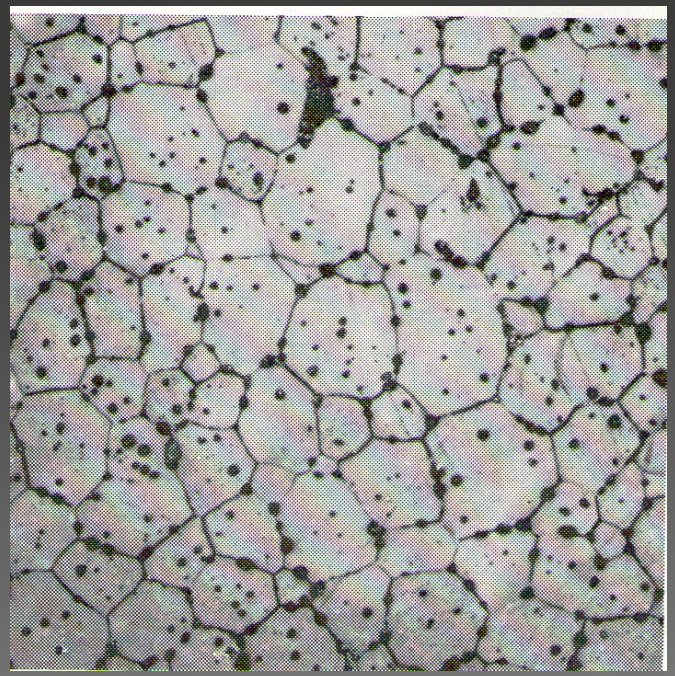

Polycrystalline flurite CaF_2 illustrating normal grain growth

PROGRESSIVE DEVELOPMENT OF MICROSTRUCTURE IN *LUCALOX ALUMINA*

a) SEM of initial particles befor sintering (5000x)

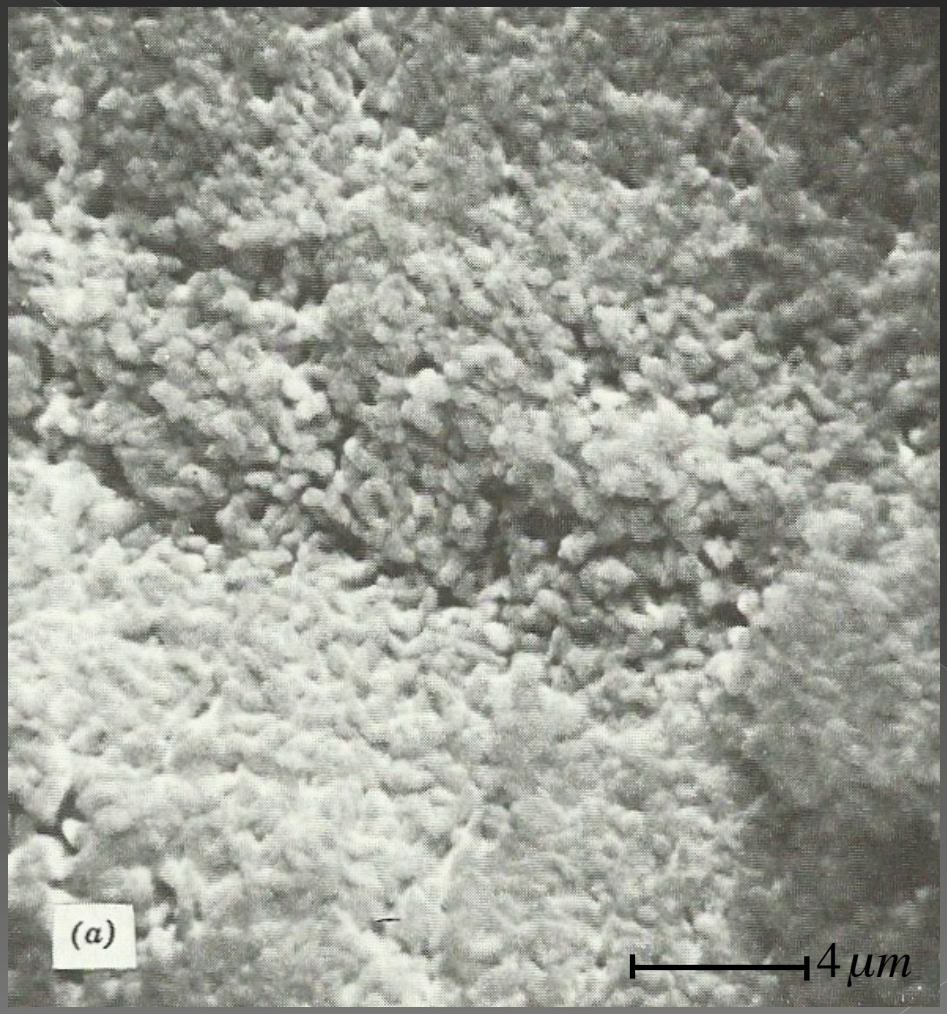

b) SEM of particles after1minute at 1700°C (5000x)

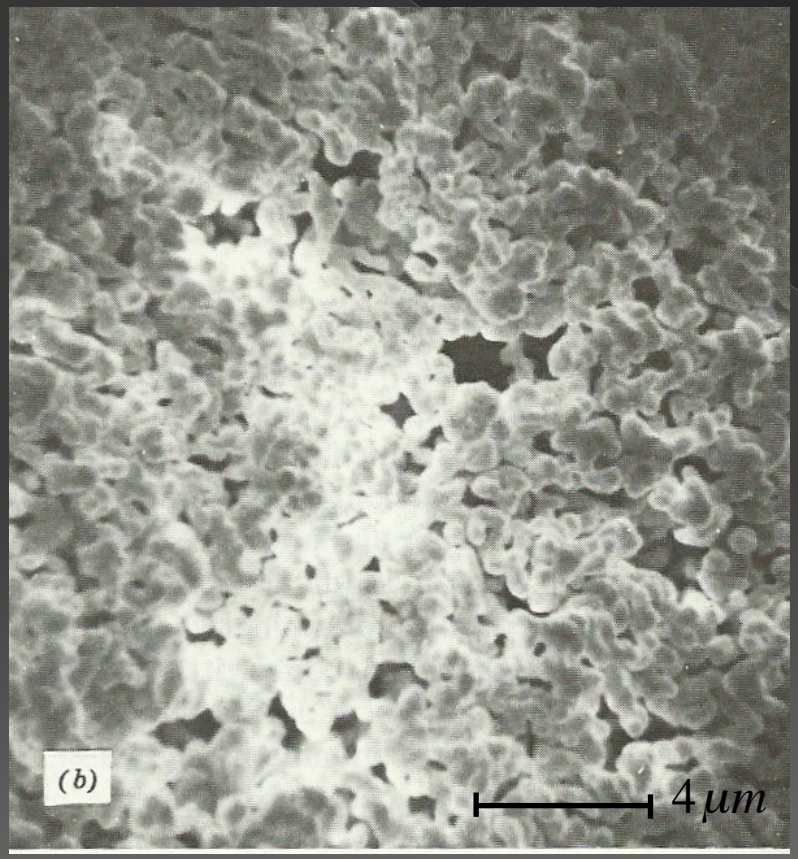

c) SEM of particles after 2 minutes at 1700°C (5000x)

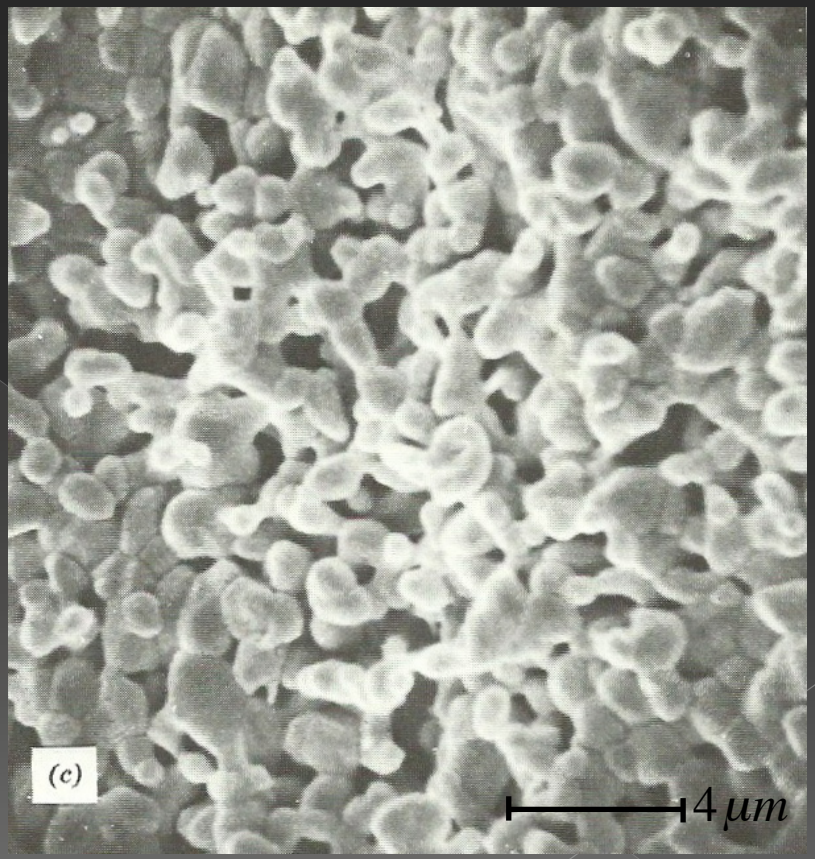

d) SEM of particles after 6 minutes at 1700°C (5000x)

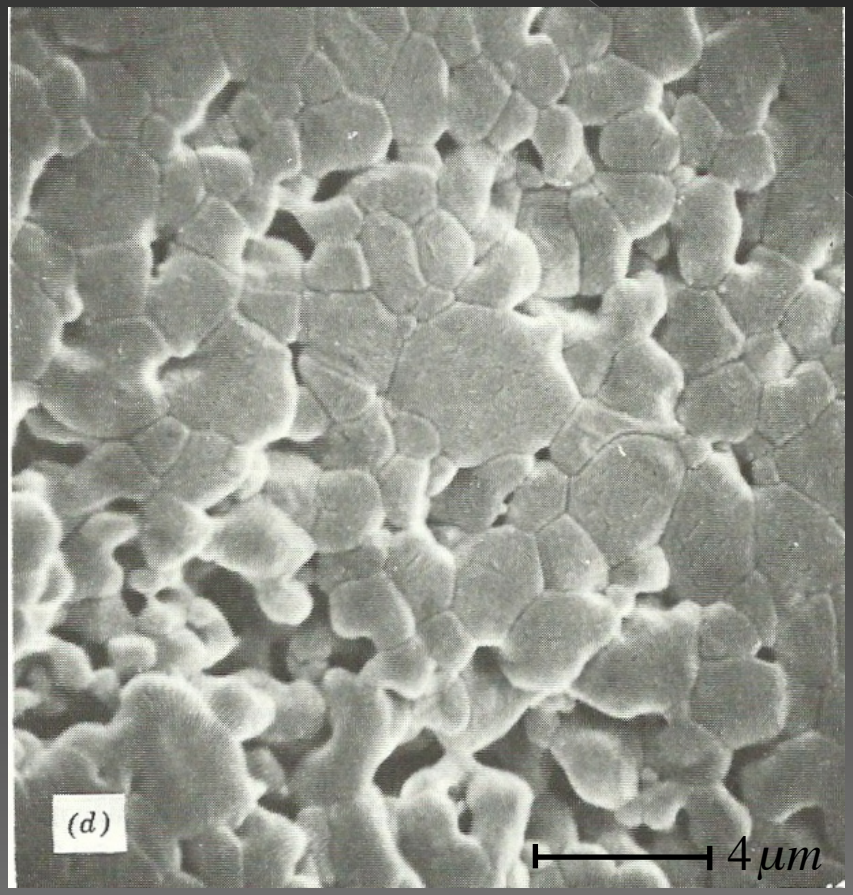

e) SEM of the final microstructure that is nearly porefree, with only a few pores located within grains (500x)

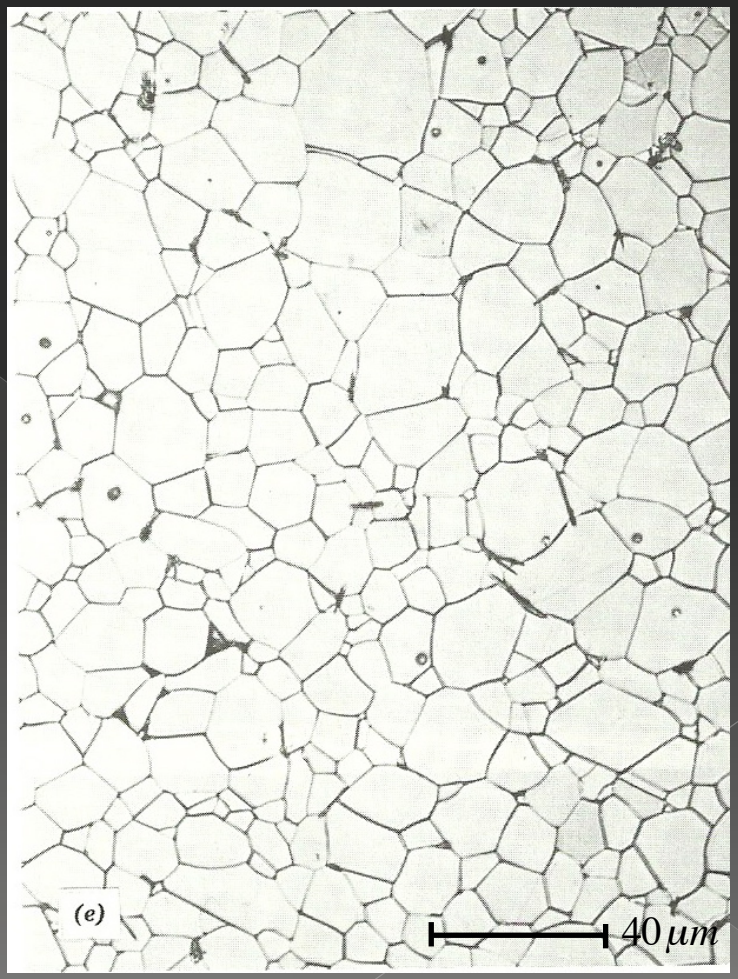

PRESSURE DIFFERENCE ACROSS A CURVED SURFACE

- The differences in the curvature of surface, causes a *pressure difference* in the various part of system, that leads to atoms transport.
- At the surface of the particle there is a positive radius of curvature, so that the vapour pressure is larger than would be observed in a flat surface.
- At the junction between particles there is a NECK whith a small negative radius of curvatures and a vapour pressure lower than that for the particle itself.

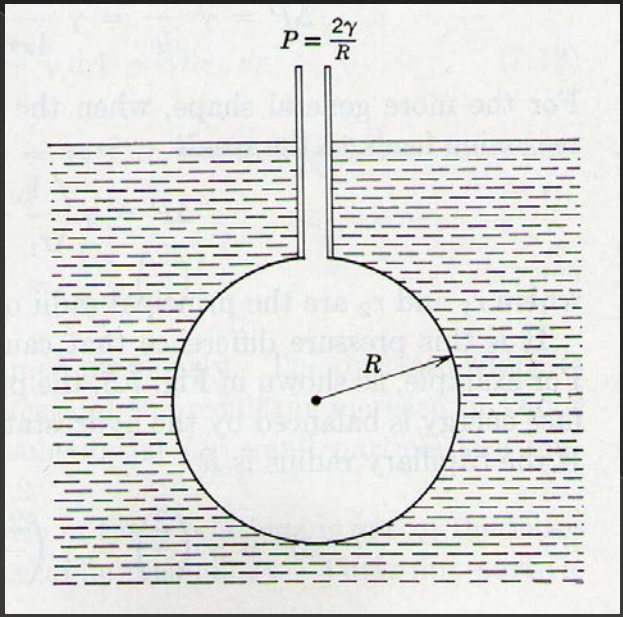

P : Supplementary pressure to create the bubble.

γ: surface tension

SPHERICAL MODEL:

$$A = 4\pi R^2 \qquad V = \frac{4}{3}\pi R^3$$

$$pdV = \gamma_{LV} dA$$

$$\Delta p 4\pi R^2 dR = \gamma_{LV} 8\pi R dR$$

$$\Delta p = \frac{2\gamma_{LV}}{R}$$

GENERICALLY:

$$\Delta p = \gamma_{LV}\left(\frac{1}{R_1} + \frac{1}{R_2}\right)$$

$$H_2O(l) \rightleftharpoons H_2O(g)$$

in equilibrium condition

$$p^\circ = K_e = e^{-\frac{\Delta G^0}{RT}}$$

vapour pressure of water
in a flat liquid-vapour interface

If the liquid-vapour interface is not flat, as in a small drops, the water has a vapour pressure that is larger than that in a flat surface:

$$e^{-\frac{\Delta G}{RT}} = e^{-\frac{\Delta G^0}{RT}} e^{-\frac{\overline{V}\Delta P}{RT}}$$

$$P_{H_2O} = P^0_{H_2O} e^{-\frac{2\gamma \overline{V}}{rRT}}$$

$P^0_{H_2O}$: standard vapour pression

Δp for water drops of different radii at STP

Droplet radius	1 mm	0.1 mm	1 μm	10 nm
Δp (atm)	0.0014	0.0144	1.436	143.6

ENERGY SURFACE

in a densification process in which the only energy is given by radius of curvature:

$$\bar{V} = \frac{MW}{\rho}$$

$$N = \frac{3MW}{4\pi a^3 \rho} = \frac{3\bar{V}}{4\pi a^3}$$

$$S_A = 4\pi a^2 N = \frac{4\pi a^2 3MW}{4\pi a^3 \rho} = 3\frac{\bar{V}}{a}$$

$$E_S = S_A \gamma = \frac{3\bar{V}\gamma}{a}$$

$\bar{V}$: molecular volume $\frac{cm^3}{mol}$

ρ : density $\frac{g}{cm^3}$

a : particle radius $\approx \mu m$

N : number of particles in a mole of powder

S_A : surface area m^2

E_S :surface energy $\frac{J}{mol}$

γ : surface tension $\approx 1\frac{J}{m^2}$

MW : molecular weight $\frac{g}{mol}$

- Energy available without added pressure in a sintering pocess of alumina:

$$E_S = \frac{3\bar{V}\gamma}{a} = 75\frac{J}{mol}$$

- Energy available with added pressure in the same sintering:

$$w = P_A\bar{V} = 750\frac{J}{mol}$$

$$P = 30Mpa$$

$$\bar{V}_{Al_2O_3} = 25\cdot10^{-6}\frac{m^3}{mol}$$

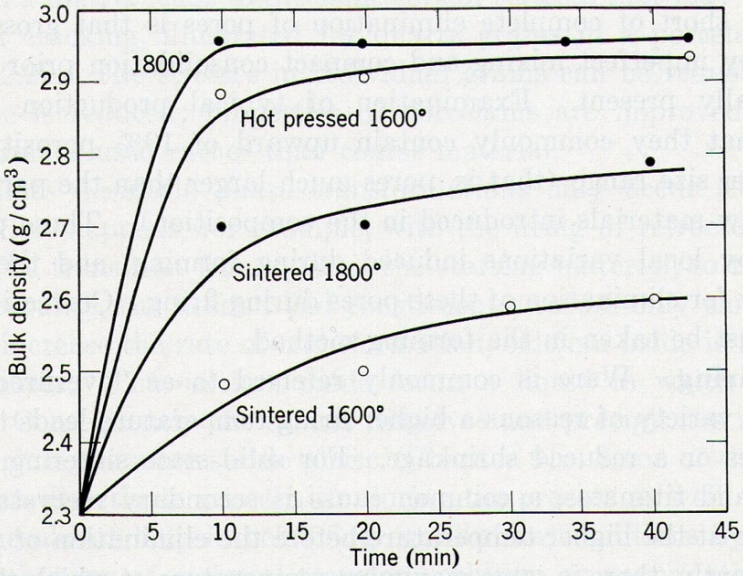

Fig. 12.30. Densification of beryllia by sintering and by hot pressing at 2000 psi.

Image from Kingery

DIFFUSION AND MOBILITY:

true in the absence of friction:

$$F = ma$$

otherwise:

$$F = m\frac{dv}{dt} + \frac{v}{M}$$

Einstein's generalized equation of mobility:

$$D = MRT$$

$\frac{v}{M}$: friction coefficient

M : mobility

D : diffusion coefficient

KINETIC MODELING OF SINTERING PROCESS

PARAMETERS TO DEFINE THE MODEL:

- *define a DRIVING FORCE*
- *define the GEOMETRY*
- *define the MECHANISM OF TRANSPORT*

STAGES OF THE SINTERING:

- *INITIAL STAGE :* from 50-55% to 75% of TD ⟶ *MODELING*
- *INTERMEDIATE STAGE :* from 75% to 92% of TD
- *FINAL STAGE :* from 92% to 100% of TD

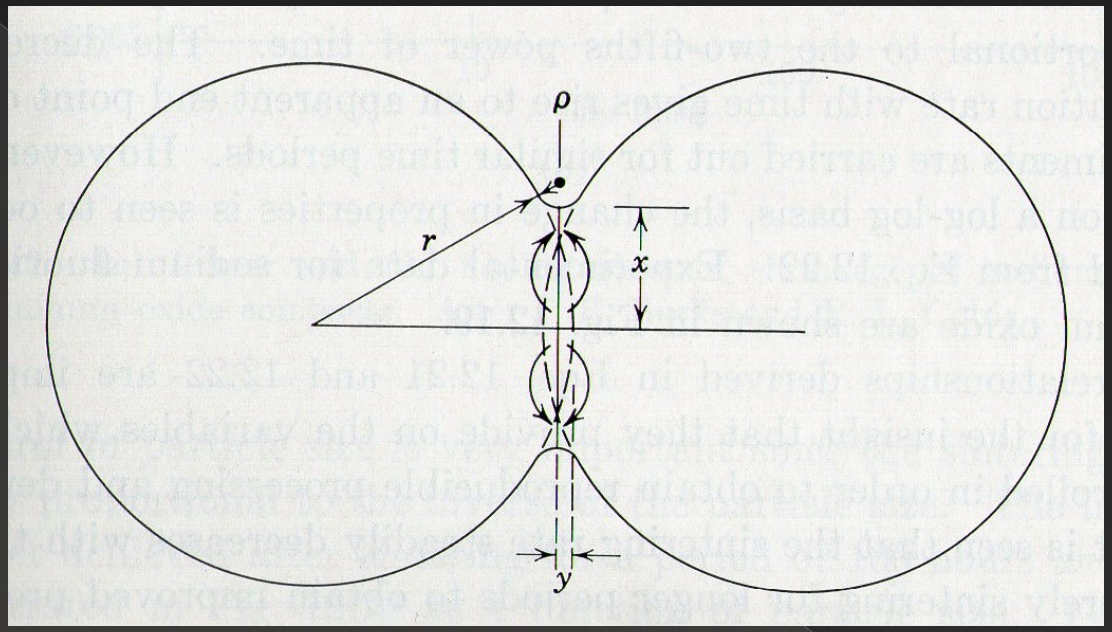

ρ : radius of the neck's curvature

r : radius of particle

x : parameter indicated the progress of the sintering

GEOMETRY

$$(r+\rho)^2 = (r-\rho)^2 + (x+\rho)^2$$

$$\rho = \frac{x^2}{4r}$$

$$A_{Neck} = 2\pi x \cdot \pi\rho = \frac{\pi^2 x^3}{2r}$$

$$V_{Neck} = \frac{\pi x^4}{8r}$$

Approximations :

$$\rho^2 = 0$$

$$x\rho = 0$$

FLUX

The material transfer is linked to the flux.
Considering the area through which the transport takes (the neck area):

$$J = \frac{1}{A_{Neck}} \frac{d}{MW} \frac{dV_{Neck}}{dt}$$

d : density
MW : molecoular weight
J : flux

$$\frac{dV_{Neck}}{dt} = \frac{4\pi x^3}{8r} \frac{dx}{dt} = \frac{\pi x^3}{2r} \frac{dx}{dt}$$

Variation of the neck volume based on the increase of the 'x' parameter:

$$J = \frac{2r}{\pi^2 x^3} \frac{d}{MW} \frac{\pi x^3}{2r} \frac{dx}{dt} = \frac{1}{\pi \bar{V}} \frac{dx}{dt}$$

FLUX expressed as a DRIVING RORCE

$$J = cMF$$

c : concentration
M : mobility of bulk and grain boundary atoms
F : force

$$M = \frac{D}{RT}$$

$J = cMF$

$$F = -\nabla G = -\frac{dG}{dx} \approx \frac{dG}{\rho}$$

Variation of the free energy during the diffusion on the neck area:

$$\Delta G = \Delta p \overline{V} = \overline{V}\gamma\left(\frac{1}{r_1} + \frac{1}{r_2}\right) = \overline{V}\gamma\left(\frac{1}{x} - \frac{1}{\rho}\right) = \frac{\overline{V}\gamma}{\rho}$$

$$F = \frac{\Delta G}{\rho} = \frac{\overline{V}\gamma}{\rho^2}$$

$$J = cMF = c\frac{D}{RT}\frac{\overline{V}\gamma}{\rho^2}$$

$$\frac{1}{\overline{V}\pi}\frac{dx}{dt} = \frac{cD}{RT}\frac{\overline{V}\gamma}{\frac{x^4}{16r^2}}$$

integration between o and x

t=o, x=o

$$\frac{1}{5}x^5 = \frac{5\pi\overline{V}^2 cD\gamma r^2}{RT}t$$

$$x = \left(\frac{5\pi\overline{V}^2 cD\gamma r^2}{RT}\right)^{\frac{1}{5}} t^{\frac{1}{5}}$$

t: sintering time

Variation of the volume of the particles in the sintering process during the time:

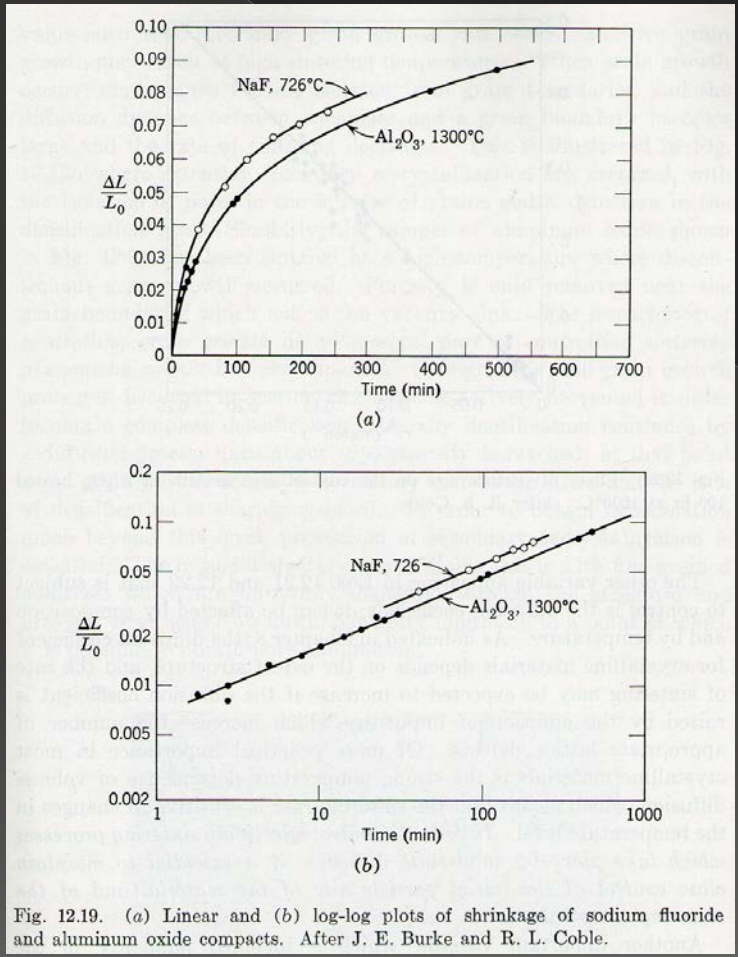

Fig. 12.19. (*a*) Linear and (*b*) log-log plots of shrinkage of sodium fluoride and aluminum oxide compacts. After J. E. Burke and R. L. Coble.

Variation of the relative density variatung time and temperature:

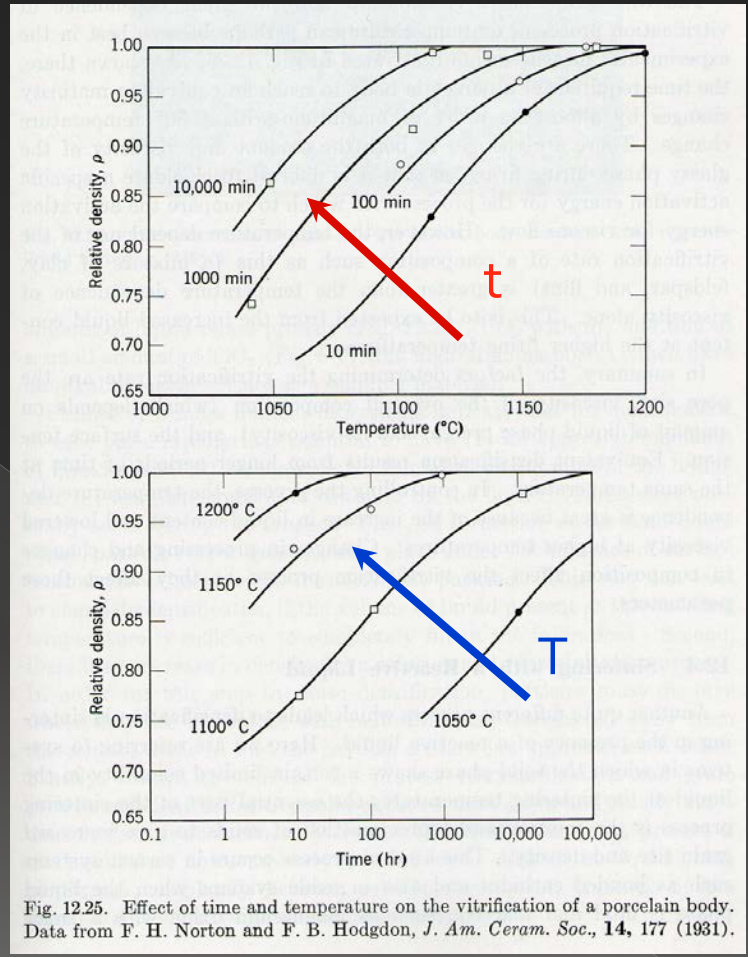

Fig. 12.25. Effect of time and temperature on the vitrification of a porcelain body. Data from F. H. Norton and F. B. Hodgdon, *J. Am. Ceram. Soc.*, **14**, 177 (1931).

The increase of a few degrees in temperature has much more influence on the grain size than the increase of a one order of magnitude of the time

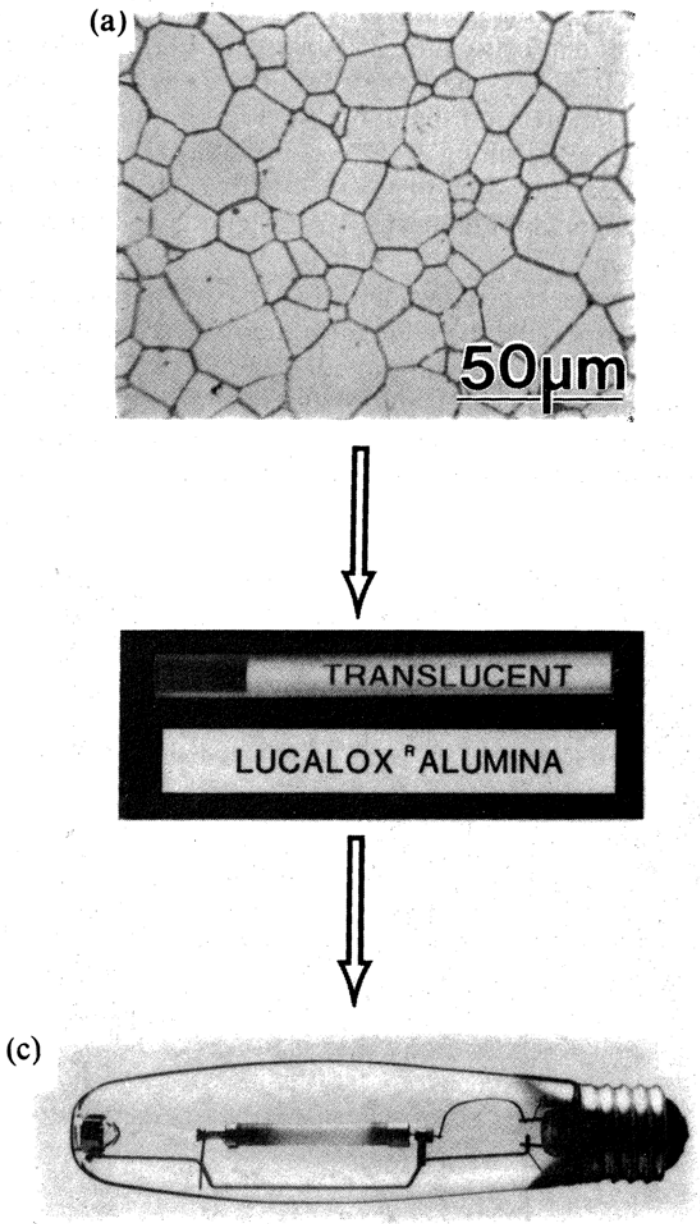

Figure 11.9 Comparison of the microstructure and translucency of relatively pore-free Al_2O_3 (a) with that of opaque Al_2O_3 containing pores trapped in grains (b). Translucent Al_2O_3 tubes are used in sodium vapor lamps that provide energy efficient street lights. (Courtesy of General Electric.)

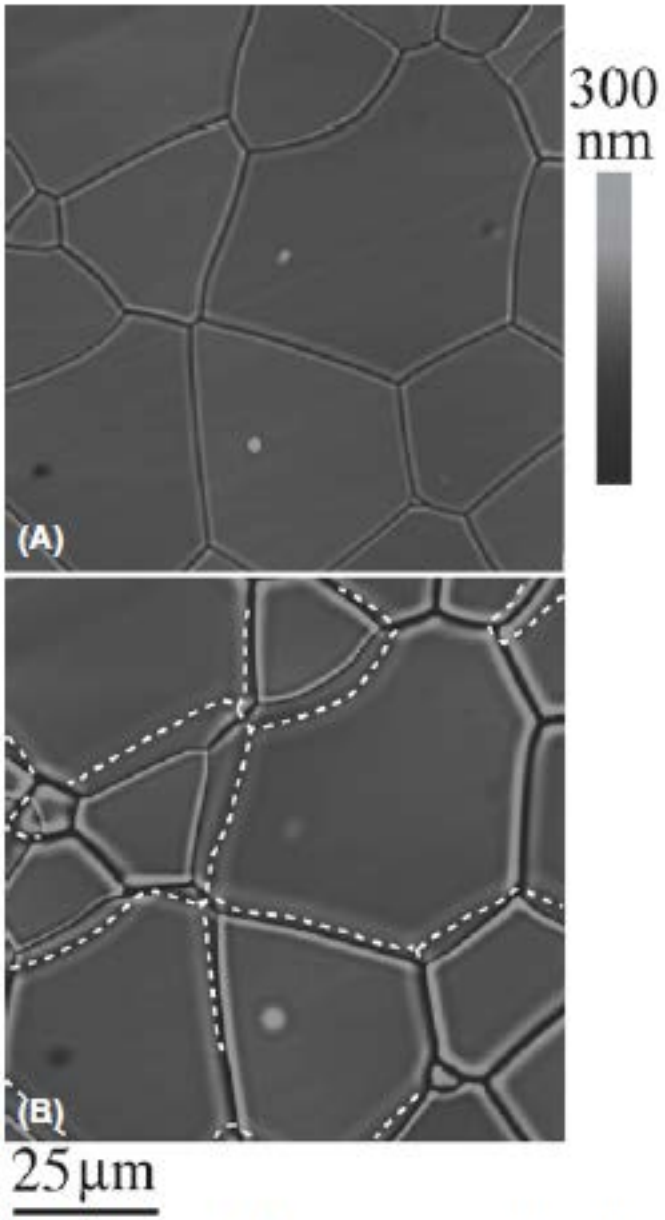

FIGURE 24.17 (a, b) AFM of grooves at migrating GBs

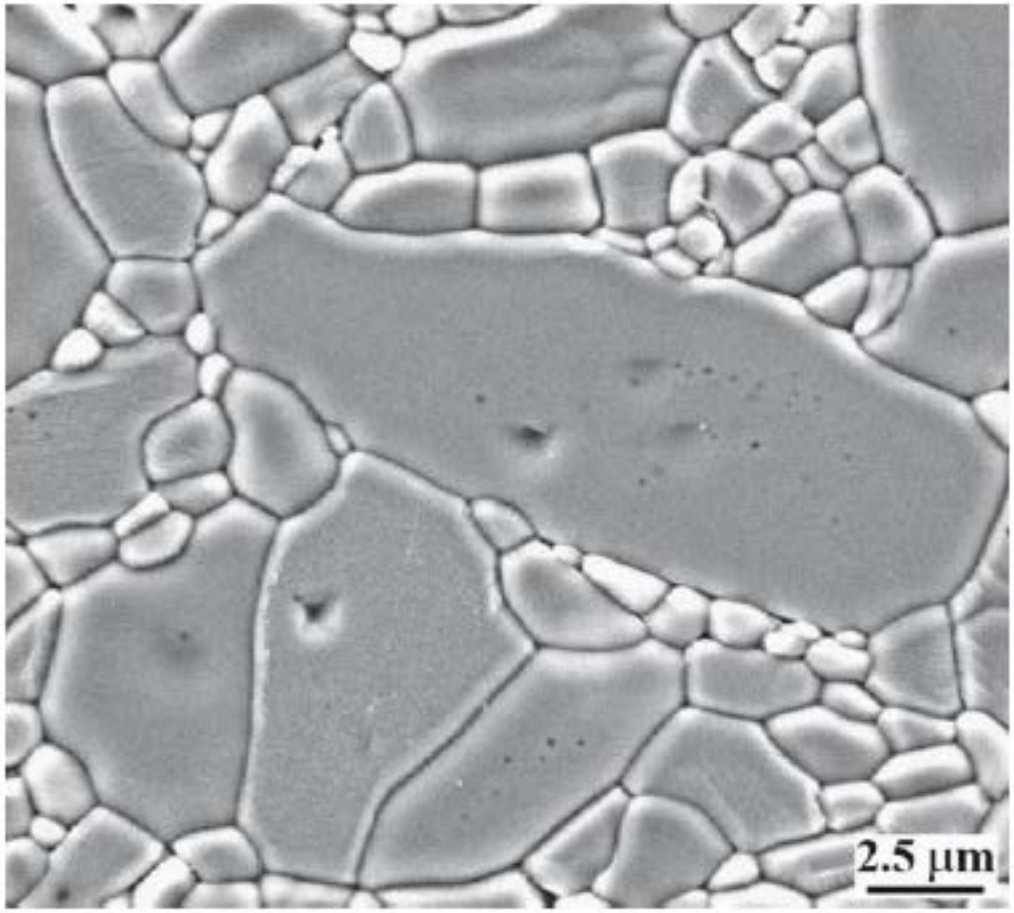

FIGURE 24.21 Elongated exaggerated grain in Al_2O_3.

- During the growth, the larger grain leaves behind a lot of pores and the piece can not achive the 100% of theoretical density (DT).
- To avoid the pore incorporation inside the grain, the speed of grain boudaries must be lower than that of the pores.
- Some impurities can segregate on grain boundary (*GRAIN BOUNDARY PINNING)* slowing the growth and so it' s possible to achive the 100% of DT.

v pore > v grain boundary

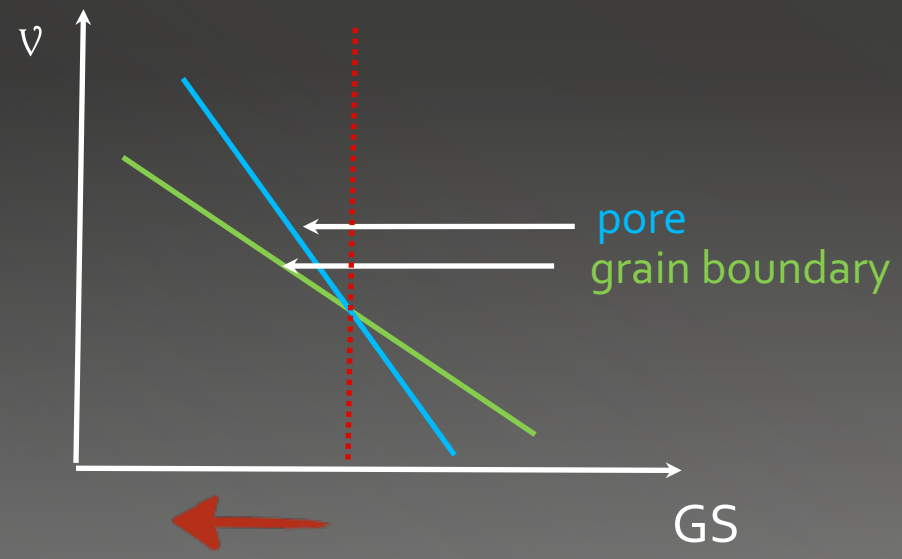

E.G. :

ALUMINA 'LUCALOX ':
polycrystalline Al_2O_3 - 1% MgO

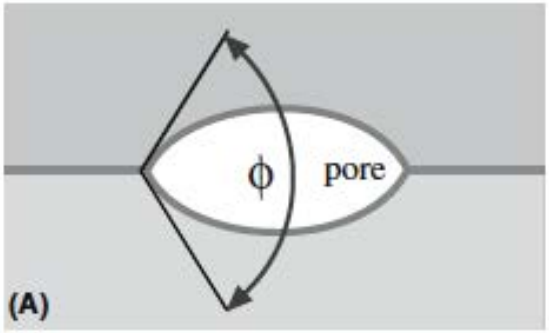

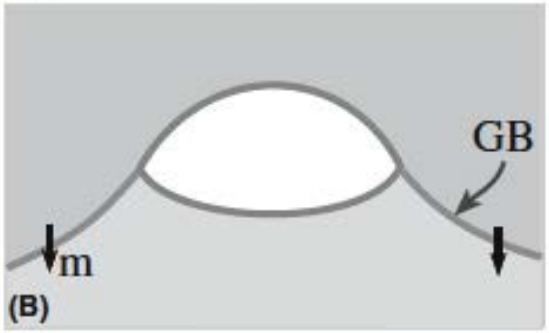

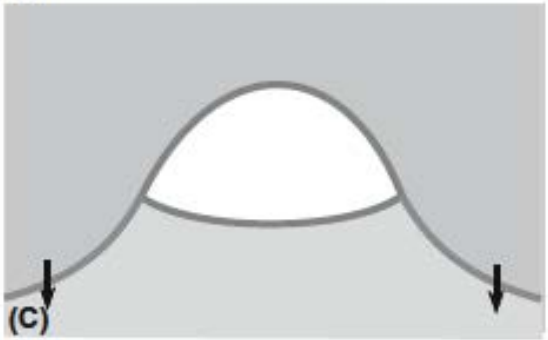

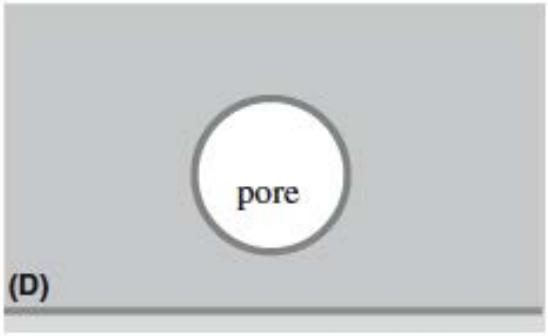

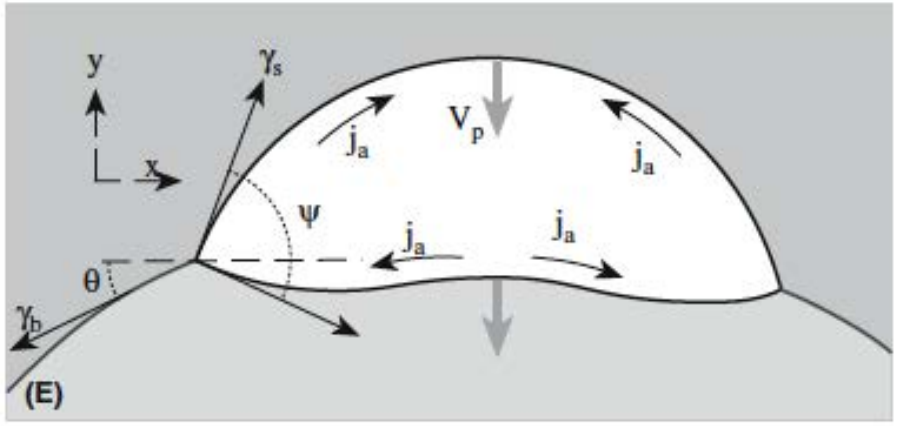

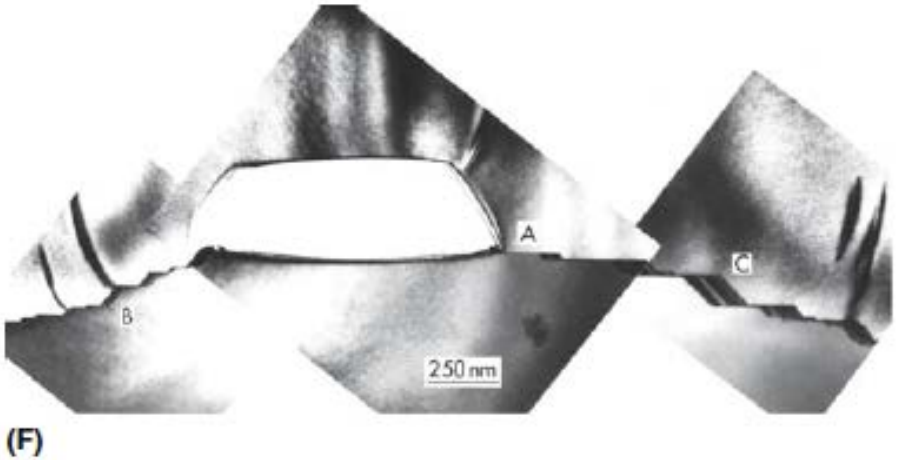

FIGURE 24.14 (a–e) GB/pore interaction: the break-away process.

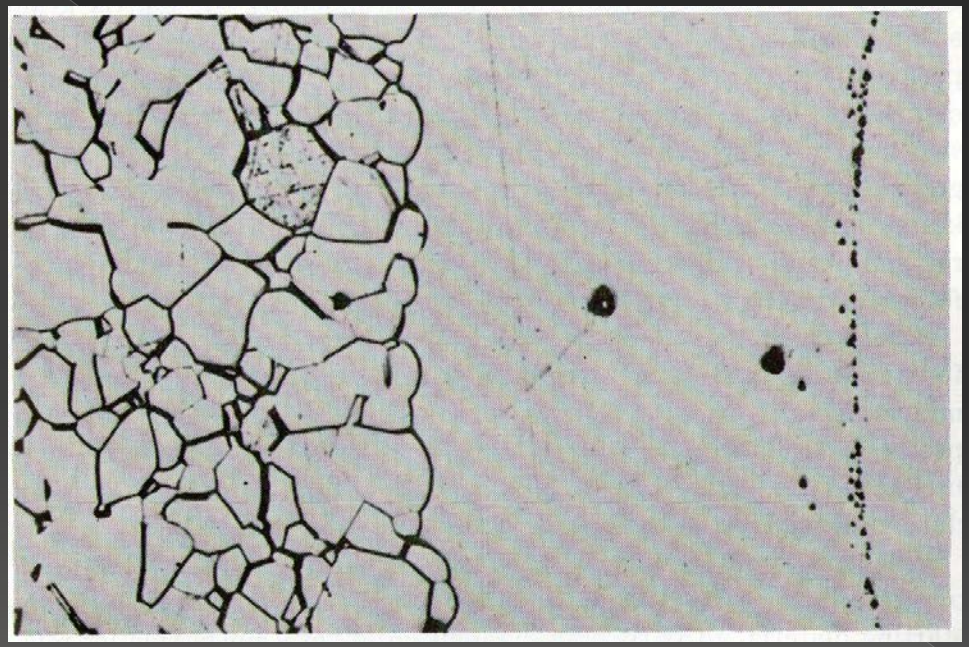

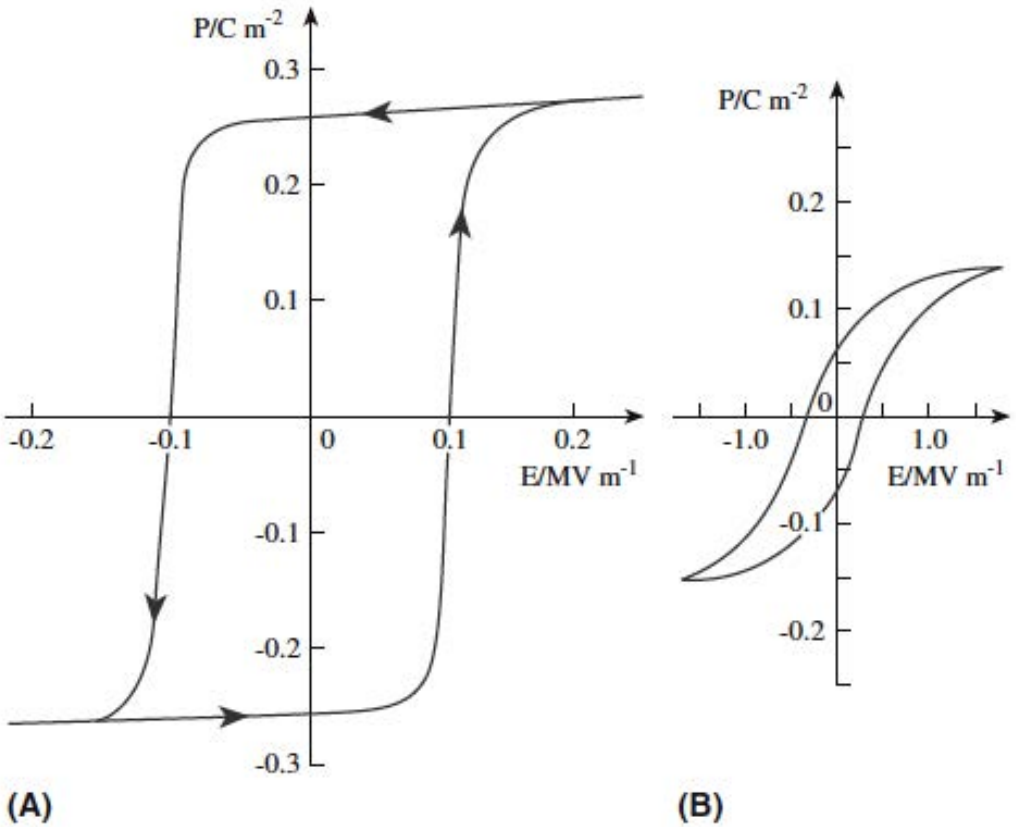

FIGURE 31.10 Hysteresis loops for $BaTiO_3$. (a) Single-domain single crystal. (b) Polycrystalline ceramic.

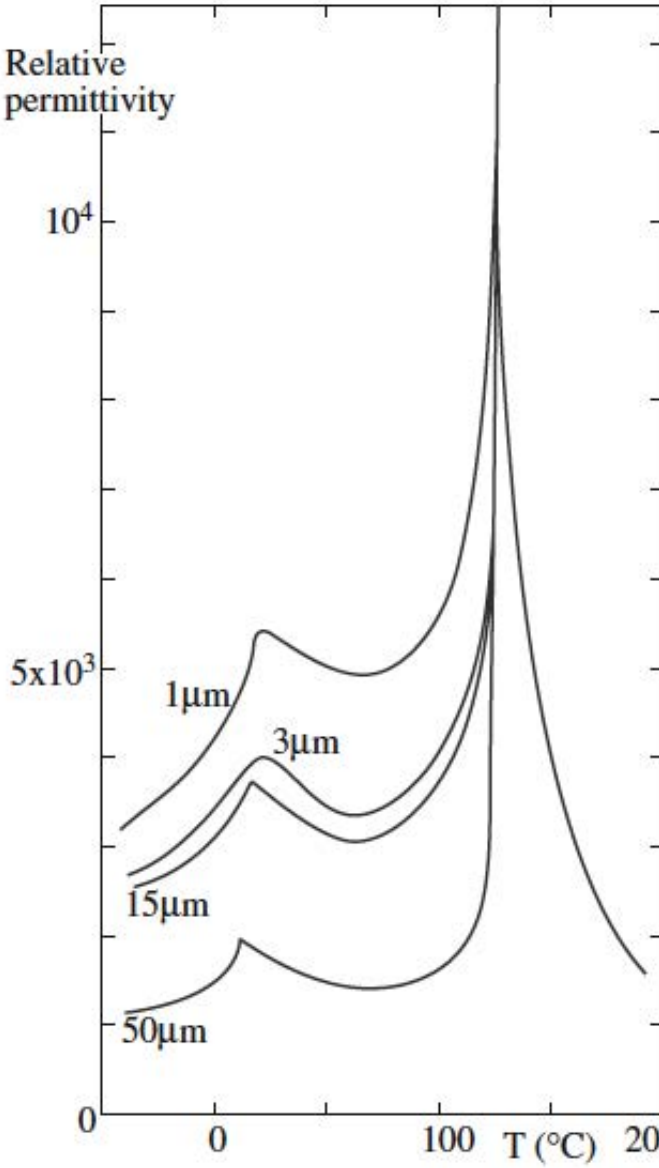

FIGURE 31.15 Effect of grain size on the dielectric con
$BaTiO_3$.

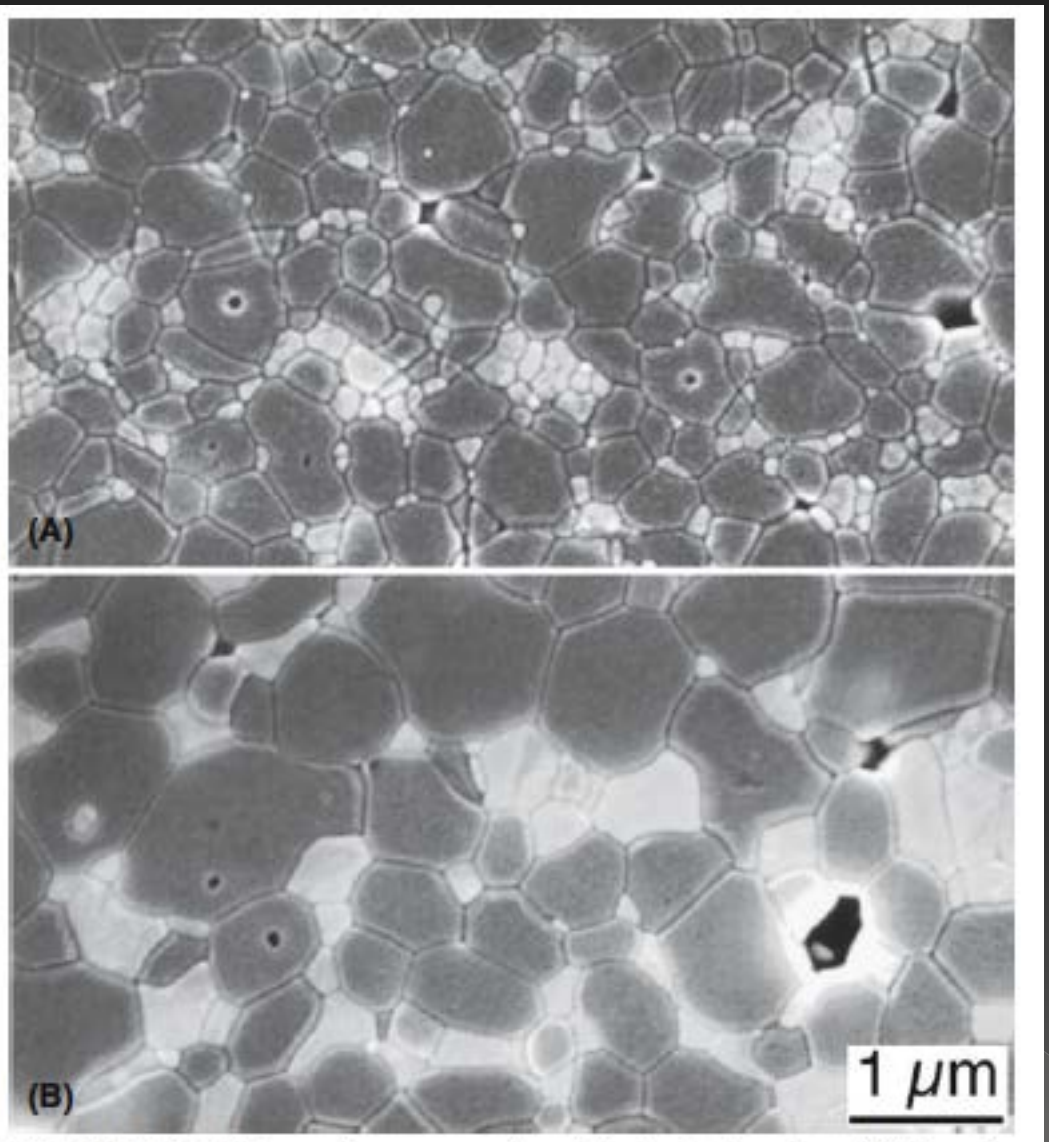

FIGURE 24.27 Two-phase ceramics. (a) As sintered and (b) heat treated at 1600°C for 30 hours. ZTA 30% (zirconia-toughened alumina with 30 vol% YSZ containing 10 molar% yttria).

WETTABILITY

Is the ability of a drop of liquid to recline on a solid surface.

Varying the pressur is changed the wettability.

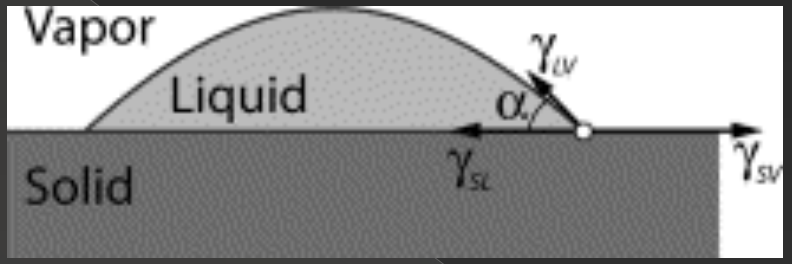

α : contact angle

γ_{LV} : liquid-vapour interfacial energy

γ_{LS} : liquid-solid interfacial energy

γ_{SV} : solid-vapour interfacial energy

The contact angle specifies the condition for minimum energy, according to the relation:

$$\gamma_{SL} + \gamma_{LV} \cos\alpha = \gamma_{SV}$$

$$\cos\alpha = \frac{\gamma_{SV} - \gamma_{SL}}{\gamma_{LV}}$$

possible cases:

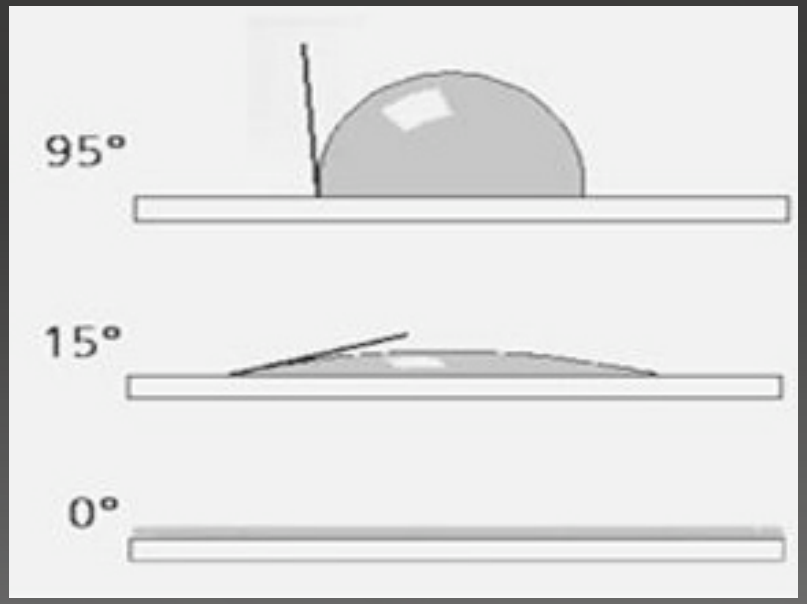

$\alpha > 90° \longrightarrow$ non-wettability

$\alpha < 90° \longrightarrow$ wettability

$\alpha = 0 \longrightarrow$ spreading

LIQUID PHASE SINTERING

- It is the process of adding an additive to the powder which will melt before the ceramic grains.
- The metal added, at high temperatures, melt and WET the grains. The intergranulary spaces are such as to have a capillary forces which attract the grain one another.
- (By lowering the temperature, the amorphous phase does not wet the grains anymore and ritires in triple junctions.)
- (This gives good mechanical proprieties.)
- E.G. : WIDIA (93% WC in a Co matrix).

Liquid phase sintered SiC

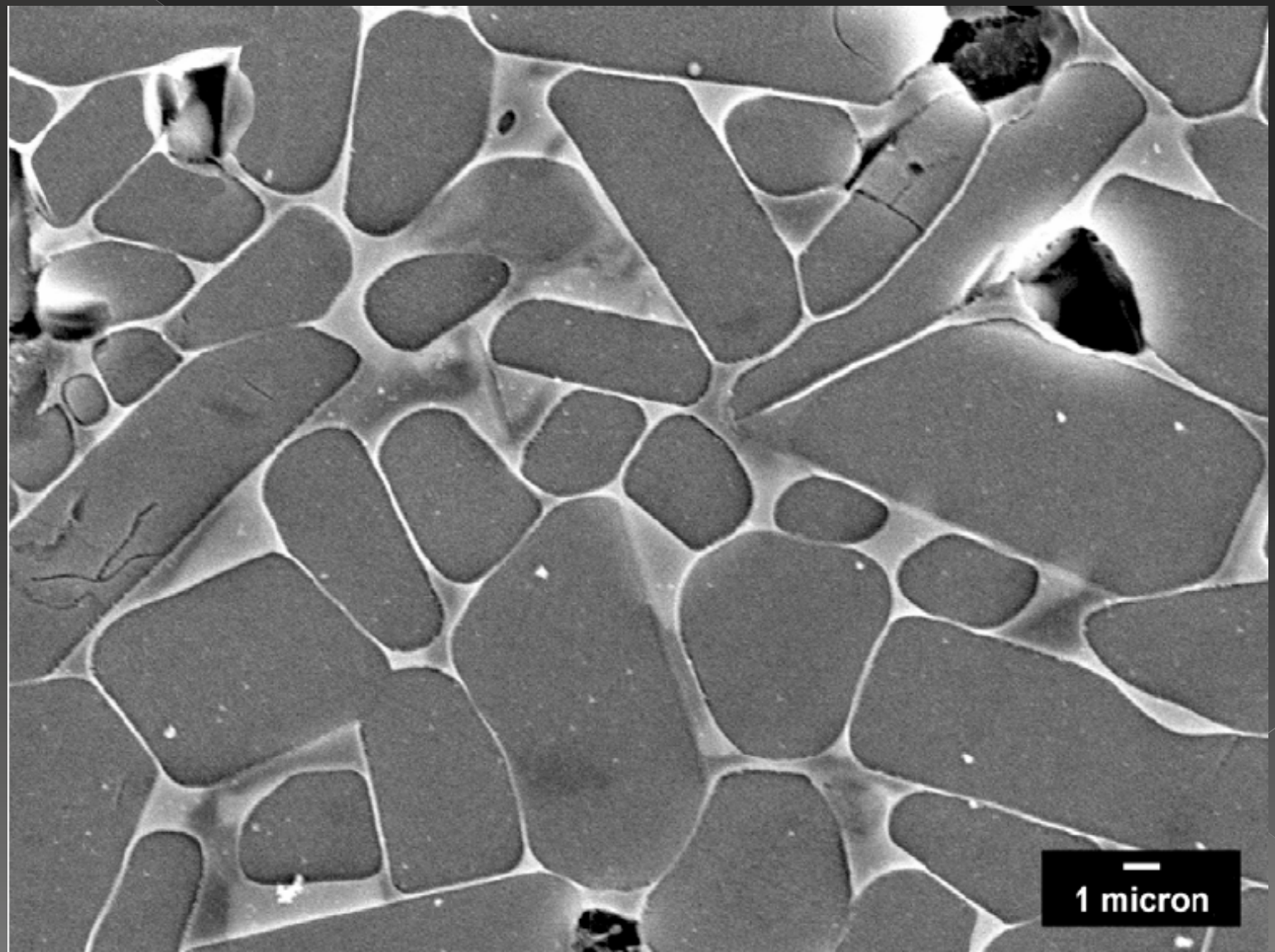

Liquid phase sintered Si_3N_4

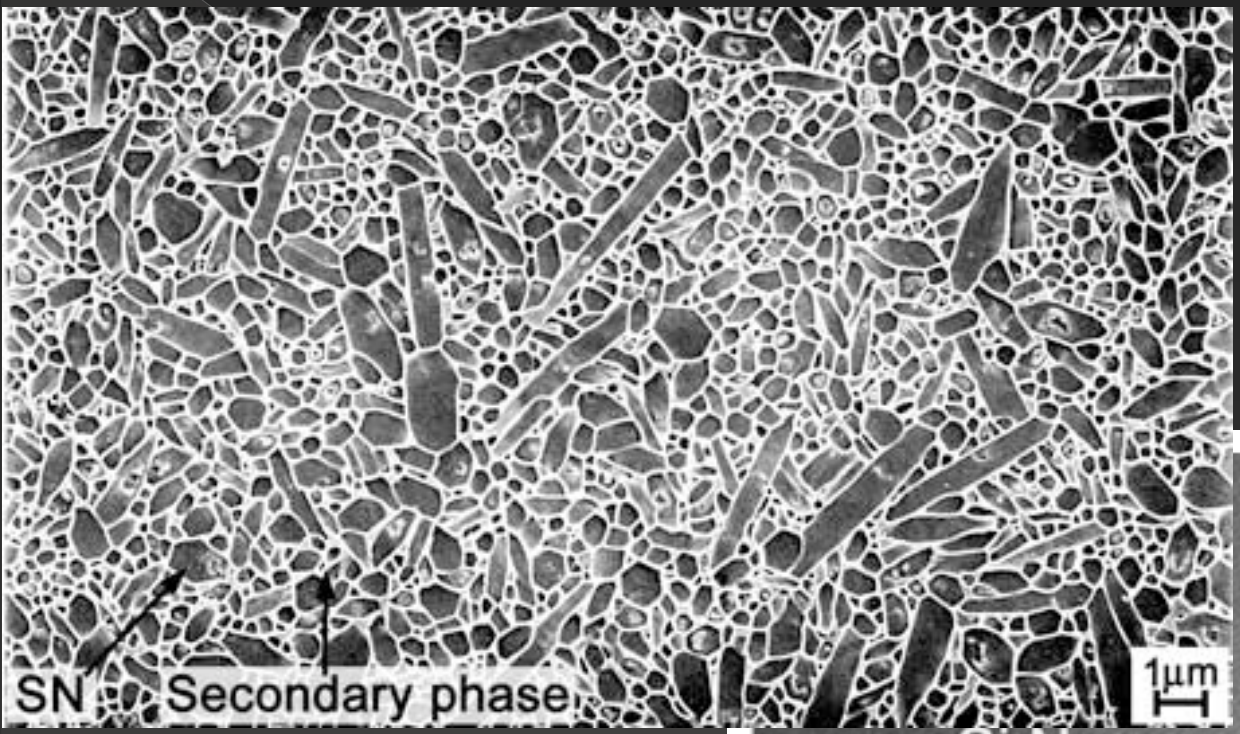

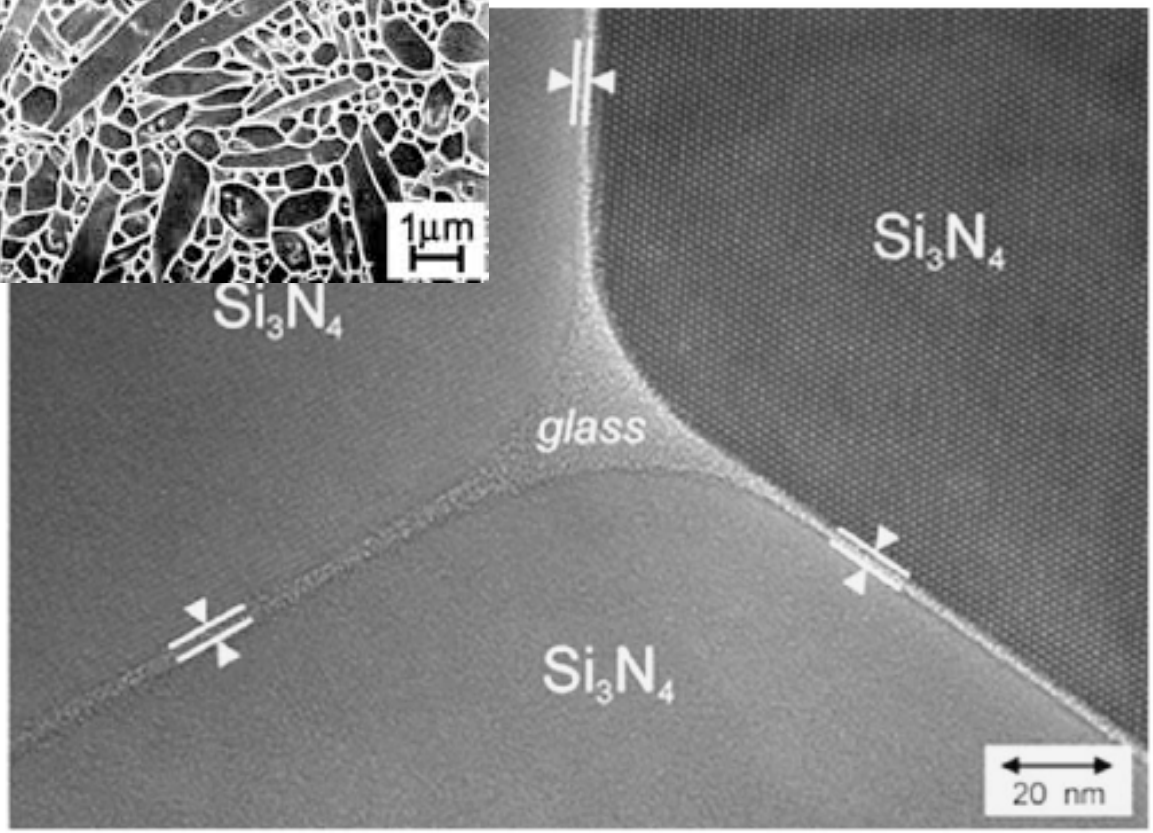

Lquid phase sintered SiAlON

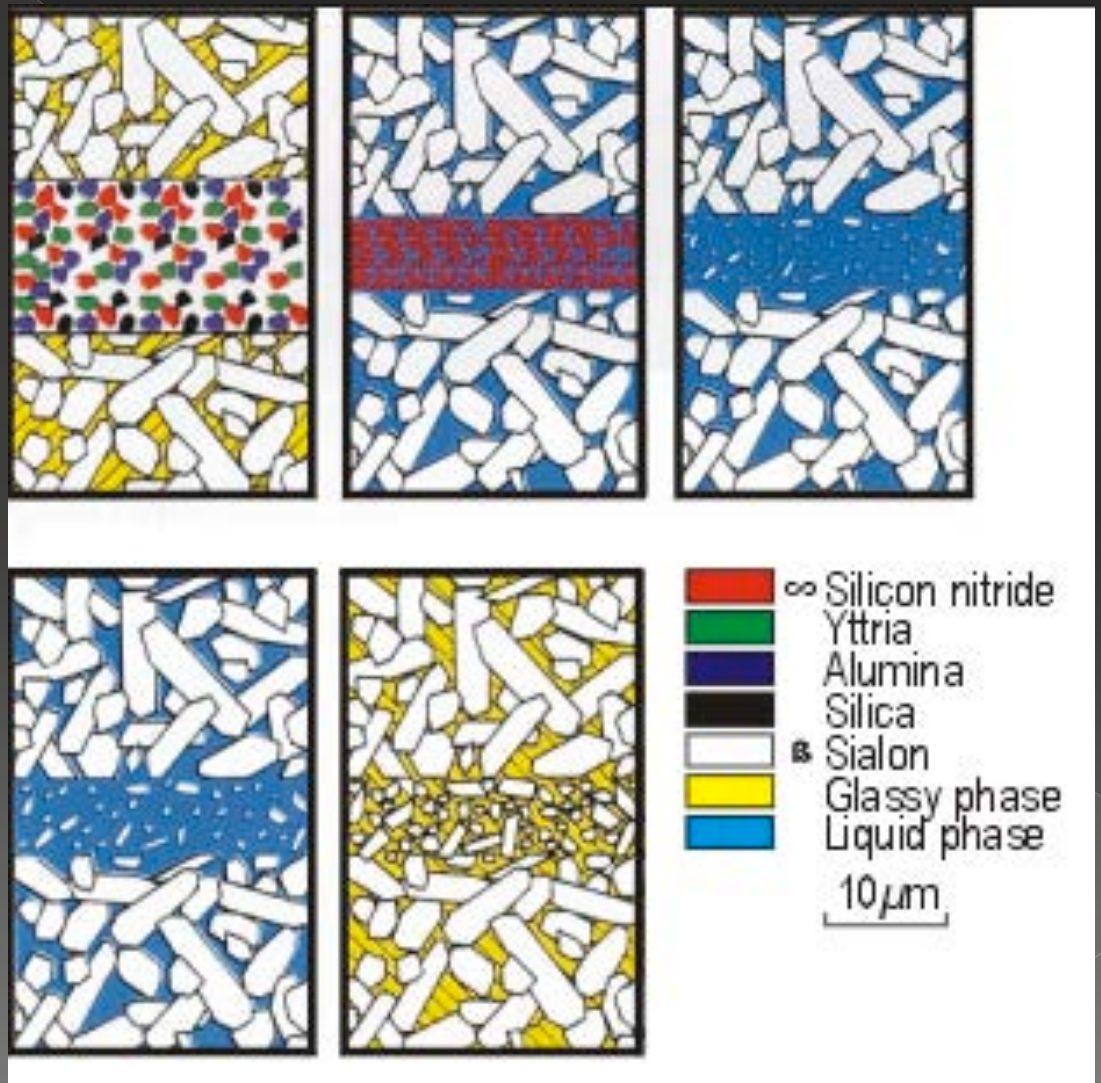

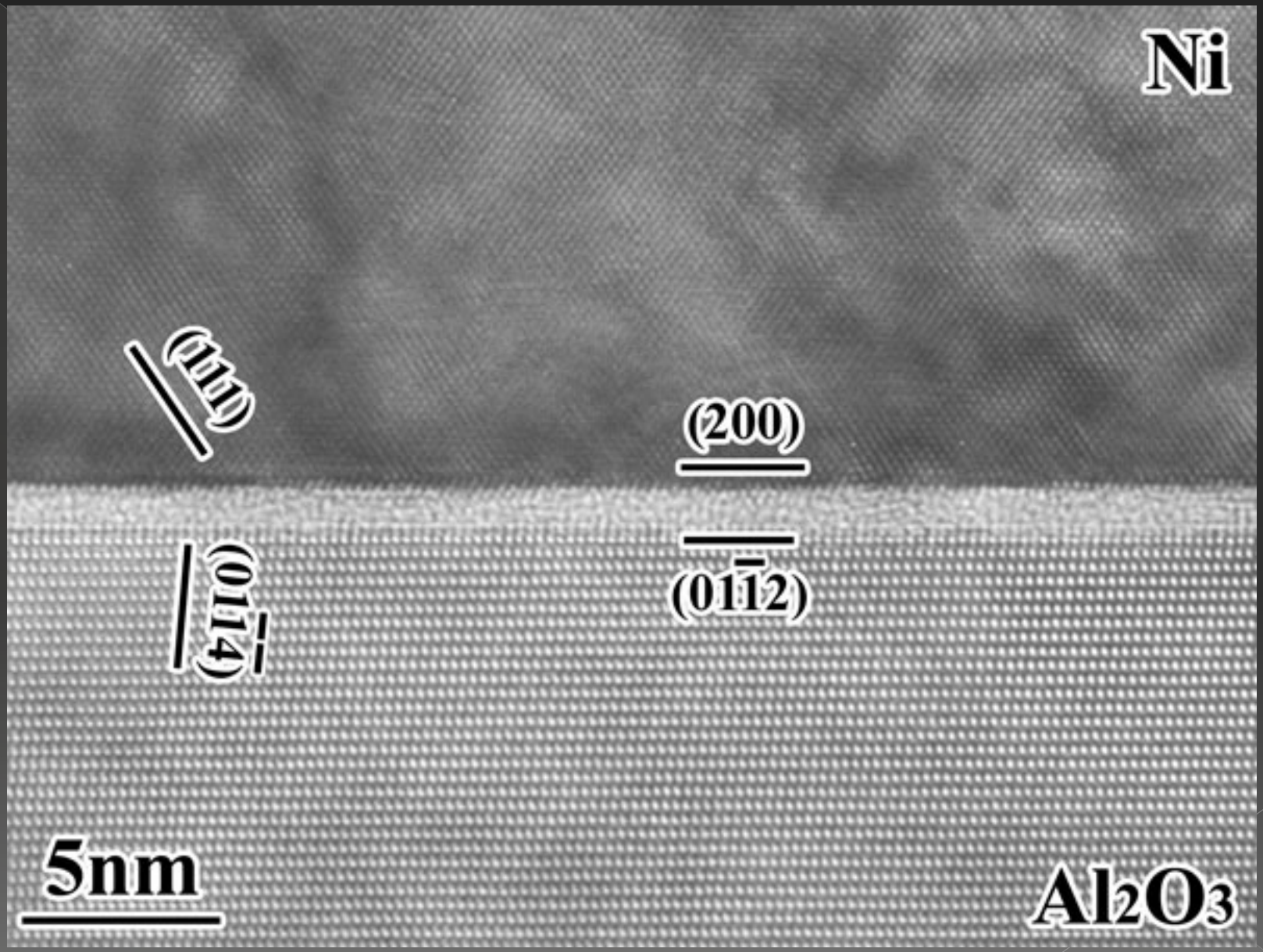
Ni
(111)
(200)
(01$\bar{1}$4)
(0$\bar{1}$12)
5nm
Al_2O_3

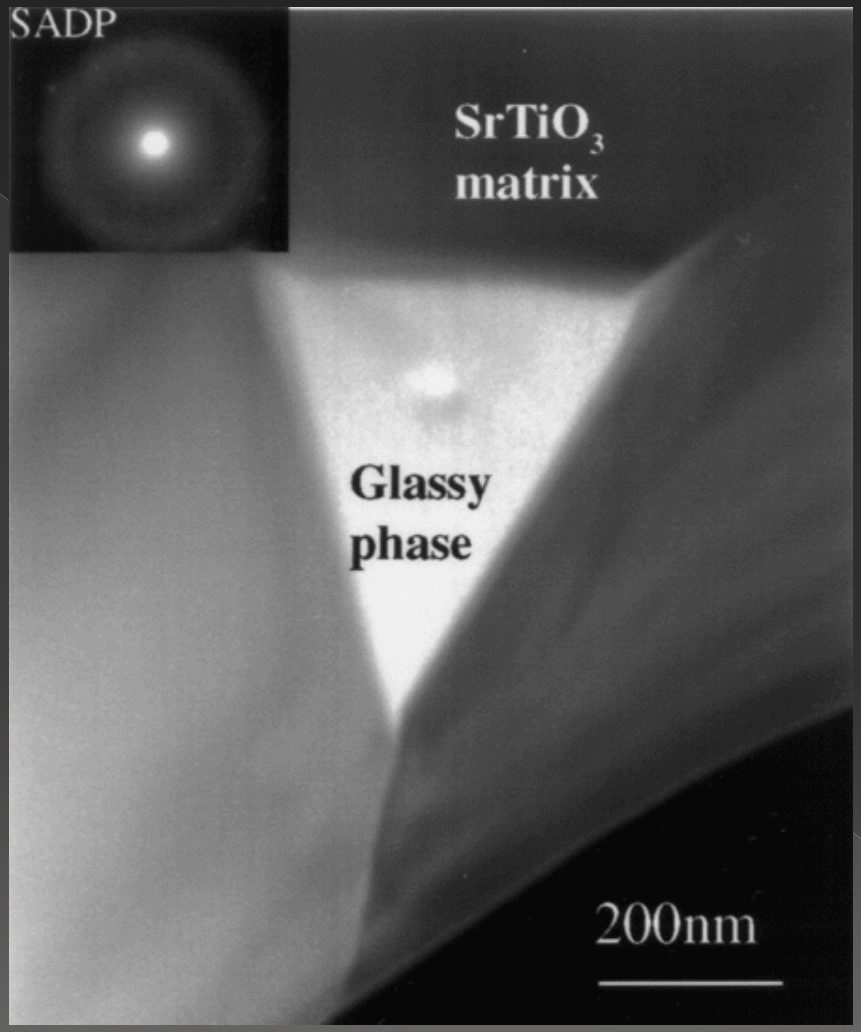
SADP
SrTiO3
matrix
Glassy
phase
200nm

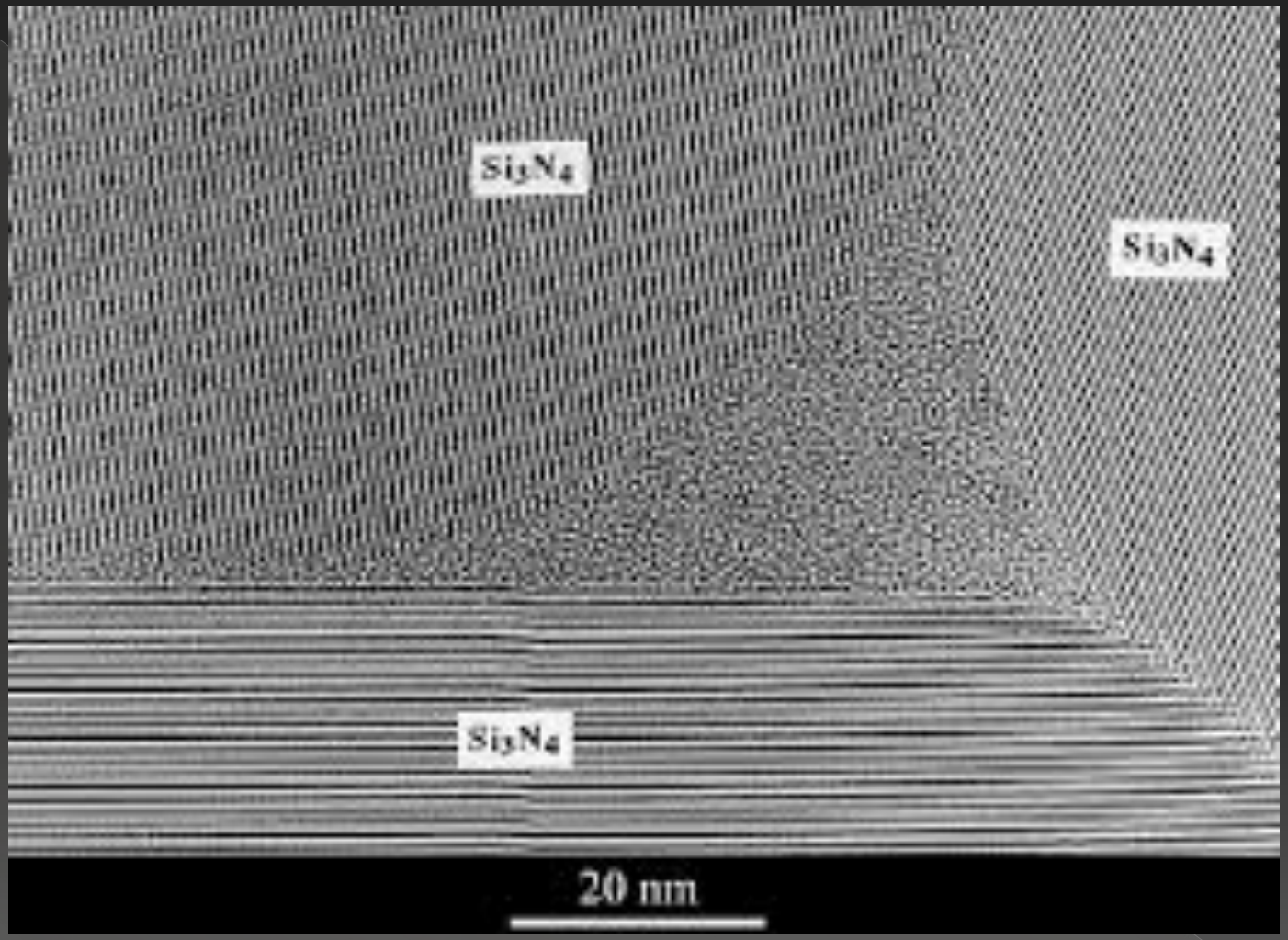
Si3N4
Si3N4
Si3N4
20 nm

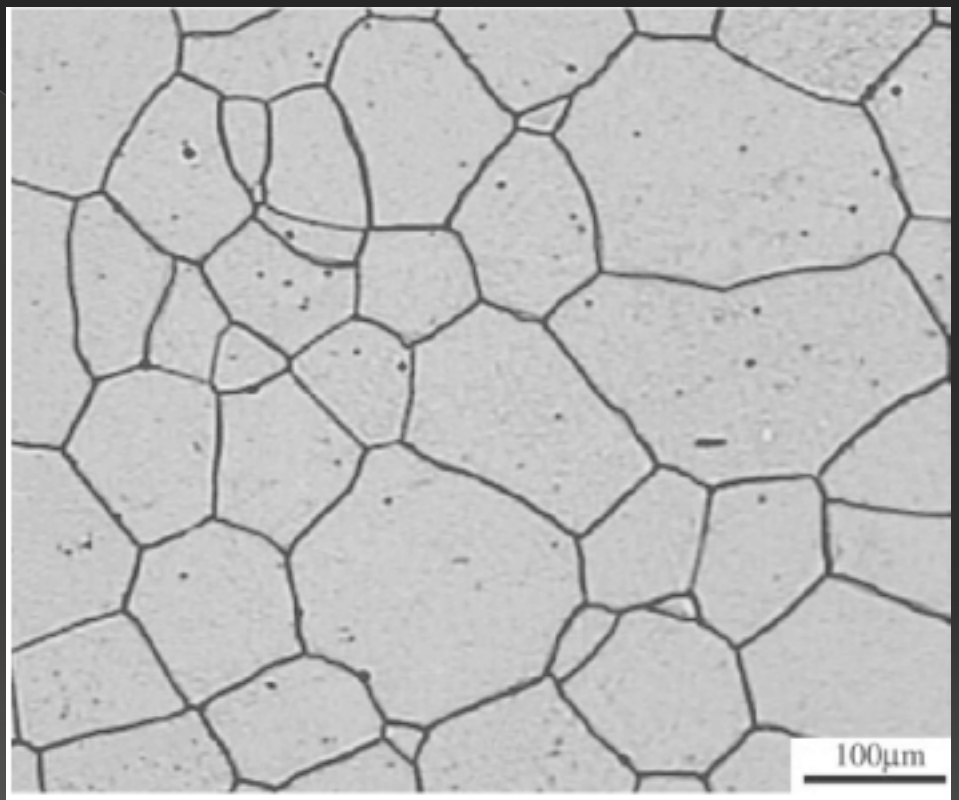

Figure 1. Typical microstructure of polycrystalline ZnO used in this work, after thermal etching at 1150 °C, for 1 h, in air.

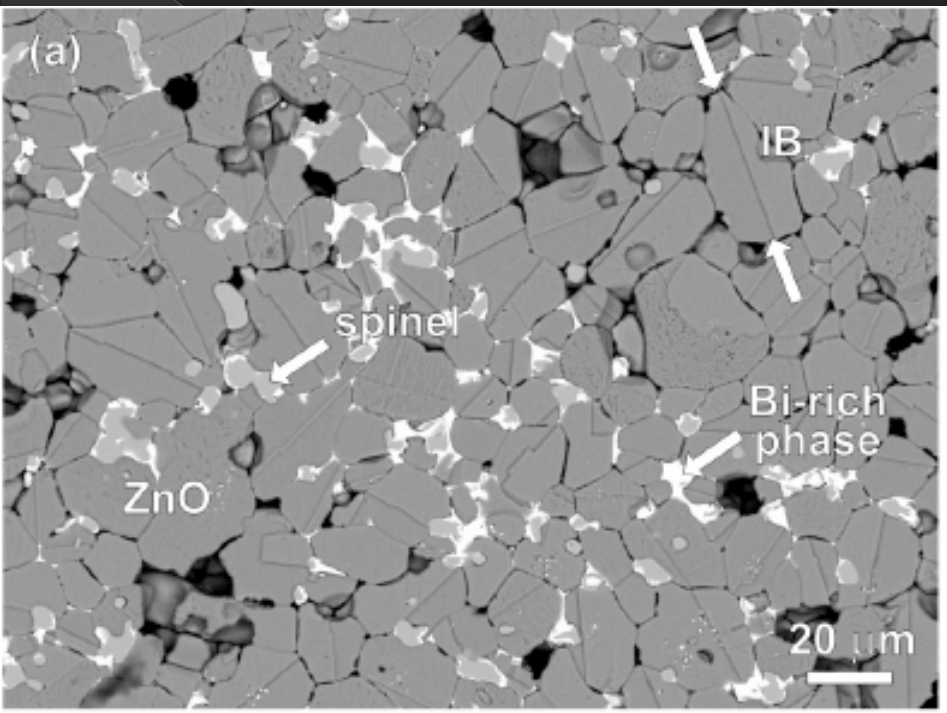
(a)
IB
spinel
Bi-rich
phase
ZnO
20 μm

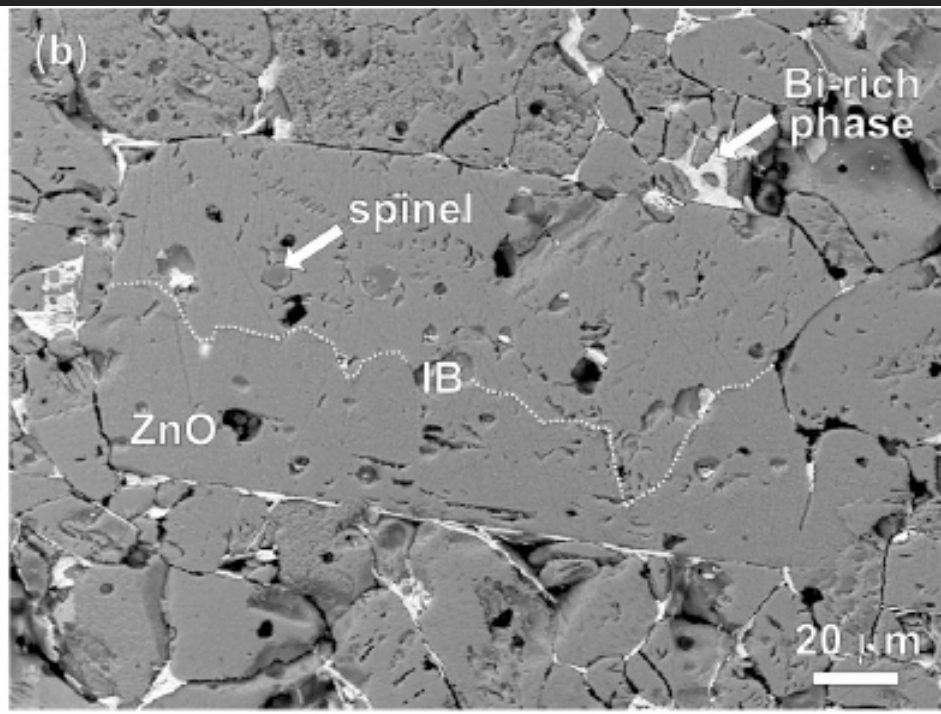
(b)
Bi-rich
phase
spinel
IB
ZnO
20 μm

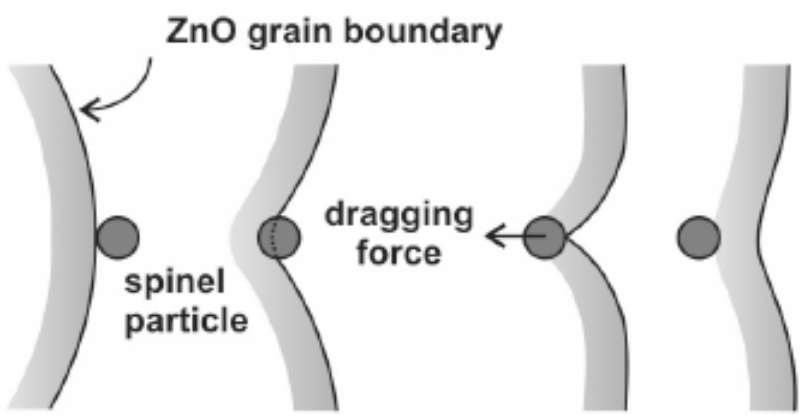
ZnO grain boundary
dragging
force
spinel
particle

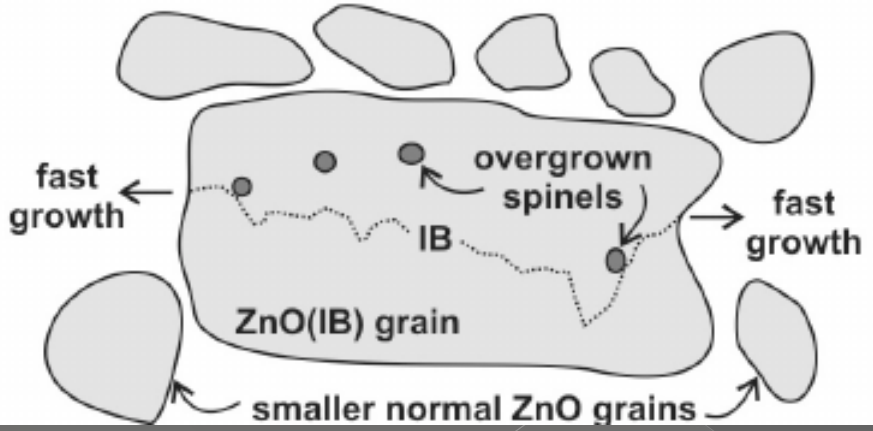
fast
growth
overgrown
spinels
fast
growth
IB
ZnO(IB) grain
smaller normal ZnO grains

PROCEDURE FOR THE SINTERING PROCESS

- Determination of the T_m $T_{sintering} = 2/3\ T_m$ E.G. : Al_2O_3
  T_m =2400°C $T_{sintering}$ = 1600°C
- CALCINATION (200°C-300°C under the sintering temperature)
  E.G. : ZrO_2 stabilized by CaO, Y_2O_3, CeO_2
- FORMING the ceramic parts
- SINTERING

$$\frac{\sqrt{D \cdot t}}{a} \approx 1$$

DENSITY DETERMINATION BY ARCHIMEDE'S PRINCIPLE

- D = dry weight
- boil the piece for 5 hours
- W = wet weight in air
- S = wet weight in water suspended
- V = external volume of the piece: $V = W - S$
- BULK DENSITY $B = D/V$
- P = apparent porosity $P = (W-D)/V$

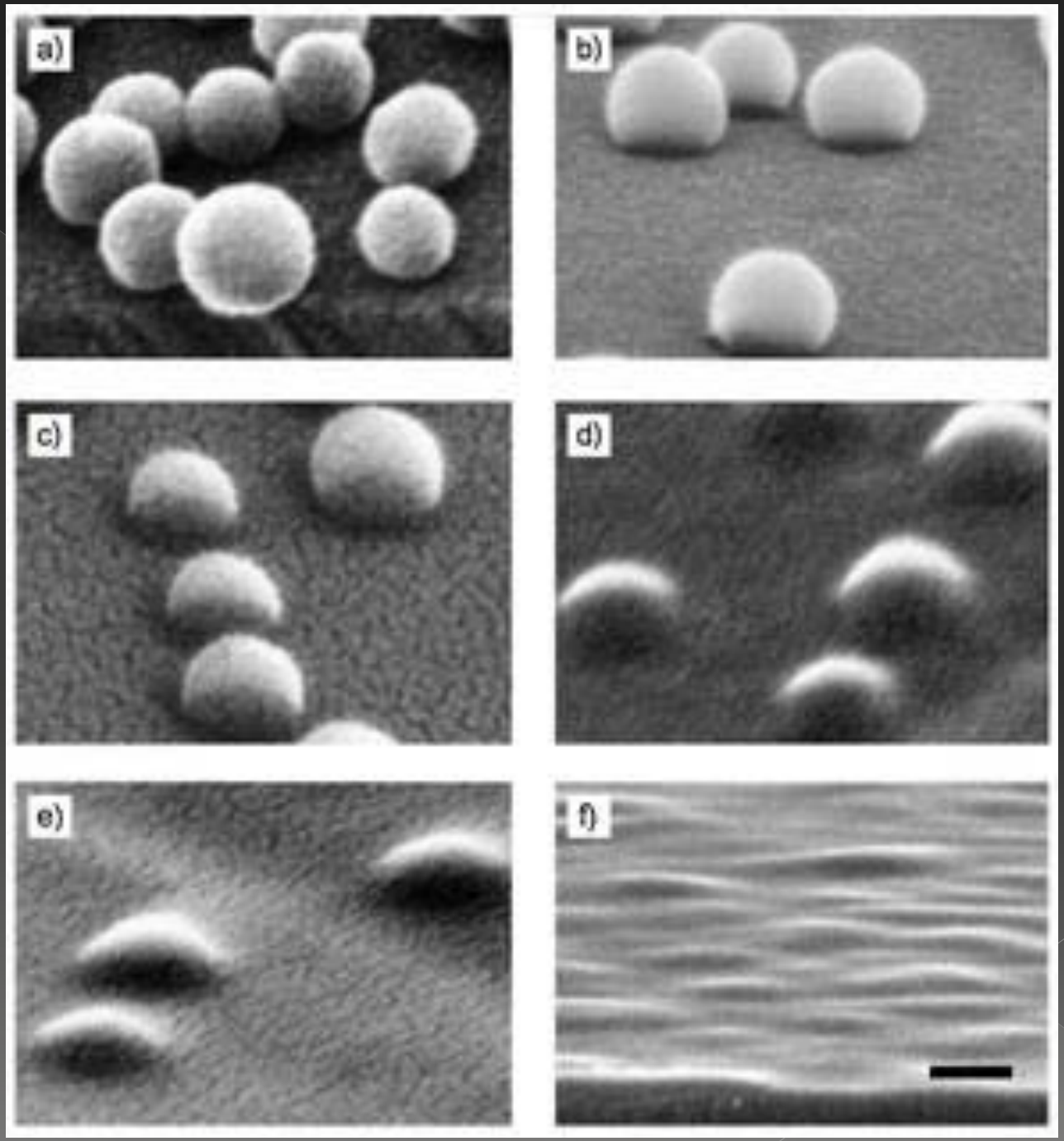
a)
b)
c)
d)
e)
f)

TYPICAL SINTERING TIME-TEMPERATURE PROFILE

Flaws are Stress Concentrators

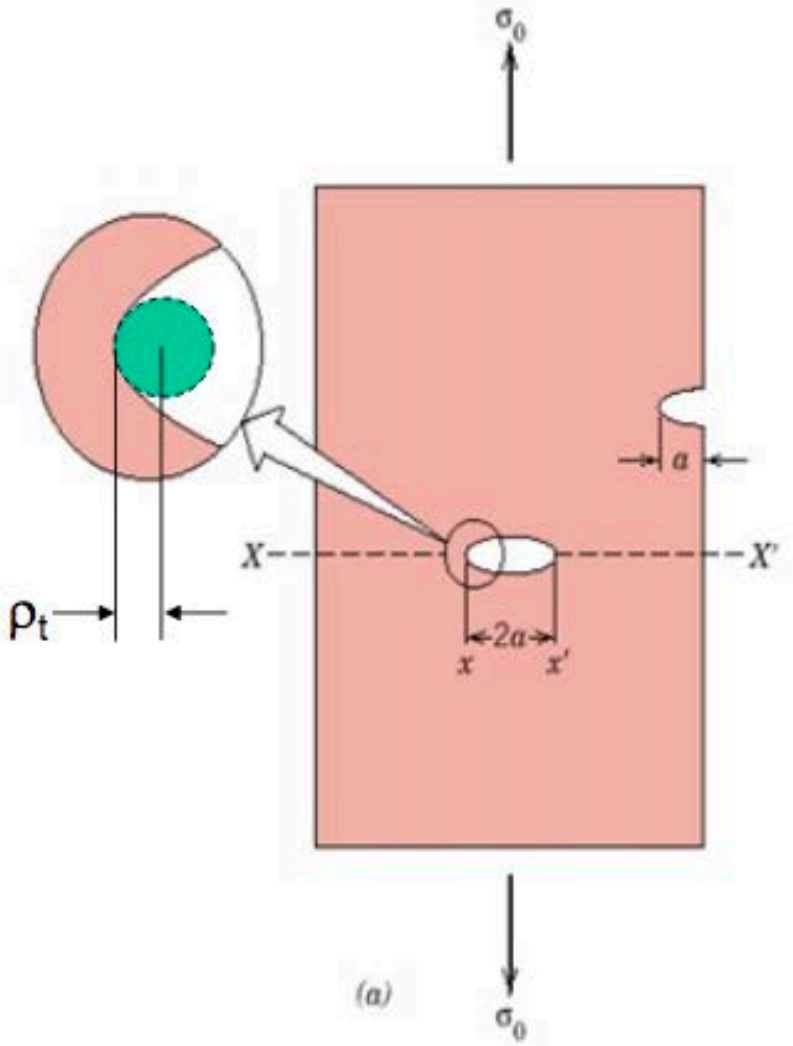

If the crack is similar to an elliptical hole through plate, and is oriented perpendicular to applied stress, the maximum stress σ_m=

$$\sigma_m = 2\sigma_o\left(\frac{a}{\rho_t}\right)^{1/2} = K_t\sigma_o$$

where

ρ_t = radius of curvature

σ_o = applied stress

σ_m = stress at crack tip

a = length of surface crack or ½ length of internal crack

$\sigma_m/\sigma_o = K_t$ the stress concentration factor

Brittle Fracture of Ceramics

- Most ceramics (at room temperature) fracture before any plastic deformation can occur.
- Typical crack configurations for 4 common loading methods.

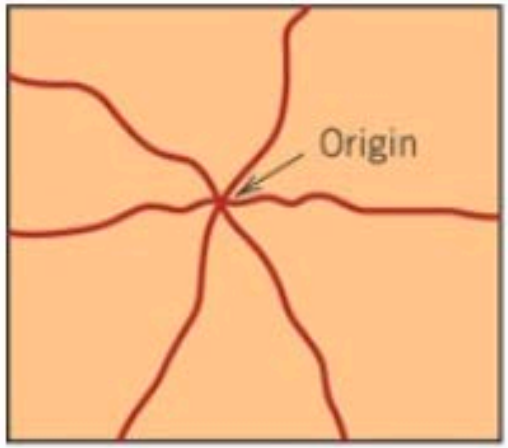

Impact or point loading

(a)

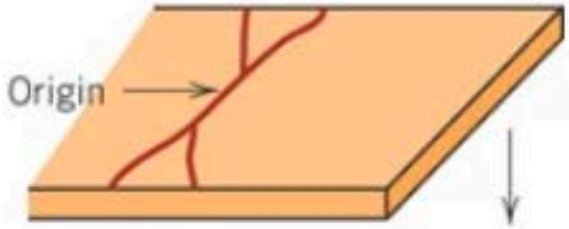

Bending

(b)

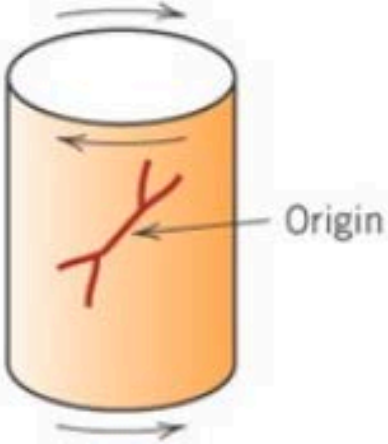

Torsion

(c)

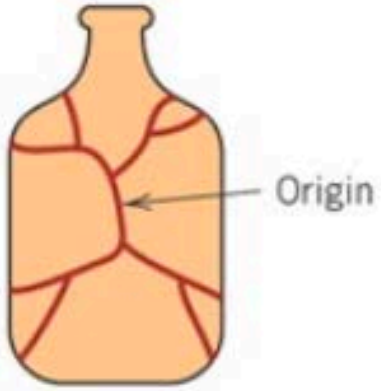

Internal pressure

(d)

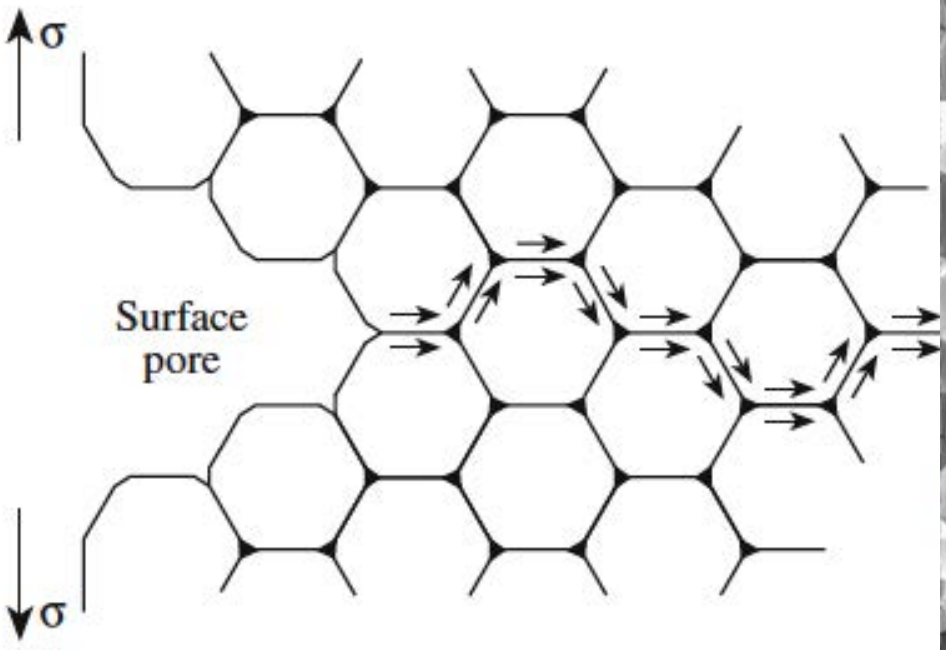

(A)

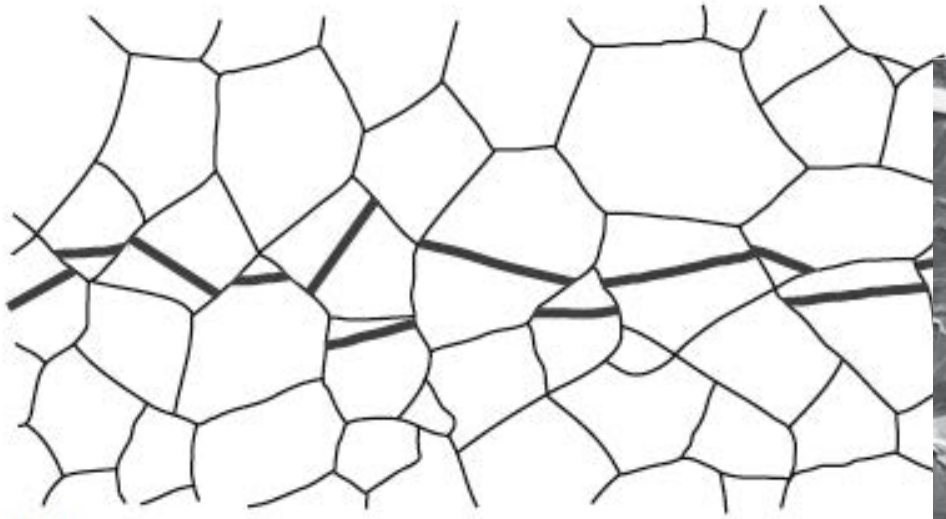

(B)

FIGURE 18.12 (a) Illustration of intergranular crackin
Illustration of transgranular cracking.

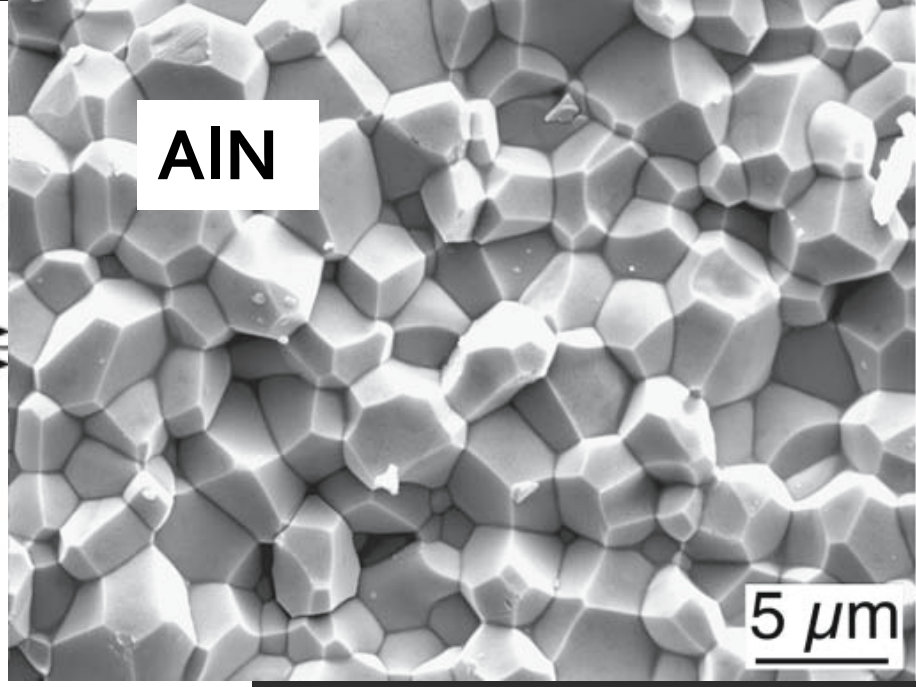

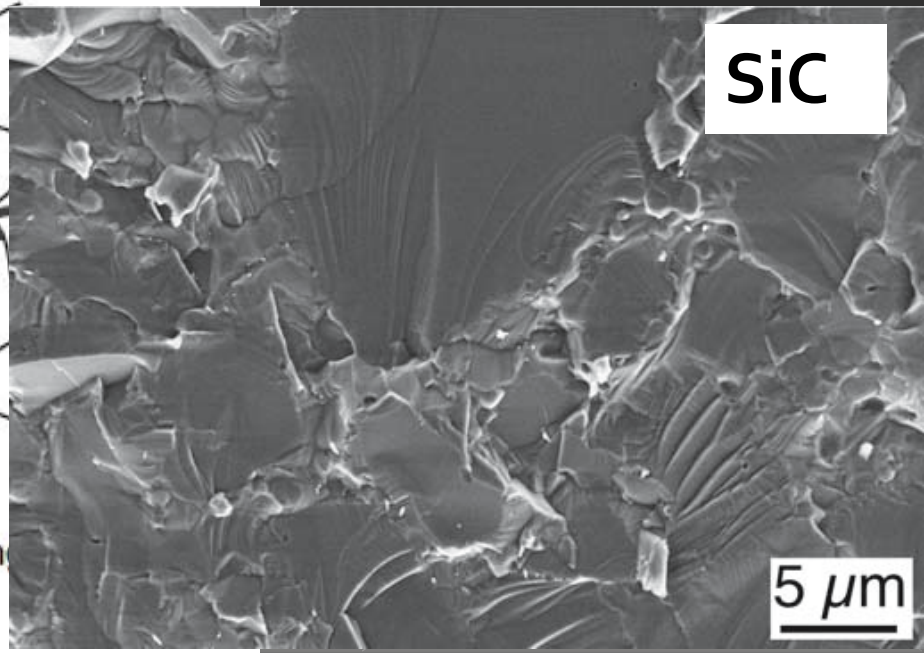

Undistinct features: brittle fracture (SiC)

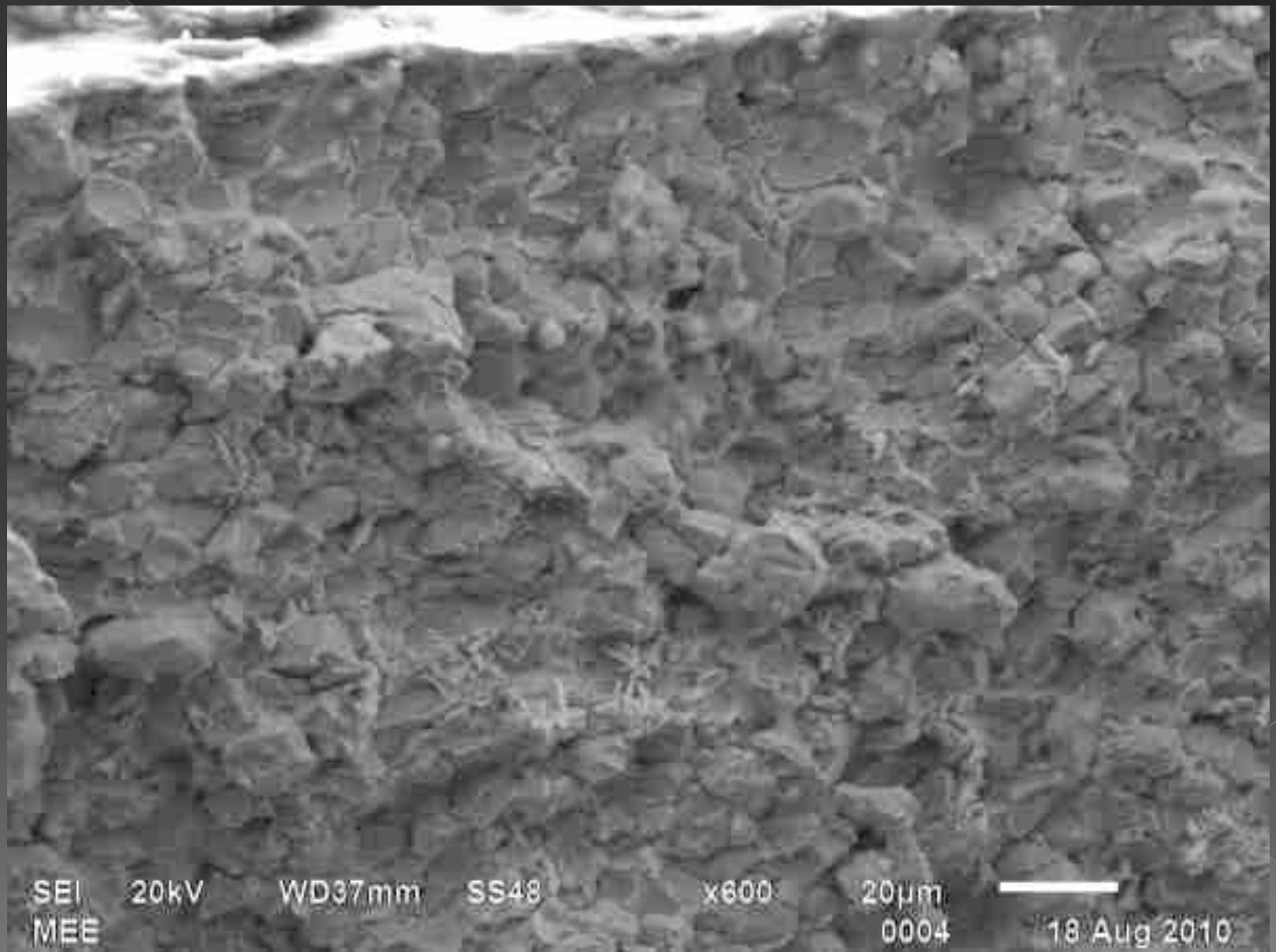

Fatigue

- Fracture surface with crack initiation at top. Surface shows predominantly dull fibrous texture where rapid failure occurred after crack achieved critical size.

- Fatigue failure
  1. Crack initiation
  2. Crack propagation
  3. Final failure

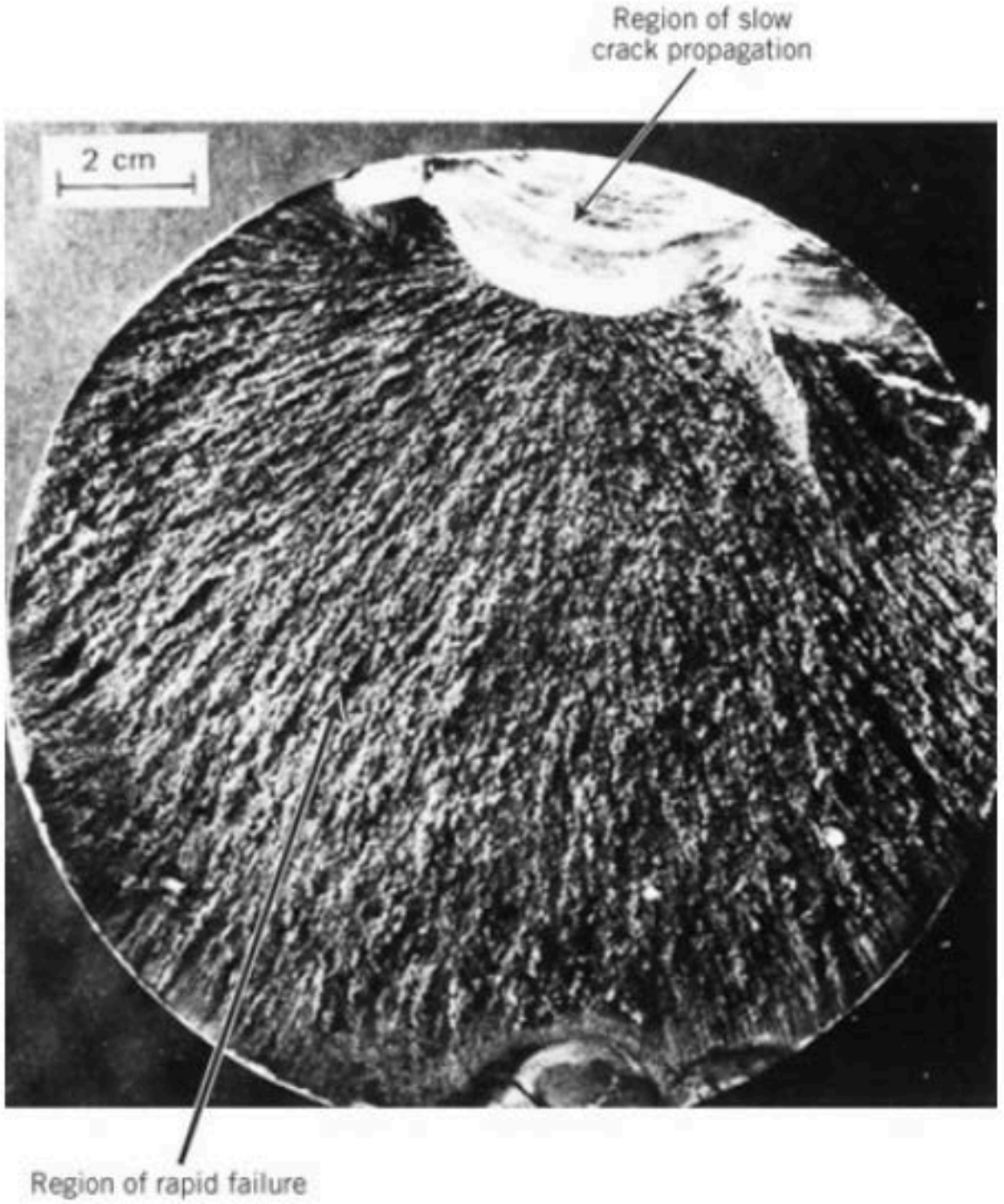

Brittle Fracture of Ceramics

- Surface of a 6-mm diameter fused silica rod.
- Characteristic fracture behavior in ceramics
  - Origin point
  - Initial region (mirror) is flat and smooth
  - After reaches critical velocity crack branches
    - mist
    - hackle

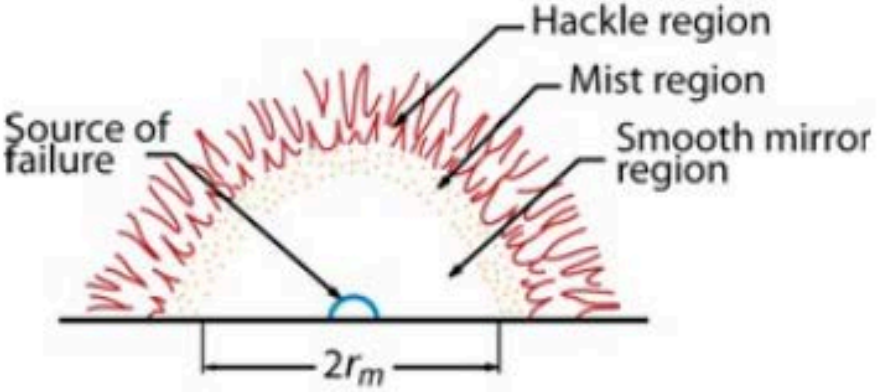

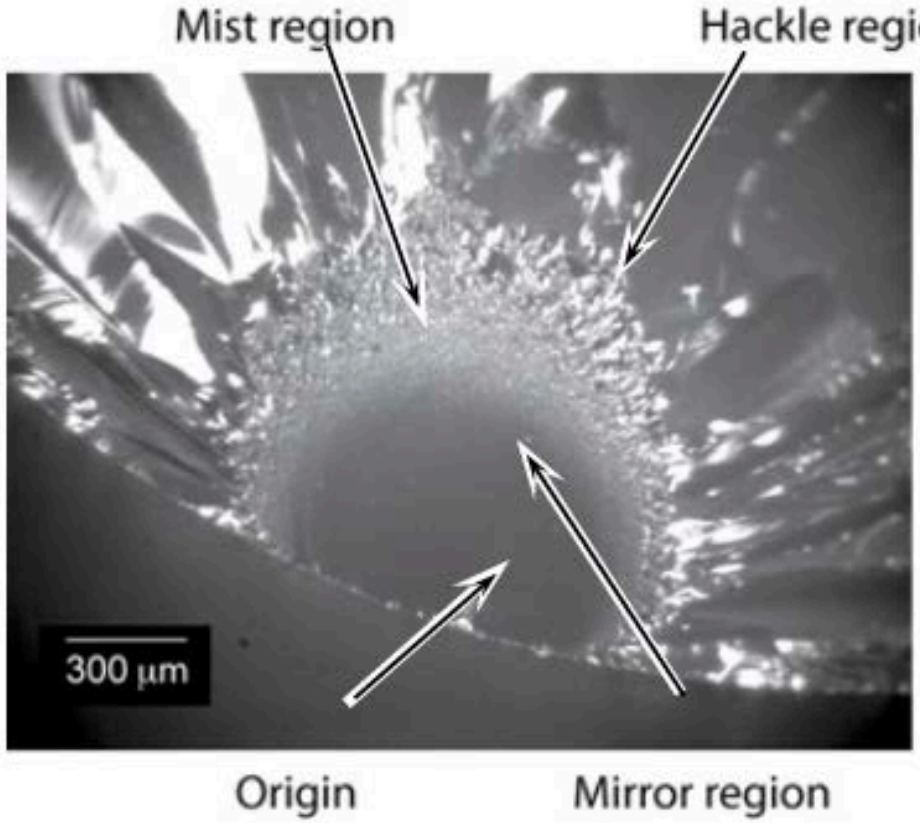

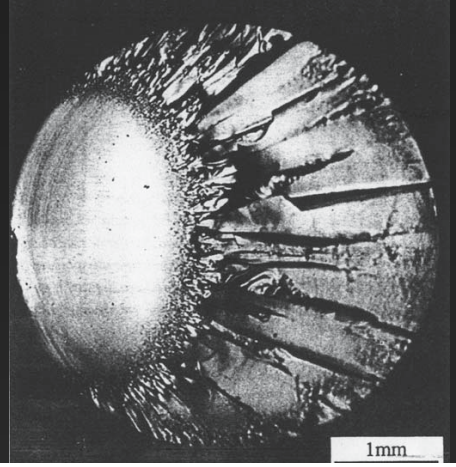
1mm

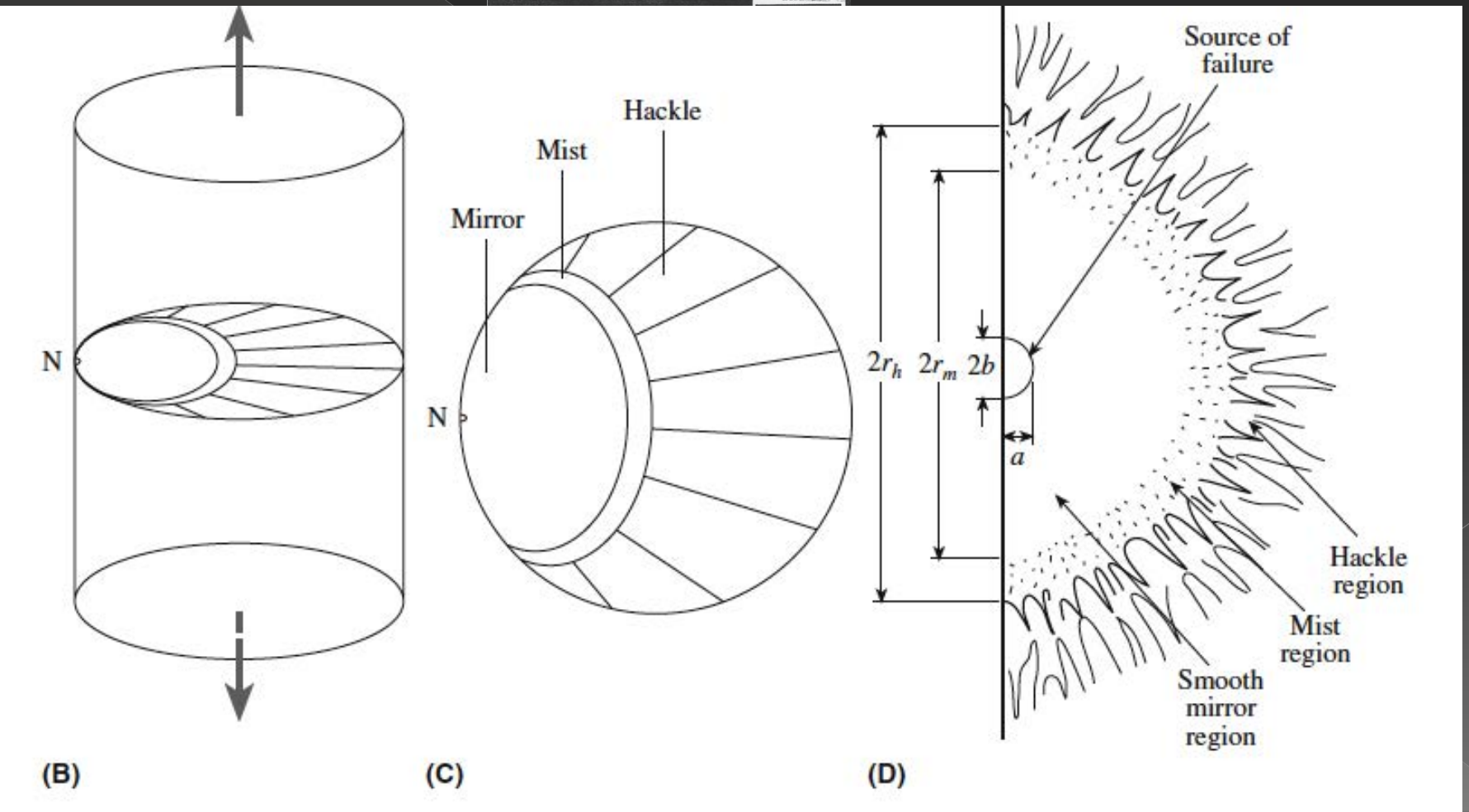
N
Hackle
Mist
Mirror
N
Source of failure
$2r_h$
$2r_m$
$2b$
a
Hackle region
Mist region
Smooth mirror region
(B)
(C)
(D)

Fracture of glass

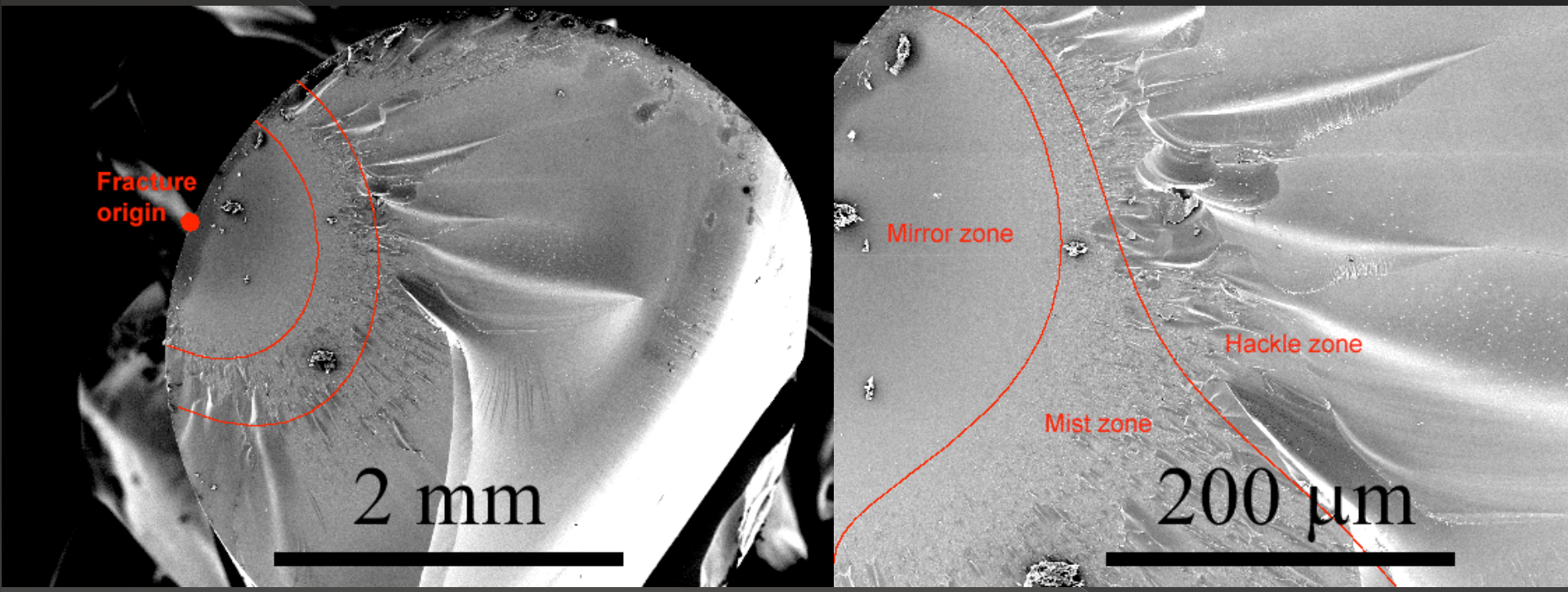

Fracture surface of silicon nitride with steel impurity

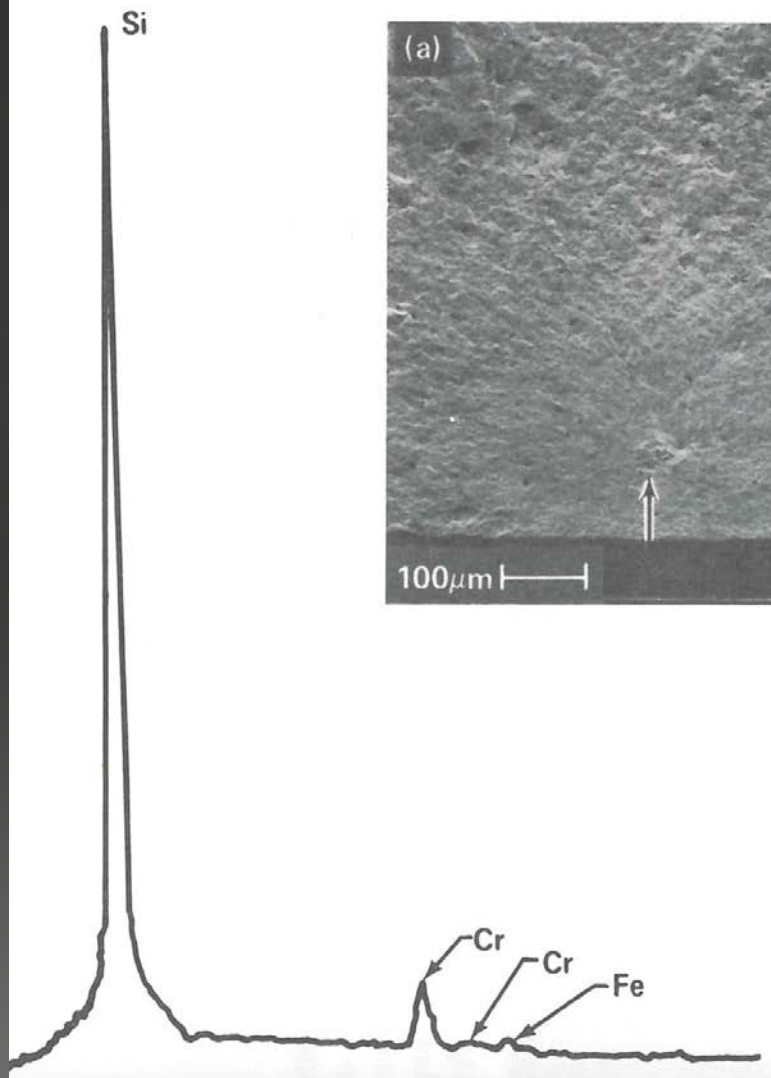

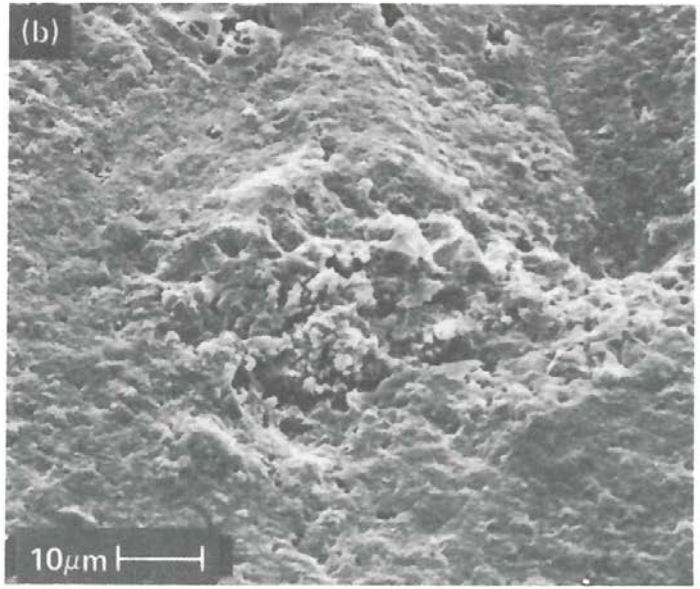

Fracture surface of lathe machined Silicon nitride

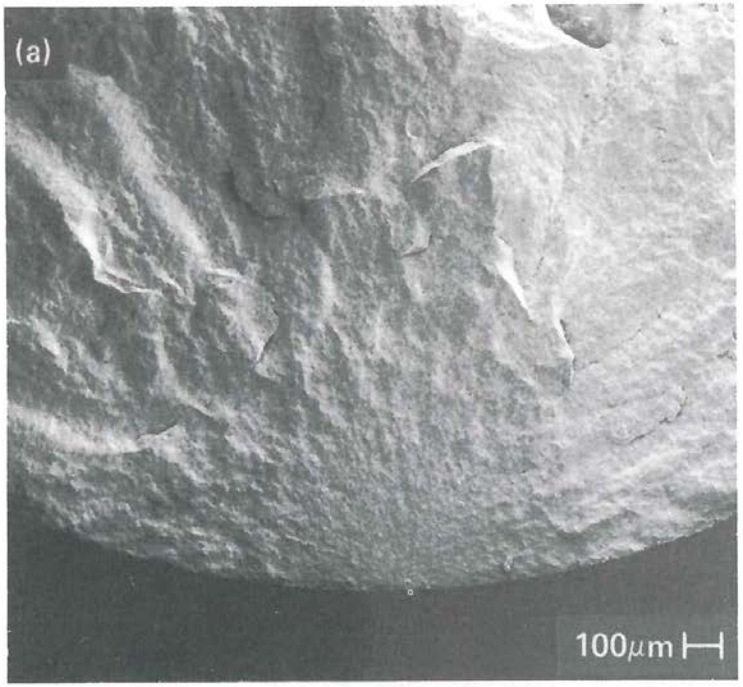

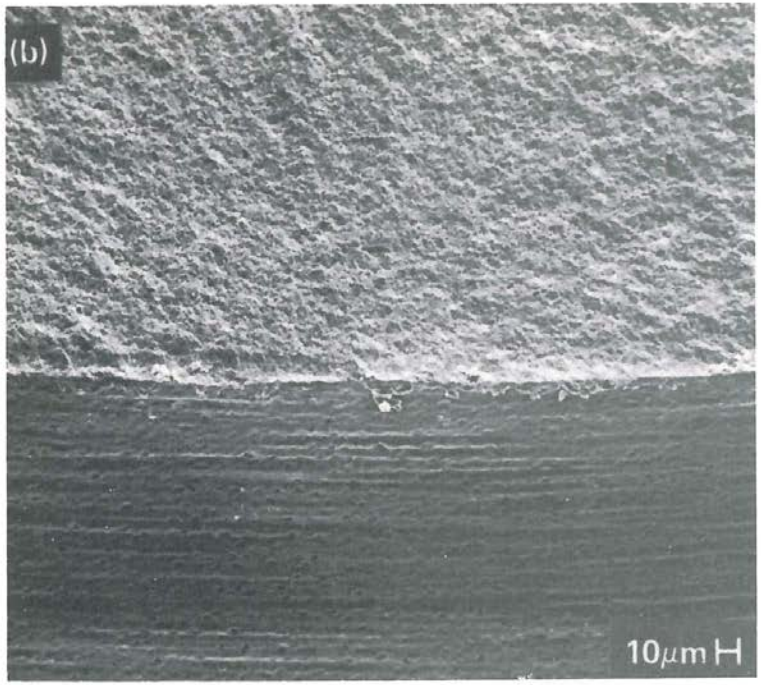

Roadmap for fractography

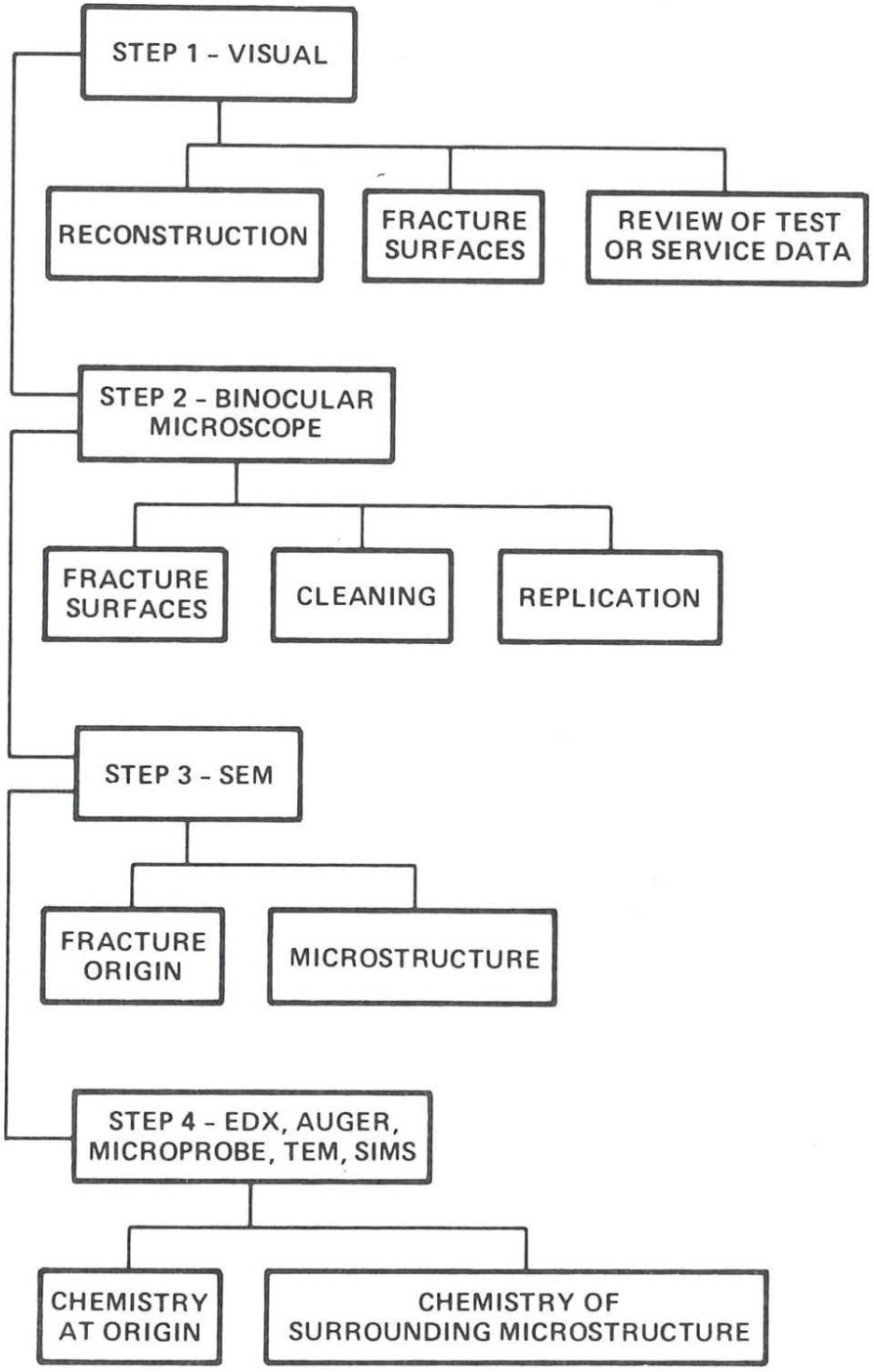

Roadmap for correcting failure

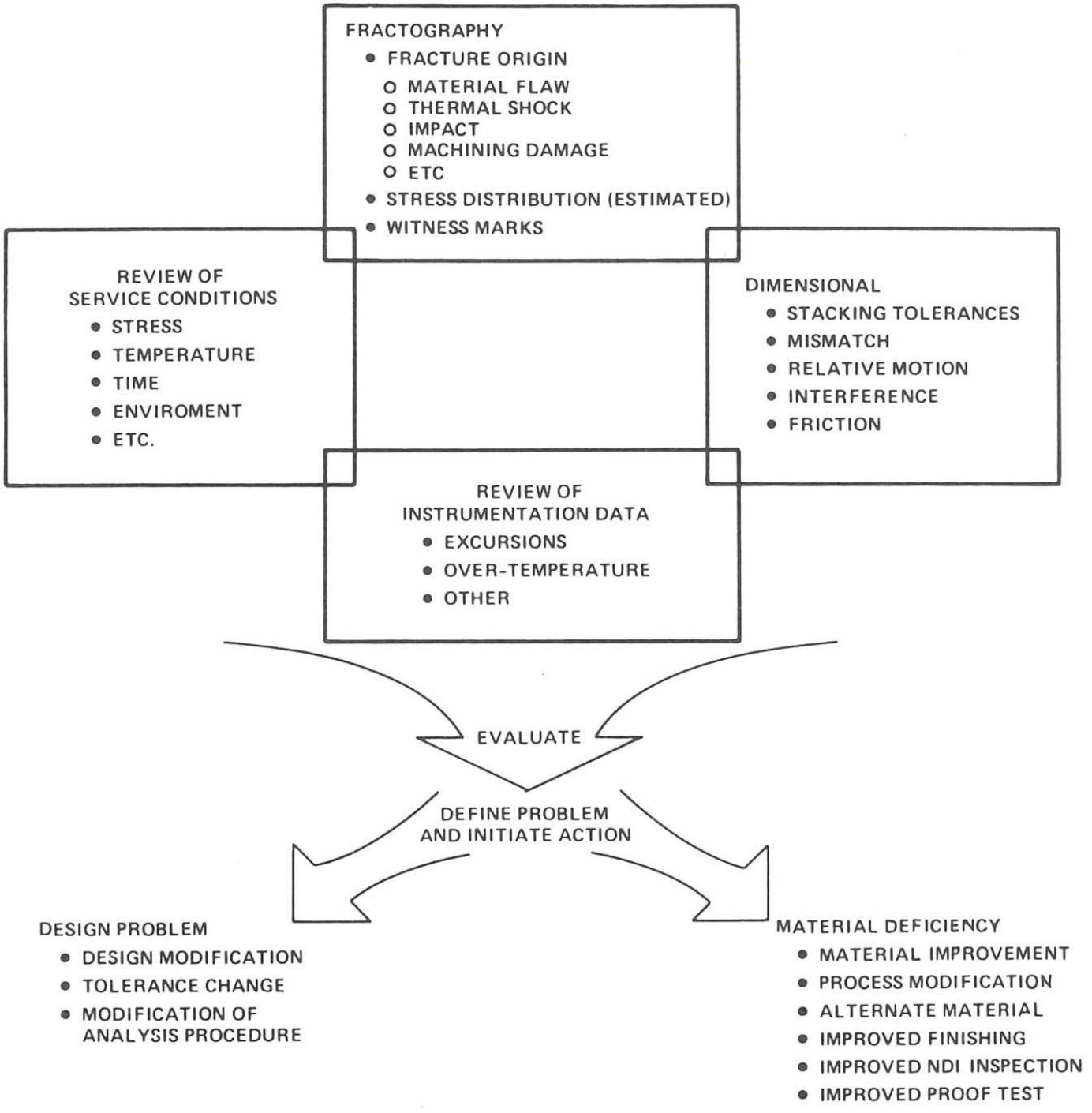

Toughening by whiskers and fibers

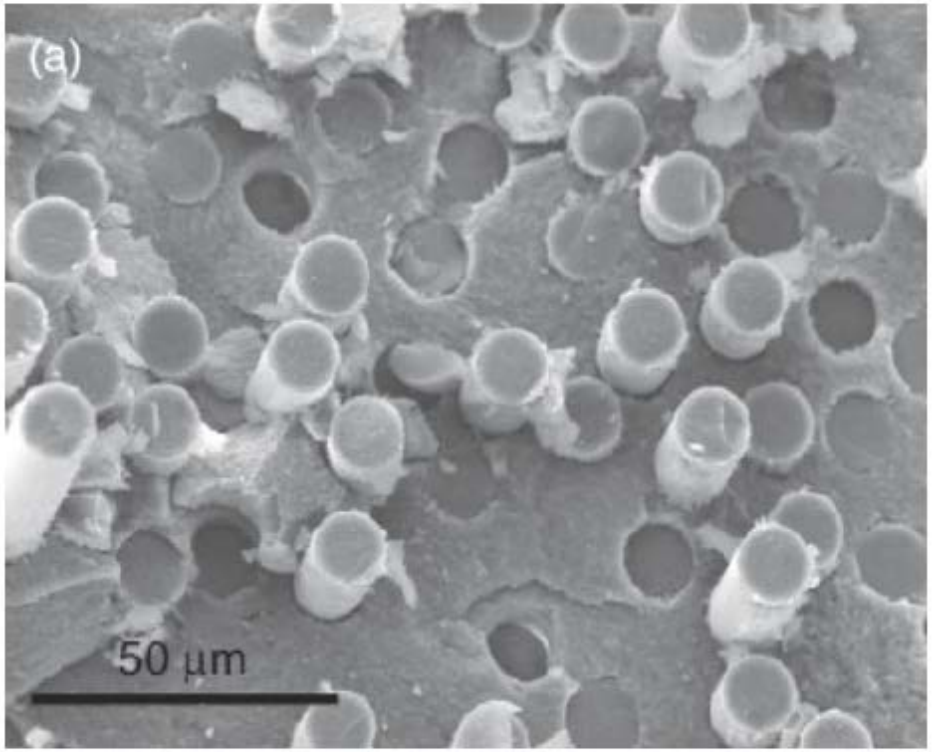

FIGURE 18.18 SEM image showing fiber pullout on the fracture surface of $AlPO_4$-coated alumina/mullite fiber/Al_2O_3 CMC, hot pressed at 1250°C for 1 h.

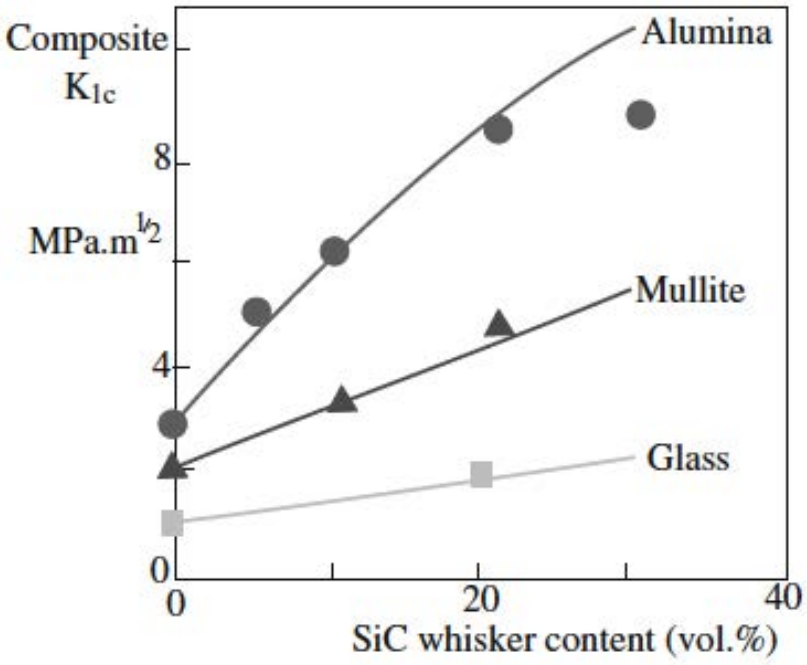

Glass theory

- Glasses lack the periodic (long range) order of a crystal
- •
- Infinite unit cell (no repeating large scale structures)
- •
- 3D network lacking symmetry and periodicity
- •
- ISOTROPIC: same average packing and properties in all directions
- •
- Crystals in different directions(see above):
- •
- different atom packing and so different properties

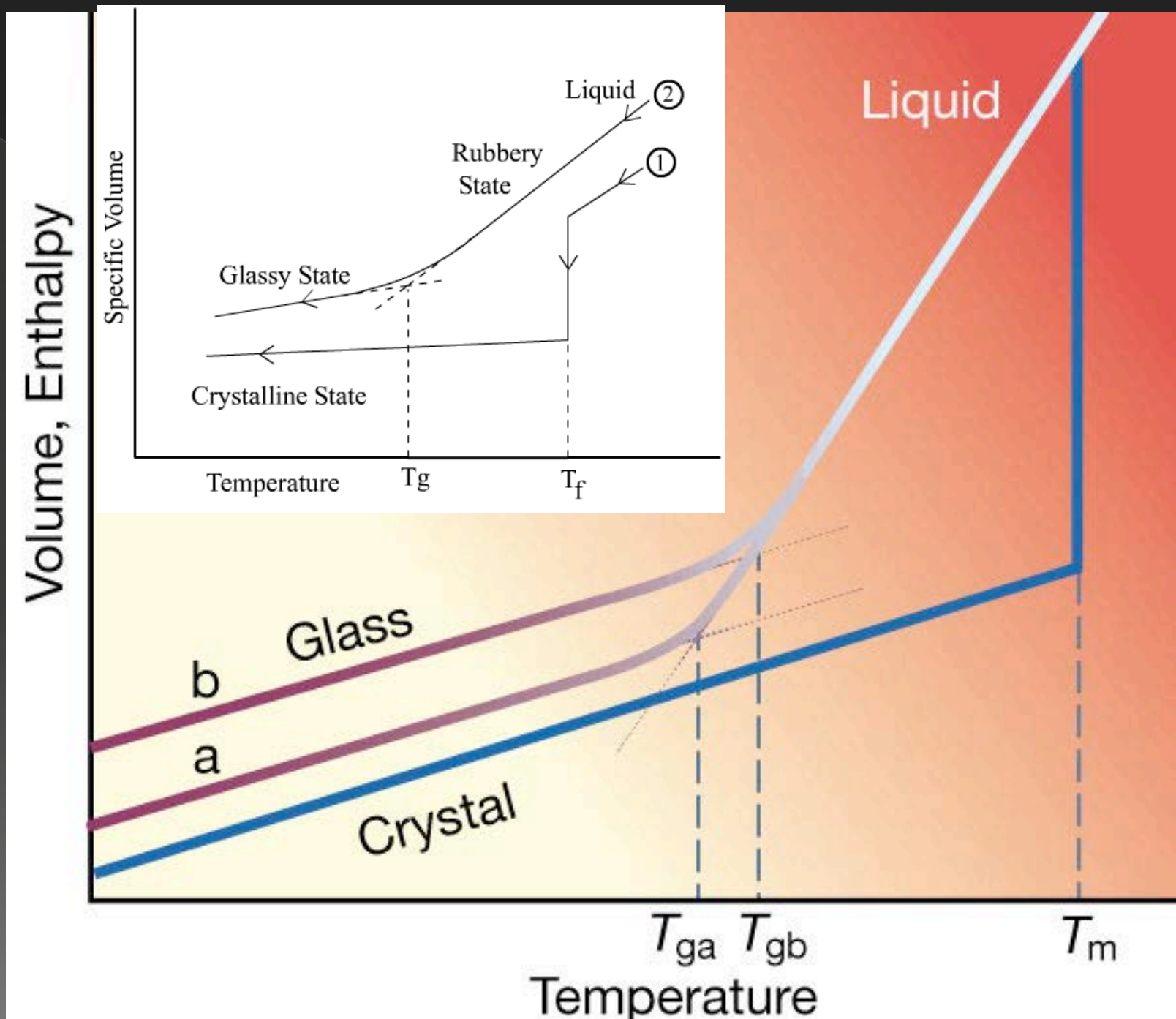
Specific Volume
Liquid
②
Rubbery
State
①
Glassy State
Crystalline State
Temperature
Tg
Tf
Volume, Enthalpy
Liquid
Glass
b
a
Crystal
Tga
Tgb
Tm
Temperature

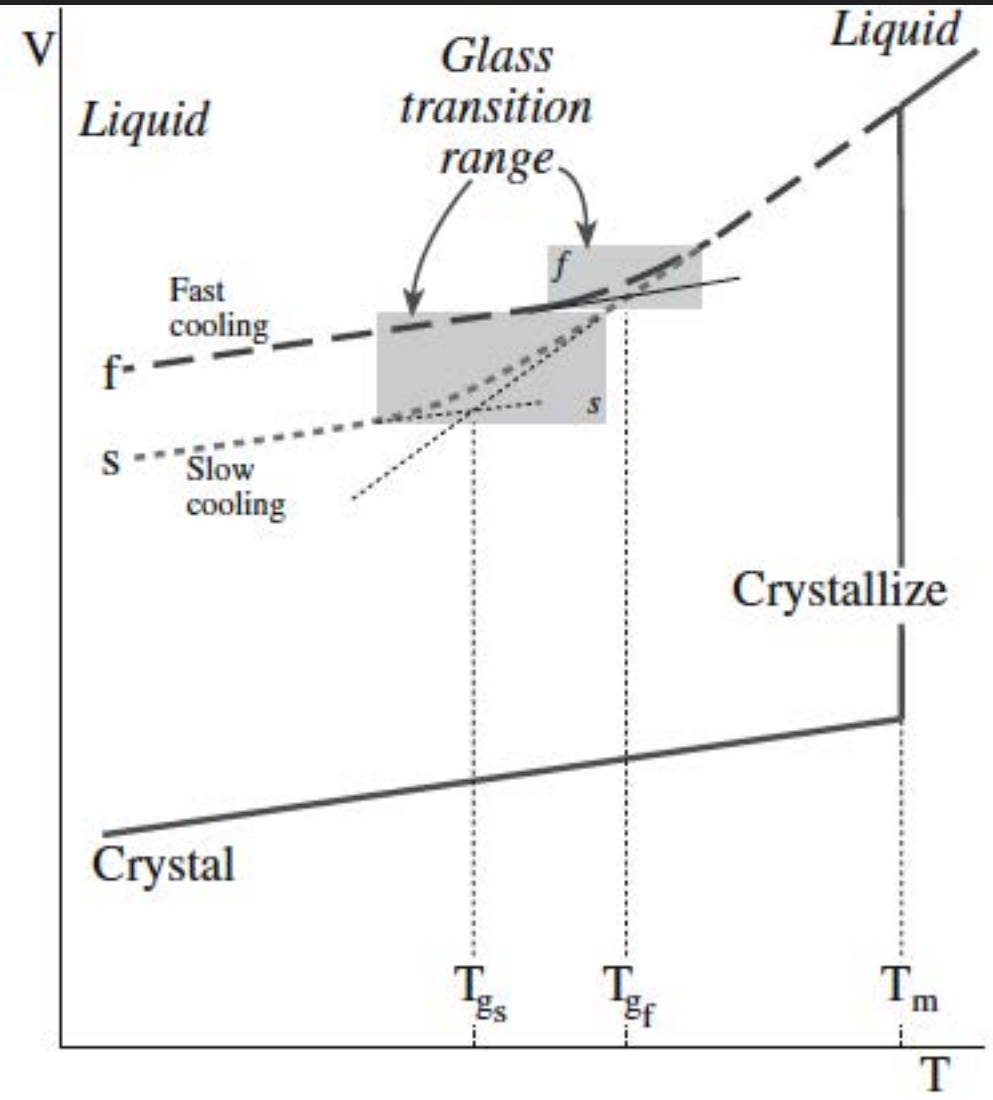

FIGURE 21.1 Plot of volume versus temperature for a liquid that forms a glass on cooling and one that forms a crystalline solid. The glass transition temperature, T_g, depends on the cooling rate and is not fixed like T_m.

Pair distribution function of SiO2 glass

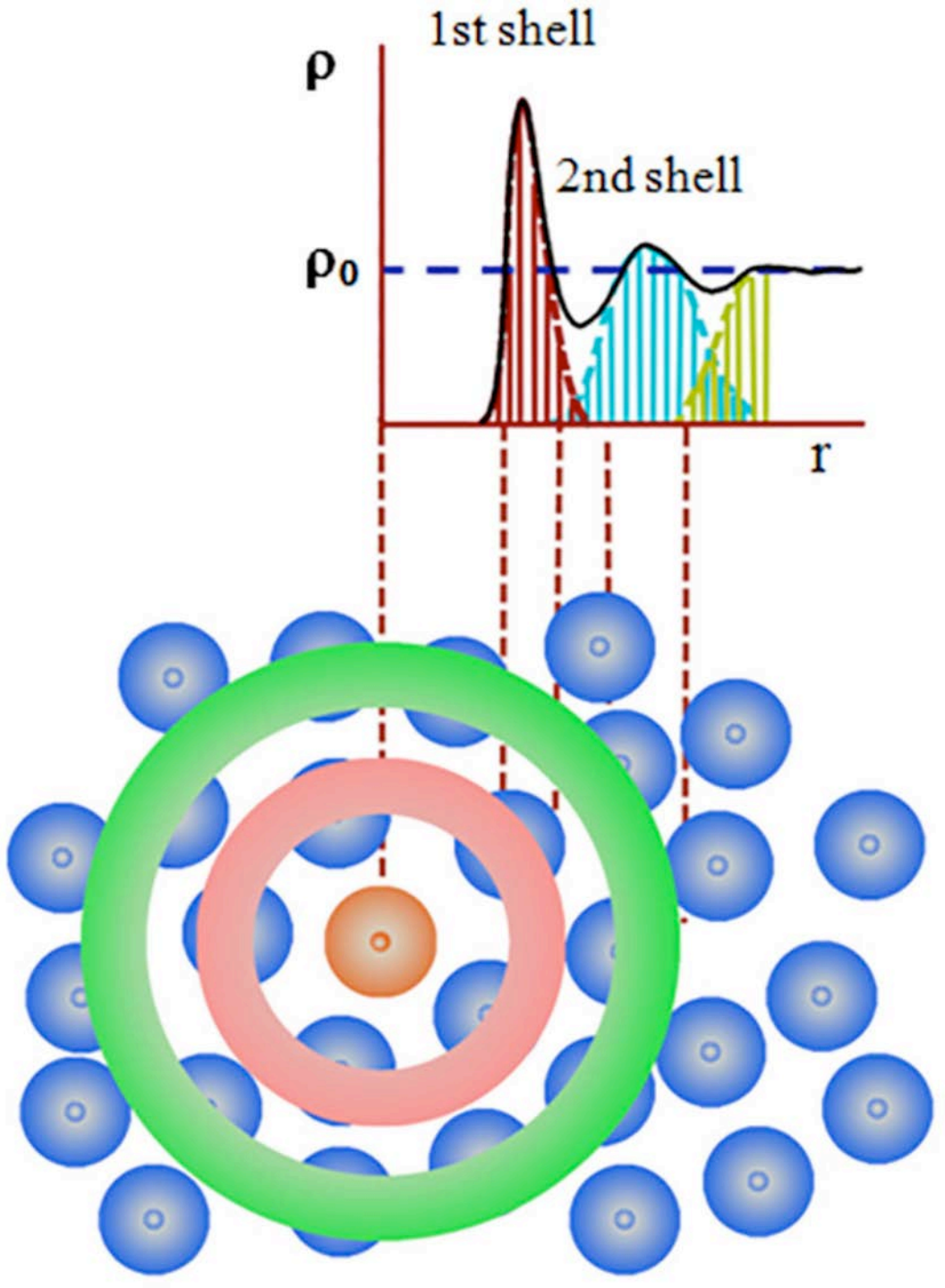

Radial distribution function for SiO_2

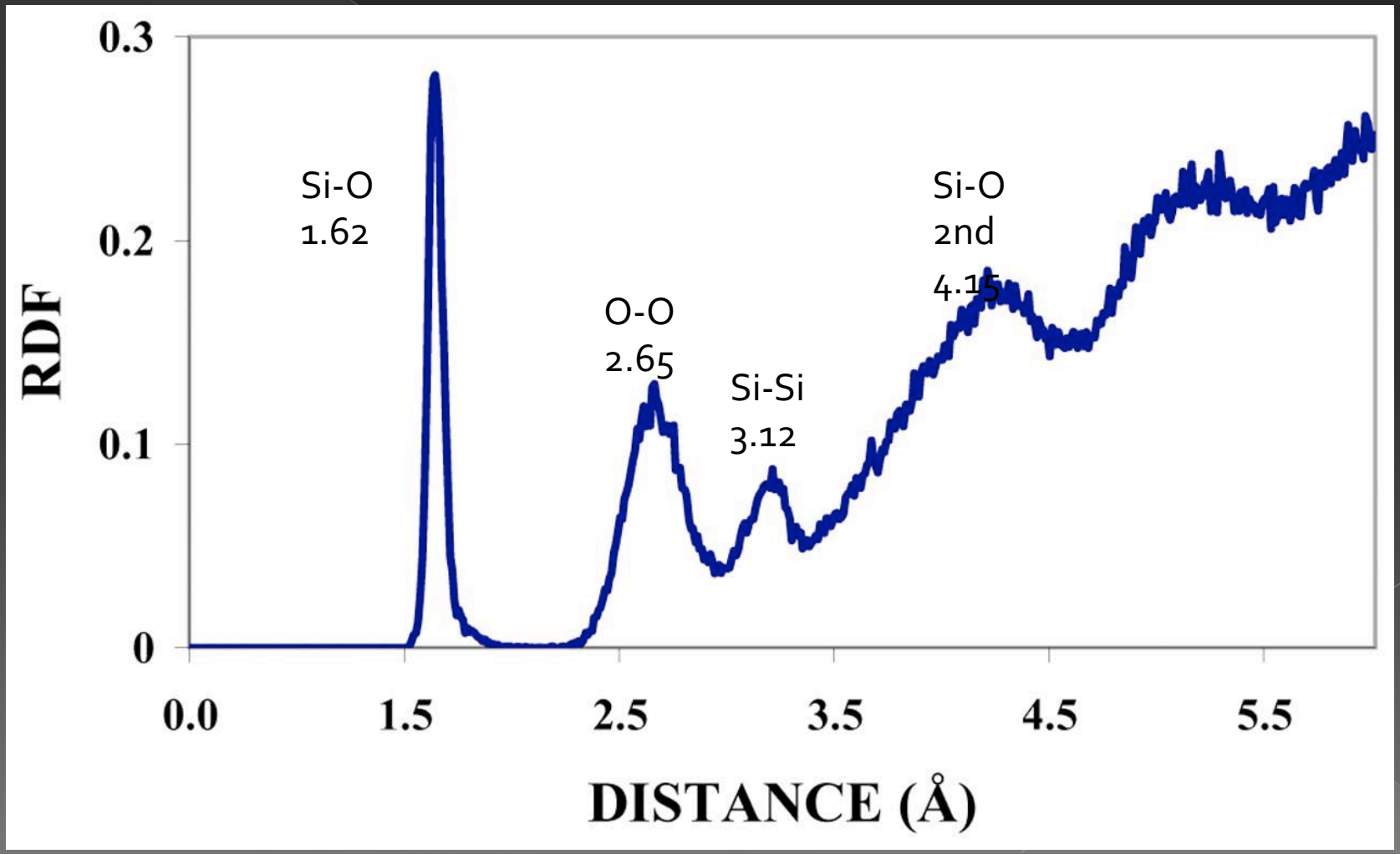

Glass structure:

SiO2 quartz compared to SiO2 glass

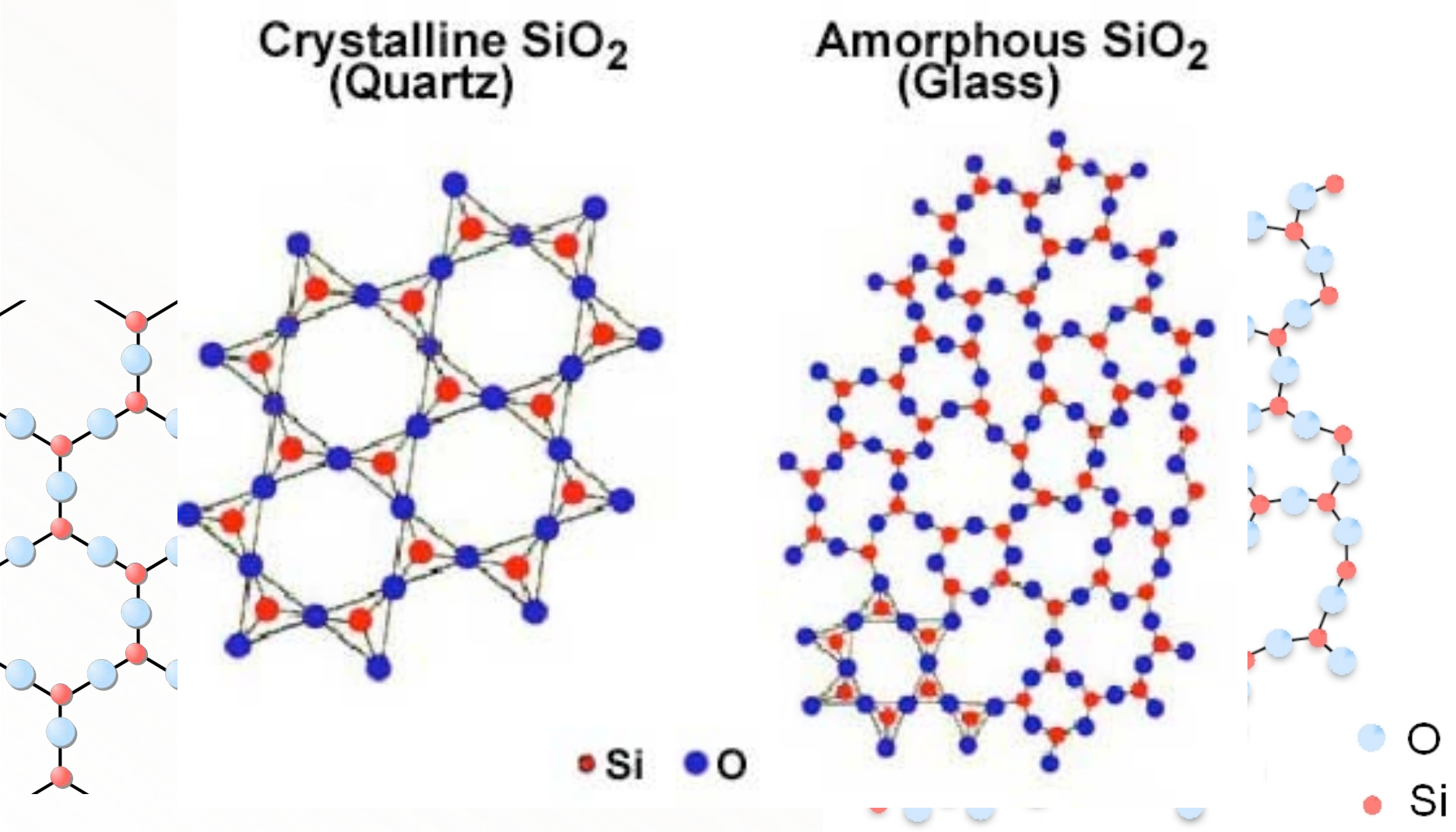

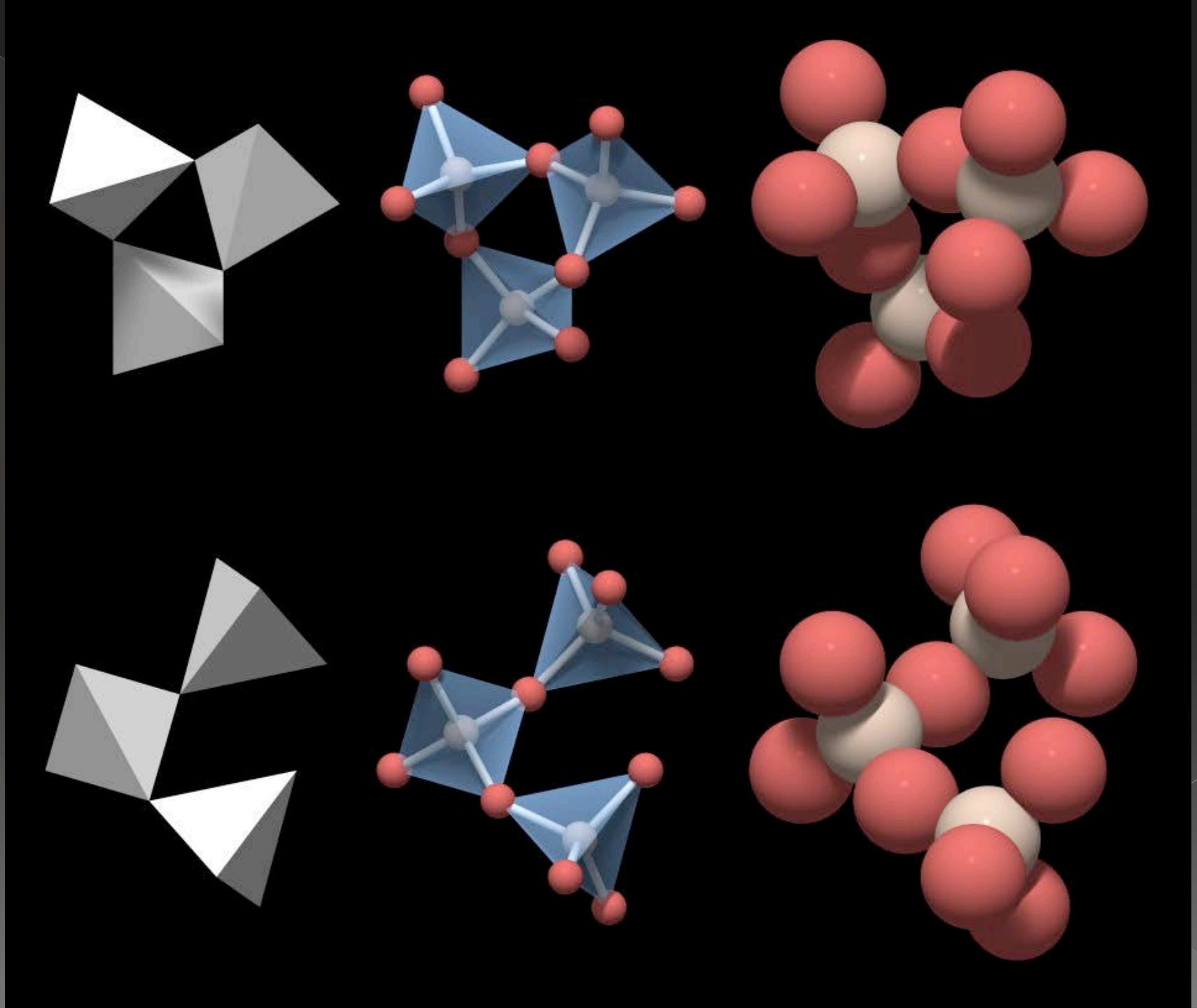

Zachariasen rules for glass A_mO_n

1) An oxygen atom is linked to no more than two glass-forming atoms A.
2) The number of oxygen atoms around each glass-forming atom A is small, perhaps 3 or 4.
3) Among the oxygen-containing polyhedra, a polyhedron cation A shares corners, but no sides or faces.
4) For three-dimensional networks of oxygen-containing polyhedra, at least three corners must be shared.

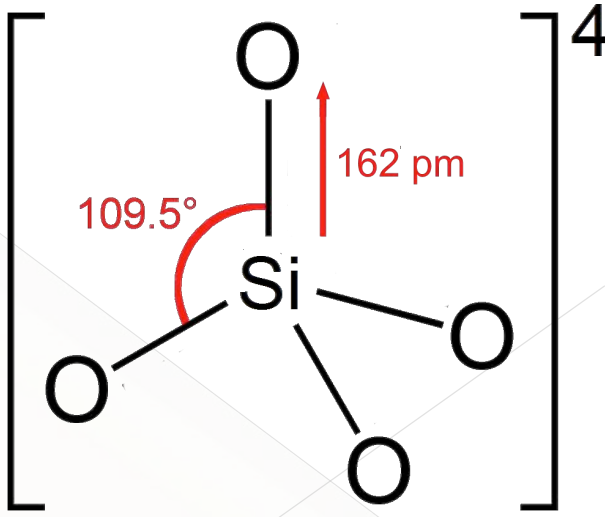

In general, all four rules should be satisfied for glass formation to occur.
Low coordination numbers, corner-sharing rules imply that glass formation is more likely with open, low density polyhedral structures.

1. Consider Silica:
    - covalent Si-O bond: sp^3 hybrid
        - tetrahedral bonding
- Pauling's packing rule:

$$\frac{r(Si^{4+})}{r(O^{2-})} = \frac{0.40}{1.40} \approx 0.29$$ *prefers tetrahedral bonding*

    - satisfies Zachariasen's rule #2.

$$\frac{charge(Si^{4+})}{CN(Si^{4+})} = \frac{4}{4} = \frac{charge(O^{2-})}{CN(O^{2-})} = \frac{2}{2}$$ $CN(O^{2-})$ *is* 2.

    - satisfies Zachariasen's rule #1.

Crystal structure: sharing four corners:

All Rules are Satisfied: SiO_2 forms a glass.

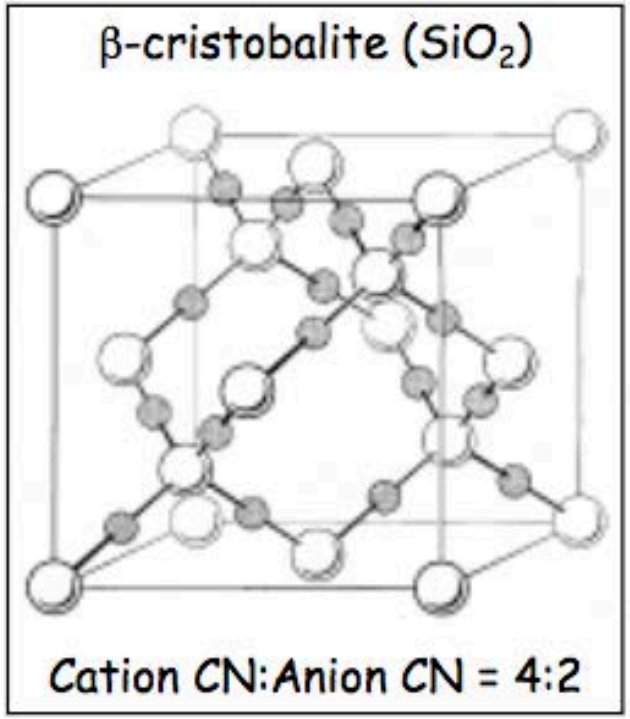

2. Consider Magnesia (MgO):

- ionic Mg-O bond
  - Pauling's packing rule:

$$\frac{r(Mg^{2+})}{r(O^{2-})} = \frac{0.72}{1.40} \approx 0.51$$ *prefers octahedral bonding*

  - violates Zachariasen's rule #2.

$$\frac{charge(Mg^{2+})}{CN(Mg^{2+})} = \frac{2}{6} = \frac{charge(O^{2-})}{CN(O^{2-})} = \frac{2}{6}$$ $CN(O^{2-})$ *is* 6.

  - violates Zachariasen's rule #1.

Crystal structure: edge-sharing polyhedra;
Rules are Not Satisfied: MgO does not form a glass.

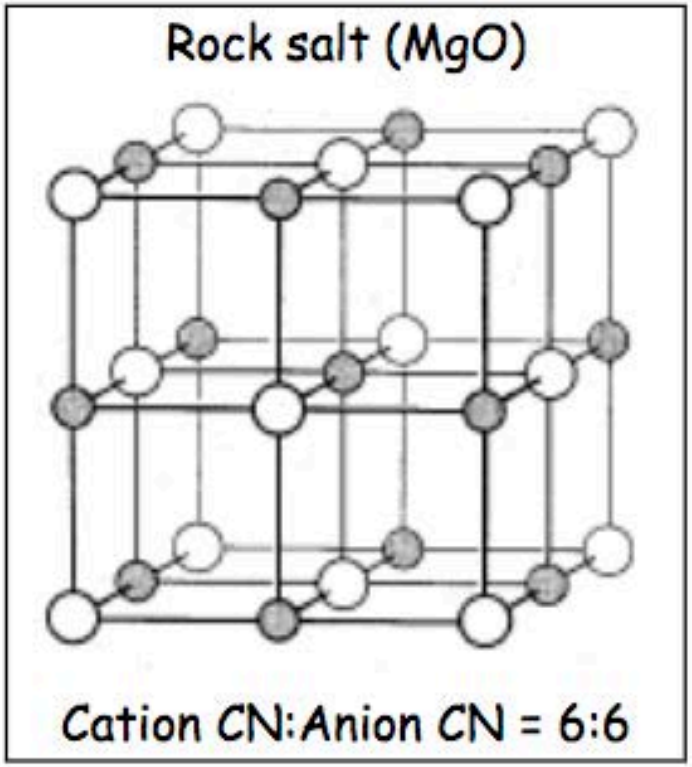

3. Consider Alumina (Al_2O_3):
   - Pauling's packing rule:

$$\frac{r(Al^{3+})}{r(O^{2-})} = \frac{0.53}{1.40} \approx 0.38$$ *octahedral / tetrahedral boundary*

   - octahedral CN preferred in Al_2O_3.

$$\frac{charge(Al^{3+})}{CN(Al^{3+})} = \frac{3}{6} = \frac{charge(O^{2-})}{CN(O^{2-})} = \frac{2}{4}$$ $CN(O^{2-})$ *is* 4.

   - violates Zachariasen's rule #1.

Al_2O_3 does not form a glass.

Elements for glass formation

Formers	Modifiers	Intermediate
B	Sc	Ti
Si	La	Zr
Ge	Na	Pb
Al	K	Al
V	Rb	Th
As	Cs	

Log Glass Viscosity vs. Temperature

- Viscosity decreases with T

- soda-lime glass: 70% SiO_2 balance Na_2O (soda) & CaO (lime)
- borosilicate (Pyrex): 13% B_2O_3, 3.5% Na_2O, 2.5% Al_2O_3
- Vycor: 96% SiO_2, 4% B_2O_3
- fused silica: > 99.5 wt% SiO_2

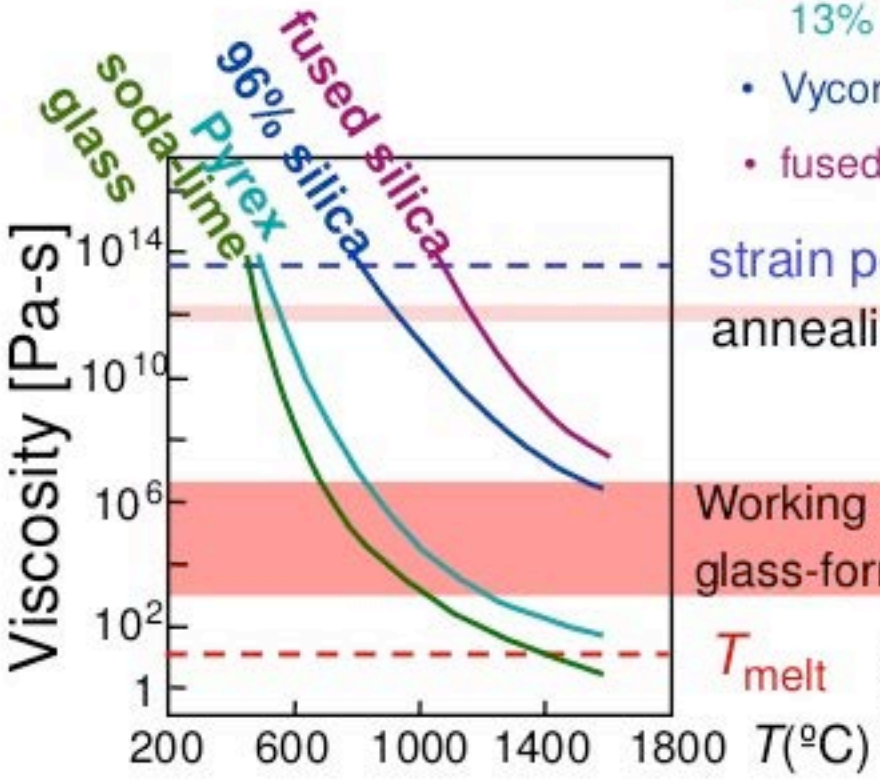

Adapted from Fig. 13.7, *Callister & Rethwisch 8e.* (Fig. 13.7 is from E.B. Shand, *Engineering Glass*, Modern Materials, Vol. 6, Academic Press, New York, 1968, p. 262.)

Glass Viscosity and Workability

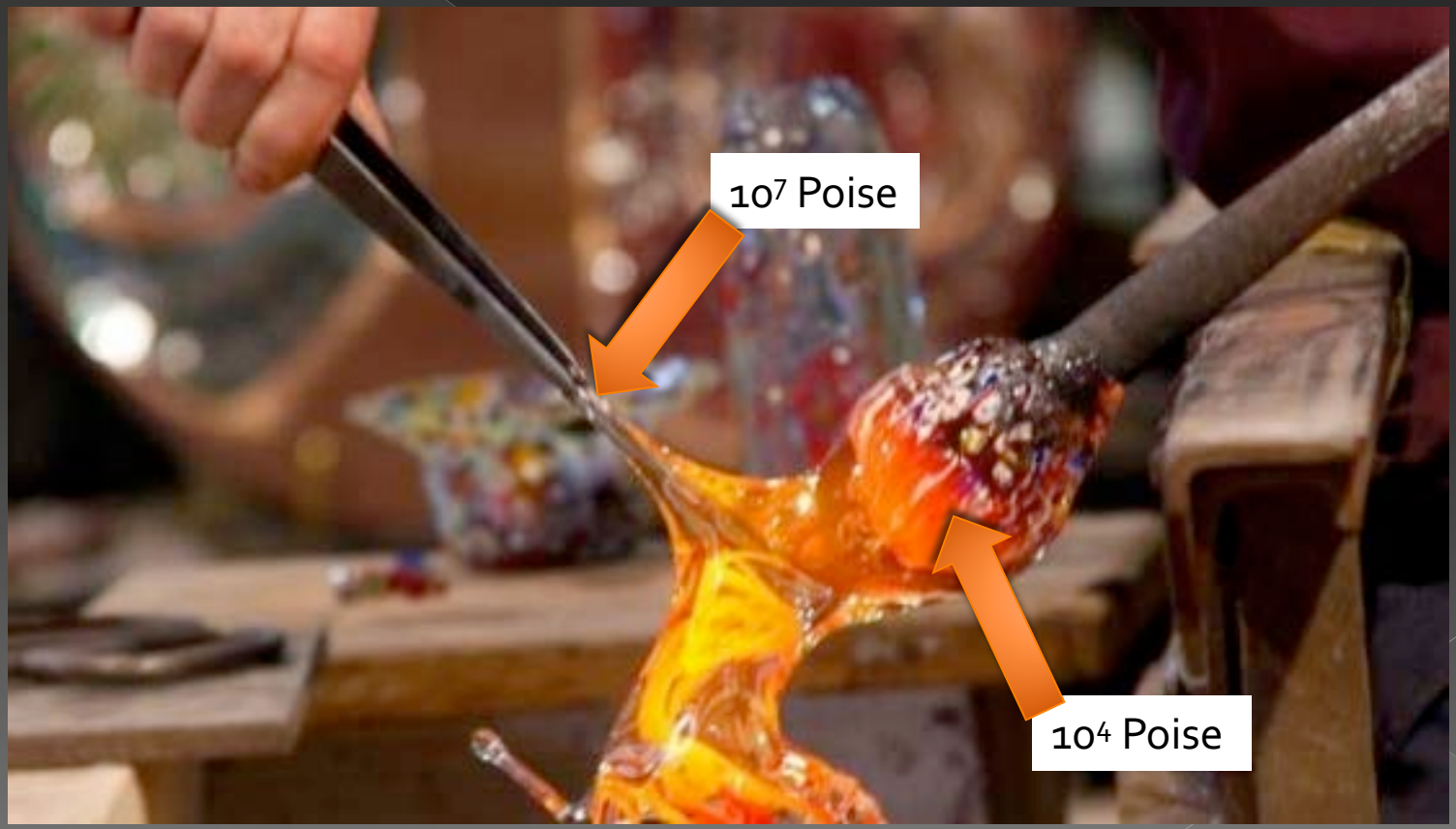

Pilkington process

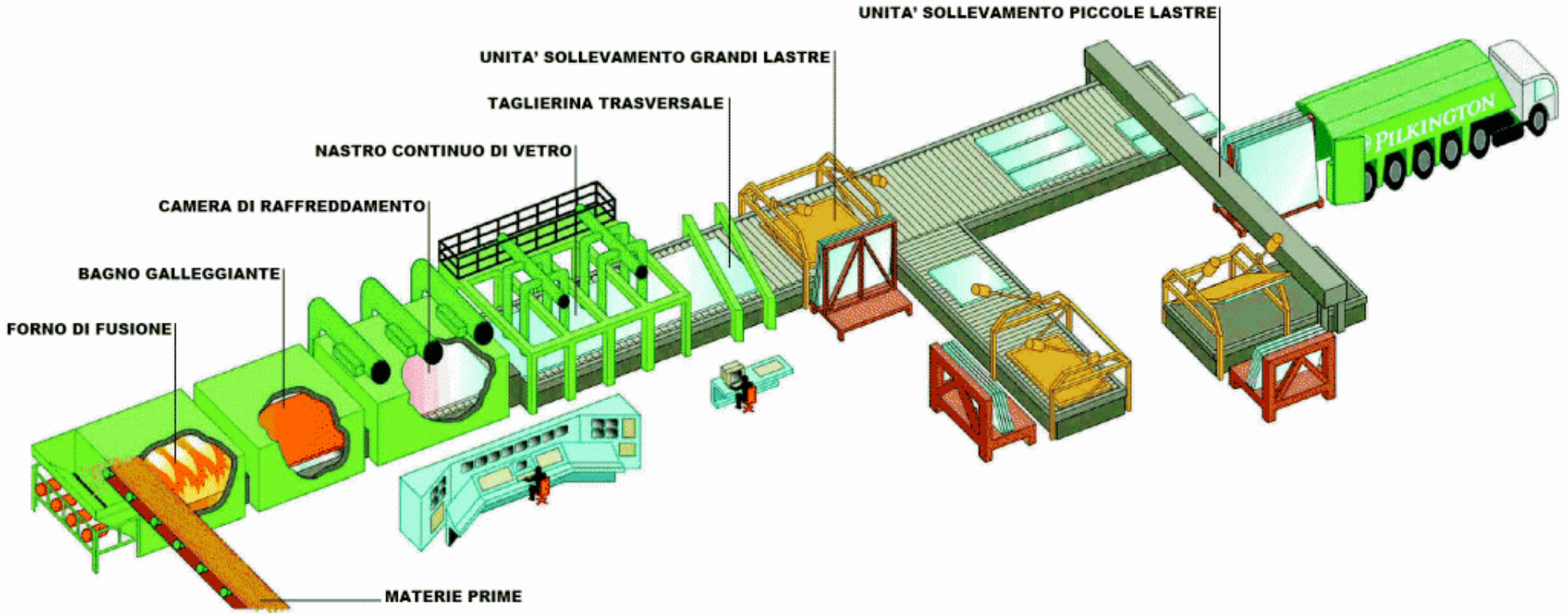

https://www.youtube.com/watch?v=ig4G5WbOMLc

Glass bending

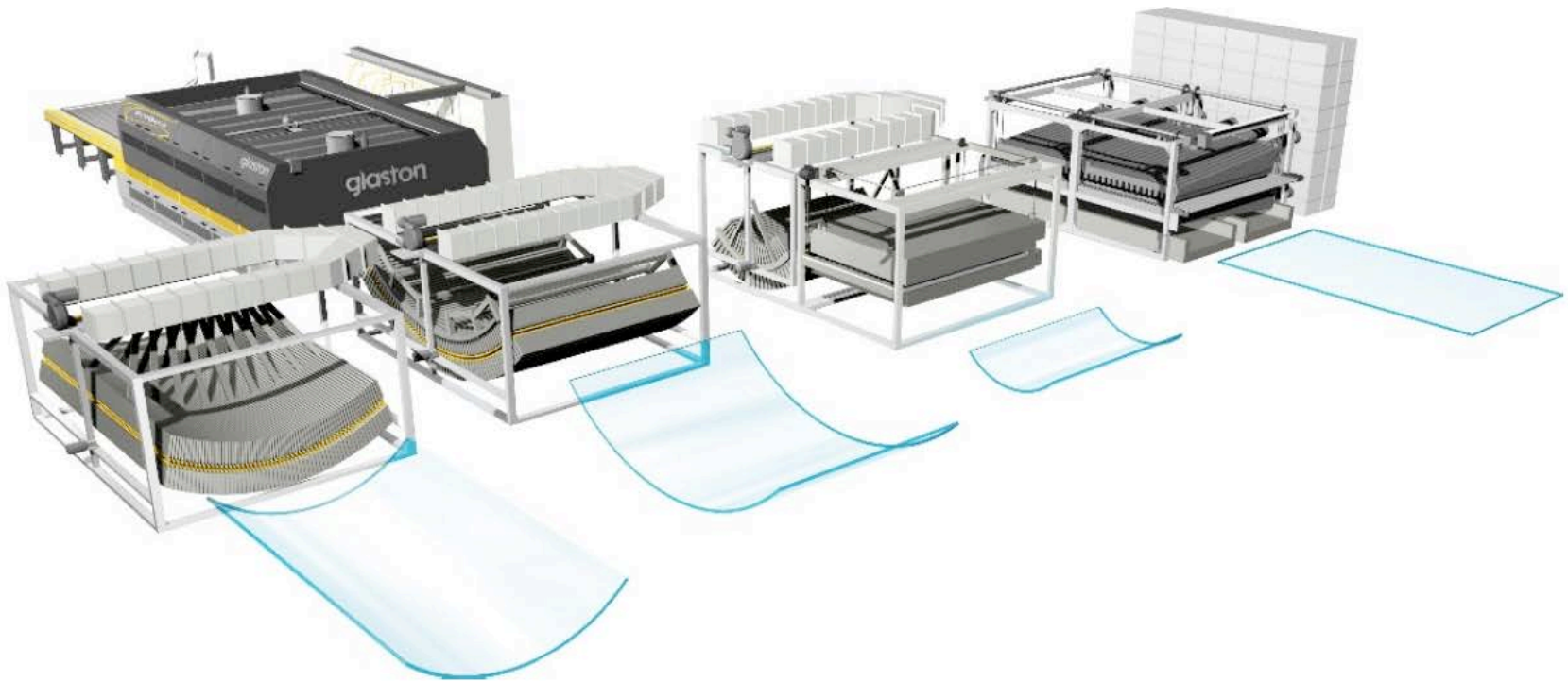

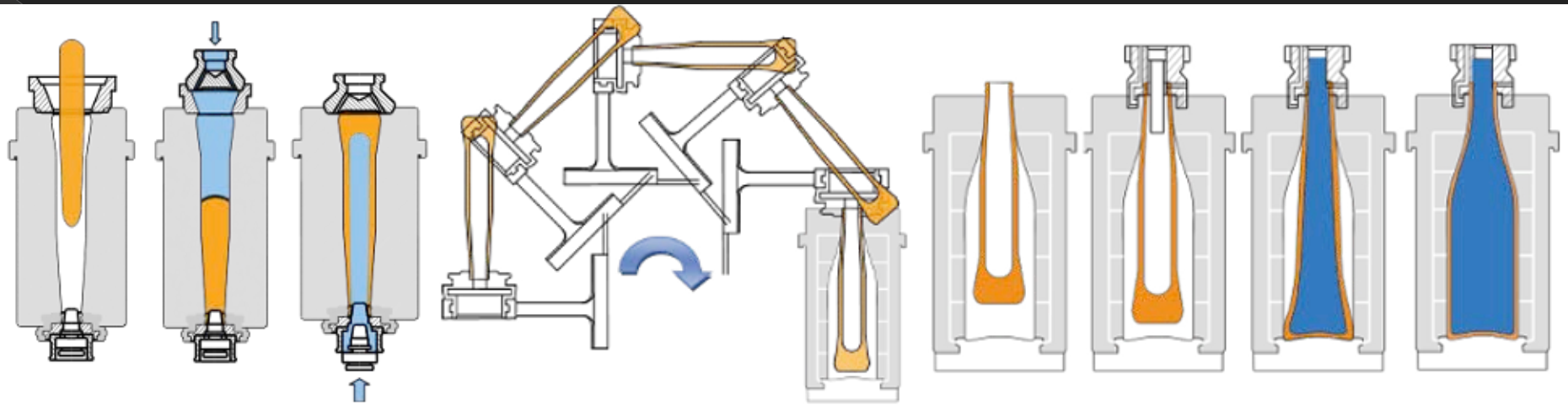

Bottle production line

http://www.youtube.com/watch?v=A_M8WBJMcMo

Dielectrics

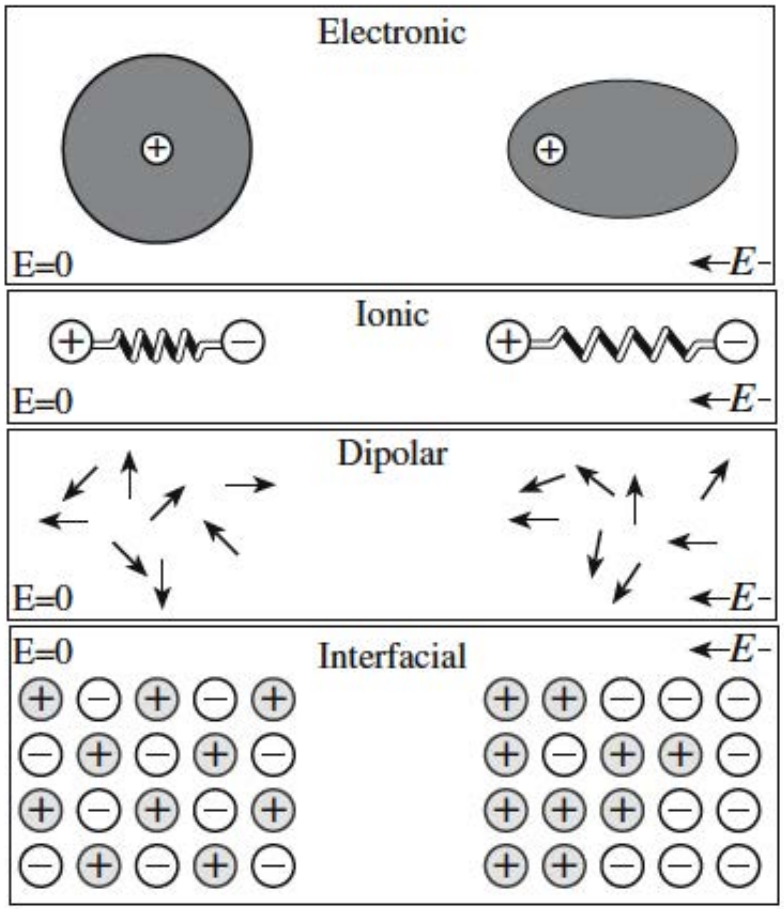

FIGURE 31.1 Illustration of the different polarization mechanisms n a solid.

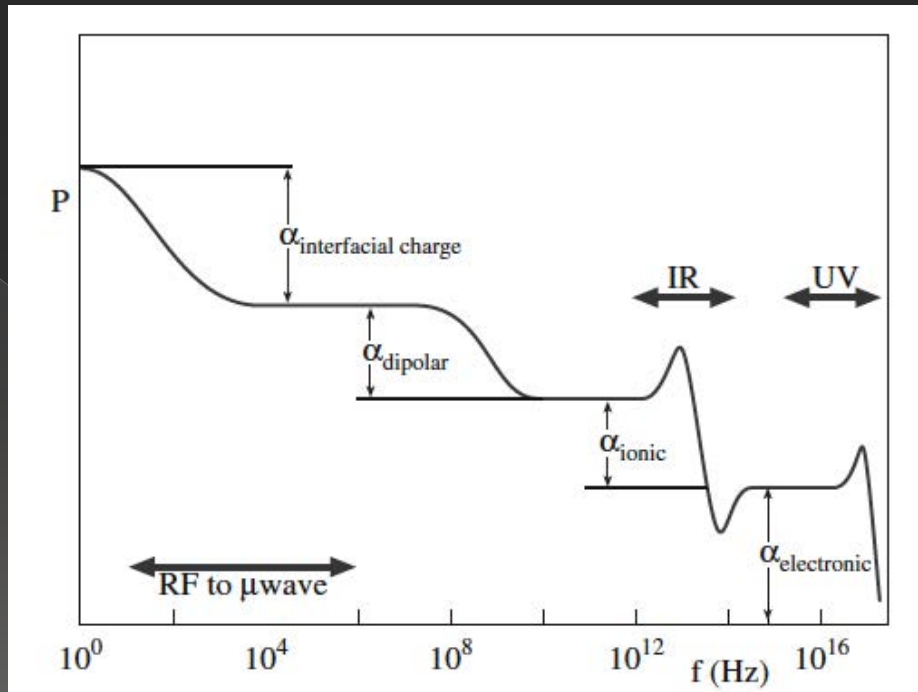

FIGURE 31.2 Frequency dependence of polarization.

TABLE 31.2 Dielectric Constants of Various Ceramics

Material	*κ at 1 MHz*	*Material*	*κ at 1 MHz*
Diamond	5.5–6.6	Al_2O_3	8.8
SiO_2	3.7–3.8	MgO	9.6
NaCl	5.9	$BaTiO_3$	3000
Mica	5.4–8.7	Pyrex glass	4.0–6.0
Soda-lime glass	7.0–7.6	TiO_2	14–110
Steatite ($SiO_2 + MgO + Al_2O_3$)	5.5–7.5	Forsterite ($2MgO \cdot SiO_2$)	6.2
Cordierite ($SiO_2 + MgO + Al_2O_3$)	4.5–5.4	Mullite	6.6
High-lead glass	19		

TABLE 31.4 Dielectric Strengths for Various Ceramics

Material	*Dielectric strength (MV/cm at 25°C)*
Al_2O_3 (99.5%)	0.18
Al_2O_3 (94.0%)	0.26
High-voltage porcelain	0.15
Steatite porcelain	0.10
Lead glass	0.25
Lime glass	2.5
Borosilicate glass	5.8
Fused quartz	6.6
Quartz crystal	6.0
NaCl [100], [111], [110]	2.5, 2.2, 2.0
Muscovite mica	10.1

Dielectric constant of $BaTiO_3$

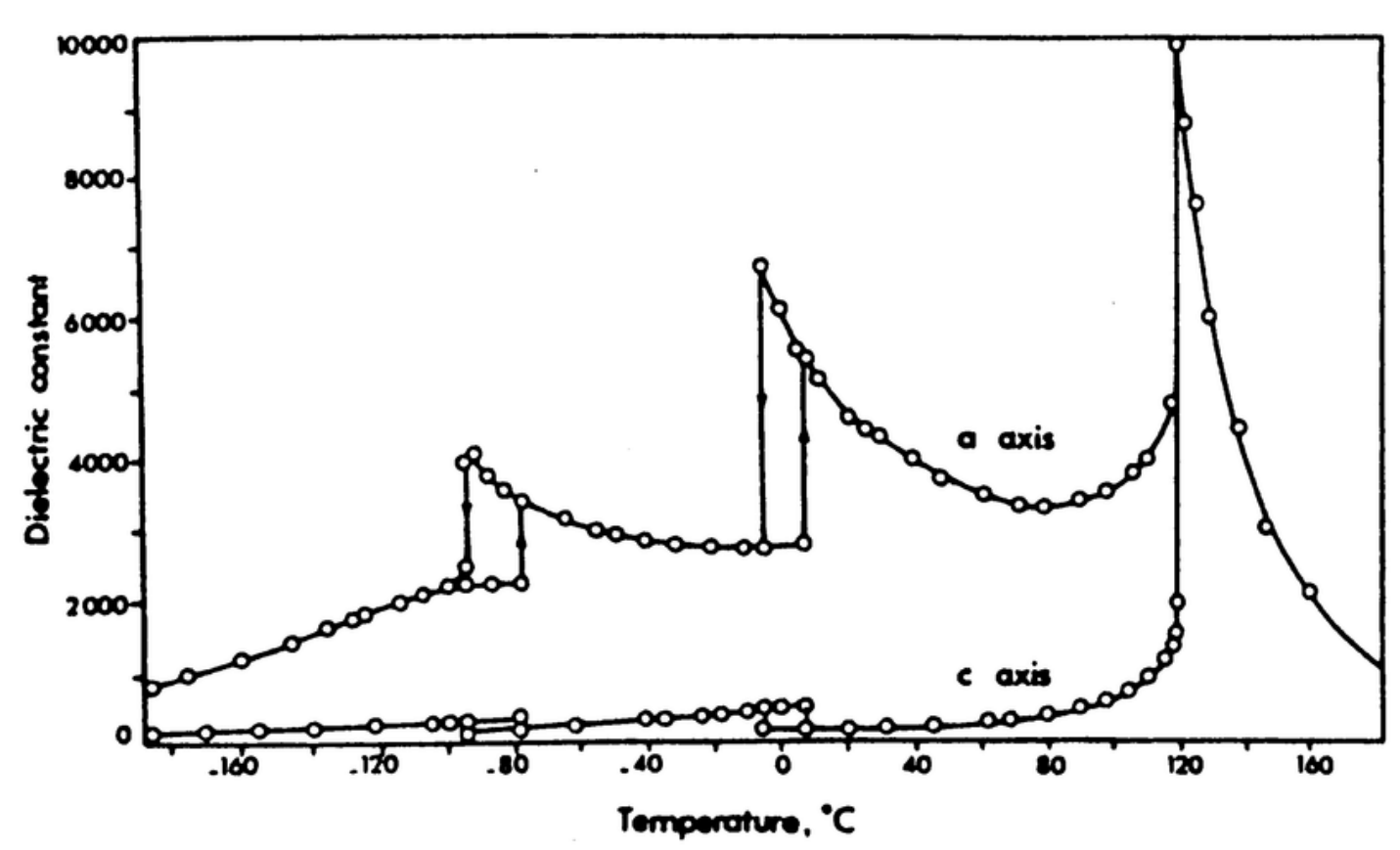

Positive Temperature coefficient, PTC of Barium Titanate

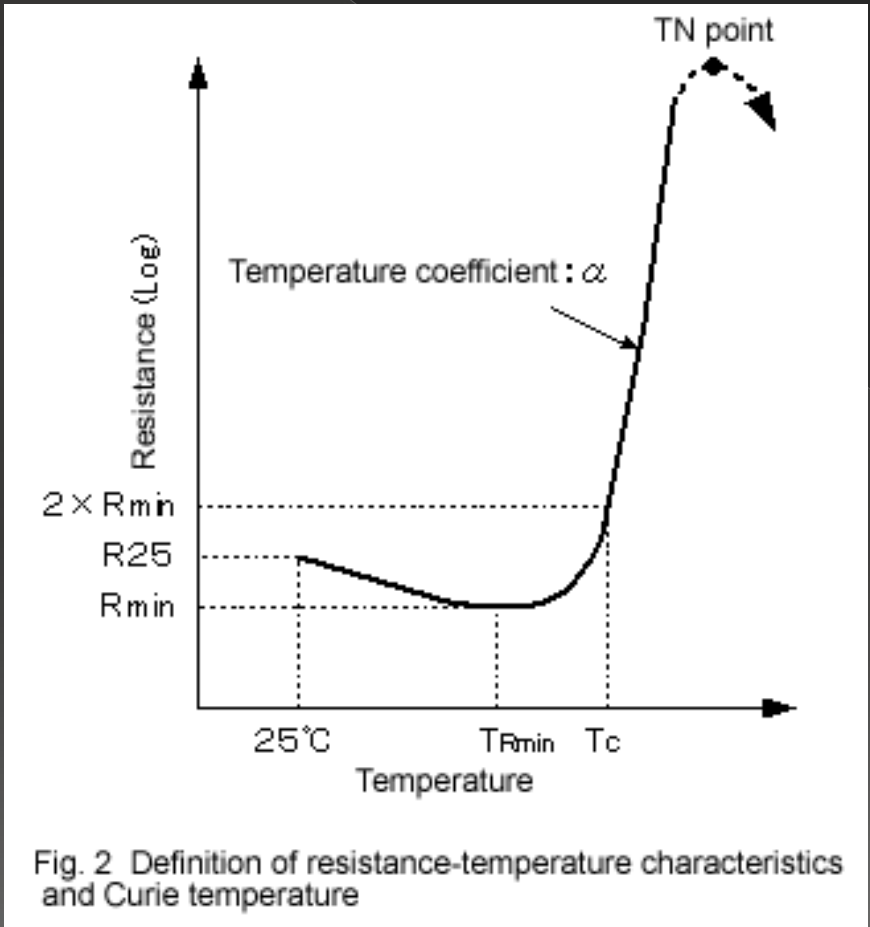

Fig. 2 Definition of resistance-temperature characteristics and Curie temperature

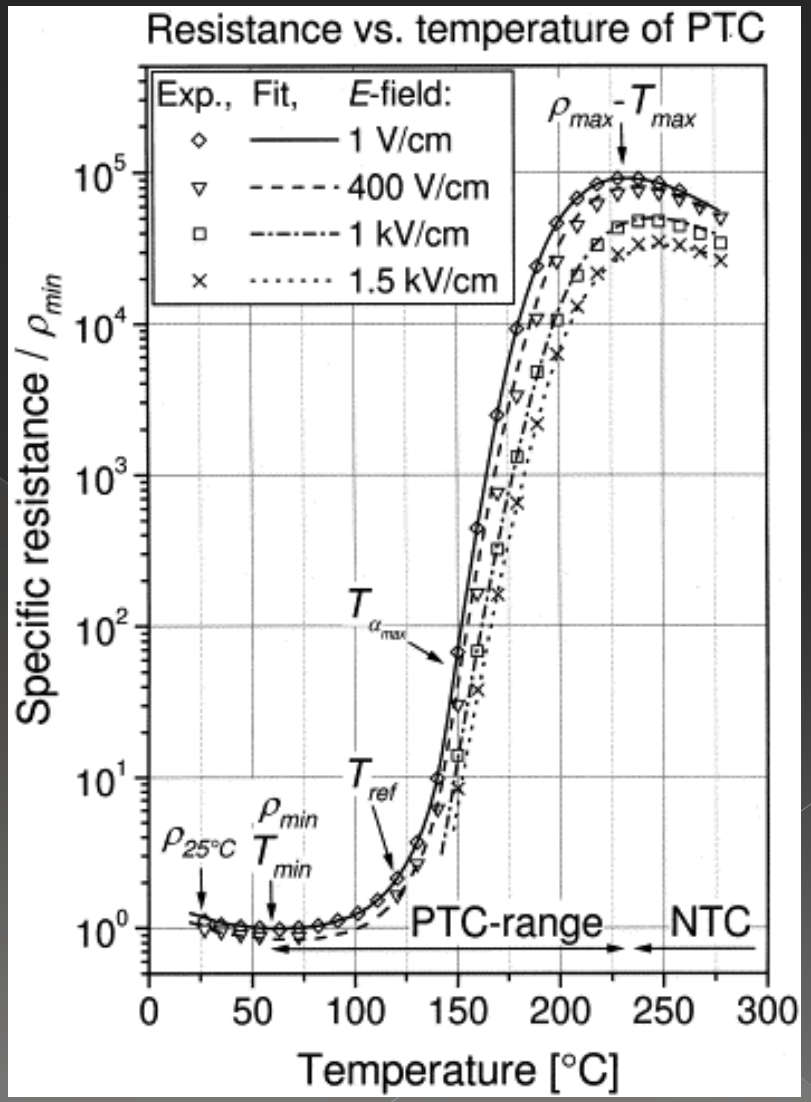

Explanation for PTC behavior of $BaTiO_3$

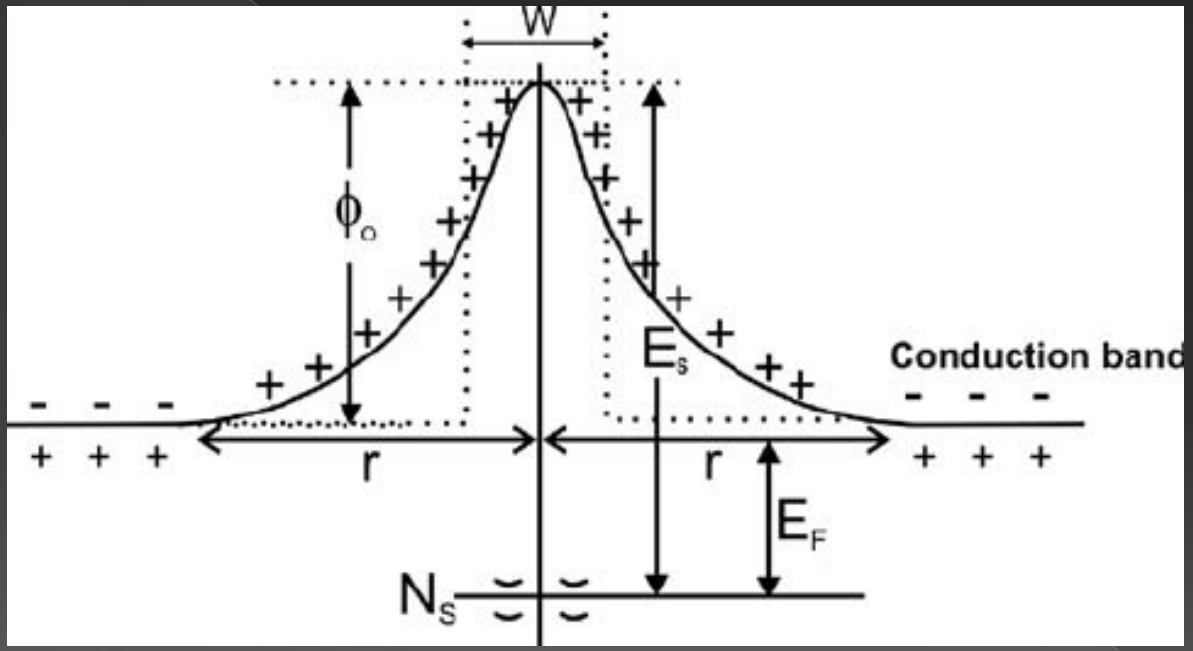

Domains in ferroelectric depend on the orientation of the polarization

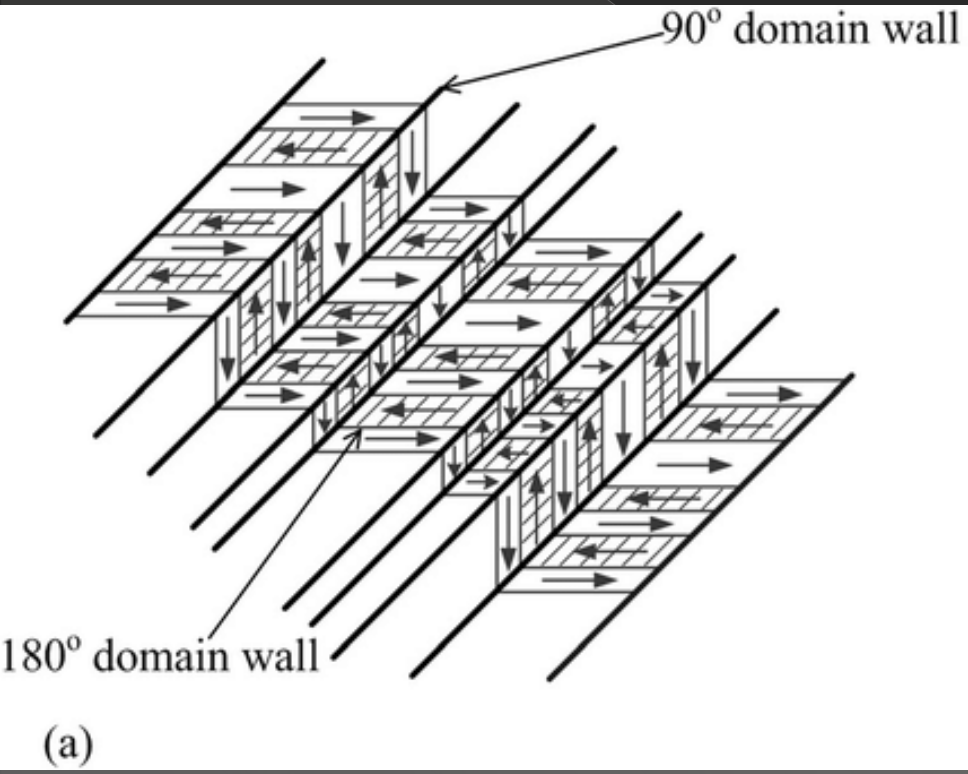

(a)

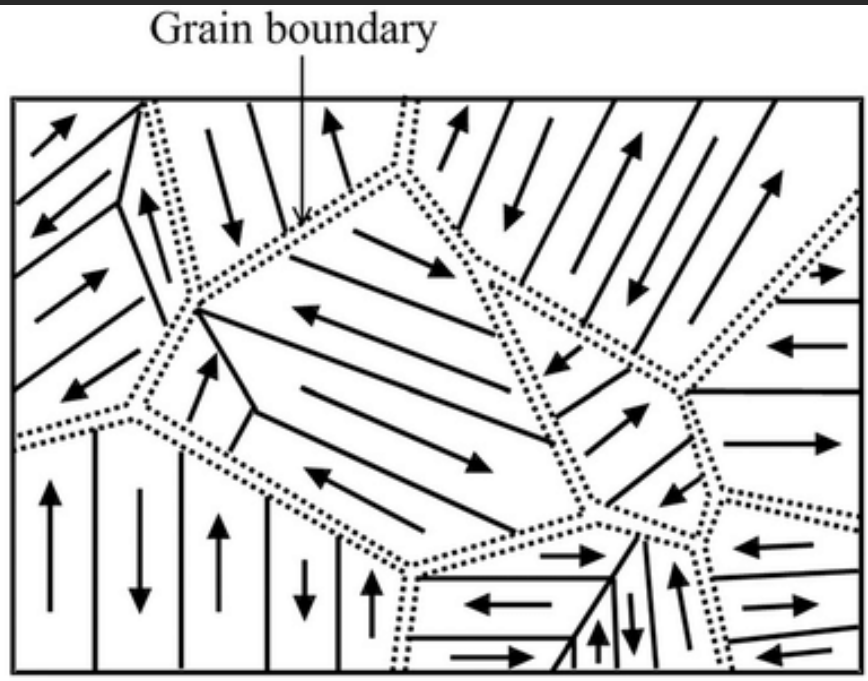

(b)

Ferroelectric domain in a ferroelectric materials

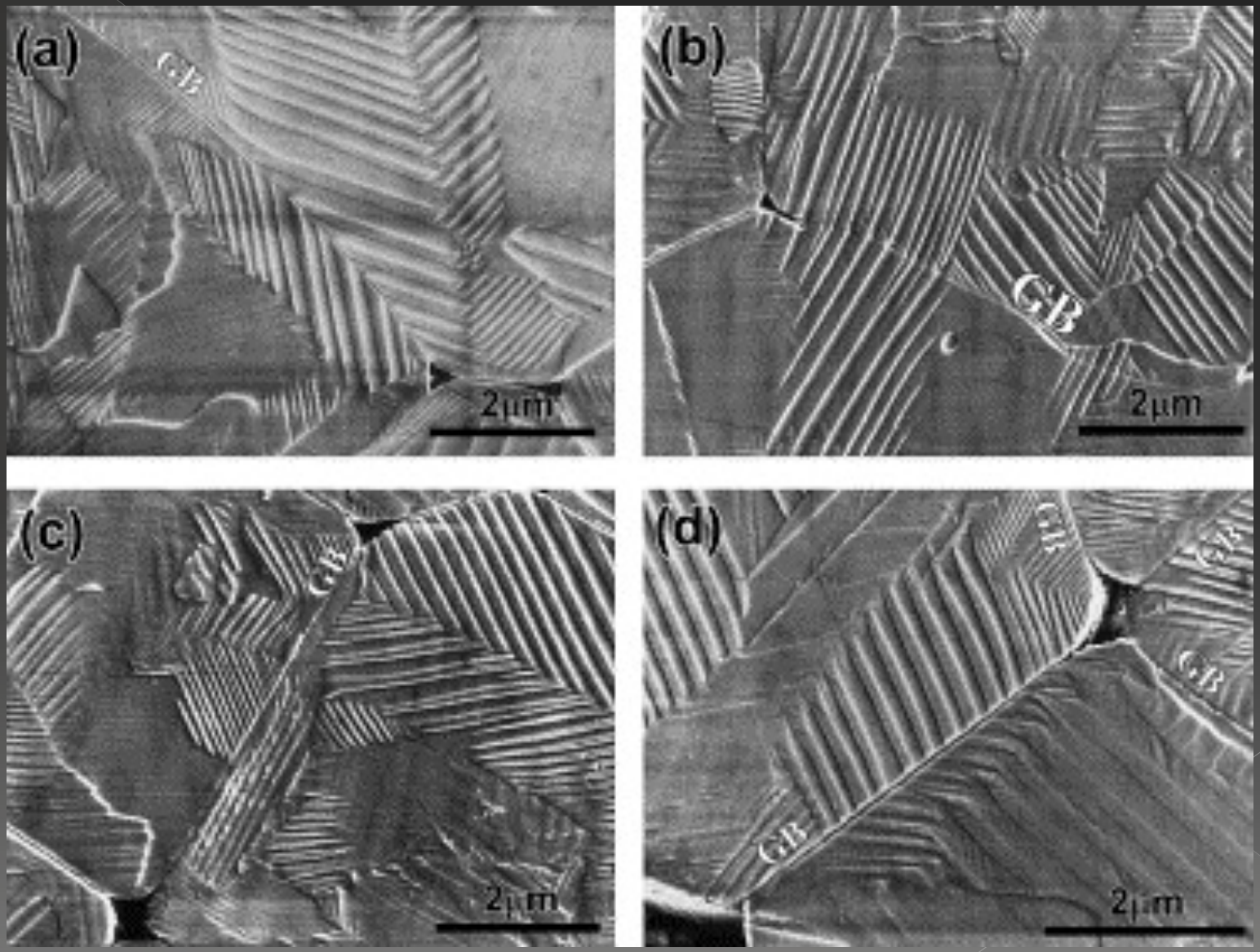

Non destructive testing Techniques

- Visual inspection
- Penetrant dyes https://www.youtube.com/watch?v=xEK-c1pkTUI
- Ultrasonic testing https://www.youtube.com/watch?v=UM6XKvXWVFA
- Radiographic testing https://www.youtube.com/watch?v=IcWjZbXiFkM
- Magnetoscopic testing
- Eddy currents

Proof testing:

1) load configuration as similar as possible to service condiction

2) one single test slightly above load/stress values in service

Liquid penetrant dyes

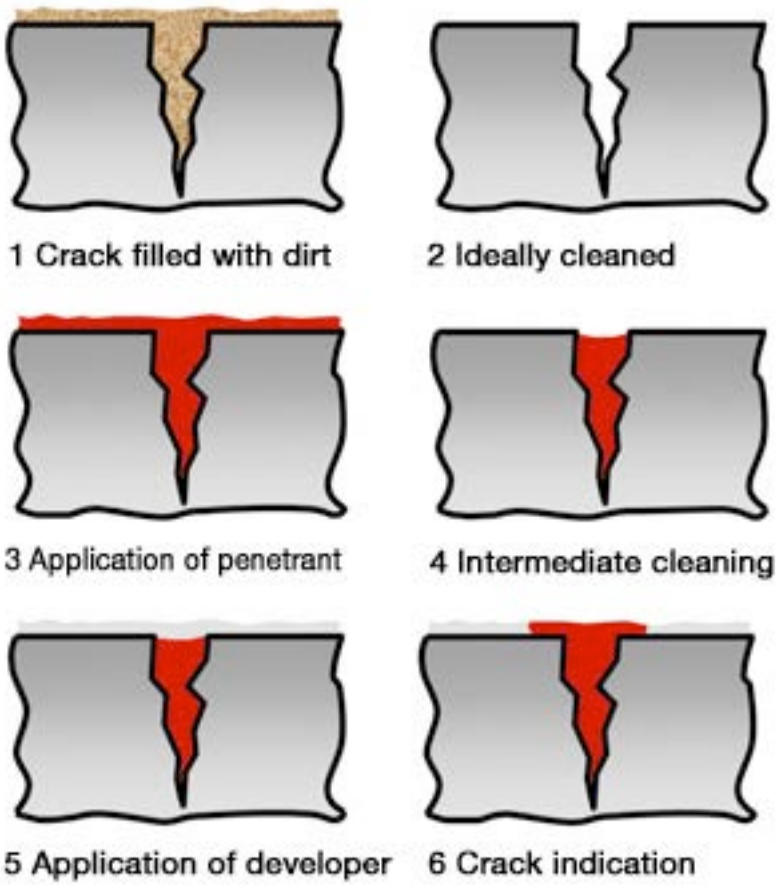

Fluorescent penetrant dye revealed with a Wood lamp

Ultrasonic testing

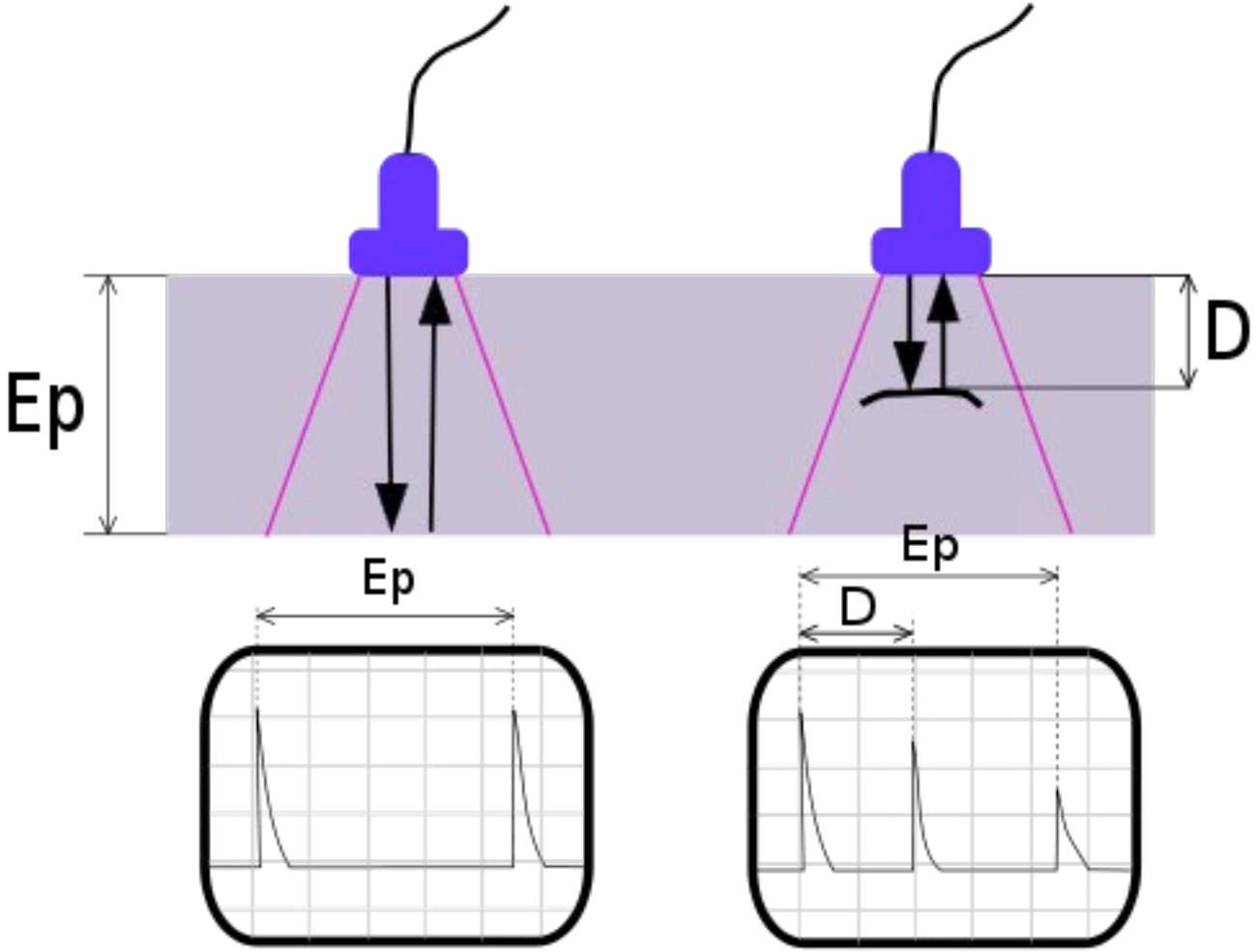


270°

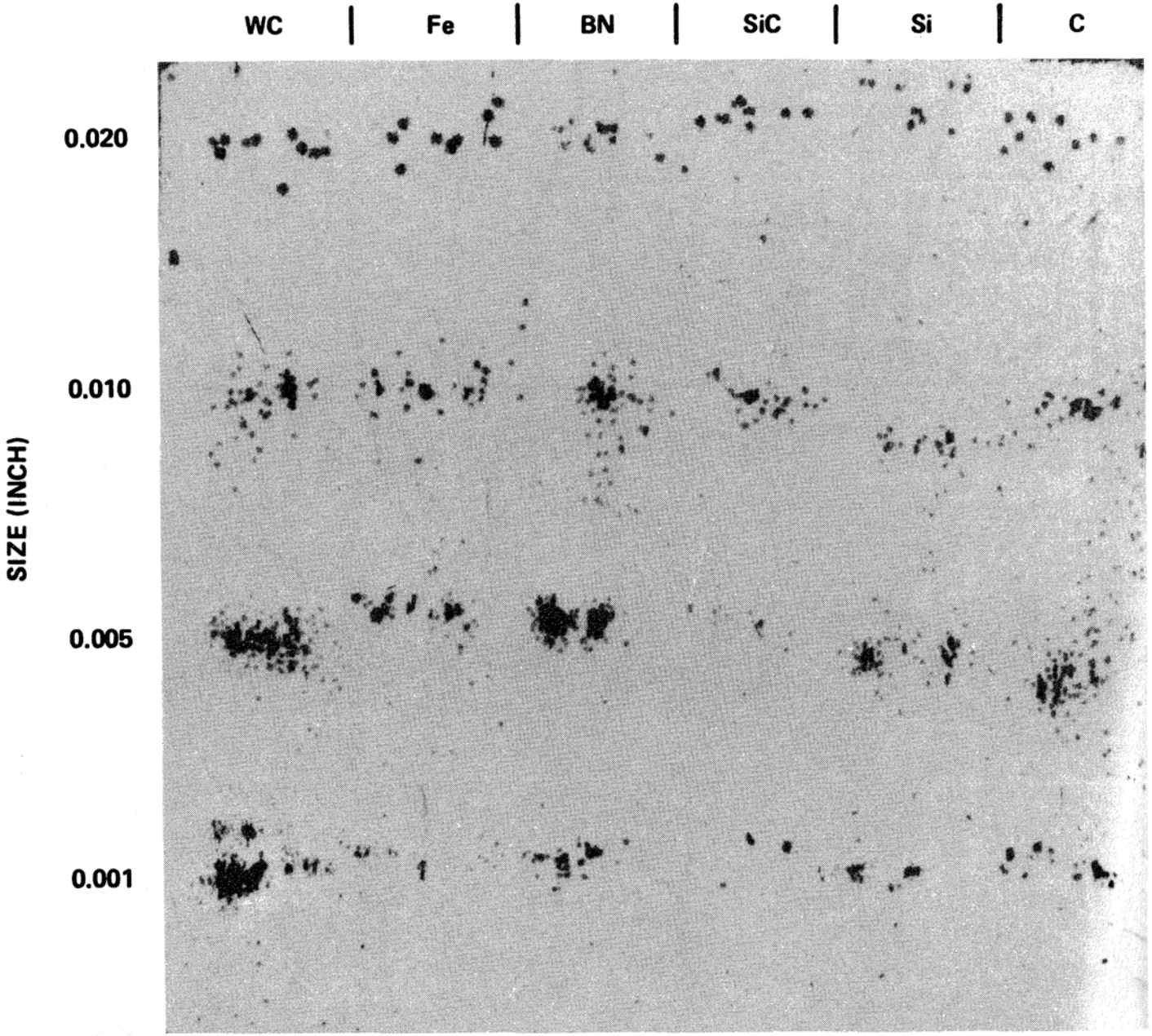

Figure 13.10 Ultrasonic C-scan with a 25-MHz transducer of a 0.64-cm (0.25-in.)-thick hot-pressed Si_3N_4 plate. (Courtesy Garrett Turbine Engine Company, Phoenix, Ariz., Division of Allied-Signal Aerospace.)

Radiographic testing

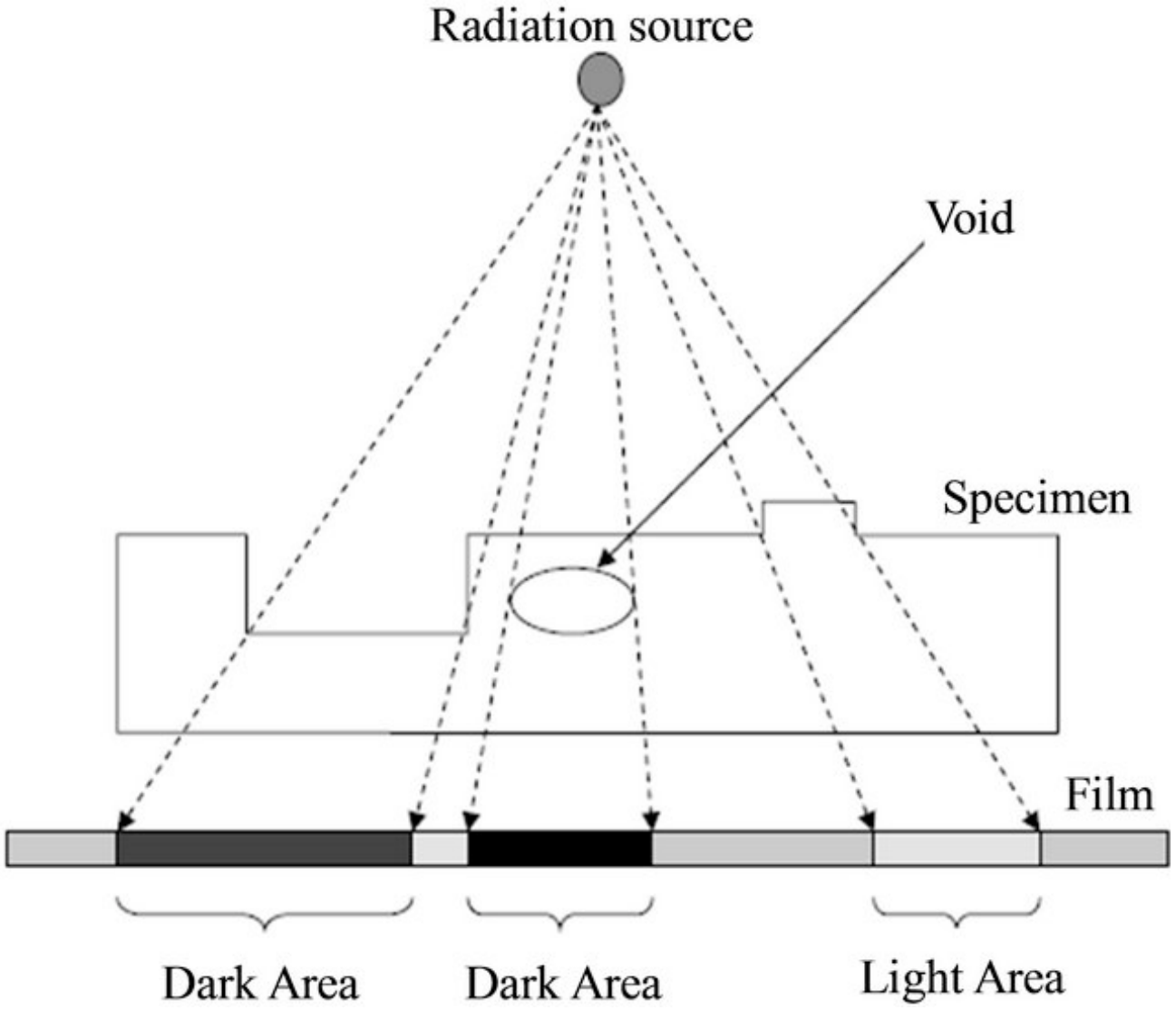

Radiographic testing of two chips

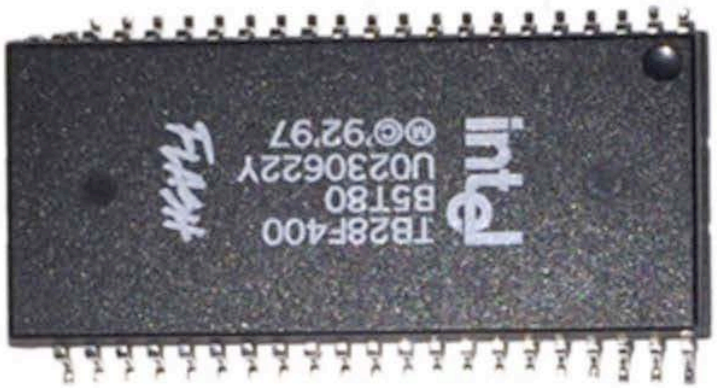

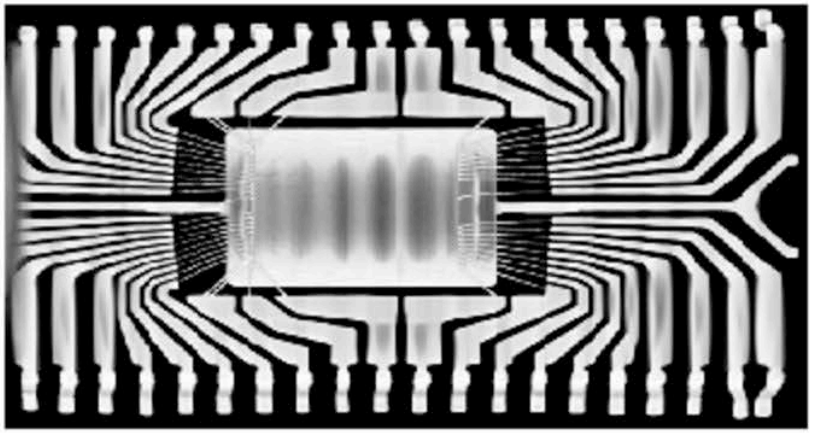

Counterfeit

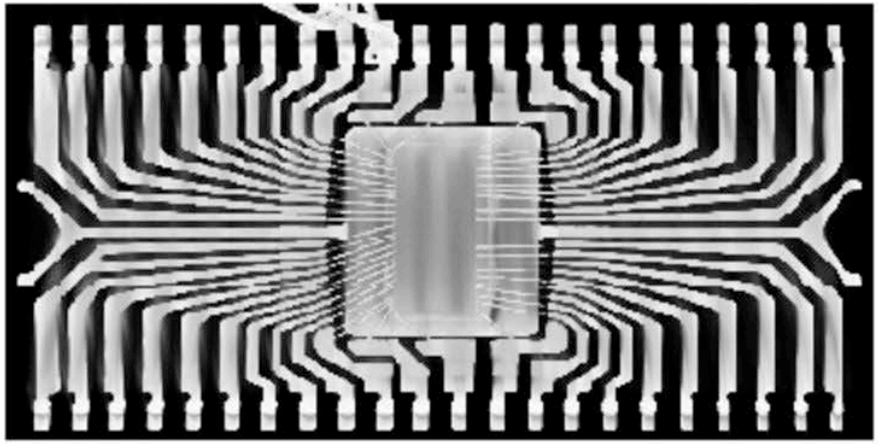

Authentic

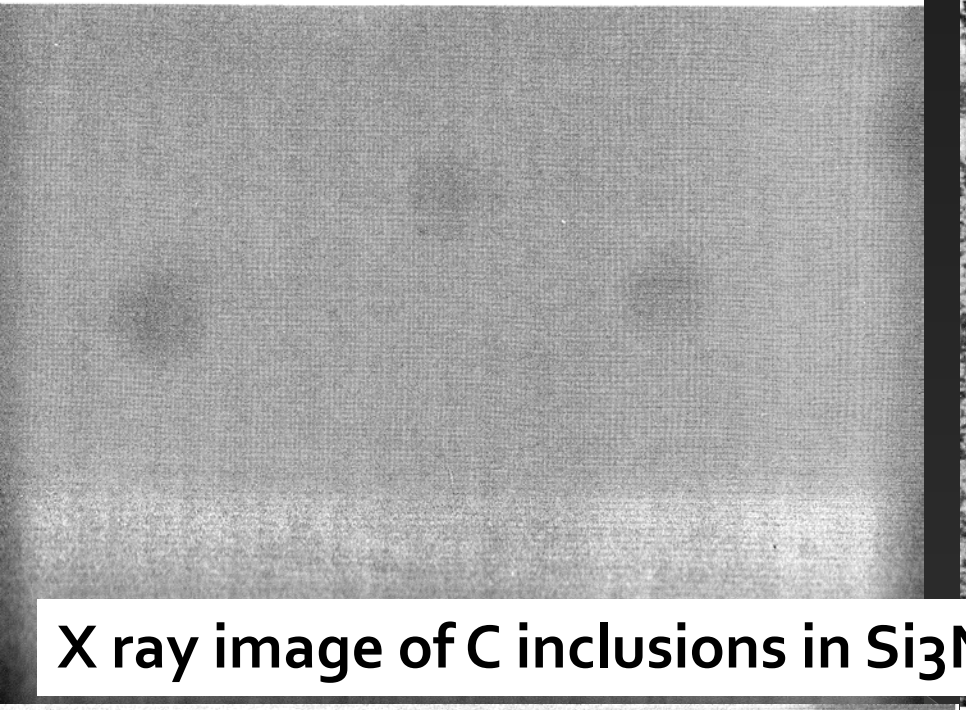

X ray image of C inclusions in Si_3N_4

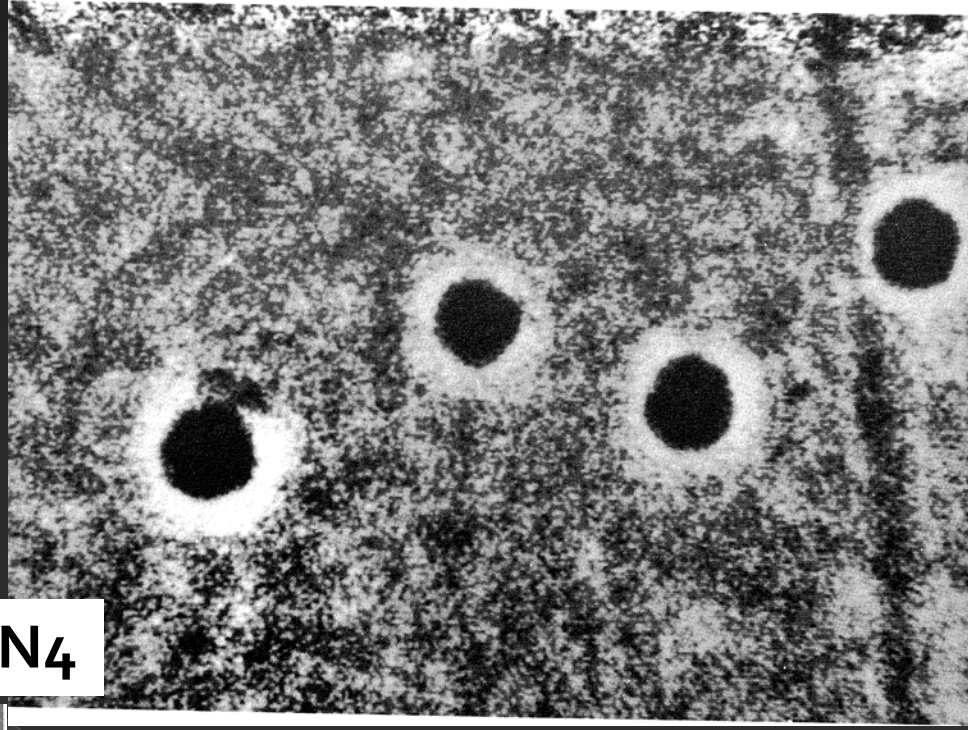

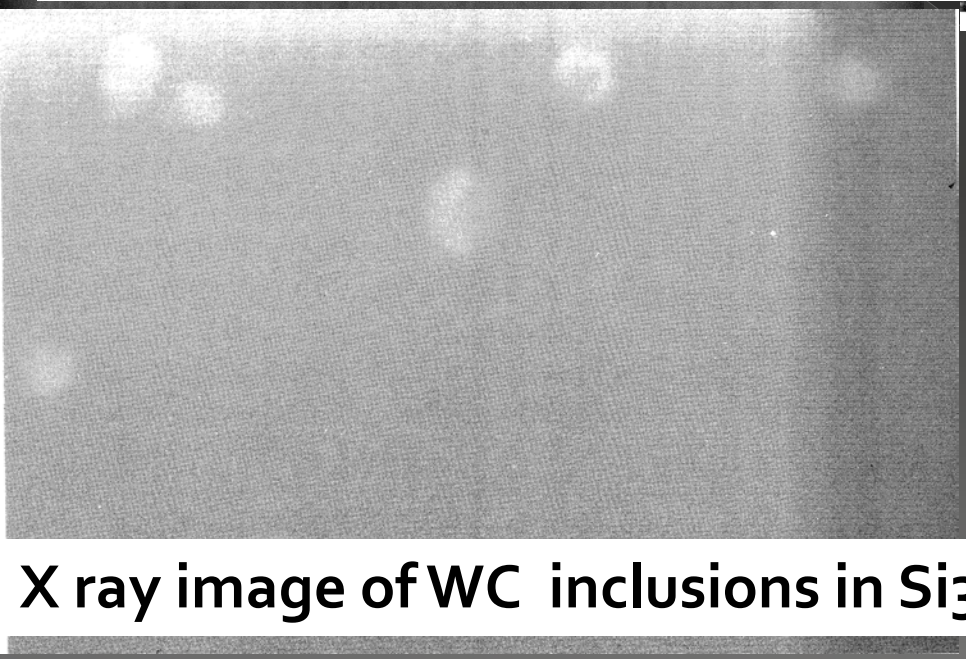

X ray image of WC inclusions in Si_3N_4

Magnetoscopic testing

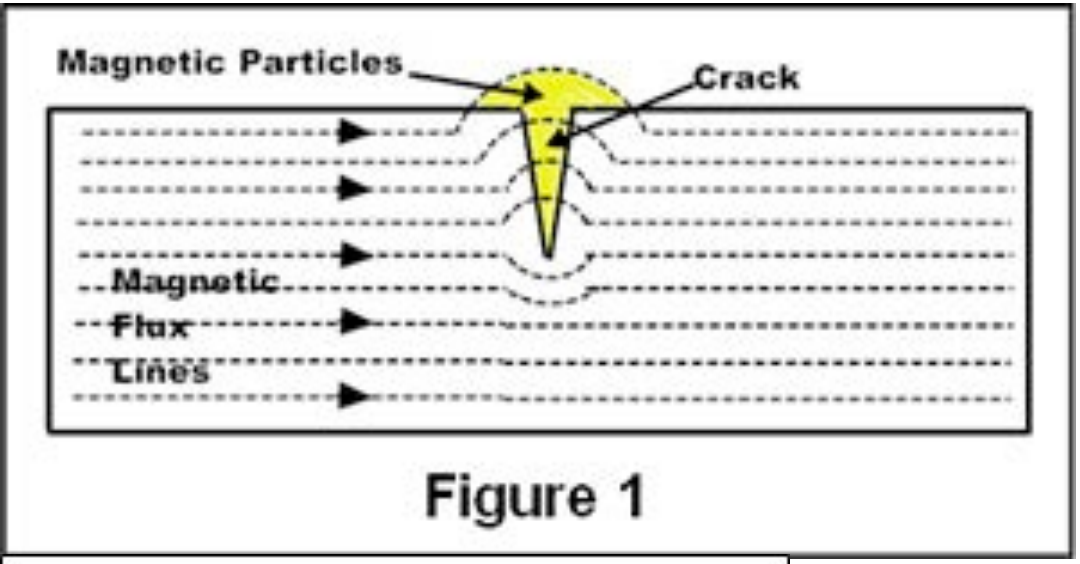

Figure 1

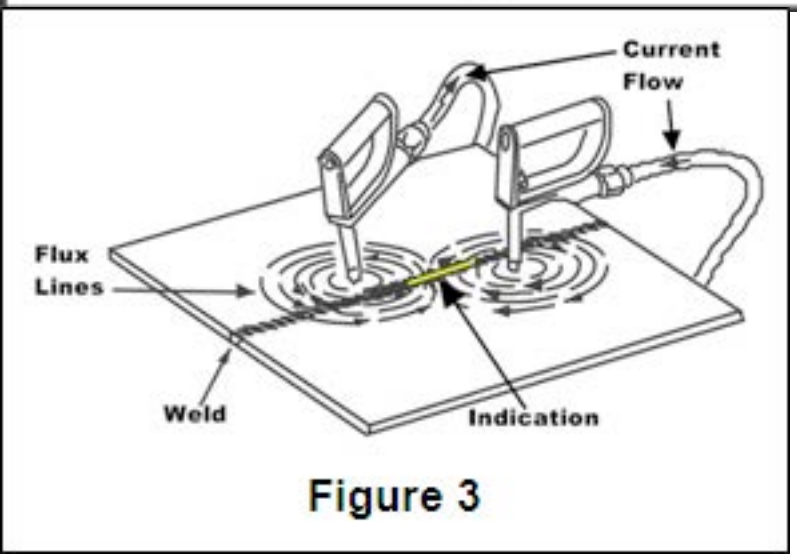

Figure 3

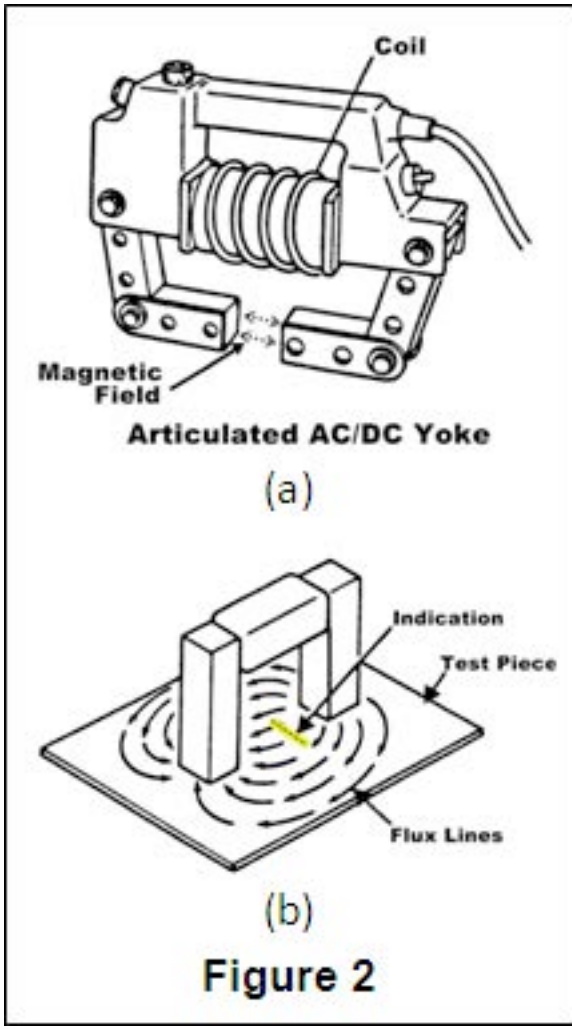

Figure 2

Eddy current testing

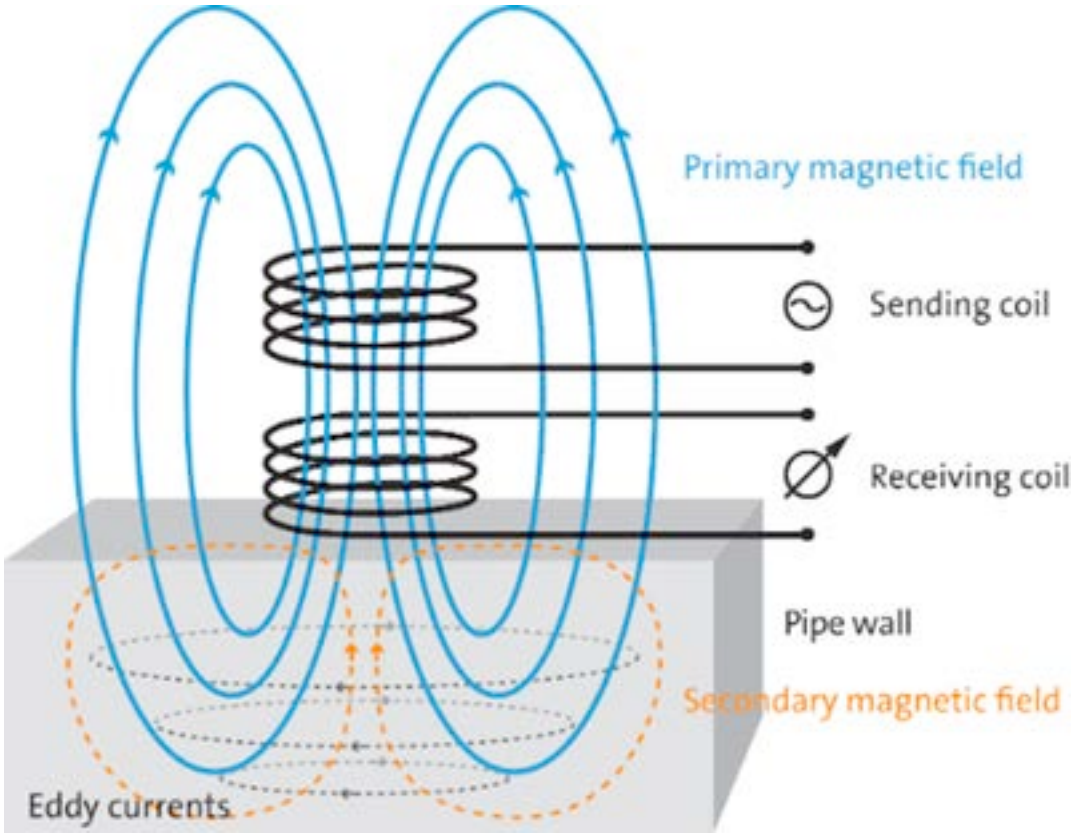

Table 14.2 Examples of Design Requirements of Various Applications and Ceramics with Properties Which Match the Requirements

Application	Requirements of the applications	Candidate ceramics	Key properties
Seal			
Turbine stator			
Heating element			
Rotary heat exchanger			
Heat sink for IC and transistor devices			
Furnace insulation			
Miniature capacitor			
High-speed, high-load bearing			
Segments of watch band			

SiC Heat exchanger

Ceramic seal for taps

Sandblast nozzles

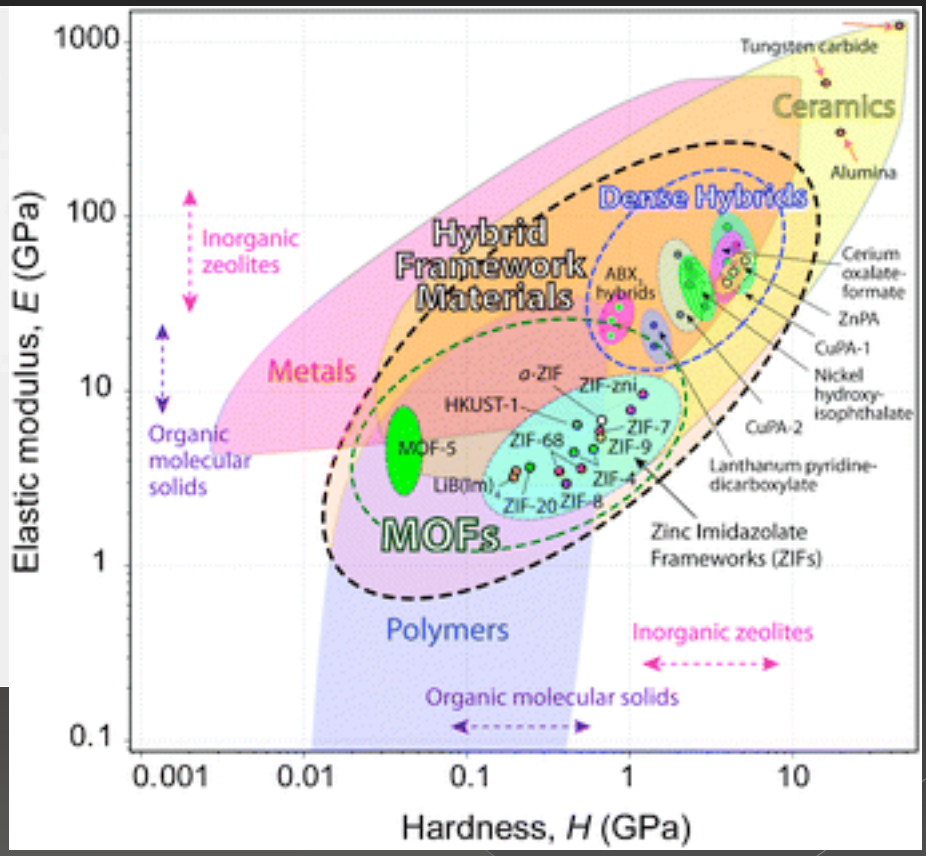

Rado watches

SEM fundamentals

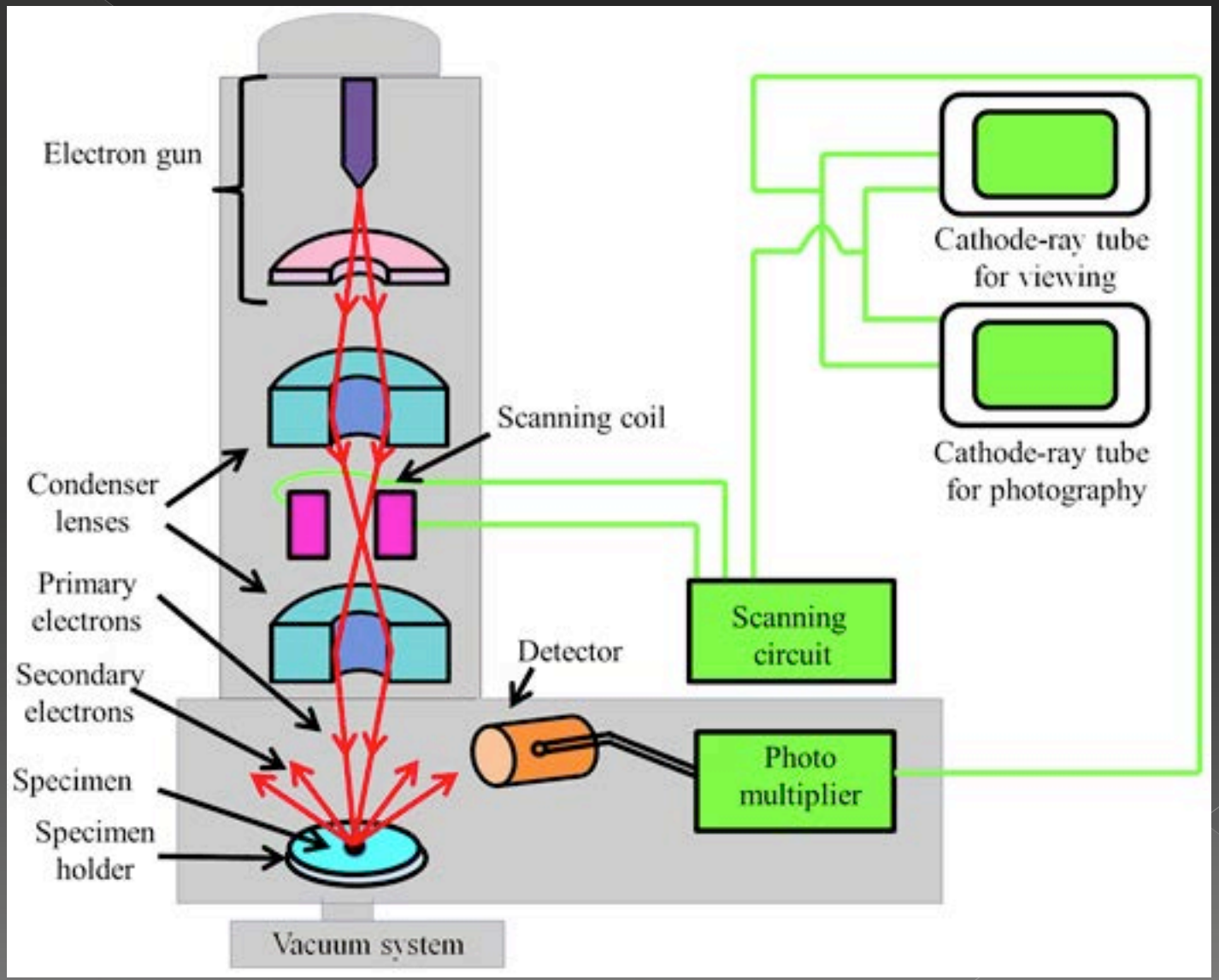

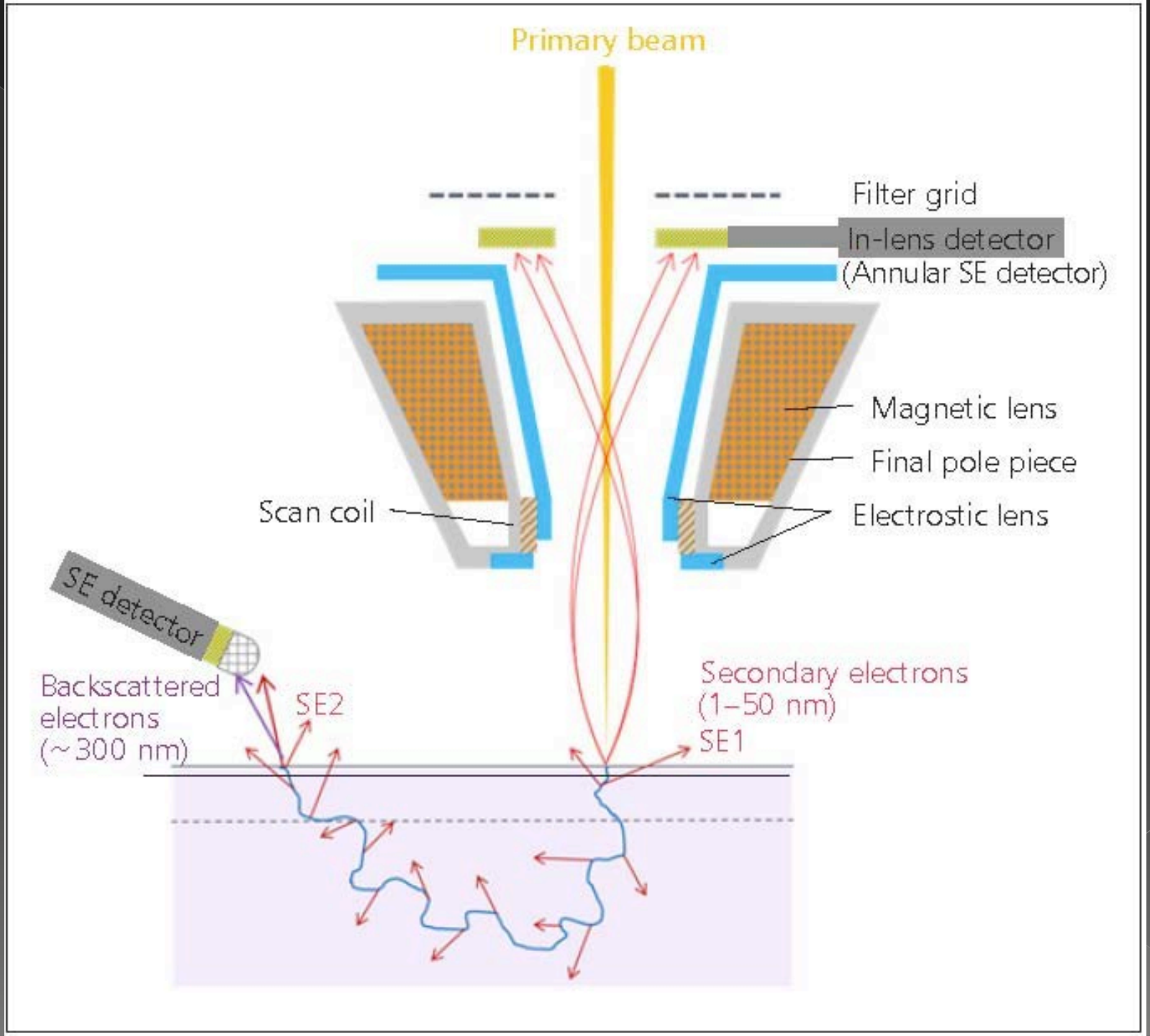
Primary beam
Filter grid
In-lens detector
(Annular SE detector)
Magnetic lens
Final pole piece
Electrostic lens
Scan coil
SE detector
Backscattered
electrons
(~300 nm)
SE2
Secondary electrons
(1–50 nm)
SE1

E-beam sample intercation

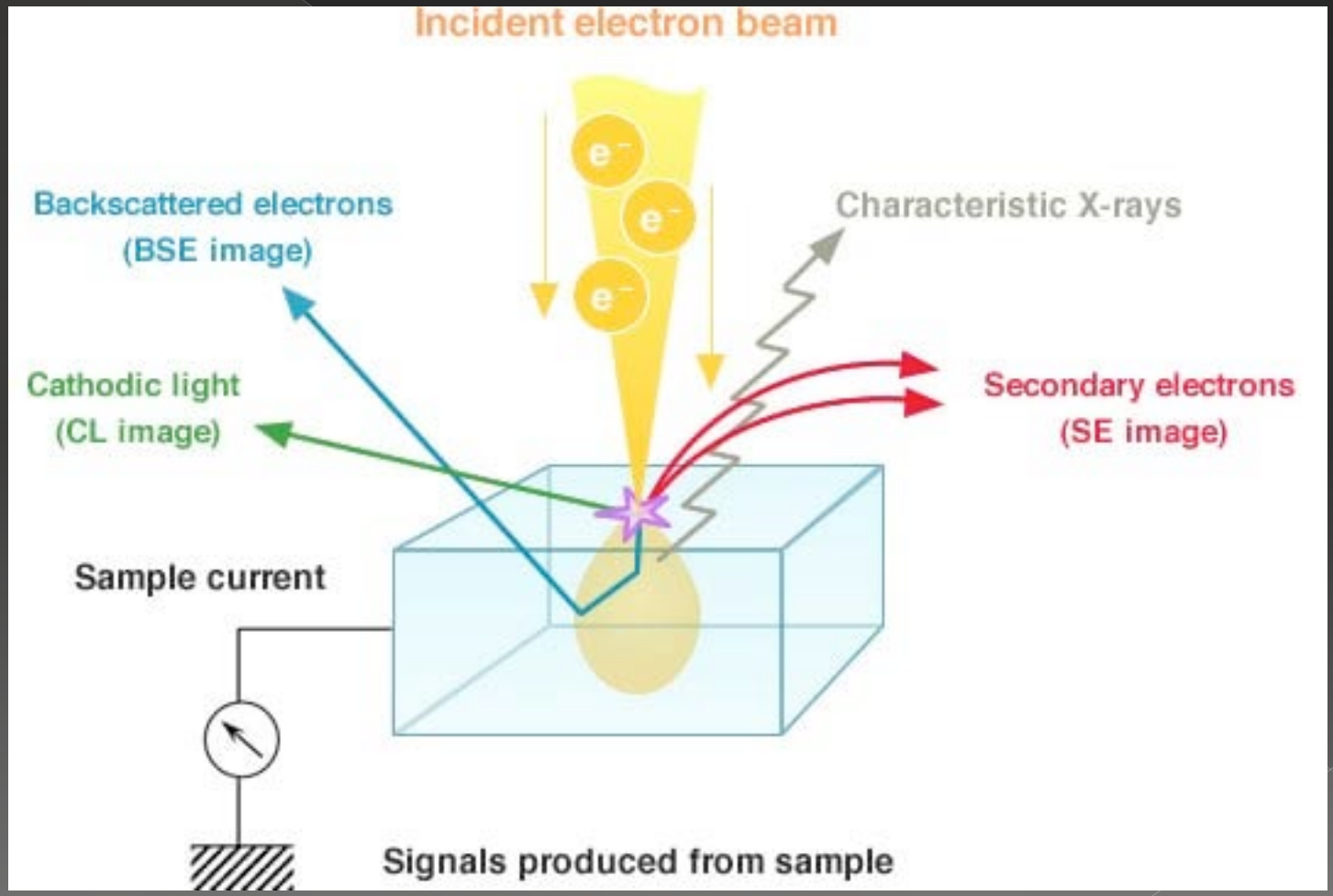

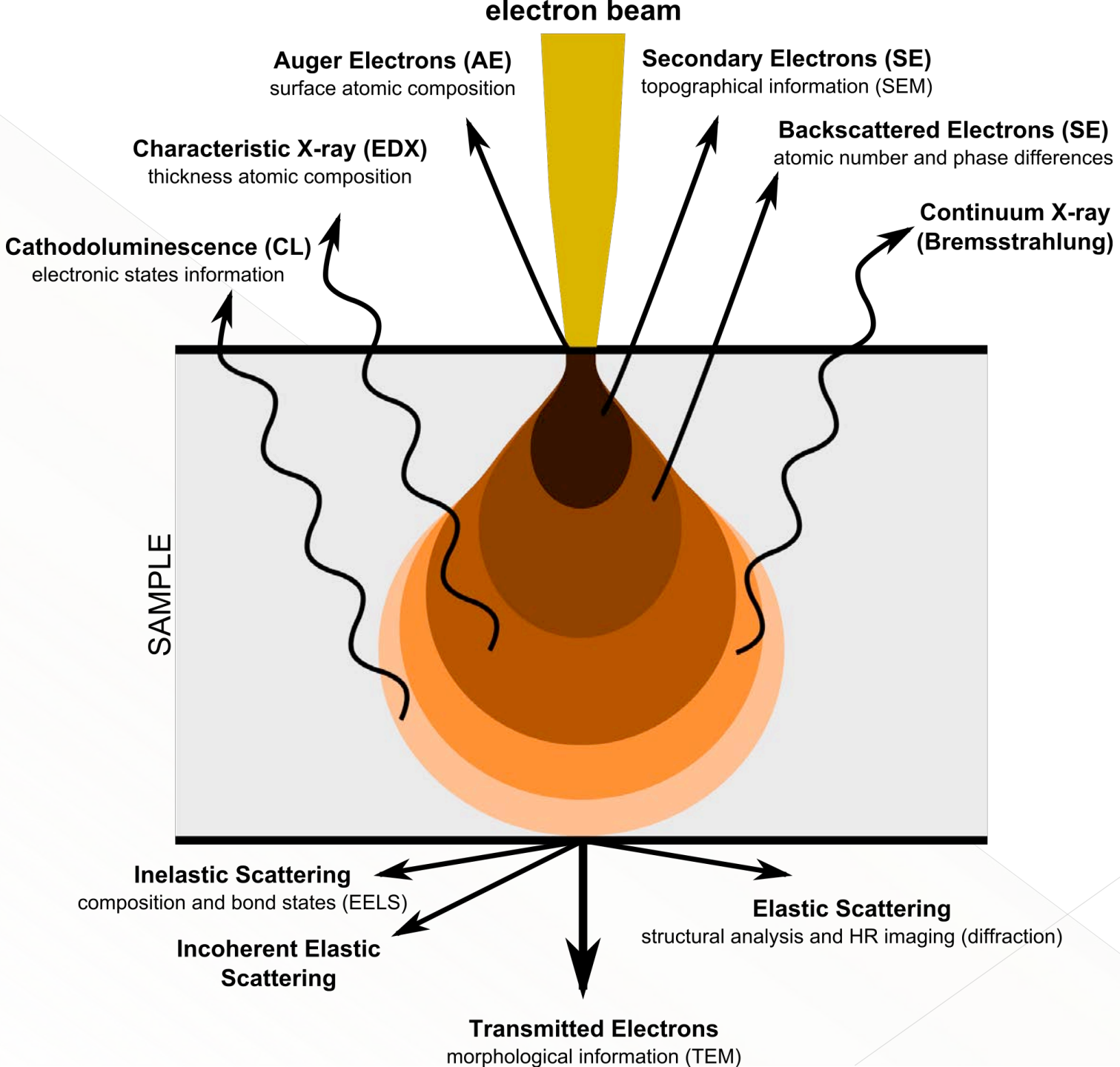
electron beam
Auger Electrons (AE)
surface atomic composition
Secondary Electrons (SE)
topographical information (SEM)
Characteristic X-ray (EDX)
thickness atomic composition
Backscattered Electrons (SE)
atomic number and phase differences
Continuum X-ray
(Bremsstrahlung)
Cathodoluminescence (CL)
electronic states information
SAMPLE
Inelastic Scattering
composition and bond states (EELS)
Elastic Scattering
structural analysis and HR imaging (diffraction)
Incoherent Elastic
Scattering
Transmitted Electrons
morphological information (TEM)

EDS spectrum of ZnO deposited on SiC

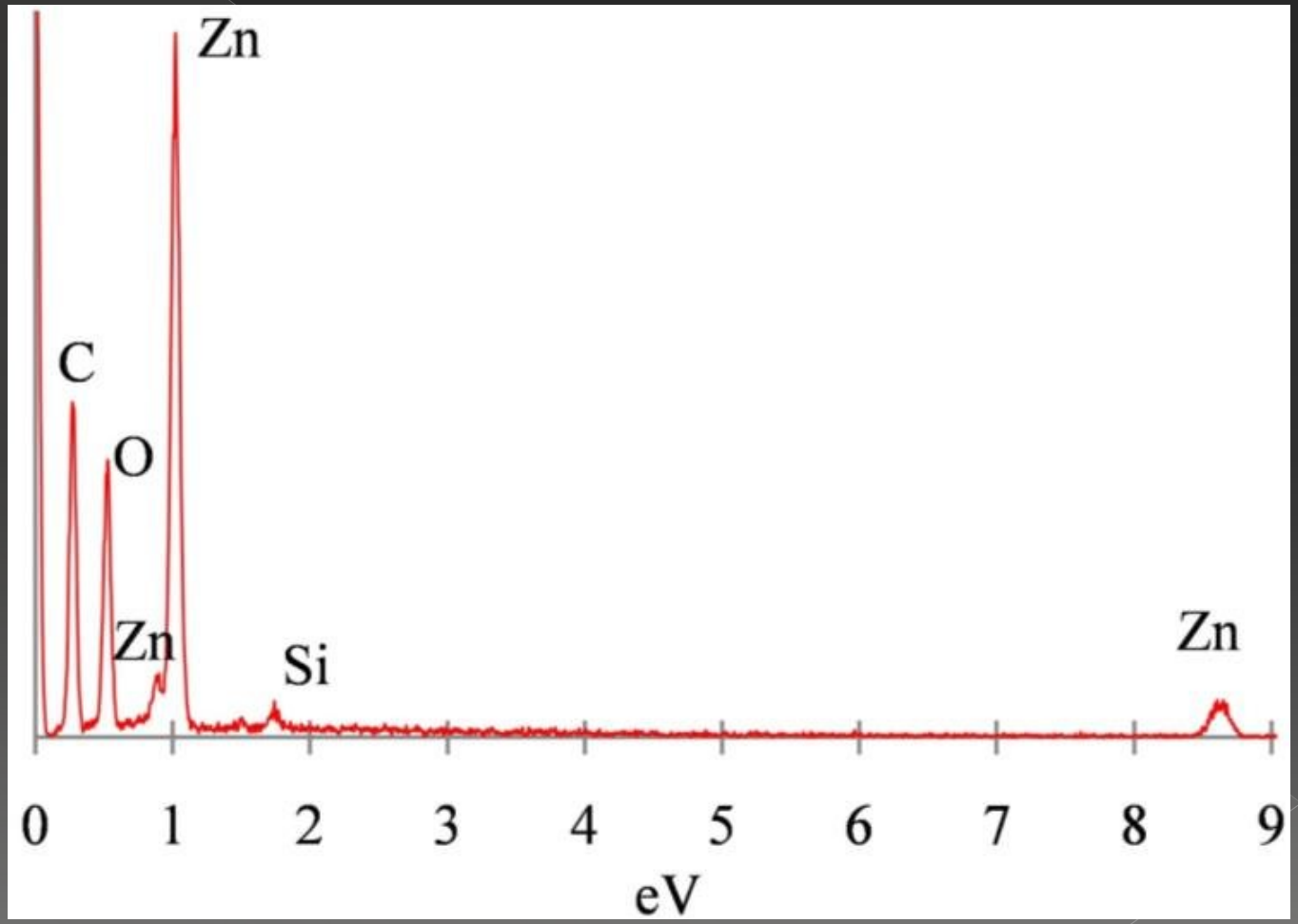

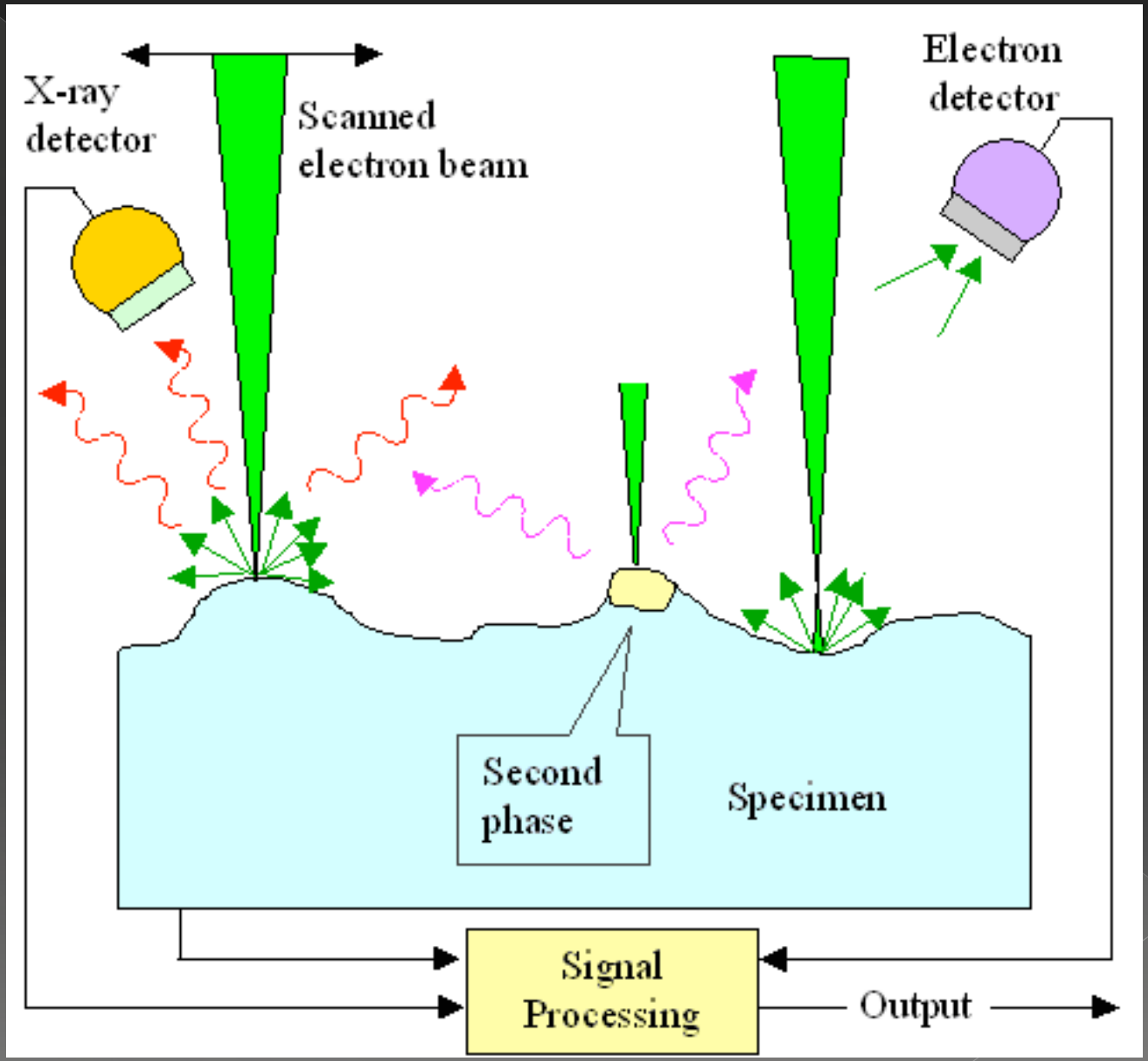
X-ray
detector
Scanned
electron beam
Electron
detector
Second
phase
Specimen
Signal
Processing
Output

Compositional contrast

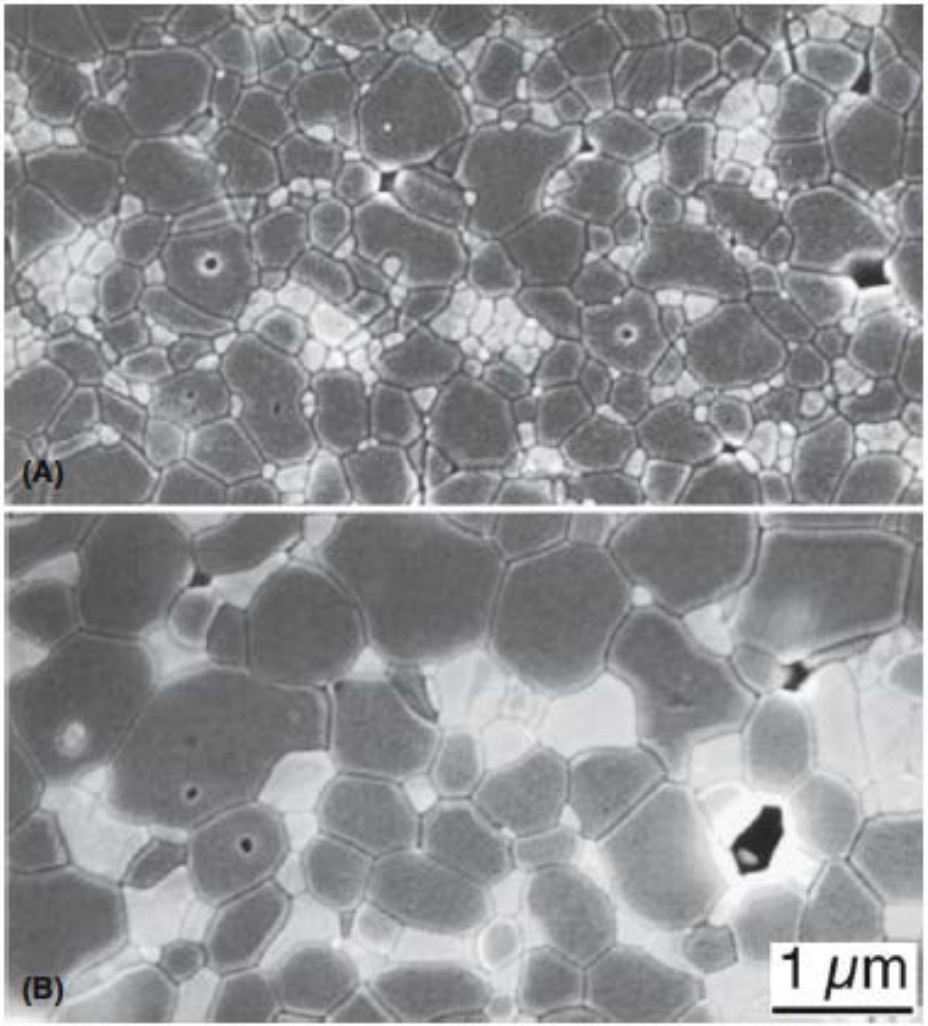

FIGURE 24.27 Two-phase ceramics. (a) As sintered and (b) heat treated at 1600°C for 30 hours. ZTA 30% (zirconia-toughened alumina with 30 vol% YSZ containing 10 molar% yttria).

Topographycal contrast

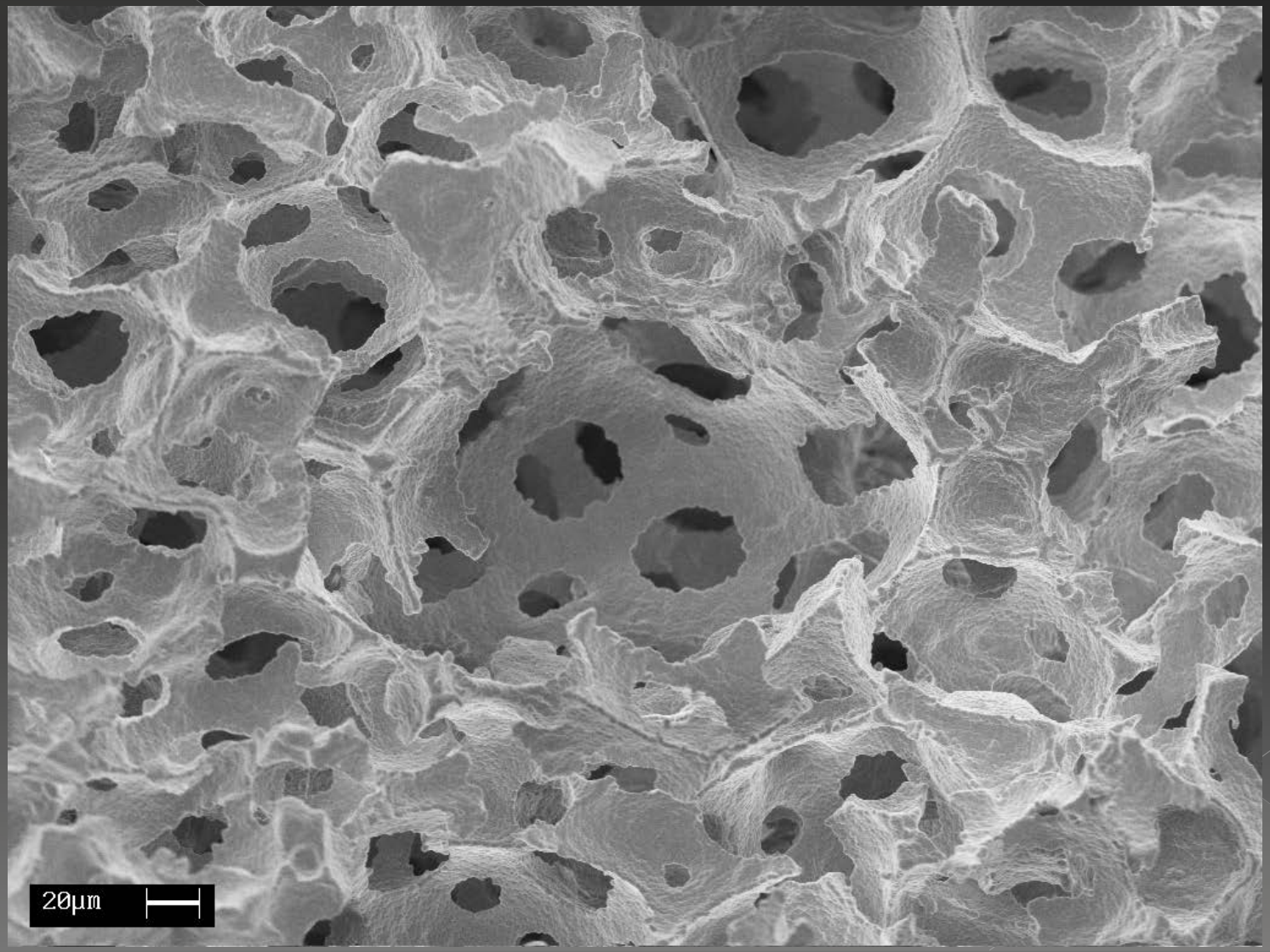

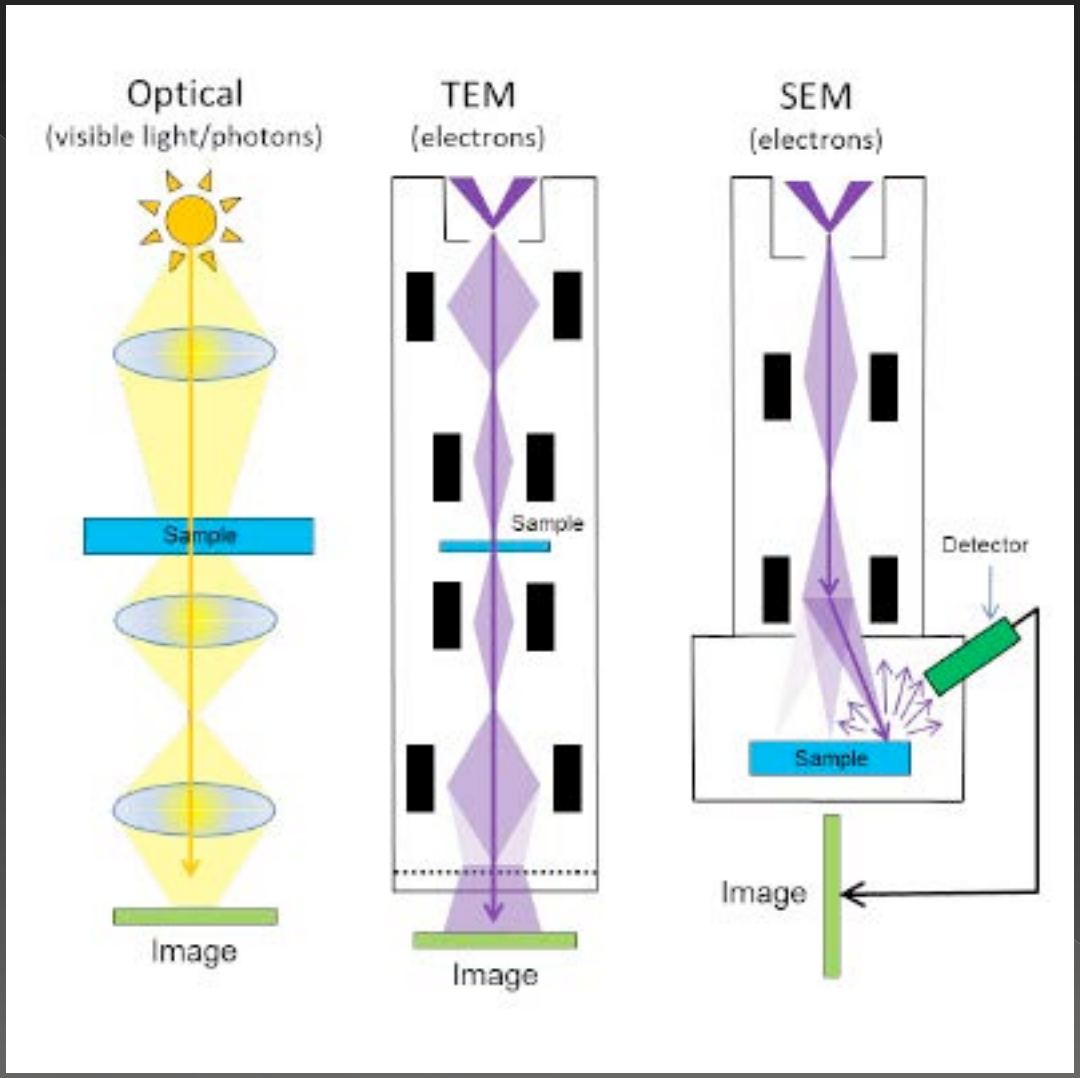
Optical
(visible light/photons)
Sample
Image
TEM
(electrons)
Sample
Image
SEM
(electrons)
Detector
Sample
Image

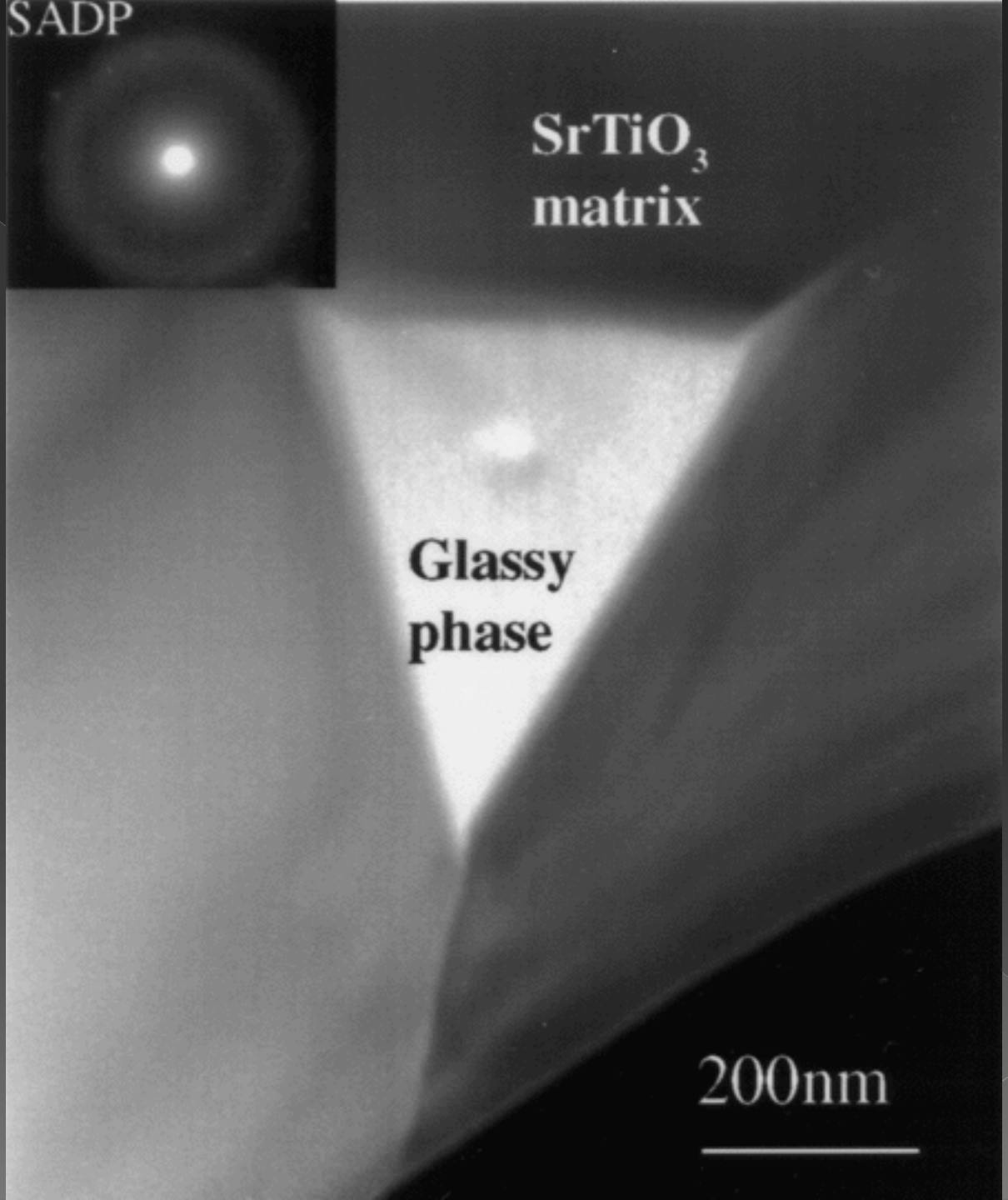
SADP
SrTiO3
matrix
Glassy
phase
200nm

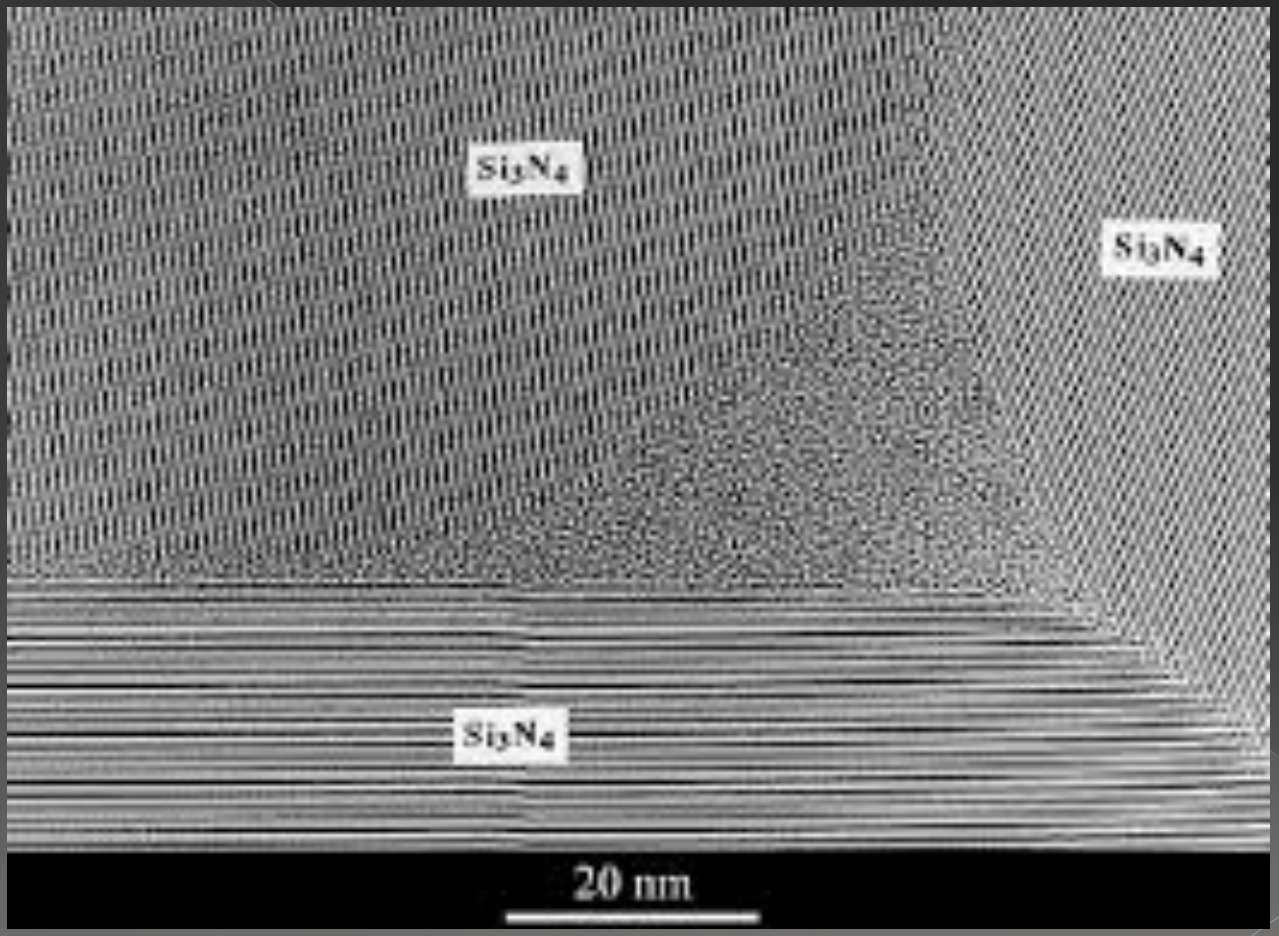
Si_3N_4
Si_3N_4
Si_3N_4
20 nm

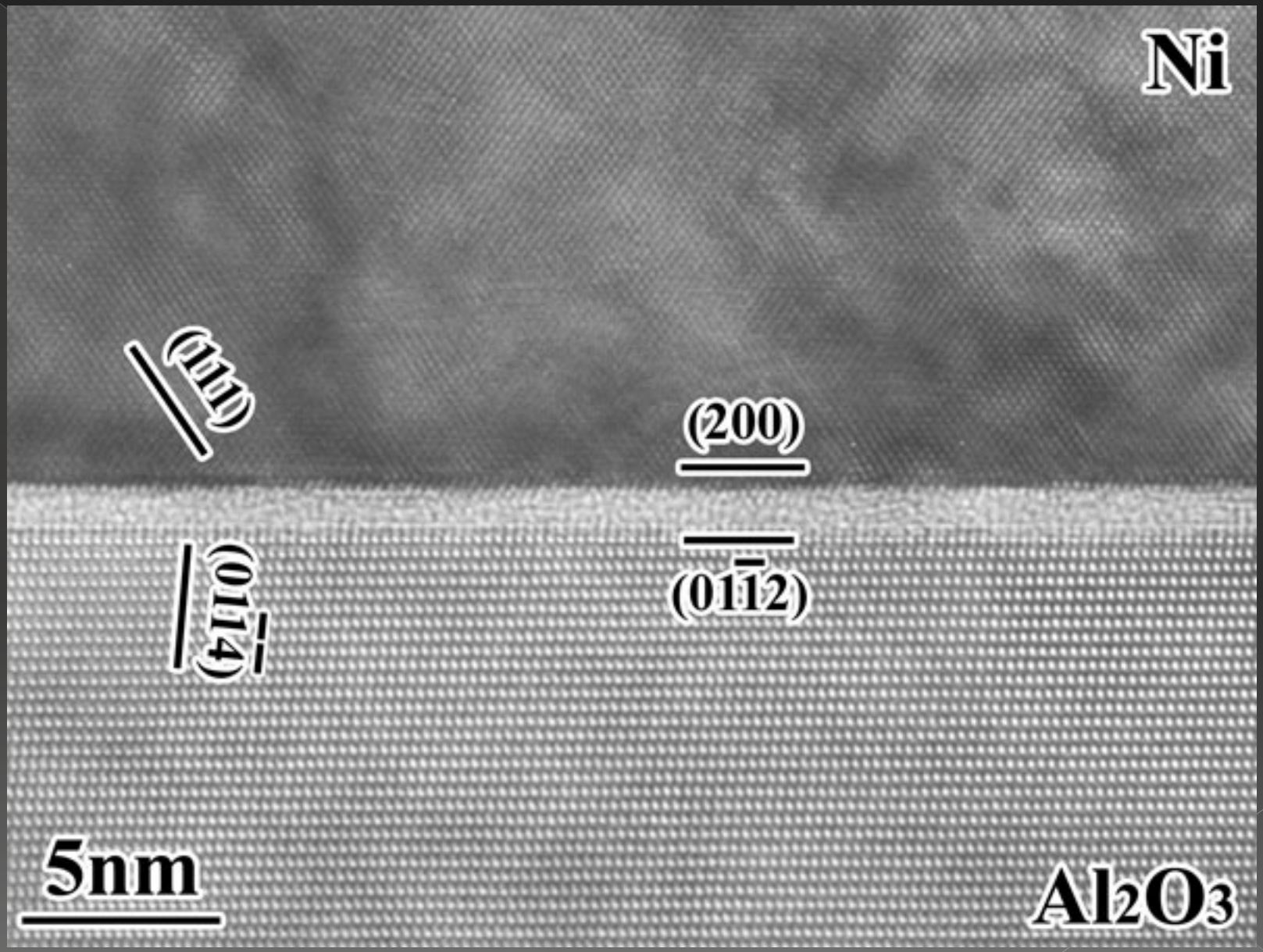
Ni
(111)
(200)
(01$\bar{1}$4)
(0$\bar{1}$12)
5nm
Al_2O_3

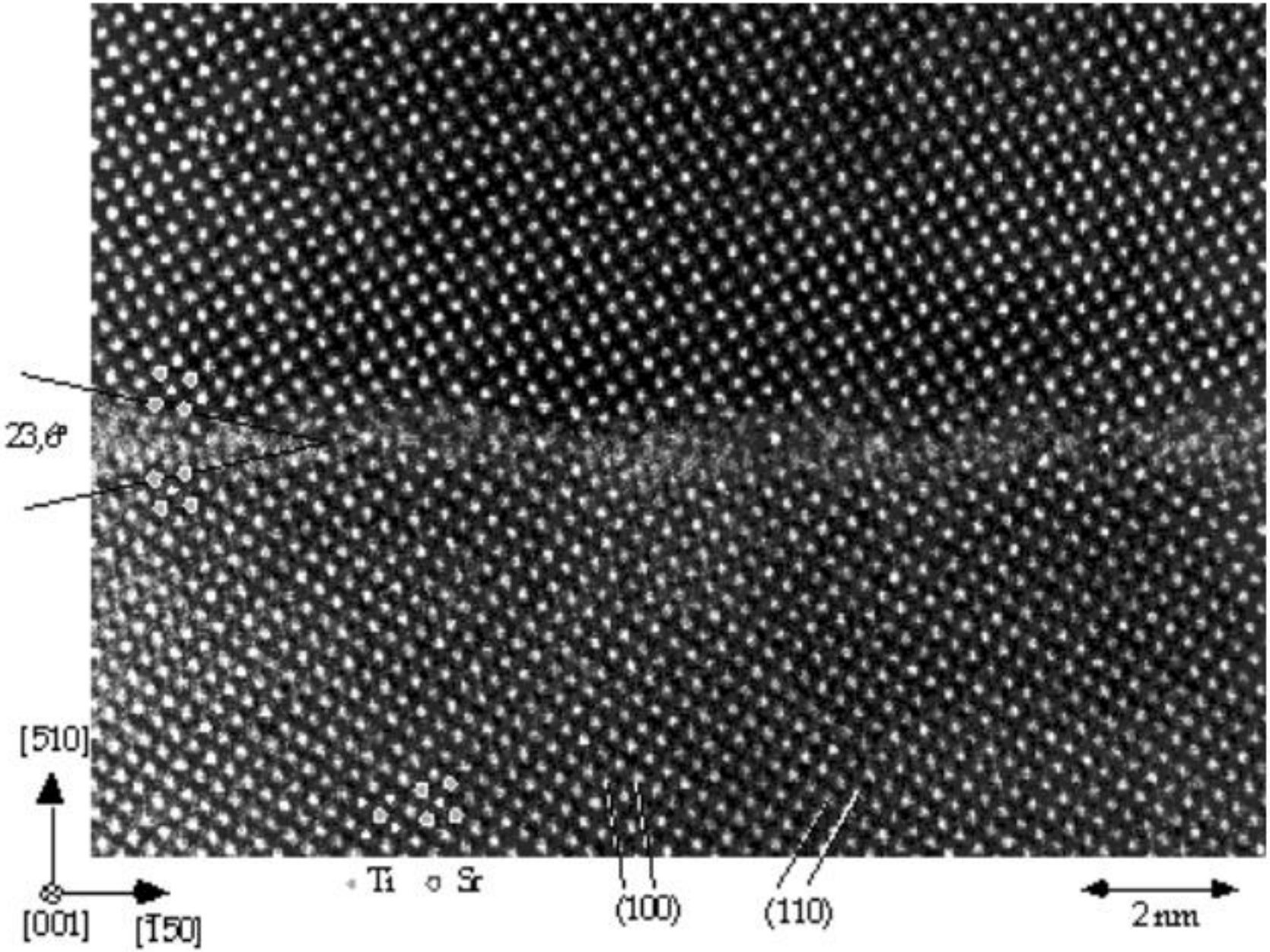
23,6°
[510]
[001]
[$\bar{1}$50]
Ti
Sr
(100)
(110)
2 nm

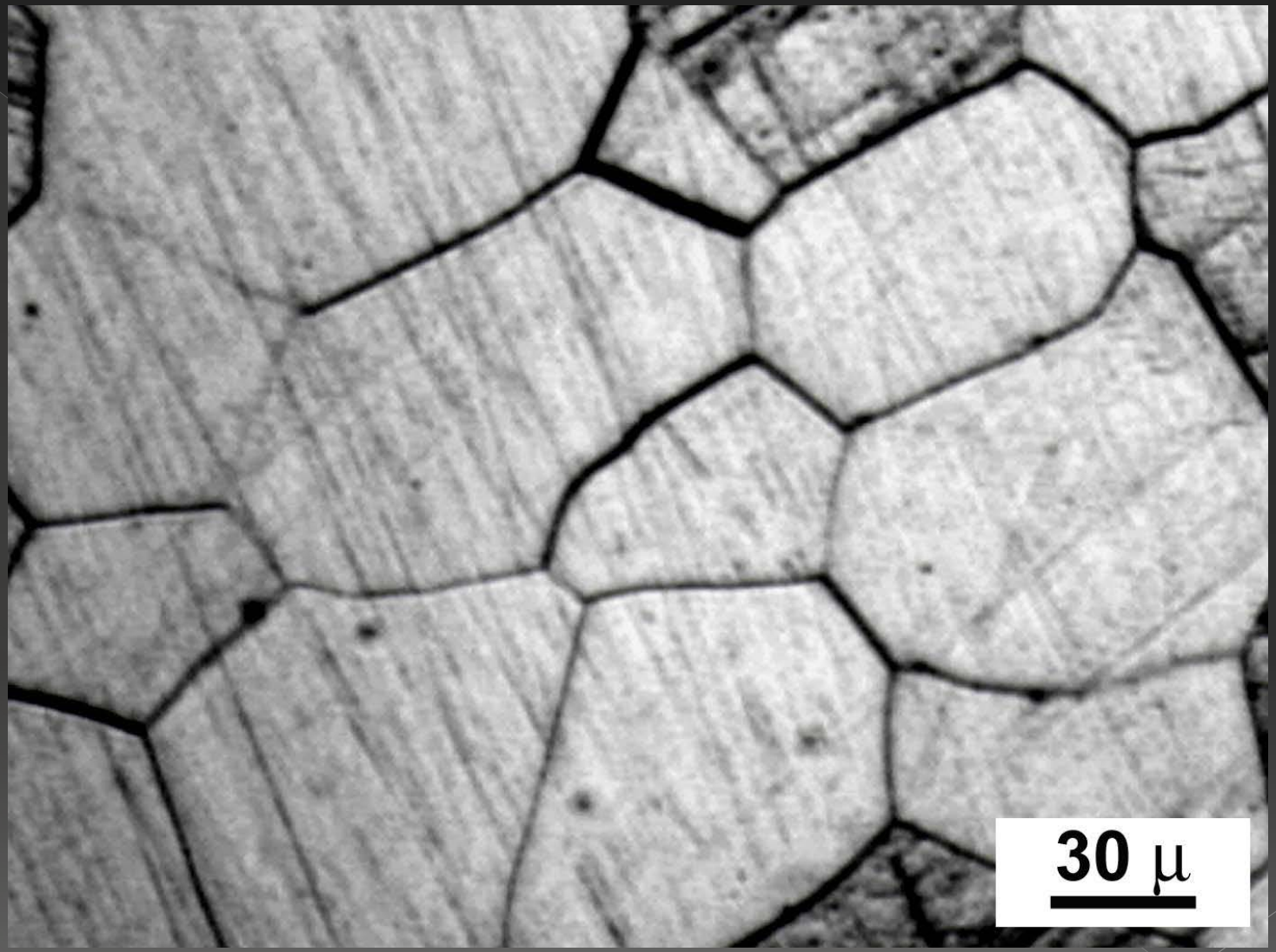
30 μ